NUI Galway
OÉ Gaillimh

The molecular mechanisms governing the colonisation of intestinal epithelial cells by *Vibrio parahaemolyticus*

Nicholas O Boyle

Thesis submitted for the degree of Doctor of Philosophy (Microbiology) at the National University of Ireland, Galway

Research Supervisor: Dr Aoife Boyd
Discipline of Microbiology
School of Natural Sciences
National University of Ireland, Galway

December 2012

Table of Contents

Chapter 2 – Materials and Methods

Chapter 5 – Confirmation of adhesin and invasin functionality and investigation into involvement in *V. parahaemolyticus* pathogenicity

Chapter 6 – Discussion

Abstract

Vibrio parahaemolyticus is a food borne gastro-intestinal pathogen of major global importance. The organism induces severe inflammatory diarrhea in individuals who become infected due to the consumption of contaminated seafood. *V. parahaemolyticus* is known to exert pathogenic effects upon host cells by the translocation of effector proteins into the host cell, using a type three secretion injectisome, however little is known about the molecular interactions which allow colonisation and persistence of the organism in the intestinal epithelium. This study analysed the adherence and invasion of *V. parahaemolyticus* using the established intestinal cell line Caco-2. *V. parahaemolyticus* was found to adhere at high levels to Caco-2 cells. A small number of the adherent bacteria became internalised and were subsequently capable of intracellular proliferation. A genomic library based approach was undertaken in order to identify novel proteins conferring adhesive and invasive traits (adhesins/invasins) upon *V. parahaemolyticus*. Bioinformatic mining was also carried out in order to identify putative adhesins/invasins based on amino acid identity to characterised adhesins/invasins from other species. One adhesin identified was confirmed as having a role in the adherence of *V. parahaemolyticus* to intestinal Caco-2. Deletion of essential components of the mannose sensitive haemagglutinin (MSHA) pilus resulted in a 40% decrease in adherence and a similar decrease in uptake by Caco-2. The decreased adhesive properties of MSHA mutants correlated with significant decreases in *V. parahaemolyticus* induced lysis, cell rounding and IL-8 induction in Caco-2. Neoglycoconjugate array comparison between the *V. parahaemolyticus* wild type and MSHA deficient mutants identified lectin functionality for the MSHA pilus with specificity towards the fucosylated blood group antigens. This study highlighted key aspects of the colonisation of intestinal tissues by *V. parahaemolyticus*. The findings discussed herein alter the currently recognised molecular mechanisms of intestinal colonisation by *V. parahaemolyticus* and have implications for the pathobiology of numerous enteric pathogens. The techniques and observations of this study may be applied to the analysis of other intestinal pathogens, with a view to understanding the processes which occur during initial interactions with host cells and eventual development of therapeutics to prevent colonisation and the subsequent onset of disease.

Acknowledgements

I would like to extend a sincere thank you to my supervisor Dr Aoife Boyd for her constant encouragement, expertise, advice and enthusiasm throughout my project. Working in the Pathogenic Mechanisms Research Group was a thoroughly enjoyable and enlightening experience. Thank you to the other members of the Pathogenic Mechanisms laboratory Dr Ana Mustel, Dr Ksenia Matlawska-Wasowska and Rebecca Finn, for their assistance and friendship throughout my time in the lab. I would like to thank Prof Lokesh Joshi, Dr Marian Kane and Benoit Houeix of the Glycoscience group, NCBES, NUI Galway for kindly providing access to their facilities and invaluable assistance with the glycan profiling carried out in my study. I would like to acknowledge Prof Lokesh Joshi and Dr Thomas Barry for the time and advice given as members of my graduate research committee. Having spent eight years interacting with the Department of Microbiology, NUI Galway, I have developed a great appreciation for their hard work and approachable nature and will always remember the time I have spent here. The academic staff, technical staff, post-doctoral and post-graduate researchers have all played a vital part in my studies throughout the years and I am very grateful to all involved. A very special thank you to my post-graduate colleagues who were ever-present during tea times and lunch breaks, when times were tough and a sympathetic ear was required. I would like to sincerely thank my parents Eilish and Raymond, and my sisters Sarah and Katie, for their love, support and continued efforts to understand and empathise. None of what I have achieved would have been possible without you guys and I am deeply grateful. Finally, a big thank you to Catherine for her patience, love and support throughout the past four years when it was needed most.

List of figures

List of tables

Chapter 1

Introduction

1.1 The *Vibrionaceae*.

The *Vibrionaceae* form a highly diverse microbial family which is found ubiquitously in marine environments. As of 2006, almost 80 different species had been classified as members of the *Vibrionaceae* family (Thompson and Swings, 2006). Vibrios have been shown to account for up to 30% of the total heterotrophic bacteria in parts of Tokyo Bay (Simidu *et al.*, 1987). Dryselius *et al.* (2007) postulated that the almost ubiquitous presence of the *Vibrionaceae* in marine environments indicated a central role in the cycling of marine nutrients. Vibrios display a pronounced environmental flexibility, a feature which has enabled their association with other marine species including plankton, copepods, shrimp, oysters and fish. These relationships may be symbiotic, as in the case of bioluminescent *V. fischeri*, which colonise the light organ of the squid *Euprymna scolopes* (Boettcher and Ruby, 1990). Many *Vibrio spp* can however also be pathogenic towards the marine animals which they colonise. *Vibrio salmonicida*, *Vibrio anguillarum* and *Vibrio vulnificus* are all capable of causing infection in fish including cod, salmonids, sea bass and turbot, a process which results in significant damage to the marine aquaculture industry (Toranzo *et al.*, 2005).

The detrimental effects of the interactions between *Vibrio spp* and human hosts have long been understood. Robert Koch first isolated and cultured *V. cholerae* from fatal victims of cholera poisoning in 1883, identifying cells which were “highly motile” and “a little bent resembling a comma or a spiral” (Brock, 1988). Importantly Koch recognised that *V. cholerae* was the causative agent of the disease and recommended the filtration of water supplies in order to prevent infections (Brock, 1988). The World Health Organisation estimate 3 to 5 million cases of toxigenic cholera infection per year, resulting in 100,000 to 120,000 deaths. Since the identification of *V. cholerae* as an important human pathogen, a number of other non-cholera *Vibrio spp* have been associated with human disease, most

notably *V. vulnificus* and *V. parahaemolyticus*, which have the ability to cause soft tissue infections and gastrointestinal illness (Blake *et al.*, 1980).

The ability to establish infections in human hosts appears to have evolved in parallel among different groups of *Vibrio spp*. Fig 1.1 contains a phylogenetic tree, constructed by Kita-Tsukamoto *et al.* (1993), comparing the evolutionary relationships between a variety of marine bacteria, predominantly *Vibrio spp*, by comparison of 16S ribosomal RNA coding sequences. As seen in Fig 1.1, *V. parahaemolyticus* is found within a closely related group of *Vibrio spp* including *V. alginolyticus*, *V. campbelli*, *V. harveyi*, *V. nereis*, *V. carchariae* and *V. fluvialis*. Of these species, only *V. parahaemolyticus*, *V. alginolyticus* and *V. fluvialis* are recognised human pathogens (Newton *et al.*, 2012; Glenn Morris, 2003; Daniels and Shafaie, 2000; Blake *et al.*, 1980). The grouping of pathogenic and non-pathogenic vibrios within the same mono-phyletic clade indicates that human pathogenicity has developed independently in each organism or that primitive pathogenic traits have selectively been lost by some species within the group. The former hypothesis is supported by the fact that each of the human pathogenic organisms possesses distinct molecular virulence mechanisms which are in many cases encoded on horizontally acquired pathogenicity islands (Makino *et al.*, 2003; Linkous and Oliver, 1999; Zanetti *et al.*, 2000). The vast majority of *Vibrio* species are non-pathogenic towards humans and it therefore seems reasonable to consider that the common ancestor of the *Vibrio* group would lack human pathogenic traits. Further support for the distinct evolutionary origins of pathogenesis is provided by the finding that the human pathogen *V. cholerae* is found on a distinct branch within the *Vibrio* clade and is therefore like *V. parahaemolyticus*, likely to have acquired pathogenicity towards humans after the speciation of the *Vibrio* group.

Figure has been removed due to copyright restrictions

Fig 1.1 Phylogenetic relationships between the *Vibrionaceae* and other related marine bacteria. The tree was constructed from 16S rRNA alignments using the neighbour joining method. *V. parahaemolyticus* is indicated by an arrow. The accompanying table includes the abbreviations used for each species within the phylogenetic tree. Figure and accompanying table adapted from Kita-Tsukamoto *et al.* (1993).

The success of the *Vibrionaceae* as colonisers of a widely diverse range of habitats can at least in part be attributed to their possession of a dynamic array of adherence and colonisation factors. Species such as *V. parahaemolyticus* possess multiple proteins which confer adhesion (adhesins), thereby allowing persistence in both shellfish and human environments (Shime-Hattori *et al.*, 2006). The possession of multi-functional adhesins such as type IV pili (TFP), which are widespread throughout the *Vibrionaceae*, has enabled unparalleled environmental adaptability – a feature which has resulted in the widespread presence of the *Vibrionaceae* in a variety of marine habitats. The involvement of adhesins, including TFP, in the colonisation of human intestinal tissue will be dealt with extensively throughout this study.

An intriguing common feature of the *Vibrionaceae* is the possession of a two chromosome genome organisation. Prior to 1989 when Suwanto and Kaplan discovered a dual chromosomal genome in *Rhodobacter sphaeroides*, it had been thought that all prokaryotes possessed a single chromosome. Pulsed field gel electrophoresis of 34 vibrios and related bacterial species identified 100% conservation of the two chromosome organisation within the *Vibrionaceae* (Okada *et al.*, 2005). The strict conservation of this feature indicates that the arrangement must have been generated prior to the diversification of the family (Thompson *et al.*, 2004). The mechanism by which this unusual genetic organisation arose has drawn vast speculation and disagreement from *Vibrio* researchers. One explanation which has been proposed is the division of a single large ancestral chromosome into two individual genetic elements (Dryselius *et al.*, 2007). Another theory which is now considered more likely, is that chromosome 2 was acquired as an ancestral megaplasmid and that its retention was brought about either through rapid acquisition of essential genes or through the activity of a toxin anti-toxin system (Dryselius *et al.*, 2007; Egan and Waldor, 2003; Heidelberg *et al.*, 2000).

Regardless of the process by which a double chromosome organisation arose, the stable maintenance of this theme throughout the *Vibrionaceae* infers an integral function in *Vibrio* biology. One group speculated that the possession of two chromosomes would enable more rapid DNA replication, a hypothesis which was based upon the observation that *V. parahaemolyticus* has a doubling time of 8 to 9 min under optimal conditions (Dryselius *et al.*, 2007; Yabuuchi *et al.*, 1974). It has also been suggested that chromosome 2 offers a potential hub for genetic variability by allowing for insertions and deletions, without the high risk of compromising essential genes that would be encountered with such manipulations of chromosome 1 (Dryselius *et al.*, 2007). Variability within chromosome 2 is supported by the fact that the size of chromosome 1 is quite conserved throughout the *Vibrionaceae*, while the interspecies size of chromosome 2 varies considerably (Okada *et al.*, 2005). While most of the *V. parahaemolyticus* genes required for growth are contained within chromosome 1, many of the genes required for environmental adaptation are encoded within chromosome 2 (Makino *et al.*, 2003). As such, it appears that the evolutionarily conserved variability of chromosome 2 in *Vibrio spp* may play a key role in facilitating vast potential for environmental adaptation without compromising the fitness of the organism.

1.2 *V. parahaemolyticus* discovery, general characteristics, clinical manifestations and epidemiology.

V. parahaemolyticus was first identified following an outbreak of food poisoning in 1950 in Osaka, Japan in which 272 individuals were infected, resulting in 20 fatalities. The cause of the outbreak was attributed to bacterially contaminated “shirasu”, a dried sardine which was consumed by all infected individuals (Fujino *et al.*, 1953). Exhaustive efforts to culture the causative agent by Fujino *et al.* in the early 1950s were eventually rewarded when a

combination of animal passaging and plating on blood agar yielded the isolation of a previously uncharacterised rod-shaped, mono-flagellated bacterium. Fujino named the organism *Pasteurella parahaemolytica* after observing that the organism failed to react with *V. cholerae* anti-sera. However, further characterisation following a second major outbreak in the 1950's resulted in the observation of halophilic properties, a trait which is typical of *Vibrio spp* (Takikawa, 1958). As such, in 1963 the causative agent of the shirasu food poisonings was given its current designation *Vibrio parahaemolyticus* (Sakazaki *et al.*, 1963).

Further characterisation of this "pathogenic halophilic bacterium" identified a strict requirement for sodium, with growth being detected from 0.1 M to 1.2 M and optimum growth conditions of 0.5 M or 3% (w/v) NaCl (Sakazaki *et al.*, 1963). The bacterium was found to be extremely sensitive to hypo-osmotic shock and was readily inactivated by incubation in distilled water for 1 to 4 min (Lee, 1972). Microscopic examination identified that *V. parahaemolyticus* cells possessed a single polar, sheathed flagellum when grown in liquid culture and were peritrichously flagellated following growth on solid media (Yabuuchi *et al.*, 1974). *V. parahaemolyticus* was found to exhibit a remarkably rapid growth rate with a generation time of 8 to 9 min being observed for many strains (Katoh, 1965). It was observed that the vast majority of clinical isolates (91.8%, n = 436) were positive for haemolysis on Wagatsuma blood agar, while very few haemolytic isolates were detected in environmental samples (0.51%, n = 396) (Miyamoto *et al.*, 1969). As such, beta haemolysis on blood agar (termed Kanagawa phenomenon (KP) by Miyamoto *et al.* [1969]) was considered a key indicator of *V. parahaemolyticus* virulence and is still used as a marker for pathogenic potential to this day.

In immunocompetent individuals the clinical manifestations of *V. parahaemolyticus* infection are mild, self-limiting gastroenteritis accompanied by abdominal cramps and watery

diarrhoea which can last for 2 to 3 days (Nair *et al.*, 2007; Honda *et al.*, 2008; Daniels and Shafaie, 2000). In some cases however, severe inflammatory diarrhoea occurs, with major destruction of gastric and intestinal epithelia, and blood being shed in the stools (Honda *et al.*, 2008). Such cases can occur due to underlying health conditions and may result in septicaemia and subsequent death of infected individuals. The most common route of infection is through the consumption of raw or undercooked seafood. The vast majority (88%) of reported cases of *V. parahaemolyticus* infection in the United States between 1988 and 1997 were due to the consumption of raw oysters (Daniels *et al.*, 2000). *V. parahaemolyticus* has also been reported to cause wound infections which can lead to necrotising fasciitis, a severe skin infection which results in extensive tissue damage (Ralph and Currie, 2007).

V. parahaemolyticus has long been recognised as the leading cause of foodborne gastroenteritis in Japan (Lee *et al.*, 2001). Advances in serotyping, molecular analysis and phylogenetics have allowed scientists to monitor the global spread of *V. parahaemolyticus* and predict which areas present the highest risk of severe illness due to *V. parahaemolyticus* outbreaks. Prior to 1995, a variety of *V. parahaemolyticus* serotypes were associated with cases of gastroenteritis and no globally relevant serovariants predominated (Boyd *et al.*, 2008). Extensive monitoring of *V. parahaemolyticus* infection in Calcutta, India identified the emergence of a new serovariant of *V. parahaemolyticus* in February 1996, which was highly virulent and caused more severe outbreaks than those observed in previous years (Okuda *et al.*, 1997). PCR detection of haemolysin genes identified the presence of the thermostable direct haemolysin (TDH), which is responsible for the Kanagawa phenomenon, but not the thermostable direct haemolysin-related haemolysin (TRH), in all of the highly virulent O3:K6 serotypes (Okuda *et al.*, 1997). Further molecular characterisation of this hypervirulent clonal variant has identified the presence of a virulence gene regulator *toxR* and the presence of two

distinct type three secretion systems (TTSS) and as such, the presence of these genetic markers is now widely used for confirmation of the pandemic status of *V. parahaemolyticus* outbreaks. The prevalence of the O3:K6 clone has since reached pandemic status, with major outbreaks occurring in South America, Africa, Europe and the United States of America (Nair *et al.*, 2007; Fig 1.2).

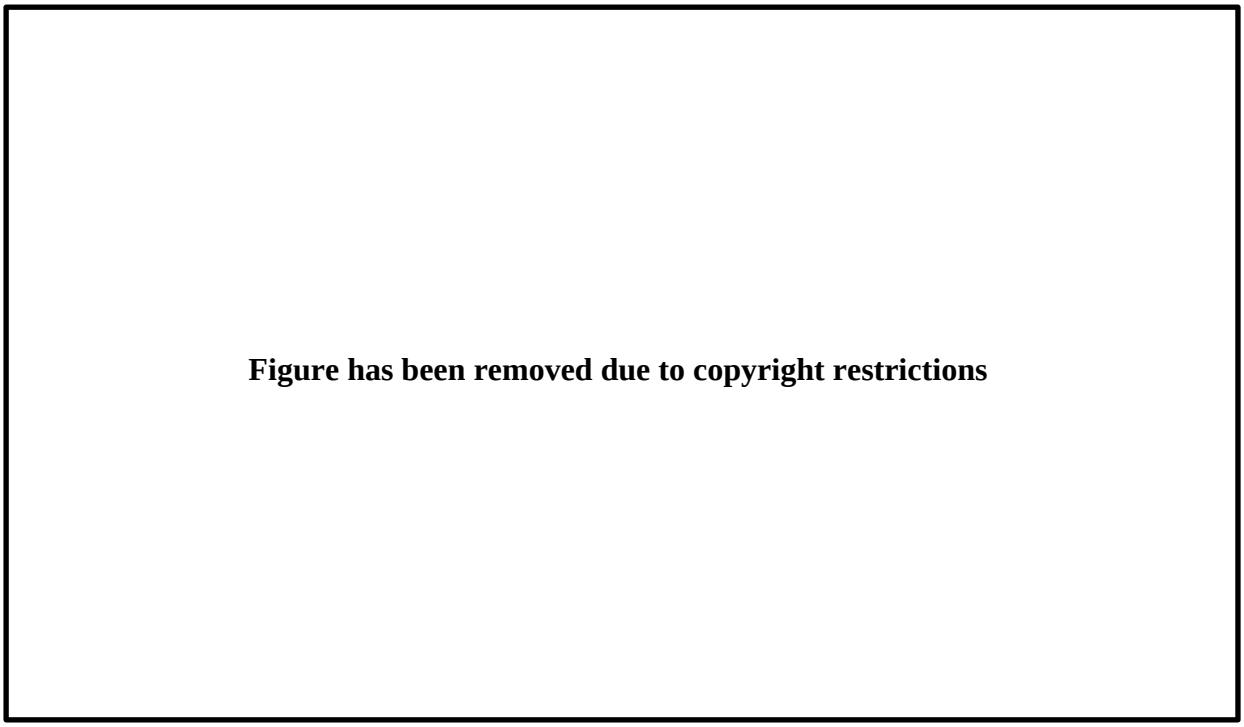

Fig 1.2 Global dissemination of the O3:K6 pandemic clone of *V. parahaemolyticus*. Figure adapted from Nair *et al.* (2007).

An example of the pathogenic and epidemic potential of this globally disseminated pandemic clone was observed during an outbreak of *V. parahaemolyticus* infection in Chile, 2005. 3,725 cases of *V. parahaemolyticus*-associated diarrhoea were detected between January and April in Puerto Monte, a large city which is the source of approximately 75% of Chilean seafood (Cabello *et al.*, 2007). As a result of the distribution of contaminated seafood products from Puerto Monte, a total of 10,783 cases of *V. parahaemolyticus* induced diarrhoea were observed, making the incident the largest documented outbreak of *V. parahaemolyticus* gastroenteritis (Cabello *et al.*, 2007). Importantly, of 60 stool samples

analysed during the outbreak, all contained O3:K6, *tdh+*, *trh-*, *toxR+ V. parahaemolyticus*, and as such the outbreak was attributed to the pandemic clone (Cabello *et al.*, 2007). Large outbreaks due to the pandemic clone have also been reported in Texas, USA in 1999; Mozambique in 2004; La Coruña, Spain in 2004; Lima, Peru in 1998 and Cambodia in 2012 (De Paola *et al.*, 2000; Ansaruzzaman *et al.*, 2005; Martinez-Urtaza *et al.*, 2005; Gil *et al.*, 2007; Vandy *et al.*, 2012). *V. parahaemolyticus* is now regarded as the leading cause of seafood-related gastroenteritis in the USA (Mc Laughlin *et al.*, 2005).

Four way whole genome BLAST analysis by Boyd *et al.* (2008) identified 24 genomic regions of at least 10 kb which were found in the pandemic O3:K6 clone RIMD2210633 but not in *V. cholerae*, *V. fischeri* or *V. vulnificus*. Interestingly, comparison of *V. parahaemolyticus* strain RIMD2210633 (isolated in 1996) with strain AQ3810, an O3:K6 serotype isolated in 1983, yielded the observation that 8 of the 24 unique regions were specific to the O3:K6 serotype from post-1995 (Boyd *et al.*, 2008). In 2011, an additional pre-pandemic O3:K6 strain and 3 additional post-pandemic clones (2 O3:K6 and 1 O4:K68) were sequenced. This study identified that 7 of the 8 loci identified by Boyd *et al.* (2008) were indeed unique to post 1996 clinical isolates of *V. parahaemolyticus* (Chen *et al.*, 2011). These 7 regions contained genomic islands and indicate that genomic flux via horizontal transfer likely contributed to the increased virulence associated with O3:K6 isolates which arose in the late 1990s (Boyd *et al.*, 2008; Chen *et al.*, 2011).

1.3 *V. parahaemolyticus* virulence factors.

The ability of the O3:K6 pandemic clone of *V. parahaemolyticus* to cause widespread, severe gastro-intestinal disease has been of great interest to microbiologists in recent years. While the involvement of TDH in the virulence of *V. parahaemolyticus* had been recognised since

the identification of the Kanagawa phenomenon in 1969, relatively little was known about the other virulence factors possessed by this enteric pathogen. Indeed, a variety of TDH-negative, KP-negative *V. parahaemolyticus* strains were isolated from patients suffering from gastroenteritis, indicating the involvement of alternative virulence factors in *V. parahaemolyticus* pathogenicity (Nishibuchi *et al.*, 1992). The sequencing of an isolate from the O3:K6 clonal serotype, RIMD2210633, by Makino *et al.* in 2003 revealed a number of insights into the pathogenesis of the organism at a molecular level and inspired a wealth of research over subsequent years.

1.3.1 Thermostable direct hemolysin (TDH).

TDH is a member of the pore-forming bacterial cytolysin family which includes the α haemolysin of *E. coli*, the *Actinobacillus* haemolysin, the adenylate cyclase-haemolysin bifunctional protein of *Bordetella pertussis* and the *Serratia marcescens* Hly haemolysin (Braun and Focareta, 1991). The TDH produced by *V. parahaemolyticus* was first documented as a key virulence factor of the pathogen when Miyamoto *et al.* (1969) recognised a strict correlation between KP-positive characteristics and isolation from clinical sources. Environmental samples by contrast were found to have extremely low rates of haemolytic activity, indicating the lack of haemolysin (Miyamoto *et al.*, 1969). Miyamoto *et al.* (1980) successfully purified the haemolysin from culture supernatants enabling further characterisation. The purified toxin was found to disrupt intestinal microvilli of infected mice, induce fluid secretion from ligated rabit ileal loops (enterotoxicity) and had a fifty percent lethal dose of 1.4 µg when injected intravenously into mice (Miyamoto *et al.*, 1980).

Recent structural analyses have demonstrated that the protein forms a tetramer ring in solution with a mass of 70 kDa and a central pore 23 Å in diameter (Hamada *et al.*, 2007;

Yanagihara *et al.*, 2010). KP-positive haemolytic strains of *V. parahaemolyticus* were found by Nishibuchi and Kaper (1990) to possess two allelic variants of TDH which possessed 97.2% amino acid identity to one another. These findings were confirmed upon sequencing of the *V. parahaemolyticus* genome, when the TDH1 and TDH2 alleles were detected in a large pathogenicity island on chromosome 2 (Makino *et al.*, 2003).

A number of *in vivo* and *in vitro* studies have demonstrated a role for TDH in the pathogenesis of *V. parahaemolyticus*. Cardiotoxicity was observed upon intravenous injection of purified TDH into rats, with disruption of heart rhythm and eventual cardiac arrest (Honda *et al.*, 1976). Honda *et al.* (1976) also observed toxicity against cultured murine cardiac tissue further highlighting the importance of cardiotoxicity in the lethal effects of TDH observed in rodents. Hiyoshi *et al.* (2010) identified a significant role for TDH in cytotoxicity towards RAW 264.7 murine macrophages, an effect which could be abrogated by preincubation with monoclonal antibodies directed against TDH.

While cardiotoxic, cytotoxic and enterotoxic effects have been observed for TDH with many infection models, the species and tissue specificities of these effects remain unclear. Hiyoshi *et al.* (2010) observed a distinct lack of involvement for TDH in cytotoxicity towards Caco-2 or HeLa human epithelial cells, a result which is directly in contrast to that observed with murine macrophages. Ritchie *et al.* (2012) carried out *in vivo* infection of rabbits with *V. parahaemolyticus* and isogenic mutants carrying deletions inactivating TDH. TDH was found to play no role in the induction of diarrhoea or lethality in infected rabbits. Surprisingly, deletion mutants lacking TDH showed increased colonisation of intestinal tissues compared with the wild type (Ritchie *et al.*, 2012). These inconsistencies cast doubt over the long-standing hypothesis of an integral role for TDH in *V. parahaemolyticus* pathogenicity. The extensive and successful use of haemolysis/Kanagawa phenomenon or PCR detection of *tdh*

as a marker of virulence may be attributable to the fact that the *tdh* genes are located in a pathogenicity island which harbours multiple alternative virulence factors. As such, a specific role for TDH in human pathogenesis at a molecular level remains unclear.

1.3.2 Type Three Secretion Systems (TTSS).

1.3.2a TTSS identification, structure and function.

Perhaps the most striking observation from the sequencing of the *V. parahaemolyticus* genome was the detection of two Type Three Secretion Systems (TTSS), one located on each chromosome, a finding which indicated a molecular mechanism of virulence distinct from that of *Vibrio cholerae* and shifted focus from predominantly TDH-centred research to molecular characterisation of *V. parahaemolyticus* TTSS (Makino *et al.*, 2003). The identification of the TTSS finally offered a clue as to the alternative virulence factors which were predicted to play a role in TDH independent cytotoxicity and enterotoxicity. The significance of TTSS in the pathogenesis of *V. parahaemolyticus* has grown with advances in the understanding of the interactions between TTSS effector proteins and host cells, such that TTSS are now regarded as the most important virulence factors of *V. parahaemolyticus*. Fig 1.3 below illustrates the annotated genome sequence of both *V. parahaemolyticus* chromosomes and the positions of the genes encoding TTSS1 and TTSS2.

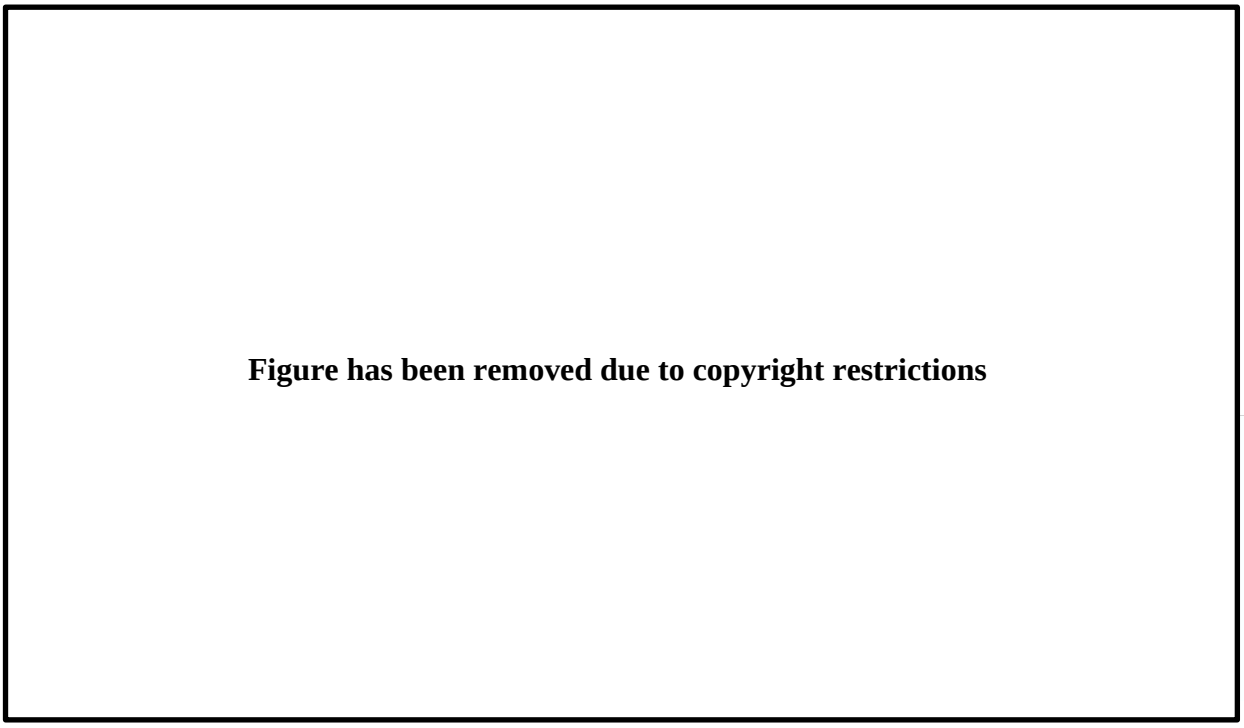

Fig 1.3 Chromosomal location of both type three secretion systems in *V. parahaemolyticus*. Figure adapted from Makino *et al.* (2003).

Bacterial TTSS have been referred to as nanomachines, capable of efficiently delivering effector proteins into host cells in order to hijack host cell signalling, thereby manipulating a variety of host cell functions. They have been identified in many gram negative bacterial species such as: *Burkholderia cepacia*, *Chlamydia trachomatis*, *Salmonella enterica*, *Pseudomonas aeruginosa*, *Shigella flexneri* and *Yersinia enterocolitica* (Mota and Cornelis, 2005). TTSS may be employed to manipulate processes such as the invasion of non-phagocytic cells, inhibition of uptake by phagocytes, inhibition of inflammation and the induction of apoptosis (Cornelis, 2006). Phylogenetic analysis and structural characterisation have identified commonalities between TTSS injectisomes and the secretory system associated with the bacterial flagellum (Cornelis, 2006). TTSS have been shown to be ancient in origin and appear to have evolved independently of the bacterial strains which possess them, indicating acquisition *via* horizontal transfer (Gophna *et al.*, 2003). Further evidence supporting the evolution of TTSS independently of the host is provided by the fact that *V.*

parahaemolyticus TTSS2 is encoded on a pathogenicity island with significantly different GC content to the genome GC content of the organism (Makino *et al.*, 2003). It should also be noted that TTSS1 belongs to the Ysc family of TTSS (also found in *Yersinia enterocolitica, Yersinia pestis* and *Aeromonas salmonicida*) whereas TTSS2 belongs to the Hrp1 family of TTSS (also found in *Pseudomonas syringae* and *Erwinia amylovora*) (Troisfontaines and Cornelis, 2005). While the secretion apparatus and needle complex are highly conserved within each family, the effector proteins responsible for modulating host cell responses are highly variable, thereby yielding widely diverse functionality even within each family (Troisfontaines and Cornelis, 2005).

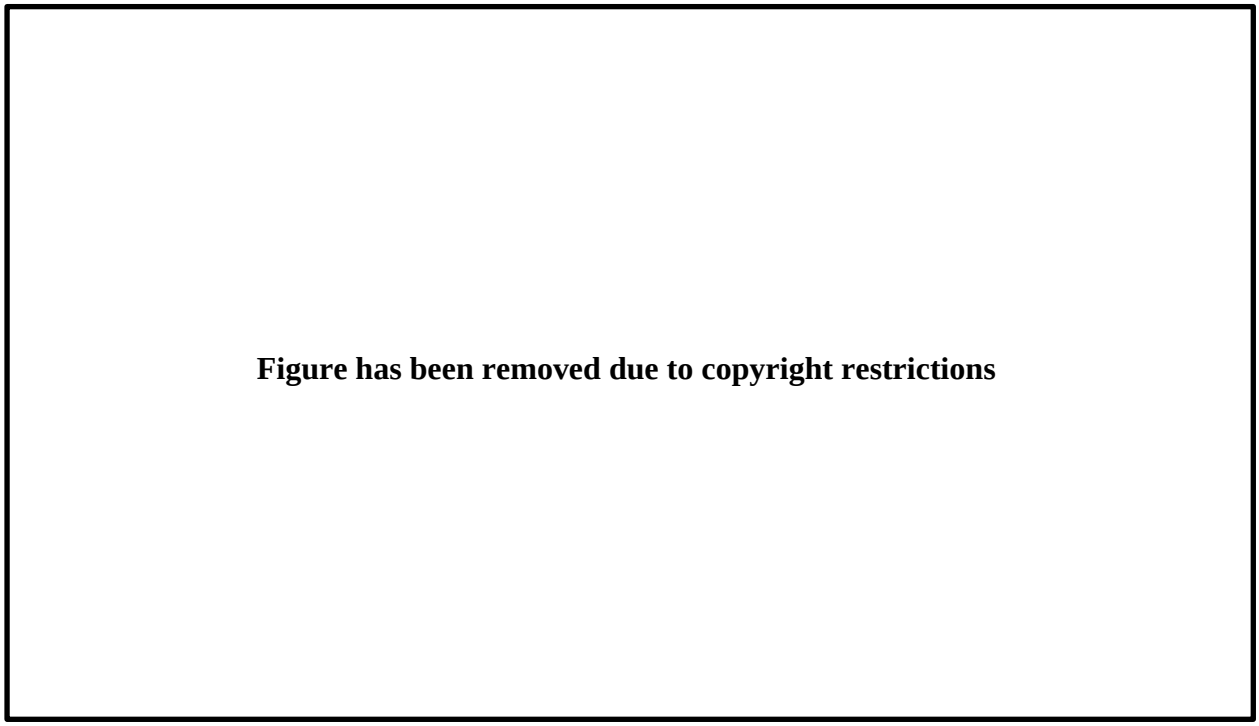

Fig 1.4 Structure of the bacterial TTSS. (**A**) Negatively stained transmission electron micrograph of TTSS needle complexes (indicated by arrows) protruding from the surface of *Y. enterocolitica*. Figure adapted from Troisfontaines and Cornelis (2005). (**B**) Schematic illustrating the structure of the membrane-associated secretion apparatus, secretory needle and translocation apparatus of the *Y. enterocolitica* TTSS. Figure adapted from Cornelis (2006). (**C**) Schematic illustrating the binding of a TTSS to a host cell via the translocation apparatus and subsequent secretion of effector proteins from the bacterial cytosol. Figure adapted from Cornelis (2006).

Fig 1.4 illustrates the structure and functionality of the *Y. enterocolitica* TTSS which has been characterised extensively. The secretion system is composed of a membrane-bound secretion apparatus, containing an ATPase, secretins and ring proteins which closely resemble the membrane structures associated with the bacterial flagellum (Cornelis, 2006). The membrane-associated components of the TTSS secrete proteinaceous needle subunits which assemble in a helical manner to form a tubular needle 60 nm in length, with an external diameter of 7 nm and an internal diameter of approximately 25 Å. The tip of the TTSS contains a translocation apparatus which inserts into the host cell membrane and forms a translocation pore, allowing the export of effector proteins from the bacterial cytosol into the host cell via the tubular needle complex (Cornelis, 2006). As the needle complex and membrane components of bacterial TTSS are highly conserved, one can expect the TTSS of *Y. enterocolitica* to closely resemble those produced by *V. parahaemolyticus*. Mutants of *Salmonella* and *Shigella* which possess inactivating deletions of TTSS ATPases lack needle complexes and as such it is believed that the ATPase (VscN in *V. parahaemolyticus*) drives the export of all non-membrane TTSS components, including the secretion of effector proteins (Kubori *et al.*, 2000; Tamano *et al.*, 2000). For this reason, Δ*vscN*1 (TTSS1 ATPase) and Δ*vscN*2 (TTSS2 ATPase) mutants have been used in many publications, and in this study, in order to inactivate each TTSS and subsequently analyse their respective involvement in *V. parahaemolyticus* pathogenesis (Park *et al.*, 2004; Matlawska-Wasowska *et al.*, 2010; Hiyoshi *et al.*, 2010; Ritchie *et al.*, 2012).

Shortly after the identification of *V. parahaemolyticus* TTSS, it was discovered that TTSS1 and TTSS2 played distinct roles in the pathogenesis of *V. parahaemolyticus*. TTSS1 was found to play a role in cytotoxicity, as observed by the lysis of cultured HeLa cells, while TTSS2 displayed enterotoxic effects, with blunting of villi and fluid secretion being induced in infected rabbit ileal loops (Park *et al.*, 2004). In subsequent years, research has been

focused on identifying and characterising the individual effector proteins responsible for these effects and assessing their relevance in *V. parahaemolyticus* infection. Table 1.1 contains a list of the currently recognised effector proteins from *V. parahaemolyticus* together with any biological activities which have been described and the effect of these activities on host cell behaviour.

1.3.2b TTSS1 effector proteins.

Table has been removed due to copyright restrictions

VopQ.

V. parahaemolyticus TTSS1 has been shown to exhibit cytotoxicity towards a variety of cell types including HeLa, Caco-2, RAW 264.7 macrophages and 3T3 fibroblasts (Park *et al.*,

2004; Burdette *et al.*, 2009; Hiyoshi *et al.*, 2010; Matlawska-Wasowska *et al.*, 2010; Krachler *et al.*, 2011). TTSS1 has also been shown to play a role in the induction of inflammatory chemokines and in the lethality of *V. parahaemolyticus* towards infected mice (Matlawska-Wasowska *et al.*, 2010; Shimohata *et al.*, 2011; Hiyoshi *et al.*, 2010). The principal effector protein involved in the lytic effects of *V. parahaemolyticus* was found by Ono *et al.* (2006) to be VopQ, encoded by *VP1680*. The mechanism by which VopQ induced the lysis of infected cells was described in detail by Burdette *et al.* (2009) who observed VopQ-dependent activation of microtubule-associated light chain 3 (LC3), a marker of autophagy. Δ*vopQ* mutants displayed a greatly reduced level of HeLa cell lysis and were unable to catalyse the conversion of LC3I to the active LC3II isoform, illustrating the central role of VopQ in *V. parahaemolyticus*-mediated autophagy. Burdette *et al.*, (2009b) speculated that the induction of autophagy by *V. parahaemolyticus* may provide a means of sequestration of cellular material in order to facilitate rapid *in vivo* growth.

VopS.

Yarbrough *et al.* (2009) identified a novel post-translational modification carried out by VopS when transfected into HeLa cells. It was observed that the Rho GTPases, RhoA, Rac1 and Cdc42, were modified by the addition of adenosine monophosphate to a conserved threonine residue (AMPylation), resulting in the inhibition of Rho GTPase signalling and collapse of the actin cytoskeleton. As such, the characteristic cell rounding associated with *V. parahaemolyticus* infection was attributed to VopS activity.

VPA0450.

VPA0450 was originally identified together with VopS and VopQ as a TTSS1-secreted protein, using 2D gel electrophoresis (Ono *et al.*, 2006). Broberg *et al.* (2010) identified that *V. parahaemolyticus* strains expressing VPA0450 displayed more rapid rounding and lysis of

HeLa cells than Δ*VPA0450* strains. It was also observed that strains possessing a functional TTSS1, but not TDH or TTSS2, caused the formation of protruding blebs in the host cell membrane – a feature which was not observed upon deletion of VPA0450 in the same background. The involvement of VPA0450 in the induction of membrane blebbing was confirmed by transfection of HeLa cells with VPA0450. Broberg *et al.* (2010) identified that hydrolysis of the D5 phosphate from the inositol ring of the membrane-associated lipid phosphoinositol (4,5) bisphosphate ($PI[4,5]P_2$) was responsible for this effect. PI(4,5)P2 plays a critical role in the regulation of cell signalling events at the plasma membrane (Kraub and Haucke, 2007). As such, Broberg *et al.* (2010) hypothesised that VPA0450 may play a complementary role with VopS and VopQ in host cell rounding and lysis by destabilising plasma membrane-cytoskeleton dynamics at late stages of infection. Interestingly, VPA0450 is the only chromosome 2-encoded TTSS1 effector protein identified to date.

VopR.

In silico screening of the *Bordetella bronchiseptica* genome for potential TTSS effector chaperones and subsequent identification of *V. parahaemolyticus* homologues confirmed the prediction of VopS, VopQ and VPA0450 as putative effector proteins (Panina *et al.*, 2005). A fourth potential effector was also identified in the TTSS1 locus, adjacent to VopS and VopQ and was hence referred to as VopR. A role for VopR in the pathogenesis of *V. parahaemolyticus* has yet to be established.

1.3.2c TTSS2 effectors.

While TTSS1 is recognised as conferring cytotoxicity of *V. parahaemolyticus* against many different cell lines, some studies involving *in vivo* infections have found that TTSS1 is not required for pathogenesis (Ritchie *et al.*, 2012). Indeed TTSS1 is present in all strains of *V. parahaemolyticus*, while TTSS2 is predominantly found in clinical isolates from patients

suffering gastrointestinal illness due to *V. parahaemolyticus* infection (Park *et al.*, 2004). The GC content of the TTSS1 locus was found to closely correlate with the genome GC content of *V. parahaemolyticus*, indicating ancestral origin, while the GC content of the pathogenicity island upon which TTSS2 is located was found to be significantly different to the genome GC content (Makino *et al.*, 2003). As such, TTSS2 is an example of a virulence factor which was recently acquired in the evolution of the pathogen. As Boyd *et al.* (2008) illustrated that recent genomic flux *via* horizontal transfer was responsible for the increased virulence associated with the pandemic clone of *V. parahaemolyticus* – the TTSS2 pathogenicity island represents a classical example of this phenomenon. Early characterisation of TTSS2 identified enterotoxic effects on rabbit intestinal tissue, with TTSS2 inducing fluid secretion from ligated ileal loops and causing pronounced blunting of the intestinal villi (Park *et al.*, 2004). Until recently, the effector proteins responsible for these enterotoxic phenotypes and their mechanisms of action have remained elusive.

VopA.

VopA was first predicted as an effector protein based upon co-localisation with TTSS2 and 55% amino acid identity the *Yersinia* effector protein YopJ (Makino *et al.*, 2003). Park *et al.* (2004) identified that the effector protein was secreted in a TTSS2-dependent manner. Further characterisation of VopA revealed that the protein was capable of inhibiting the MAPK cell signalling pathway, a central pathway in regulation of host cell survival during the response to infection (Trosky *et al.*, 2004). It was also observed that expression of VopA in yeast resulted in inhibition of growth, a feature consistent with the related *Yersinia* effector YopJ. YopJ has been shown to function as an acetyltransferase which binds to and acetylates the MAPK kinase (MKK) superfamily, thereby preventing the subsequent activation of MAPK and NF-κB (Orth *et al.*, 1999). Trosky *et al.* (2007) identified that VopA was capable

of inhibiting MAPK signalling by a novel mechanism involving acetylation of a conserved lysine residue found in the catalytic domain of MKK proteins. This had the result of inhibiting MAPK activation in mammalian cells, but unlike YopJ, VopA did not affect the activation of NF-κB.

VopT.

In conjunction with the TTSS1 effector protein VopS, TTSS2 effectors VopT and VopC were also found to target the low molecular weight G proteins which are involved in the regulation of cell proliferation, vesicular trafficking and cytoskeletal homeostasis. VopT was shown by Kodama *et al.* (2007) to post-translationally modify the Ras GTPase by ADP ribosylation. Expression of VopT resulted in inhibition of growth in yeast and Δ*vopT* mutants were found to have decreased TTSS2-mediated cytotoxicity towards Caco-2. It is important to note that Kodama *et al.* (2007) used mutant backgrounds which were deficient in TTSS1 in order to assess TTSS2-mediated cytotoxicity. The inactivation of TTSS1 allowed for co-incubations of up to 6 h before reaching 100% lysis of host cells, thereby allowing analysis of TTSS2 factors which may play a role in cytotoxicity at later stages of infection. Kodama *et al.* (2007) speculated that ADP-ribosylation of Ras may have resulted in disruption of Ras-mediated cell signalling, ultimately leading to cell death. However the precise mechanism by which Ras modification influences *V. parahaemolyticus* cytotoxicity has yet to be determined.

VopC.

Activation of Rho family GTPases has been described as a means for bacteria to induce cellular uptake in non-phagocytic cells (Etienne-Manneville and Hall, 2002; Hardt *et al.*, 1998; Cossart and Sansonetti, 2004; Kerr and Teasedale, 2009). Zhang *et al.* (2012) identified that TTSS2 was required for the invasion of HeLa cells by *V. parahaemolyticus*. It was observed that strains lacking TTSS1, but possessing a functional TTSS2 were capable of

invading at a similar efficiency to *Shigella*, while inactivation of both secretion systems resulted in a non-invasive phenotype. Zhang *et al.* (2012) further characterised this invasive phenotype by determining that the effector protein VopC, which was secreted by TTSS2 was specifically required for invasion and that invasion was mediated by constitutive activation of the Rho GTPases Rac1 and Cdc42. The activation of Rac1 and Cdc42 was dependent on the cysteine^{220} residue of VopC and resulted in modifications in the actin cytoskeleton of infected HeLa cells (Zhang *et al.*, 2012). These results indicate that VopC functions as an invasin in a similar manner to the *Salmonella* TTSS effector protein SopE by modulating actin dynamics through the activation of Rac1 and Cdc42 (Friebel *et al.*, 2001).

VopL.

The TTSS2 effector proteins VopV and VopL have also been associated with manipulations of the cytoskeleton of host cells. Maintenance of correct cell shape and regulation of the cell cycle require a constant turnover of actin, with dynamic conversion between globular and filamentous forms (F-actin). The formation of actin filaments is stimulated by nucleation events which are brought about through the recruitment of globular actin monomers by proteins such as formins, SPIRE and the Arp2/3 complex (Quinlan and Kerkhoff, 2008). The formation of a trimeric nucleus of globular actin is a critical step in the stimulation of actin filament extension. Nucleation *via* the Arp2/3 complex results in the formation of branched filaments at a 70° angle to existing filaments, while formins and SPIRE stimulate the formation of straight filaments (Quinlan *et al.*, 2005). The VopL effector protein secreted by TTSS2 presents an intriguing example of bacterial host mimicry. VopL possesses 3 proline rich motifs and 3 WH2 domains, both of which are found in eukaryotic proteins which carry out actin nucleation (Liverman *et al.*, 2007). Like its eukaryotic counterparts SPIRE and formin, VopL can bind and nucleate globular actin *in vitro*, independent of eukaryotic factors

(Liverman *et al.*, 2007). *In vivo* transfection of HeLa cells led to more rapid extension of actin fibres, at lower concentrations than that observed for the eukaryotic nucleators SPIRE and Arp2/3, indicating that VopL is a more potent activator of actin assembly than host proteins, thereby enabling *V. parahaemolyticus* to override actin homeostasis in infected cells (Liverman *et al.*, 2007). Modulation of actin dynamics by a *V. cholerae* effector protein VopF which shares 57% amino acid identity with VopL has been shown to play a role in the colonisation of the small intestine during *in vivo* infections of mice (Tam *et al.*, 2007). Establishment of the significance of VopL activity in *V. parahaemolyticus* infection will yield new insights into the importance of actin remodelling during *V. parahaemolyticus* pathogenesis.

VopV.

While research involving the TTSS2 effector proteins VopC, VopT, VopA and VopL has provided fresh insights into the pathogenesis of *V. parahaemolyticus*, until recently the effector protein responsible for the TTSS2-mediated enterotoxic effects (fluid accumulation and villus blunting) of the organism had not been identified. Like VopL, VopV was found by Hiyoshi *et al.* (2011) to possess multiple F-actin binding domains. Transfection of HeLa cells with GFP-tagged VopV resulted in direct binding of the effector protein to F-actin (Hiyoshi *et al.*, 2011). VopV also disrupted actin dynamics in transfected host cells with bundling of F-actin into concentrated foci being observed (Hiyoshi *et al.*, 2011). Mutants lacking VopV did not cause blunting of rabbit ileal villi upon infection and deletion of any VopV domains required for actin binding resulted in an inability to induce fluid accumulation from ligated ileal loops (Hiyoshi *et al.*, 2011). These results demonstrated for the first time that actin binding of VopV was responsible for the enterotoxic effects associated with TTSS2. The mechanism by which F-actin binding by VopV leads to enterotoxicity is not yet understood

and as such, research in this area will prove invaluable in determining the mechanism by which *V. parahaemolyticus* induces secretory diarrhoea in infected individuals.

1.3.2d TTSS regulation.

As observed by the examples above, *V. parahaemolyticus* TTSS are capable of manipulating a remarkably diverse range of host cell processes by virtue of the secretion of multiple effectors, each having distinct activities, during infection. As TTSS1 effectors are associated with biological activities distinct from those of TTSS2, one can imagine how differential regulation of TTSS activity would influence the effect of *V. parahaemolyticus* activity on host cell response.

The TTSS1 locus of *V. parahaemolyticus* was found to encode two putative transcriptional regulators, ExsA and ExsD with 40% and 30% amino acid identity respectively, to ExsA and ExsD from *P. aeruginosa* (Zhou *et al.*, 2008). ExsA was found to function as a transcriptional activator of *P. aeruginosa* TTSS genes at low calcium concentrations, while ExsD was found to function as an inhibitor of the same subset of genes when overexpressed (Yahr and Frank, 1994; McCaw *et al.*, 2002). The activities of ExsA and ExsD have been shown in both *P. aeruginosa* and *V. parahaemolyticus* to depend on the anti-anti-activator ExsC and its cognate chaperone ExsE. The currently recognised model for ExsACDE regulation of TTSS genes is summarised in Fig 1.5.

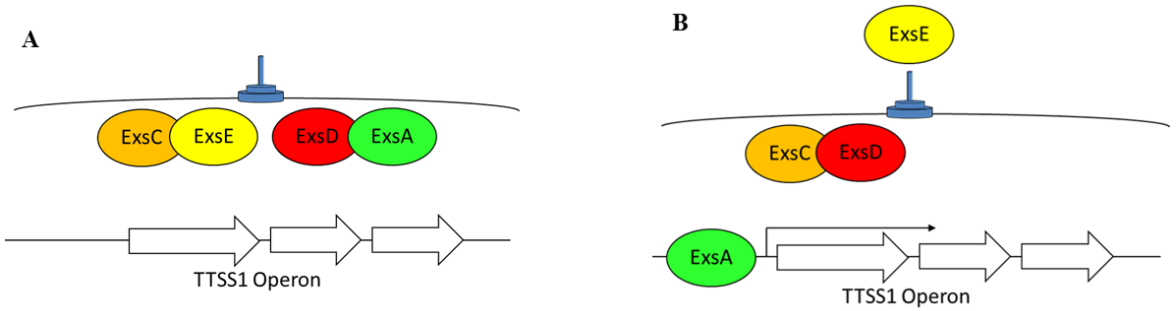

Fig 1.5 ExsACDE regulation of the TTSS1 regulon. (**A**) Non-inducing conditions, transcription is repressed. (**B**) Inducing conditions, transcription is derepressed.

In conditions of high Ca^{2+}, the *V. parahaemolyticus* TTSS secretion channel remains closed, the anti-activator ExsD remains bound to ExsA, thereby repressing transcription, while the anti-anti-activator ExsC remains bound to its chaperone ExsE (Fig 1.5A; Kodama *et al.*, 2010). When low Ca^{2+} concentrations are encountered, the TTSS secretion channel is opened, allowing the export of ExsE. ExsC then sequesters the anti-activator ExsD, freeing ExsA to bind to upstream regulatory elements of TTSS1 genes, enhancing transcription levels (Fig 1.5B; Kodama *et al.*, 2010).

In addition to the ExsACDE regulatory cascade, TTSS1 genes were also shown to be controlled by the transcriptional regulator H-NS (histone-like nucleoid structuring protein) (Kodama *et al.*, 2010). This protein is one of the most abundant DNA-associated proteins in the bacterial cell and plays a central role in the regulation of gene expression by manipulating DNA topology (Hulton *et al.*, 1990). H-NS was shown to inhibit the expression of many virulence genes within the ToxR regulon of *V. cholerae* (Nye *et al.*, 2000). As such Kodama *et al.* (2010) hypothesised that H-NS regulation may play a role in TTSS1 gene expression. Indeed Kodama *et al.* (2010) observed that Δ*hns* mutants displayed a pronounced increase in TTSS1 activity. Further to this, Kodama *et al.* (2010) identified that the expression of H-NS

was inversely proportional to the promoter activity of *exsA*, thereby indicating that H-NS could manipulate TTSS1 gene expression by regulating the transcription of *exsA*.

Kodama *et al.* (2010b) identified two transcriptional regulators, VtrA and VtrB, which were encoded within the same pathogenicity island as TTSS2. It was found that VtrA controlled the transcription of *vtrB* and that VtrB in turn induced the transcription of a variety of TTSS2-related proteins including a variety of structural components and the effector genes *vopC*, *vopT*, *vopV*, *vopL* and *vopA*. TDH genes were also significantly affected by deletion of *vtrA* or *vtrB*, with *tdhA* exhibiting 11-fold higher transcription in the wild type than the Δ*vtrB* mutant and *tdhS* exhibiting 9-fold higher transcription (Kodama *et al.*, 2010). The effects of the VtrAB regulatory system were found to be TTSS2-specific and had no effect on expression of TTSS1 genes. Further to these findings, Gotoh *et al.* (2011) identified that crude bile could serve as an effective inducer of the VtrAB regulon by activating VtrA-mediated transcription of *vtrB*. It was found that addition of cholestyramine (a bile salt sequestrant) abrogated VtrB activation and subsequent expression of TDH and TTSS2 proteins. Gotoh *et al.* (2011) identified that purified bile salts taurodeoxycholate and glycodeoxycholate were potent activators of VtrB while many other bile salts proved ineffective. These results indicated the first host-derived inducer for *V. parahaemolyticus* pathogenicity, thereby revealing an intriguing sensory mechanism which allows *V. parahaemolyticus* to adapt its cellular processes and cause infection in human hosts.

In conclusion, the TTSS of *V. parahaemolyticus* provide an innovative means of facilitating the fine regulation of host cell behaviour during gastrointestinal infection. The possession of two distinct secretion systems with differential regulatory mechanisms allows the organism to adapt its virulence in response to environmental conditions. Although reductionist in its approach, analysis of the discrete roles of individual effector proteins has yielded a variety of

fascinating insights into the complex array of host cell manipulations which *V. parahaemolyticus* is capable of inducing in infected cells. Alterations in cytoskeletal dynamics, membrane integrity and signal transduction facilitate a model of infection which enables persistence of *V. parahaemolyticus* through the colonisation of tissues, sequestration of nutrients, invasion of host cells and manipulation of various components of the innate immune system. While molecular analyses have proved useful in establishing an understanding of the roles of *V. parahaemolyticus* effector proteins in the process of pathogenesis, significant gaps exist in current knowledge of tissue specificity and species specificity of the secretion systems and their respective effector proteins. Murine infections have established a critical role for TTSS1 and TDH in lethality, while infections of rabbits identified TTSS2 as the principal virulence mechanism with TTSS1 and TDH not playing significant roles in the induction of diarrhoea or lethality (Hiyoshi *et al.*, 2010; Ritchie *et al.*, 2012). As such, further research using such *in vivo* infection models is warranted in order to develop an understanding of the importance of each TTSS-associated biological activity in the overall induction of human disease by *V. parahaemolyticus*.

1.4 Bacterial adherence mechanisms.

Both commensal and pathogenic bacteria share a common requirement for adherence to host tissues. The commensal microflora of the gastrointestinal tract establish a highly complex, dense biofilm which serves to prevent colonisation by pathogenic species, while facilitating the growth of commensal organisms in a nutrient rich environment. This symbiotic relationship is critical for gastrointestinal function and plays a vital role in innate immunity. In order to establish a successful infection, pathogens such as *V. parahaemolyticus* must compete with commensal species for access to underlying tissues and host cell receptors. The

process by which bacterial pathogens colonise the intestinal epithelium may be summarised as follows:

1. Initial attachment. Bacterial adhesins bind to molecules on the surface of host epithelia, thereby anchoring the pathogen to the host cell. Adhesins involved at this stage are typically filamentous (pili) and interactions may occur between extracellular matrix components, mucus, commensal bacteria or host cell receptors.

2. Intimate attachment. Once anchored on the host cell, further interactions occur between the pathogen and the host. A number of adhesins bind to distinct receptors on the host cell enhancing the efficiency of binding and increasing the force required for removal of the pathogen. Pili may retract, drawing attached bacteria closer to the host cell (Pujol *et al.*, 1999). As bacteria multiply on the host epithelium, pili from distinct cells may interact with one another, forming a microcolony (Craig *et al.*, 2004).

3. Manipulation of the host cell. Following efficient attachment, pathogens exert detrimental effects upon the host *via* an immensely diverse array of pathogenic mechanisms. Bacteria such as *V. parahaemolyticus, Y. enterocolitica* and enteropathogenic *E. coli* secrete effector proteins into the host cell using TTSS (Park *et al.*, 2004; Sory and Cornelis, 1994; Kenny *et al.*, 1997). *V. cholerae* produces cholera toxin, which binds to host cell receptors, inducing cytosolic translocation (Merritt *et al.*, 1994). *L. monocytogenes* binds to host cell receptors such as E-cadherins, thereby triggering invasion of non-phagocytic enterocytes (Lecuit *et al.*, 1997). The downstream effects of these pathogenic activities are as diverse as the mechanisms by which they are elicited. Host cell lysis, cytoskeletal disruption, secretion of cytoplasmic contents, inflammation and tissue disruption are all common outcomes of enteric bacterial pathogenesis.

4. Host cell response. During the infection, innate inflammatory responses of the host cell may be triggered, causing recruitment of granulocytic phagocytes which may engulf and destroy the pathogen (Qadri *et al.*, 2003). Inflammation may also induce fluid secretion, resulting in mechanical removal of adherent bacteria. Recognition of pathogen-associated antigens by macrophages may trigger an antibody response in the host, enhancing the rate of pathogen clearance (Qadri *et al.*, 2003). Many enteric infections are self-limiting, however in cases of severe intestinal destruction, traversal of pathogens into the bloodstream may occur. Systemic infections arising from septicaemia may result in rapid mortality (Daniels *et al.*, 2000).

As indicated above, the binding events which occur during initial attachment are vital in the establishment of enteric infections. These binding events may involve the interaction of bacterial adhesins with host cell proteins, glycoproteins, lipids and glycolipids. Importantly, adhesin binding has implications not only for the colonisation of host cells but can also manipulate host cell signalling events, thereby altering immune responses, actin cytoskeleton homeostasis, invasion and intracellular survival (Kline *et al.*, 2009). Disruption of this critical early stage of pathogenesis is among the most promising targets for prevention of infection by intestinal pathogens.

A number of studies have confirmed that deletion of genes coding for adhesins results in severe abrogation of downstream pathogenic processes. Deletion of the monomeric BabA glycan binding protein of *Helicobacter pylori* resulted in a significant reduction in pro-inflammatory chemokine secretion compared with wild type strains upon infection of cultured MDCK cells (Ishijima *et al.*, 2011). Importantly, chemokine responses were found to require functional expression of the Lewis B receptor, indicating the specificity of the adhesin-receptor interaction in the pathogenesis of *H. pylori* (Ishijima *et al.*, 2011).

Disruption of the *V. cholerae* toxin-coregulated pilus (TCP) by deletion of the major pilin subunit TcpA resulted in complete abrogation of the typical diarrhoeal effects associated with infection, during a volunteer study (Tacket *et al.*, 1998). Faecal shedding of *V. cholerae* from volunteers who were administered Δ*tcpA* mutants was also observed to be considerably lower than the levels detected with wild type administration, indicating that TCP played a central role in intestinal colonisation (Tacket *et al.*, 1998).

The above examples indicate the central roles played by adhesins in enteric bacterial pathogenesis. Definitive links between adhesin function and pathogenesis have not been illustrated in *V. parahaemolyticus*. As such, this study aimed to identify any such adhesins and establish functionality through detailed molecular characterisation. Fig 1.6 illustrates the structural variability of bacterial adhesins and their respective biogenesis components.

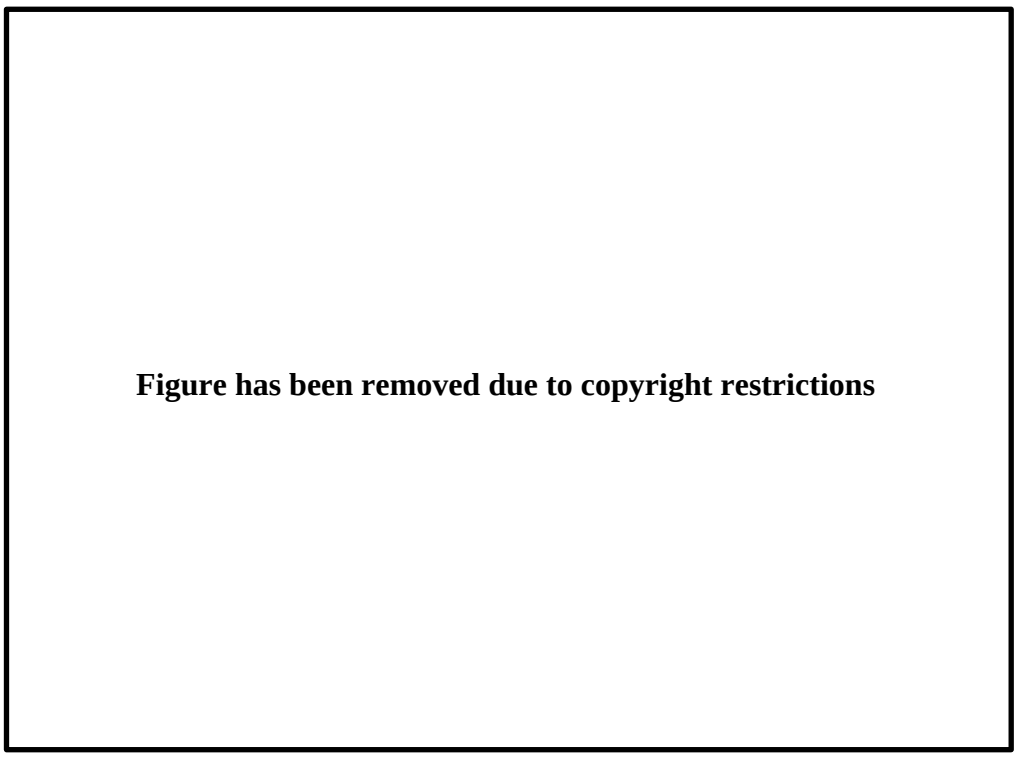

Fig 1.6 Schematic representation of a variety of characterised gram negative bacterial adhesins. *Porphyromonas gingivalis* pili, UPEC type I pili, *Yersinia enterocolitica* YadA trimeric autotransporter adhesin, *S. enterica* curli and *Neisseria gonorrhoeae* type IV pili. Structural variation, secretion pathways and associated biogenesis mechanisms. SecYEG indicates the Sec translocon apparatus. Figure adapted from Kline *et al.* (2009).

1.4.1 Filamentous adhesins.

Many bacterial pathogens produce hair-like appendages which play specific roles in the process of tissue colonisation. These appendages are termed pili (occasionally fimbriae) and are produced by a highly organised cell surface secretory system. The majority of characterised bacterial pili are produced by either the chaperone usher pathway, as in type I pili of enteropathogenic and uropathogenic *E. coli*, or a type II secretion system, as observed for TFP such as those found in *Vibrio spp* (Soto and Hultgren, 1999). Type I and TFP have been characterised as having central roles in the pathogenicity of a vast number of bacterial species and as such, only these will be further discussed. Filamentous adhesins offer considerable advantages compared with cell-associated adhesins in the initial phases of attachment to host epithelia. Due to outward extension from the bacterial cell, pili may become entangled in mucus, extracellular matrix components or commensal bacteria, thereby anchoring the pathogen on the host epithelium. Phylogenetic comparison of the biogenesis components of pili has revealed that in many cases, the pili have co-evolved with the parent organism indicating ancient ancestral origin (Aagesen and Häse, 2012). This ancestral origin suggests that a strong selective pressure exists for retention of pili, likely as a result of critical functionality. Indeed pili have been observed to play diverse roles in a wide range of bacterial activities such as DNA uptake, twitching motility, aggregation and adhesion. The aggregative and adhesive properties of these dynamic organelles may be explained by their functionality in promoting both cell-cell interactions and cell-host cell interactions. These processes form integral steps in biofilm formation and colonisation during infection. As such, the significance of these filamentous adhesins should not be underestimated in the process of bacterial pathogenesis.

1.4.1a Type I pili.

Uropathogenic *E. coli* (UPEC) present an excellent example of a pathogen which uses a proteinaceous adhesin to adhere with high specificity to host tissue. UPEC produce type I pili, a helical rod-shaped organelle which is assembled on the bacterial cell surface. Individual pilin subunits are secreted into the periplasm where they bind to a chaperone protein, thereby priming the pilins for secretion (Kline *et al.*, 2009). The chaperone-pilin complex binds to an outer membrane usher protein which catalyses the orderly export of polymerised pilin subunits onto the cell surface to form a functional pilus (Allen *et al.*, 2012). The major subunit of UPEC type I pili is FimA, however the tissue binding capacity of the pilus is conferred by a tip located adhesin, FimH (Krogfelt *et al.*, 1990; Jones *et al.*, 1995). Krogfelt *et al.* (1990) found that FimH was capable of binding to mannosylated BSA *in vitro*, thereby indicating mannose specific lectin functionality. Further to this finding, it was observed by Zhou *et al.* (2001) that a urinary epithelial tissue specific glycoprotein uroplakin Ia was the functional mannosylated receptor for FimH. Zhou *et al.* (2001) also highlighted that binding of multiple pili to uroplakin Ia would result in a highly efficient, highly specific binding to urinary epithelial cells.

1.4.1b Type IV pili (TFP).

TFP have been identified in many bacterial species and have been shown to have highly diverse functionality, leading to involvement in a wide range of activities such as twitching motility, the uptake of DNA, binding to both abiotic and biotic surfaces and the formation of aggregates. Like type I pili, TFP are helical, proteinaceous filaments. TFP however are anchored in the inner membrane and are assembled by a completely distinct mechanism from that of type I pili. The biogenesis of *Neisseria meningitidis* TFP represents perhaps the most thoroughly characterised TFP assembly mechanism. Mutational analysis identified that

expression of a total of 15 genes was required for pilus production and subsequent cell surface localisation (Carbonnelle *et al.*, 2005). TFP major pilin subunits are produced as prepilins, which possess an N-terminal signal sequence. This sequence directs the prepilin to a prepilin peptidase located in the inner membrane, where cleavage of the signal sequence by the peptidase primes the major pilin subunits for secretion (Craig *et al.*, 2004). Secretion of pilin subunits is driven by a membrane-associated ATPase and an outer membrane pore protein (secretin) is required for cell surface localisation of pilus subunits (Carbonnelle *et al.*, 2005; Pelicic, 2008; Kline *et al.*, 2009).

TFP have been described as "bacteria's favourite colonisation factors" and indeed a role in pathogenesis has been described for TFP from many different bacterial pathogens (Pelicic, 2008). The *Pseudomonas* strain K pilin has been shown to bind to the glycosphingolipids asialo-GM1 and asialo-GM2 (Krivan *et al.* 1988; Sheth *et al.*, 1994). *P. aeruginosa* is an opportunistic pathogen which colonises epithelial tissues using TFP, resulting in severe infections in patients suffering from chronic pulmonary conditions such as cystic fibrosis. It was observed that the PAK pilus was the principal virulence factor involved in adherence to cultured pulmonary epithelial cells and the pilus also played a central role in conferring lethality of *P. aeruginosa* towards infected mice (Hahn, 1997).

The TFP produced by *Neisseria* species are multi-functional virulence factors. These TFP have been shown to play a role in the natural competence of *Neisseria meningitidis* by binding to DNA and enabling cellular uptake through pilus retraction (Mattick, 2002; Cehovin *et al.*, 2011). The genetic variability conferred by such transformations may play a role in promoting antigenic variability or environmental adaptation during infection. Interestingly, the forces generated from pilus retraction are sufficient to confer a twitching motility phenotype, which may also play a role in pathogenesis (Mattick, 2002). The CD46

complement control protein has been described as a receptor for the *Neisseria* TFP (Källström *et al.*, 1997). Disruption of glycosylated regions of the CD46 receptor resulted in abrogation of *Neisseria* pilin binding and as such it appears that the *Neisseria* TFP may possess lectin functionality (Källström *et al.*, 2001). Specific glycan motifs have not yet been identified as functional receptors for *Neisseria* TFP.

Extensive insight into the structure and function of TFP will be provided in Chapter 5.

1.4.2 Non-pilus adhesins.

While pili play pivotal roles in initial attachment, a successful colonisation typically requires multiple interactions with the host cell. A number of cell-associated non-pilus adhesins have been characterised and have been shown to play central roles in pathogenesis. These adhesins may be expressed on the cell surface prior to attachment or expression may be induced following docking on the host cell surface. The combinatorial effect of pilus and cell-associated adhesin binding results in intimate attachment to the host cell and reduced risk of removal by shear forces or mucus entrapment.

H. pylori is an intriguing pathogen which is capable of causing persistent, chronic infections of the gastric epithelium. Two glycan binding proteins produced by *H. pylori* have been described in detail. BabA was shown to be cell surface located and bound specifically to Lewis B type glycans, while the SabA adhesin was shown to bind to sialylated forms of the Lewis X glycans (Ilver *et al.*, 1998; Mahdavi *et al.*, 2002; Moran and Gupta, 2011). These adhesin-glycan interactions are believed to be the principal means of colonisation employed by *H. pylori* and as such present an attractive target for potential therapeutics. In addition to the binding of human Lewis type glycans, *H. pylori* LPS commonly contains modifications which form molecular mimics of these host antigens (Moran and Gupta, 2011). This may have implications not only in the masking of the pathogen from the immune system, but also

in the binding of the bacterium to lectin expressing cells (Evans and Evans, 2000; Edwards *et al.*, 2000).

As described in section 1.3.2, TTSS of *V. parahaemolyticus* are the principal virulence mechanisms used by the organism during infection of human hosts. As TTSS function in a contact-dependent manner, one can imagine how disruption of adhesins may adversely affect TTSS activity. The *Yersinia enterocolitica* adhesin YadA provides an example of an adhesin which is required for TTSS activity. Translocation of the *Y. enterocolitica* TTSS effector protein YopE into HeLa cells was shown to require functional expression of YadA (Sory and Cornelis, 1994). YadA was shown to mediate attachment to host cells by binding to the extracellular matrix proteins fibronectin and collagen (Tertti *et al.*, 1992; Leo *et al.*, 2008). Mutants lacking functional YadA were found to display reduced adherence to HeLa cells and were unable to colonise infected mice, highlighting the importance of YadA-mediated adherence in an *in vivo* context (Schutz *et al.*, 2010). The results obtained with *Y. enterocolitica* provide a clear indication of the importance of adherence for TTSS functionality and downstream pathogenesis.

1.5 Current understanding of *V. parahaemolyticus* adherence mechanisms.

While the identification and characterisation of TTSS as major virulence factors of *V. parahaemolyticus* has led to a vast increase in our understanding of the molecular basis of *V. parahaemolyticus* pathogenicity, the mechanism governing the attachment of the organism to host cells has been somewhat ignored. It is generally accepted that TTSS function in a host cell contact-dependent manner, a process which would require the activity of bacterial adhesins. This process has been demonstrated in other pathogens, such as *Y. enterocolitica*,

however until recently, the role of adhesins in *V. parahaemolyticus* TTSS activity has been poorly understood.

1.5.1 *V. parahaemolyticus* TFP.

As described previously, TFP can function as mediators of bacterial virulence by facilitating attachment to host cells, aggregation and in some cases, subversion of host cell signalling. Two distinct TFP of *V. parahaemolyticus* have been characterised at a molecular level using deletion mutants which lack functional pili.

In 1990, Nakasone and Iwanaga first identified a link between pilus production and adherence of *V. parahaemolyticus* to rabbit intestinal explants. Nakasone *et al.* have since purified and characterised pili from three distinct strains of *V. parahaemolyticus*, including strain Ha7 (serotype, O2:K3), strain Na2 (serotype O4:K12) and a representative from the recently emerged pandemic O3:K6 clone, LVP9 (Nakasone and Iwanaga, 1990; Nakasone and Iwanaga, 1991; Nakasone *et al.*, 2000). The pili from all three strains were identified as distinct unbundled fibres, approximately 7 nm in diameter. Purified pili were found to adhere to rabbit intestinal explants and adherence of the parent organism could efficiently be inhibited by pre-treatment of host cells with purified pili or by pre-treatment of *V. parahaemolyticus* with anti-pilus antibodies. Purified pili did not agglutinate red blood cells, regardless of the haemagglutination capacity of the parent strain. Importantly, cross reactivity of anti-pilus antibodies was found to be serogroup specific, indicating a high degree of antigenic variability at an intra-species level (Nakasone and Iwanaga, 1990; Nakasone and Iwanaga, 1991; Nakasone *et al.*, 2000). At the time of analysis, the specific protein composition of these adhesive pili was not known and the genes coding for the pilus subunits were not identified.

The sequencing of the *V. parahaemolyticus* genome offered a new opportunity to further develop understanding of *V. parahaemolyticus* pilus biology as the operons encoding the pilin proteins and their respective biogenesis machineries were revealed. The first molecular characterization of *V. parahaemolyticus* RIMD2210633 TFP using mutational analysis was carried out by Shime-Hattori *et al.* (2006). In that study, it was observed that two distinct TFP with PilA and MshA1 as major pilin subunits played distinct roles in *V. parahaemolyticus* biofilm formation. The MshA1 pilus was constitutively expressed under normal growth conditions, while the addition of a mixture of chito-oligosaccharide and *N*-acetly glucosamine was required for induction of *pilA* promoter activity. The MshA1 pilus was required for initial attachment to abiotic surfaces, while expression of the PilA pilus induced the formation of aggregates. It was suggested by Shime-Hattori *et al.* (2006) that the differential regulation of expression of each pilus may serve as a response to the sensing of nutritive chitinous environments in which the bacterium would thrive by eliciting enhanced colonisation. Prior to our study, a role for the PilA and MshA pili in the pathogenicity of *V. parahaemolyticus* RIMD2210633 had not been investigated.

The findings of Shime-Hattori *et al.* (2006) directly correlate with the characterised roles of the MshA pilus in *V. cholerae*. *V. cholerae* possesses three TFP, with TcpA, MshA and PilA functioning as the respective major pilin subunits. While TcpA has been shown to mediate virulence by facilitating colonisation of host tissues, MshA was described as an environmental persistence factor and was found to play no role in the virulence of *V. cholerae* (Thelin and Taylor, 1996; Attridge *et al.*, 1996; Tacket *et al.*, 1998; Marsh and Taylor, 1999). Characterisation of the *V. cholerae* MshA pilus has led to the identification of a role in attachment to abiotic surfaces and attachment to zooplankton (Watnick *et al.*, 1999; Chiavelli *et al.*, 2001). PilA was observed to have a similar role in environmental persistence, being induced upon binding to nutritive chitinous surfaces (Meibom *et al.*, 2004). The biosynthetic

operons in which the *V. cholerae* MshA and PilA pilus components are encoded is virtually identical to those observed in *V. parahaemolyticus* (Marsh and Taylor, 1999; this study, Fig 5.3). As such, one might speculate that there could be conserved pilus functionality and hence a lack of involvement for MshA or PilA in *V. parahaemolyticus* pathogenicity. However, sequence analysis has confirmed a high level of variability in major pilin proteins from the *Vibrionaceae*, particularly in the predicted substrate binding C-terminal regions (Aagesen and Häse, 2012). As a result, a role in pathogenicity should be considered for the *V. parahaemolyticus* TFP, particularly upon consideration of the early observations of Nakasone *et al.* who observed a definitive role for *V. parahaemolyticus* pili in binding to rabbit enterocytes.

1.5.2 Cell-associated haemagglutinin.

Nagayama *et al.* (1994) found a direct correlation between the ability of a variety of *V. parahaemolyticus* strains to agglutinate red blood cells in a mannose sensitive manner and the ability to bind to Caco-2 intestinal cells. Interestingly no correlation between adhesiveness and piliation was observed, with less than 10% of all cells analysed (n = 539) exhibiting piliation. The protein responsible for haemagglutination was purified by Nagayama *et al.* in 1995. It was found to have a mass of 26 kDa and was shown by immunogold labelling to be located on the cell surface, and as such was deemed a cell-associated haemagglutinin (cHA). Adherence to cultured rabbit enterocytes was efficiently inhibited by antibodies raised against purified cHA and D-mannose, indicating that cHA was responsible for both mannose sensitive haemagglutination and adherence to rabbit enterocytes. For this reason Nagayama *et al.* (1995) stated “Thus, we do not believe that pili of *V. parahaemolyticus* participate in the adherence”. This hypothesis clearly contradicts the findings of Nakasone *et al.* (1990) who observed that pili were indeed mediators of *V. parahaemolyticus* adherence to rabbit

enterocytes and likely indicates that adherence mechanisms of *V. parahaemolyticus* are strain specific. cHA function has not been described in *V. parahaemolyticus* RIMD2210633, nor has the identification of the gene encoding cHA been reported. As such it remains unclear whether or not cHA plays a role in adherence-mediated virulence of *V. parahaemolyticus* RIMD2210633.

1.6 Invasion of intestinal cells by bacterial pathogens.

During the process of colonisation of the intestinal epithelium, pathogens are exposed to a number of threats from the host organism. Entrapment by mucus, removal by shear forces, competition with commensals and targeting by the innate immune system all pose a threat to the efficient colonisation of the human host. In order to counteract these issues, a number of bacterial species have developed complex strategies to invade into host tissues and persist or even proliferate within the intracellular environment. Following invasion, the host cell may respond by inducing lysosomal fusion with phagocytic vacuoles. Another major issue for internalised pathogens lies in the ability of epithelial cells to recognise pathogen-associated molecular patterns (PAMPS), such as lipopolysaccharide, flagellar antigens or capsular polysaccharides and subsequently stimulate inflammatory immune responses to facilitate removal of the unwanted intruder. Some particularly resourceful intracellular pathogens have developed effective mechanisms of subverting these host cell responses and as such can cause persistent and damaging infections.

While the cells of the gastro-intestinal tract (particularly M cells located in the Peyer's patches of the small intestine) passively sample material from the intestinal lumen, truly

invasive pathogens manipulate non-phagocytic cells in such a way as to promote engulfment of bacterial cells and traversal into the intracellular environment. Fig 1.7 illustrates a number of well characterised invasion mechanisms used by enteric bacterial pathogens.

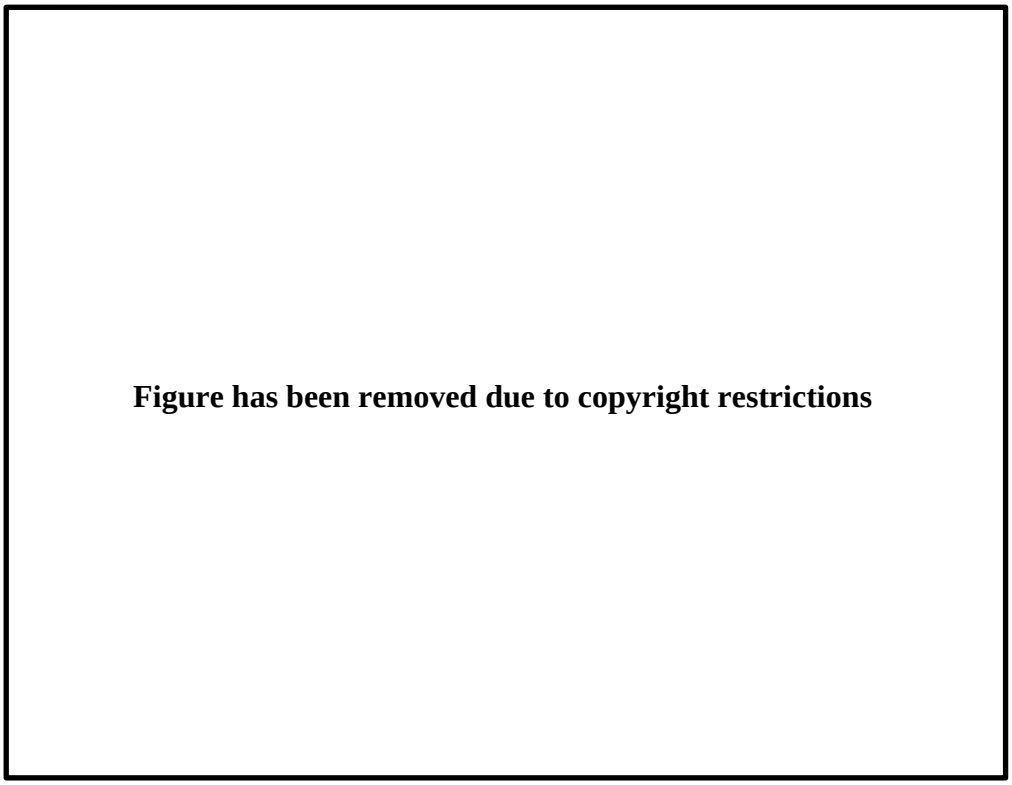

Fig 1.7 Schematic representation of two well characterised mechanisms of epithelial invasion. (**A**) The zipper mechanism as employed by *Yersinia spp* and *Listeria monocytogenes*. (**B**) The trigger mechanism as employed by *S. enterica* and *Shigella flexneri*. Figure adapted from Cossart and Sansonetti, 2004.

As shown in Fig 1.7, the stimulation of phagocytosis in non-phagocytic cells requires the manipulation of host cell signalling pathways, eventually leading to alterations in the actin cytoskeleton which cause engulfment of the bacterial cell. *Yersinia spp.* and *L. monocytogenes* trigger cellular uptake using protein-protein interactions between the bacterial cell surface invasin and a host cell receptor. The *Yersinia* invasin protein binds to host cell β1 integrins, which are cell surface located proteins that anchor the cell to the extracellular matrix (Isberg and Barnes, 2001). The C-terminal domain of β1 integrins commonly binds to focal adhesion kinases (FAKs) and as such, invasin-integrin binding may activate a FAK-

dependent signalling cascade which leads to actin remodelling (Alrutz and Isberg, 1998). It has been shown that this invasin-integrin interaction also activates the small Rho GTPase Rac1, which leads to Arp2/3-mediated branched actin filament formation in an N-WASp independent manner (Alrutz *et al.*, 2001). The end result of these signalling alterations is extension of filipodia around the bacterial cell, forming a phagocytic cup which engulfs the bacterium, translocating it to the intracellular environment.

L. monocytogenes also employs protein-protein interactions, using cell surface internalin proteins InlA and InlB to activate filipodium formation and subsequent internalisation. InlA binds to E-cadherins, while InlB binds to the Met receptor on host cells (Mengaud *et al.*, 1996; Shen *et al.*, 2000). E-cadherins bind directly to α and β catenins, which are associated with the actin cytoskeleton and as such, the binding and clustering of E-cadherins by InlA provides an efficient means of actin sequestration at the site of attachment (Lecuit *et al.*, 2000). The InlA-E-cadherin interaction has been demonstrated to cause two critical post-translational modifications of E-cadherins. The tyrosine kinase Src mediates phosphorylation of E-cadherins, while E-cadherins are ubiquitinated by the ubiquitin ligase Hakai (Bonazzi *et al.*, 2008). These post-translational modifications have the effect of stimulating two independent endocytic pathways: caveolar endocytosis and clathrin-mediated endocytosis (Bonazzi *et al.*, 2008). The binding of InlA to E-cadherin has also been shown to cause activation of Rac1 which may play a role in Arp2/3-dependent filipodium production (Sousa *et al.*, 2007).

L. monocytogenes possesses a second internalin InlB, which is also capable of manipulating cell signalling pathways for the promotion of bacterial uptake. The binding of InlB to the host cell receptor Met results in the activation of PI3-kinase, a central regulator of actin dynamics and autophagy (Ireton *et al.*, 1999). This results in increased membrane-associated

phosphatidyl inositol 3-phosphate (PI[3]P) in the host cell membrane. PI(3)P is commonly associated with early endosomes and is produced during clathrin-mediated endocytosis (Kraub and Haucke, 2007). As such, this may indicate a co-operative role for InlB with InlA-mediated activation of the clathrin endocytic pathway. InlB has also been implicated in the activation of Rac1 at the site of bacterial entry, further supporting a role in actin filament extension *via* recruitment of WASp family proteins (Seveau *et al.*, 2007).

Key differences exist between the zipper mechanism of invasion used by *Yersinia* and *Listeria*, and the trigger mechanism used by *Salmonella* and *Shigella*. Importantly *Yersinia* invasin or *Listeria* InlA coated latex beads have been shown to be efficiently internalised, highlighting the specificity of their respective roles in the induction of invasion *via* the zipper mechanism (Wiedemann *et al.*, 2001; Lecuit *et al.*, 1997). The zipper mechanism involves the orderly extension of finger-like projections (filipodia) at the point of bacterial entry, facilitated by invasin-receptor interactions and subsequent alterations in cytoskeletal dynamics (Cossart and Sansonetti, 2004). The trigger mechanism by contrast induces enormous cytoskeletal reorganisation with the extension of large sheet-like projections (lamellipodia) which engulf the bacterium, allowing access to the intracellular milieu (Cossart and Sansonetti, 2004). The trigger mechanism in general also involves secretion of numerous bacterial effector proteins into the host cell, which often serve to mimic modulators of host cell cytoskeletal organisation, thereby allowing the bacterium to manipulate its own uptake (Cossart and Sansonetti, 2004).

The *Salmonella* TTSS effector proteins SopE1, SopE2 and SopB play a central role in initiating the formation of the macropinocytic pocket by directly or indirectly activating Rho GTPase signalling cascades. SopE1 and SopE2 were found to function as guanine nucleotide exchange factors (GEFs), which catalysed the binding of GTP to Rac1 and Cdc42 GTPases,

thereby activating downstream signalling (Friebel *et al.*, 2001). SopB was shown to activate an endogenous GEF (SH3-containing GEF), which caused specific activation of RhoG (Patel and Galan, 2006). The activation of Rac1 and RhoG was found to be critical for rearrangement of the actin cytoskeleton, while Cdc42 activation was found to play a central role in MAPK-dependent IL-8 induction (Patel and Galan, 2006). A fourth effector protein, SipA was found to bind directly to polymerised actin filaments within the macropinocytic pocket, preventing de-polymerisation (Zhou *et al.*, 1999). *Salmonella spp* have developed an intriguing strategy to minimise host cell responses by temporally regulating Rho GTPase activity following invasion. The effector protein SptP is secreted in parallel with the aforementioned invasins but functions in an antagonistic manner by acting as a GTPase activating protein (GAP), which catalyses the hydrolysis of active Rho GTPases to inactive GDP bound forms (Fu and Galan, 1999). This results in closure of the macropinocytic pocket and a recovery of normal host cell actin homeostasis (Fu and Galan, 1999). Temporal regulation is achieved as a result of the rapid proteasomal degradation of SopE and the relative persistence of SptP (Kubori and Galan, 2003).

Shigella spp orchestrate a similarly complex subversion of host cell cytoskeletal arrangements via TTSS, forming lamellipodia which are similar in appearance to those induced by *Salmonella spp* (Cossart and Sansonetti, 2004). The plasmid-encoded TTSS effector protein VirA initiates cytoskeletal rearrangement by causing destabilisation of microtubules, a process which leads to RhoA inhibition and Rac1 activation (Yoshida *et al.*, 2002). The formation of an activated Rac1-WAVE2 complex induces Arp2/3-dependent filament extension at the entry focus (Ogawa *et al.*, 2008). Actin nucleation is also induced by the C-terminus of the IpaC translocation protein which is exposed to the host cell cytoplasm (Tran Van Nhieu *et al.*, 1999). The recovery of normal cytoskeletal organisation in cells infected with *Shigella* is brought about through the activity of IpaA, a TTSS secreted

effector protein. IpaA has been shown to induce the expression of vinculin, a protein which catalyses the depolymerisation of actin filaments in the macropinocytic pocket (Bourdet-Sicard *et al.*, 1999).

As shown by the examples in Fig 1.7, bacterial invasion is a hugely complex process, which requires the manipulation of multiple host cell targets, either through interactions with host cell receptors or through direct manipulation of host cell signalling cascades *via* translocation of bacterial effector proteins. *V. parahaemolyticus* possesses significant potential for either induction or inhibition of phagocytosis due to its ability to secrete a vast array of effector proteins into host cells during infection. However, a number of contradictory reports have been published regarding *V. parahaemolyticus* invasion and as such, the importance of invasion for *V. parahaemolyticus* pathogenicity remains poorly understood.

1.7 Current understanding of *V. parahaemolyticus* invasion.

The activities of the *V. parahaemolyticus* TTSS effectors which have been described to date indicate that the Rho GTPases are major host cell targets during infection (Table 1.1). As described in section 1.6, these host cell signalling modulators play a critical role in the regulation of actin re-organisation during the process of bacterial invasion. As such, it is highly likely that inhibition or induction of invasion occurs by manipulation of GTPase activity during the process of *V. parahaemolyticus* infection. A summary of the involvement of GTPase signalling in *V. parahaemolyticus* invasion of various cell types is shown in Fig 1.8.

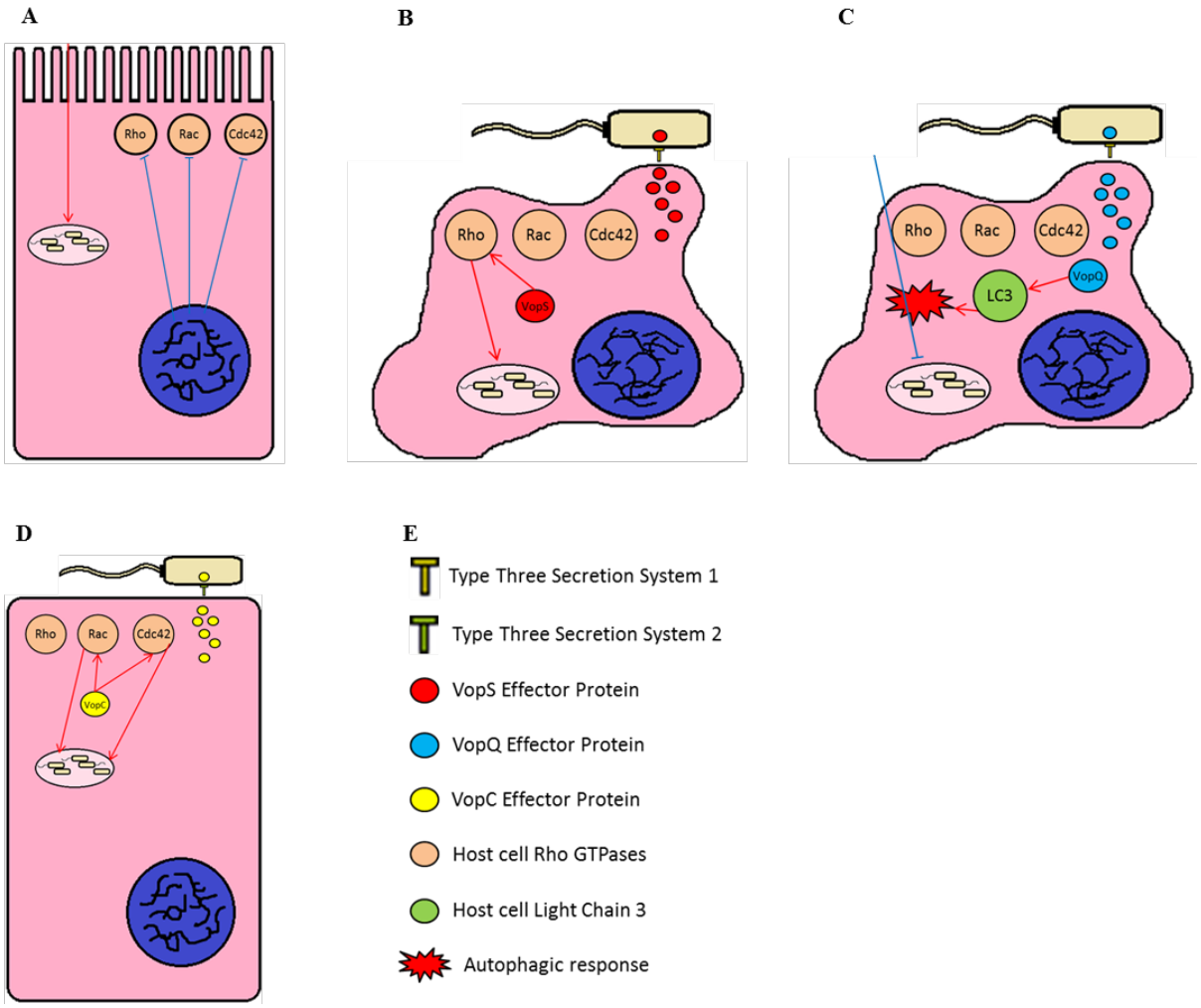

Fig 1.8 Modulation of Rho GTPase signalling affects the invasion of *V. parahaemolyticus*. (**A**) Inhibition of Rho GTPases by expression of dominant negative allelic variants increases entry into Caco-2 (Akeda *et al.*, 2002). (**B**) TTSS1 effector VopS causes increased expression of RhoB, leading to enhanced macrophage phagocytosis (Bhattacharjee *et al.*, 2008). (**C**) TTSS1 effector VopQ activates LC3 leading to autophagy, a process which redirects cellular activity and prevents phagocytosis by macrophages (Burdette *et al.*, 2009). (**D**) TTSS2 effector VopC activates Rac and Cdc42, increasing cellular uptake by HeLa cells (Zhang *et al.*, 2012) (**E**) Symbol nomenclature.

Prior to the sequencing of the *V. parahaemolyticus* genome and the identification of TTSS1 and TTSS2 as major virulence factors, the invasiveness of *V. parahaemolyticus* was investigated by a number of groups. The first reports of an invasive phenotype for *V. parahaemolyticus* were published by Akeda *et al.* (1997) who identified that a number of clinical isolates of *V. parahaemolyticus* were capable of invading into Caco-2 cells. Akeda *et*

al. (1997) observed that one particular isolate was capable of invading at a similar efficiency to that observed for *S.* Typhimurium. Further to these findings, it was observed that inhibition of the Rho GTPases RhoA, Rac1 and Cdc42 by expression of dominant negative allelic variants resulted in increased uptake of *V. parahaemolyticus* into Caco-2 (Akeda *et al.*, 2002). The TTSS1 effector protein VopS has been shown to play a role in the inhibition of the same subset of GTPases and as such may represent a means of induction of invasion in Caco-2 (Yarbrough *et al.*, 2009). While a role for VopS in the upregulation of phagocytosis by RAW 264.7 murine macrophages has been reported, a similar involvement in the invasion of epithelial cells has not yet been described (Bhattacharjee *et al.*, 2008). The TTSS2 effector protein VopC was recently identified and characterised by Zhang *et al.* (2012). VopC was found to be required for the invasion of HeLa epithelial cells by *V. parahaemolyticus*. Zhang *et al.* (2012) also characterised the molecular basis for VopC-mediated invasion, with the effector being implicated in the activation of Rac1 and Cdc42 and subsequent actin cytoskeletal rearrangements which were required for invasion. While the Rho GTPases involved in VopC-mediated invasion have been identified, downstream targets such as the WASp family of actin regulators have not been described. It also remains to be seen whether VopC has a similar role in intestinal cells, such as Caco-2. This would provide particularly interesting insights into *V. parahaemolyticus* invasion as the findings of Akeda *et al.* (2002) indicated that inhibition, not activation, of Rho GTPases in Caco-2 resulted in increased cellular uptake.

While cellular invasion has been described as a key pathogenicity determinant by multiple groups, there is also evidence to suggest that *V. parahaemolyticus* may actively inhibit uptake by host cells, favouring a cell surface infection model. Burdette *et al.* (2009) observed that VopQ caused PI3-kinase independent autophagy, a process which resulted in the inhibition of phagocytosis. VopQ-dependent autophagy was observed in both HeLa cells and RAW 264.7

macrophages. Burdette *et al.* (2009b) speculated that inhibition of phagocytosis was due to redirection of cellular responses towards autophagy, thereby interfering with the induction of phagocytosis, and that the simultaneous inhibition of phagocytosis and induction of autophagy may provide a pool of host cell-derived nutrients to facilitate rapid bacterial growth. As shown by the examples in Fig 1.7, the induction of invasion by bacterial pathogens commonly requires the activation of GTPases. Investigation into GTPase activation levels in cells transfected with VopS may provide direct evidence of the phenomenon proposed by Burdette *et al.* (2009b).

As a result of contradictory reports in published data and the importance of cellular invasion for the pathogenicity of many enteric pathogens, it is clear that further research is warranted in this poorly understood area of *V. parahaemolyticus* pathobiology. As much of the invasion-related research which has been carried out to date has involved the use of either murine cell models or HeLa cervical cell models, the use of an intestinal cell culture model may provide more representative information regarding the molecular mechanisms governing *V. parahaemolyticus* invasion during *in vivo* infections.

1.8 Objectives of study.

This project aimed to further current understanding of the molecular interactions governing cellular adherence and invasion of *V. parahaemolyticus* in Caco-2 intestinal epithelial cells. Although the cytotoxic and enterotoxic effects of *V. parahaemolyticus* have been attributed to the translocation of TTSS effector molecules into host cells, a significant gap exists in current understanding of the role played by adhesins and invasins in this process. Furthering current knowledge in this area will be critical not only for developing a more complete understanding of *V. parahaemolyticus* pathogenicity but also for the development of efficient therapeutics.

As TTSS play a role in the invasion of many enteric pathogens, their involvement in *V. parahaemolyticus* invasion and adherence was assessed. In order to better understand the importance of cellular invasion in relation to *in vivo* infections, the ability of invasive bacteria to proliferate intracellularly was also evaluated.

Next, this study aimed to identify novel adhesins and invasins by employing the functional screening of a random *V. parahaemolyticus* genomic library in a non-adherent, non-invasive library host, *E. coli* HB101. A similar approach has been used recently by Waterfield *et al.* (2008) and was shown to prove particularly useful for the characterisation of virulence-related genes which previously lacked functional annotations. As the number of sequenced genomes continues to grow, assigning functionalities to the vast amount of sequence data generated is of prime importance. A bioinformatics based approach was also undertaken in combination with extensive literature analysis in order to predict putative adhesins based upon characterisation in other species.

Following the selection of a number of putative adhesins and invasins, this study aimed to characterise the selected proteins through functional analysis of *V. parahaemolyticus* deletion mutants. Assessment of adherence and invasion using the Caco-2 cell model was employed in order to confirm a role for each protein in these processes. The relative importance of the confirmed adhesins and invasins for *V. parahaemolyticus* pathogenesis was then assessed by analysing a variety of phenotypes associated with *V. parahaemolyticus* TTSS activity in Caco-2 cells.

Overall, this study aimed to examine the interactions between *V. parahaemolyticus* and host cells, a process which is critical in the establishment of intestinal colonisation but has remained poorly understood.

Chapter 2

Materials and Methods

2.1 General microbiological techniques.

All chemicals and reagents were obtained from Sigma Aldrich, unless otherwise stated.

2.1.1 Bacterial growth conditions.

2.1.1a General bacterial growth conditions.

V. parahaemolyticus and *V. parahaemolyticus* deletion mutants were grown in LBN broth (LB + 3% NaCl) at 37°C with shaking. LBN agar (LBN broth + 1.5% agar) and the selective and differential medium thiosulphate citrate bile salts sucrose agar (TCBS) were also used for cultivation of *V. parahaemolyticus*. 5 μg ml^{-1} chloramphenicol, 30 μg ml^{-1} kanamycin or 25 μg ml^{-1} gentamicin was included where required for vector selection in *V. parahaemolyticus*. *E. coli* and *Salmonella* strains were grown in LB broth at 37°C with shaking. LB agar was also used for growth of *E. coli* and *Salmonella* strains. 100 μg ml^{-1} ampicillin, 20 μg ml^{-1} chloramphenicol, 40 μg ml^{-1} kanamycin or 25 μg ml^{-1} gentamicin was included where required for vector selection in *E. coli*. Where induction of protein expression from *lac* and T7 promoters was required, isopropyl β-D-1-thiogalactopyranoside (IPTG) was added to growth medium for *E. coli* and *V. parahaemolyticus* at a concentration of 100 μM. Expression was induced for 1.5 h at 37°C.

2.1.1b Bacterial growth conditions for co-incubations.

For co-incubation with Caco-2, overnight cultures of bacterial strains were used to inoculate LBN or LB broth to an OD_{600} of 0.05. Cultures were incubated at 37°C until exponential phase was reached (OD_{600} of 0.3 to 1.3). 1 ml aliquots of exponential phase cultures were centrifuged at 10,000 X *g* for 2 min. Supernatants were discarded and pellets were washed with 1 ml Phosphate Buffered Saline (PBS). Centrifugation was repeated and pellets were resuspended in 1 ml PBS. Suspensions of bacteria equivalent to 0.1 (0.2 for *E. coli* HB101

only) OD_{600} were prepared by dilution in PBS. 45 µl aliquots of 0.1 or 0.2 OD_{600} suspensions (section 2.1.2) were added to each well of 7 day cultured Caco-2 in 24 well plates, resulting in a multiplicity of infection (MOI) of 10, assuming 450,000 cells per confluent well of Caco-2. Co-incubations were performed at 37°C, 5% CO_2.

2.1.2 Caco-2 cell culture conditions.

Caco-2 cells were cultured in DMEM complete (Dulbecco's Minimal Eagles Medium containing 20% (v/v) foetal bovine serum (FBS), 1 X non-essential amino acids, 20 mM L-glutamine, 100 U ml^{-1} penicillin and 100 µg ml^{-1} streptomycin) at 37°C, 5% CO_2. Cells were routinely cultured in T25 flasks for 5 to 7 days following seeding at a density of 100,000 cells in 5 ml DMEM complete. For co-incubation experiments, cells were seeded at 20,000 cells per well with 1 ml DMEM complete per well in 24 well tissue culture plates. Cells were cultured for 6 days, at which point DMEM complete was removed, and monolayers were washed with 1 ml PBS per well. 1 ml DMEM (DMEM complete, without addition of penicillin and streptomycin) was added per well and plates were returned to 37°C, 5 % CO_2 for a further 24 h. To allow for vector selection, antibiotics were included at the following concentrations: 100 µg ml^{-1} ampicillin, 20 µg ml^{-1} chloramphenicol and 1 µg ml^{-1} gentamicin (higher gentamicin concentrations had adverse effects on bacterial growth). Low level expression was induced by inclusion of 10 µM IPTG.

2.1.3 DNA agarose gel electrophoresis.

DNA was routinely analysed and isolated by agarose gel electrophoresis. Agarose gels were prepared at a concentration of 0.8% (w/v) in TAE buffer (40 mM Tris, 20 mM glacial acetic acid, 1 mM EDTA), with the incorporation of 800 ng ml^{-1} ethidium bromide. Samples were prepared for electrophoresis by mixing with 10X loading buffer (1.25 mg ml^{-1} xylene cyanol, 1.25 mg ml^{-1} bromophenol blue, 6.25 mg ml^{-1} SDS, 62.5% (v/v) glycerol). Electrophoresis

was carried out at 100 V for 45 min and the gels were visualised using the Syngene G:Box Gel Documentation system with Syngene GeneSnap software.

2.1.4 Polymerase chain reaction (PCR).

PCR was routinely carried out using Biomix PCR mix (Bioline). Where high fidelity amplification was required (amplification of deletion alleles/generation of constructs for expression), Accuzyme PCR mix (Bioline) was used. The PCR mixes contain appropriate concentrations of dNTPs, ATP, DNA polymerase and $MgCl_2$ at 4.0 mM. Reaction mixes were composed of 1X Biomix/Accuzyme, 10 pmol forward primer, 10 pmol reverse primer, 0.5 µl template DNA and PCR grade H_2O to 25 µl. PCR templates routinely used included: 1:1,000 dilution of miniprep DNA; 1:1,000 dilution of *V. parahaemolyticus* RIMD 2210633 genomic DNA; 50 µl resuspension of a bacterial colony.

PCR was carried out using an Eppendorf Mastercycler Gradient thermocycler programmed as follows: Cell lysis/initial denaturation at 95°C for 5 min, denaturation at 95°C for 1 min, annealing at 50°C to 65°C (optimised for each primer pair), extension at 72°C for 30 s per 1,000 bp to be amplified (for Accuzyme, the extension temperature was adjusted to 68°C and 1 min was allowed per 1,000 bp to be amplified). The PCR cycle was repeated at least 30 times, followed by a final extension step carried out for 10 min at the appropriate temperature.

2.1.5 Plasmid miniprep.

Plasmids were isolated using 5 ml overnight cultures of *E. coli* grown in LB broth with the appropriate selective agent for vector retention. Cultures were centrifuged at 8,000 X *g* for 10 min. Pellets were resuspended in 250 µl buffer P1. 250 µl buffer P2 was added and incubated at room temperature for 5 min. 350 µl buffer N3 was added, the tubes were inverted and

centrifuged at 16,000 X *g* for 10 min. Supernatants were then applied to Qiaprep Spin columns and centrifuged at 16,000 X *g* for 1 min. 500 µl buffer PB was added to each column and centrifugation was repeated. Columns were washed with 750 µl buffer PE and dried by centrifuging at 16,000 X *g* for 5 min. Plasmid/cosmid DNA was eluted with 50 µl PCR grade H_2O.

2.1.6 DNA purification using Wizard SV Gel/PCR Cleanup kit (Promega).

DNA was purified from PCR reactions, vector digests and gel excisions using SV cleanup kit. Membrane binding buffer was added to the DNA sample in a 1:1 ratio. (Gel fragments were heated to 65°C for 10 min in order to melt the agarose). Samples were then applied to SV spin columns and incubated at room temperature for 1 min. Columns were centrifuged at 16,000 X g for 1 min and washed with 750 µl membrane wash buffer. The wash was repeated with 500 µl membrane wash buffer and columns were dried by centrifugation at 16,000 X g for 10 min. DNA was eluted with 30 µl PCR grade H_2O.

2.1.7 TOPO TA cloning of PCR products into pCR2.1 and pET101.

PCR products were generated as outlined in section 2.1.4. Where non-specific amplification occurred, the specific product of interest was isolated by gel electrophoresis and purified from a gel excision as outlined in section 2.1.6. 2 µl PCR product, 1 µl salt solution and 2 µl of PCR grade H2O were mixed in a micro-centrifuge tube. 1 µl of TOPO ready vector was added and reaction was again mixed. Samples were incubated at room temperature for 20 min to allow for integration into the vector. Transformation was carried out as described in section 2.1.11.

2.1.8 Restriction endonuclease digestion.

Restriction digests were carried out using either Fermentas Fast Digest or Promega restriction endonucleases. Digests were prepared by mixing 2 µl restriction enzyme (~20 U), 2.5 µl appropriate 10X enzyme buffer, 2.5 µl bovine serum albumin (BSA) and 18 µl of miniprep DNA (~200 ng μl^{-1}). The reaction mix was incubated at 37°C for 2 h. The efficiency of digestion was assessed by agarose gel electrophoresis (section 2.1.3). Where appropriate, gel fragments were excised and purified by Promega SV Gel/PCR Cleanup (section 2.1.6).

2.1.9 Phosphatase treatment of vector DNA.

Digested vector DNA was treated with shrimp alkaline phosphatase (SAP, Promega) prior to ligation. 3 µl SAP (3U), 3 µl 10X SAP buffer and 25 µl purified vector (~25 ng μl^{-1}) were mixed and incubated at 37°C for 30 min. SAP was inactivated by incubating at 65°C for 15 min.

2.1.10 Ligation.

Column purified insert DNA was ligated into purified, phosphatase treated vectors as follows: 2 µl T4 ligase, 2 µl 10X ligase buffer, 20 ng vector and a 3:1 molar ratio of insert to vector (~30 ng) were mixed and completed to 20µl with PCR H_2O [For blunt end ligations PEG 4000 was included at 5% (v/v)]. The reaction mixture was incubated at 16°C overnight.

2.1.11 Transformation of competent cells.

Cryovials containing 50 µl of chemically competent *E. coli* Top10, PIR1, BL21/DE3 (Invitrogen) or HB101 (Promega) were allowed to thaw on ice. 3 µl vector DNA was added (~5 ng) and cryovials were incubated on ice for 20 min. Heat shock was carried out by incubating at 42°C for 30 s. Cells were placed on ice and 250 µl SOC medium was added.

100 µl of the transformation mix was spread plated on LB agar with appropriate antibiotic selection.

2.1.12 Preparation of glycerol stocks.

Isolated colonies were inoculated in the appropriate medium and cultured at 37°C overnight with shaking. Three 1 ml aliquots for each strain were centrifuged at 16,000 X g for 2 min. Pellets were washed with 1 ml fresh medium. Pellets were resuspended in 1 ml fresh medium and transferred to labelled cryovials. 500 µl sterile 60% glycerol (v/v) was added to each cryovial and stocks were stored at -80°C.

Table 2.1 Bacterial strains used in this study.

Strain name	Description/Genotype		Source
V. parahaemolyticus			
WT	Wild type RIMD2210633		Boyd Lab
Δ*ompA*	Outer membrane protein A deletion mutant	*VPA0248*$_{\Delta 22\text{-}987}$ allele encoding OmpA$_{\Delta Ala^{7}\text{-}Gln^{323}}$	This study
Δ*mshE*	Type IV pilus ATPase deletion mutant	*VP2701*$_{\Delta 7\text{-}1689}$ allele encoding MshE$_{\Delta Ile^{3}\text{-}Gly^{563}}$	This study
Δ*mshL*	Type IV pilus outer membrane secretin deletion mutant	*VP2704*$_{\Delta 7\text{-}1638}$ allele encoding MshL$_{\Delta Lys^{3}\text{-}Ala^{546}}$	This study
Δ*pilA*	Chitin regulated pilus deletion mutant	*VP2523*$_{\Delta 43\text{-}405}$ allele encoding PilA$_{\Delta Ile^{15}\text{-}Asp^{136}}$	This study
Δ*mshA*1	Major type IV pilin subunit deletion mutant	*VP2698*$_{\Delta 7\text{-}492}$ allele encoding MshA1$_{\Delta Arg^{3}\text{-}Gly^{164}}$	This study
Δ*mshA*2	Putative major pilin subunit deletion mutant	*VPA0747*$_{\Delta 61\text{-}483}$ allele encoding MshA2$_{\Delta Thr^{21}\text{-}Ala^{161}}$	This study
Δ*mshA3*	Putative major pilin deletion mutant	*VP2697*$_{\Delta 13\text{-}231}$ allele encoding MshA3$_{\Delta Lys^{6}\text{-}Gly^{77}}$	This study
Δ*pilA*/Δ*mshA*1	Double deletion of *pilA* and *mshA*1		This study
Δ*pilA*/Δ*mshA*2	Double deletion of *pilA* and *mshA*2		This study
Δ*mshA*1/Δ*mshA*2	Double deletion of *mshA*1 and *mshA*2		This study
Δ*pilA*/Δ*mshA*1/Δ*mshA*2	Triple deletion of *pilA*, *mshA*1 and *mshA*2		This study
Δ*pilA*/Δ*mshA*3	Double deletion of *pilA* and *mshA*3		This study
Δ*mshA2*/Δ*mshA*3	Double deletion of *mshA*2 and *mshA*3		This study
Δ*pilA*/Δ*mshA*2/Δ*mshA*3	Triple deletion of *pilA*, *mshA*2 and *mshA*3		This study
Δ*vscN*1	Deletion of TTSS1-associated ATPase	*VP1668*$_{\Delta 142\text{-}1065}$ allele encoding VscN1$_{\Delta Cys^{48}\text{-}Arg^{355}}$	Boyd Lab
Δ*vscN*2	Deletion of TTSS2-associated ATPase	*VPA1338*$_{\Delta 132\text{-}1154}$ allele encoding VscN2$_{\Delta Val^{45}\text{-}Glu^{385}}$	Boyd Lab
Δ*vscN*1/Δ*vscN*2	Double deletion of *vscN*1 and *vscN*2		Boyd Lab

Table 2.1 continued.

E. coli		
Top 10	*mcrA*, Δ (*mrr-hsd*RMS-*mcrBC*), φ80*lacZ*Δ*M15*, Δ*lacX*74, *deoR*, *recA*1, *araD*139, Δ (*ara-leu*)7697, *galU*, *galK*, *rpsL* (Sm^R), *endA*1, *nupG*	Invitrogen
Pir1	Δ*lac*169, *rpoS* (Am), *robA*1, *creC*510, *hsdR*514, *endA*, *recA*1, *uidA*, *(ΔMluI)::pir-116*	Invitrogen
CC118 λ*pir*	λ*pir* lysogen of CC118 Δ (*ara-leu*), *araD*, ΔlacX74, *galE*, *galK*, *phoA*20, thi-1, *rpsE*, *rpoB*, *argE* (Am), *recA*1	E. Stabb (University of Georgia)
DH5α λpir	λ *pir* lysogen, *endA*1, *glnV*44, thi-1, *recA*1, *relA*1, *gyrA*96, *deoR*, *nupG*, φ80*lacZ*ΔM15, Δ (*lacZYA-argF*) U169, *hsdR*17	E. Stabb (University of Georgia)
HB101	*mcrB*, *mrr*, *hsdS*20, *recA*13, *leuB*6, ara-14, *proA*2, *lacY*1, *galK*2, xyl-5, mtl-1, *rpsL*20 (Sm^R) *glnV*44	ATCC
BL21/DE3	*ompT*, *gal*, *dcm*, *lon*, *hsdS*, λ (DE3 [*lacI*, *lacUV*5-T7 gene 1, *ind*1, *sam*7, *nin*5]	Invitrogen

Table 2.2 Plasmids used in this study.

Plasmid name	Description	Source
pWEB-TNC	High capacity cosmid vector derived from pWE15 ColE1 origin, Amp^R, Cm^R	Epicentre
pCR2.1-TOPO	General cloning vector with topoisomerase for efficient insertion, Amp^R, Km^R	Invitrogen
pET-101	Expression vector with IPTG inducible T7 promoter and overhang for directional cloning, Amp^R	Invitrogen
pEVS104	pRK2013-derived conjugal transfer helper plasmid. R6Kγ replication origin, Km^R	Stabb and Ruby, 2002
pDS132	pCVD442-derived suicide vector with R6Kγ replication origin, *oriT* and *sacB*, Cm^R	Philippe *et al.*, 2004
pDS-*ompA*	pDS132 with deletion cassette for *ompA*	This study
pDS-*mshE*	pDS132 with deletion cassette for *mshE*	This study
pDS-*mshL*	pDS132 with deletion cassette for *mshL*	This study
pDS-*pilA*	pDS132 with deletion cassette for *pilA*	This study
pDS-*mshA*1	pDS132 with deletion cassette for *mshA*1	This study
pDS-*mshA*2	pDS132 with deletion cassette for *mshA*2	This study
pDS-*mshA3*	pDS132 with deletion cassette for *mshA3*	This study
pVSV102	pES213-derived vector encoding pQBI63-derived *gfp* downstream of *lac* promoter, R6Kγ and pES213 replication origins, Km^R	Dunn *et al.*, 2006
pVSV208	pES213-derived vector encoding pDSRed.T3-N1-derived *rfp* downstream of *lac* promoter, R6Kγ and pES213 replication origins, Cm^R	Dunn *et al.*, 2006
pVSV105	pES213-derived shuttle vector containing lacZα, R6Kγ and pES213 replication origins, CmR	Dunn *et al.*, 2006
pVSV-*ompA*	pVSV105 containing *ompA* with native promoter	This study
pLM1877	pMMB66EH derived low copy number expression vector with *lac* promoter, Gm^R, Amp^R	Fürste *et al.*, 1986
pLMSAC	pLM1877 with Gm^R gene removed by *Sac*I digest followed by ligation	This study

Table 2.2 continued.

pLM-*mshE*	pLM1877 with *mshE* cloned downstream of *lac* promoter	This study
pLM-*mshL*	pLM1877 with *mshL* cloned downstream of *lac* promoter	This study
pLM-*pilA*	pLM1877 with *pilA* cloned downstream of *lac* promoter	This study
pLM-*mshA*1	pLM1877 with *mshA*1 cloned downstream of *lac* promoter	This study
pLM-*mshA*2	pLM1877 with *mshA*2 cloned downstream of *lac* promoter	This study
pLMSAC-*ompA*	pLMSAC with *ompA* wild type allele cloned downstream of *lac* promoter	This study

Table 2.3 Oligonucleotides used in this study.

Oligonucleotide	Sequence 5' – 3'	Binding site
VP2523.DelA	GAA TAC GCA GAA ACC GGA G	Binds 353bp upstream of *pilA* ATG start
VP2523.DelB	TGC AAC CAT CCA GAG TGA AAC CCT G	Binds 42bp downstream of *pilA* ATG start with 10bp overhang complementary to 5' end of CD product
VP2523.DelC	TTC ACT CTG GAT GGT TGC AGT TAA TAC	Binds 15bp upstream of *pilA* TAA stop with 9bp overhang complementary to 3' end of AB product
VP2523.DelD	CCG CCA ACA CCA ACT CAA C	Binds 388bp downstream of *pilA* TAA stop
VP2523.For	ATC ATT AAA AAG GGC CAC TAG G	Binds 208bp upstream of *pilA* ATG start
VP2523.Rev	CCG TGT ATT AAC TGC AAC CAT C	Binds 7bp downstream of *pilA* TAA stop
VP2523.Int	TCG ACG GTG GGA TAC TAA C	Binds 95bp upstream of *pilA* TAA stop
VP2697.DelA	ACC CAG TAG CAG CAG ATA AC	Binds 304bp upstream of *mshA*3 ATG start
VP2697.DelB	GTT ATT TTG CAT ATG AAC CAT TCC GAG	Binds 12bp downstream of *mshA*3 ATG start with 9bp overhang complementary to 5' end of CD product
VP2697.DelC	TCA TAT GCA AAA TAA CTA GAT ATT GG	Binds 12bp upstream of *mshA*3 TAG stop with 7bp overhang complementary to 5' end of CD product
VP2697.DelD	CGA TTA ACC TGC ACT TGG C	Binds 291bp downstream of *mshA*3 TAG stop
VP2698.For	AGA TAC AGT ATC CAC TTC ACG G	Binds 135bp upstream of *mshA*1 ATG start
VP2698.Rev	GCT GGC CTT TAT AAC ACC G	Binds 20bp downstream of *mshA*1TAA stop
VP2698.Int	GCA GCT AAG GTA AAA GCA GG	Binds 96bp upstream of *mshA*1 TAA stop
VP2701.For	TCT CGA ATC AGT CGC AAG C	Binds 67bp upstream of *mshE* ATG start
VP2701.Rev	TTC ACC GCA TCG ACT TTG CC	Binds 79bp downstream of *mshE* TAG stop
VP2701.Int	AAA CTA CAA ACC GCT TCT TGC C	Binds 124bp upstream of *mshE* TAG stop
VP2704.For	TAA AGC GTG GTA GCC GTC AG	Binds 79bp upstream of *mshL* ATG start

Table 2.3 continued.

VP2704.Rev	AGC TAA CGT TTC TTC TGC G	Binds 20bp downstream of *mshL* TAA stop
VP2704.Int	ACT TGT TCC GCA ACA CTT C	Binds 146bp upstream of *mshL* TAA stop
VPA0747.DelA	AGT CCC ATC GCA AGC AAG	Binds 415bp upstream of *mshA*2 ATG start
VPA0747.DelB	TAG TTG GCG GGC CGA GTA TCA CAA TCA C	Binds 60bp downstream of *mshA*2 ATG start with 10bp overhang complementary to 5' end of CD product
VPA0747.DelC	ACT CGG CCC GCC AAC TAC ATC AAA C	Binds 54bp upstream of *mshA*2 TAA stop with 7bp overhang complementary to 3' end of AB product
VPA0747.DelD	GAT ACT TTG GCG TCG TCA GG	Binds 414bp downstream of *mshA*2 TAA stop
VPA0747.For	TCG CTC TAT AAT GCT GAC CC	Binds 103bp upstream of *mshA*2 ATG start
VPA0747.Rev	TTA TCG CTC ATC AAG CAC	Binds 61bp downstream of *mshA*2 TAA stop
VPA0747.Int	CTC CGC CAA CTA CAT CAA AC	Binds 56bp upstream of *mshA*2 TAA stop
VPA0248.DelA	TAA CAA CCA CCC TGA TCC G	Binds 557bp upstream of *ompA* ATG start
VPA0248.DelB	TTA TTG AGC TGC AAT AGC GAT TTT TTT C	Binds 21bp downstream of *ompA* ATG start with 9bp overhang complementary to 5' end of CD product
VPA0248.DelC	TAT TGC AGC TCA ATA ATT TGT TGC	Binds 9bp upstream of *ompA* TAA stop with 7bp overhang complementary to 3' end of AB product
VPA0248.DelD	CAT TCG GTA CCG TGT TGG	Binds 610bp downstream of *ompA* TAA stop
VPA0248.For	CTT GCT TAA TTT GTG TTG CTT TGT G	Binds 47bp upstream of *ompA* ATG start
VPA0248.Rev	GCT GGC TTT TTG CTT TGT TGG	Binds 34bp downstream of *ompA* TAA stop
VPA0097.For	CAC CAT GAG CGG CGA CAT C	Binds on *emrA* ATG start with CACC overhang for directional pET cloning , used for amplification of *emrA* and *emrAB*

Table 2.3 continued.

VPA0097.Rev	GTA ATT TGA TGG CTC ATT G	Binds 13bp downstream of *emrA* TGA stop, used for amplification of *emrA*
VPA0098.For b	CAC CAT GAG CCA TCA AAT TAC GGC AG	Binds on *emrB* ATG start with CACC overhang for directional pET cloning, used for amplification of *emrB*
VPA0098.Rev	AAA CGC CTC TCA AGC TGA CAC	Binds 64bp downstream of *emrB* TAA stop, used for amplification of *emrAB*
VPA0098.Revb	AAC GCC TCT CAA GCT GAC AC	Binds 63bp downstream of *emrB* TAA stop, used for amplification of *emrB*
EMRAB.Flank_For	TGC GTG GTA TGC AAA CAT TG	Binds 350bp upstream of *emrA*, used to construct template for *emrB* and *emrAB* nested PCR
EMRAB.Flank_Rev	ACA TGC AGC GAC AAG AGT G	Binds 224bp downstream of *emrB* TAA stop, used to construct template for *emrB* and *emrAB* nested PCR
pLM1877.For	ACC CTG AAT TGA CTC TCT TCC	Binds 370bp upstream of *EcoR*I in MCS on pLM1877
pLM1877.Rev	CAC GTA GAT CAC ATA AGC ACC	Binds 700bp downstream of *EcoR*I in MCS on pLM1877
T7.For	TAA TAC GAC TCA CTA TAG GG	Binds 93bp upstream of CACC insert site on pET101
T7.Rev	CTA GTT ATT GCT CAG CGG T	Binds 170bp downstream of insert site on pET101
pWEB.For	TCG TCT TCA AGA ATT CGC GGC	Binds 31bp upstream of *Sma*I insert site on pWEB-TNC
pWEB.Rev	ACG ACT CAC TAT AGG GAG AGG	Binds 21bp downstream of *Sma*I insert site on pWEB-TNC
M13.For	TGT AAA ACG ACG GCC AGT	Binds 111bp downstream of PCR insert site on pCR2.1
M13.Rev	GAG CGG ATA ACA ATT TCA CAC AGG	Binds 111bp upstream of PCR insert site on pCR2.1

All oligonucleotides in the above table were designed throughout the course of this study.

2.2 Methods to evaluate adherence and invasion efficiency

2.2.1 Analysis of bacterial adherence

2.2.1a Enumeration of adherence efficiency.

Bacterial strains were prepared for co-incubation as described in section 2.1.1b. Inoculum count was determined by serial dilution of the inoculum followed by plating on LBN agar (*V. parahaemolyticus*) or LB agar (*E. coli*). Bacteria were added to quadruplicate wells of Caco-2 at an MOI of 10. Co-incubation was carried out for 1 h. The medium was discarded and non-adherent bacteria were removed by washing monolayers three times with 1 ml PBS per wash. Caco-2 cells were lysed by incubation in PBS + 1% (v/v) Triton X-100 for 10 min. The lysate was serially diluted and plated on LBN agar (*V. parahaemolyticus*) or LB agar (*E. coli*). Plates were incubated at 37°C overnight and the numbers of colony forming units (cfu) were recorded. The adherence efficiency was calculated as the number of adherent cfu expressed as a percentage of the number of cfu in the inoculum.

2.2.1b Microscopic analysis of *V. parahaemolyticus* adherence by giemsa staining.

For microscopic visualisation of adherence, Caco-2 were cultured as described in section 2.1.2. Bacteria were added at an MOI of 10 and incubated for 1 h. The medium was discarded and the monolayers were washed 3 times with PBS. The monolayers were fixed by incubation in 300 µl 4% paraformaldehyde per well for 20 min. 300 µl 5% giemsa was added per well and incubated for 20 min. The stain was removed and a 20 µl drop of PBS was placed in the centre of each well in order to keep cells hydrated during visualisation.

The cells were visualised using a Leica DMI3000 B inverted microscope and a 40X objective. 10 fields were analysed per strain. The number of cell-associated *Vibrio* was calculated per field. The number of cell-associated bacteria per cm^2 was calculated using the

field size of 157 µm X 118 µm. Three experimental replicates were carried out and results were expressed as mean plus standard deviation Log_{10} cfu cm^{-2}.

2.2.1c Visualisation of *V. parahaemolyticus* adherence by epifluorescence microscopy.

V. parahaemolyticus wild type and TTSS mutants carrying the plasmid pVSV102, which allows for constitutive expression of green fluorescent protein (GFP) were prepared for co-incubation as described in section 2.1.1b. Caco-2 cells were cultured for 9 days on sterile 12 mm glass coverslips as described in methods section 2.1.2 (9 days growth required for confluency. Medium was changed after 4 days and medium without antibiotics was added after 8 days). The adherence assay was carried out as described previously (section 2.2.1). Following the removal of non-adherent bacteria, the Caco-2 cells were fixed in 4% paraformaldehyde for 20 min at room temperature. The cells were permeabilised by incubation in PBS + 0.1% (v/v) Triton X-100 for 5 min and then stained by incubation in staining solution (165 nM phalloidin-Alexa Fluor 568, 1.6 µg ml^{-1} Hoechst 33258 in PBS + 0.1% (w/v) BSA or 100 nM phalloidin-FITC, 1.6 µg ml^{-1} Hoechst 33258 in PBS + 0.1% (w/v) BSA) for 20 min at room temperature. Coverslips were washed twice with 1 ml PBS per wash and mounted on 5 µl drops of polyvinyl alcohol mounting medium.

Cells were visualised using a Leica DMI3000 B inverted microscope and a 40X objective. The following Leica filter cubes were used: D (hoechst), GFP (GFP and phalloidin-FITC), and N2.1 (RFP and phalloidin-Alexa568). Overlays were created using Leica Application Suite.

2.2.2 Gentamicin protection assay to enumerate invasion efficiency.

Bacterial strains were prepared for co-incubation as described previously (section 2.1.1b). Inoculum count was determined by serial dilution of the inoculum followed by plating on

LBN agar (*V. parahaemolyticus*) or LB agar (*E. coli*). Bacteria were added to quadruplicate wells of Caco-2 at an MOI of 10. Co-incubation was carried out for 1 h. The medium was discarded and the monolayers were washed with 1 ml PBS per well. Extracellular bacteria were killed by incubating in 1 ml DMEM + 50 μg ml^{-1} gentamicin per well for 1 h. The DMEM with gentamicin was discarded and the monolayers were again washed with 1 ml PBS per well. Caco-2 cells were lysed by incubation in PBS + 1% (v/v) Triton X-100 for 10 min. The lysate was serially diluted and plated on LBN agar (*V. parahaemolyticus*) or LB agar (*E. coli*). Plates were incubated at 37°C overnight and the numbers of cfu were recorded. Invasion efficiency was calculated as the number of invasive cfu expressed as a percentage of the number of cfu in the inoculum.

2.2.3 Enumeration of intracellular proliferation.

The gentamicin protection assay was carried out as described in section 2.2.2. Following killing of extracellular bacteria, the DMEM + 50 μg ml^{-1} gentamicin was removed and DMEM + 10 μg ml^{-1} gentamicin was added. Prolonged incubations at high concentrations of gentamicin can kill intracellular bacteria (Brown and Percival, 1978). At selected time points following the addition of DMEM + 10 μg ml^{-1} gentamicin, the medium was removed, the monolayers were washed with 1 ml PBS per well and the Caco-2 cells were lysed by incubation in PBS + 1% (v/v) Triton X-100 for 10 min. The lysate was serially diluted and plated on LBN agar. Plates were incubated at 37°C overnight and the number of cfu was recorded. Proliferation was recorded by calculating the percentage of the initial cfu (point at which DMEM + 10 μg ml^{-1} gentamicin was added) present at each time point.

2.3. Genomic library preparation and selection methods.

2.3.1 Library preparation.

A 40 kb genomic library of *V. parahaemolyticus* RIMD2210633 was prepared in the cosmid pWEB-TNC, using the pWEB-TNC Cosmid Cloning Kit (Epicentre) according to the manufacturer's instructions. First, *V. parahaemolyticus* genomic DNA was isolated using the Promega Wizard Genomic DNA Purification Kit according to manufacturer's instructions. DNA was passed through a Hamilton 51 μm bore syring needle four times to achieve the appropriate level of shearing. Sheared DNA was end-repaired with the End-Repair Enzyme Mix from the pWEB-TNC Cosmid Cloning Kit.

Size selection was carried out by pulsed field gel electrophoresis in a 1% Seakem Gold agarose gel. The gel was stained by incubation in 1X Sybr Gold (Invitrogen) (pH 7.5) gel stain for 30 min with gentle shaking. The gel was visualised using blue light in the Syngene G:Box. Insert DNA of approximately 40 kb was excised.

DNA was purified from the excised gel fragment using Gelase reagents from the pWEB-TNC Cosmid Cloning Kit. Gelase and SYBR gold were removed by ethanol and ammonium acetate precipitation. The DNA pellet was resuspended in TE buffer.

Ligation was carried out with 383 ng insert DNA, 2 U Fast-Link DNA Ligase (Epicentre) and 0.5 μg pWEB-TNC Cosmid Vector. Ligated cosmids were packaged using Max Plax lambda packaging extract (Epicentre) according to manufacturer's instructions. The library was titered and aliquots of packaged cosmids containing a 5X coverage of the *V. parahaemolyticus* genome with a 99.9% probability of containing a given sequence were prepared. Packaged library aliquots were stored at -80°C in 20% (v/v) glycerol.

3 clones from the initial library titering were selected at random and sent for sequencing with pWEB.For and pWEB.Rev primers in order to verify the presence of distinct fragments of *V. parahaemolyticus* DNA. Sequence data from the extremities of the inserts in each clone were aligned with *V. parahaemolyticus* sequence data in the NCBI BLAST database. Clones were labelled C1, C2 and C3.

For selection of the bacterial genomic library, an aliquot of packaged, titered cosmids was adsorbed on to exponential phase *E. coli* HB101 at 37°C for 30 min with gentle mixing. 100 µl aliquots were spread on to LB agar + ampicillin and plates were incubated at 37°C overnight. Following overnight growth, each plate was rinsed with LB broth + 100 µg ml^{-1} ampicillin and colonies were gently scraped from the plate with a spreader. This rinse solution containing pWEB-TNC clones was aspirated and pooled.

The first library invasion selection (section 2.3.2) was started immediately using a 1 ml aliquot of the pooled library. Glycerol stocks were also prepared from the pooled library and stored at -80°C for future experiments.

2.3.2 Selection of invasive library clones with one round of selection.

A 1 ml aliquot of pooled bacterial genomic library was added to a 1.5 ml microcentrifuge tube and, without further growth was washed and prepared for co-incubation as described in section 2.1.1b. Bacteria were added at an MOI of 10 to 4 wells of confluent 7 day Caco-2. The gentamicin protection assay was employed to isolate invasive library clones as per section 2.2.2. The entire lysate was spread plated on LB agar + ampicillin. The 37 invasive clones were labelled A1 to A37. The experiment was repeated the following day and a further 18 invasive clones were isolated (B1 to B18). Subsequently the invasion efficiency of each clone was enumerated by further gentamicin protection assays, using pure cultures of each clone on duplicate wells of Caco-2.

2.3.3 Selection of invasive library clones using multiple rounds of selection.

For the first round of selection a 1.5 ml aliquot of library glycerol stock was added to 20 ml LB + chloramphenicol and the flask was incubated for 3 h 30 min (OD_{600} = 0.5). 1 ml culture was added to a 1.5 ml microcentrifuge tube and then prepared for co-incubation as described in method section 2.1.1b. Bacteria were added at an MOI of 10 to 10 wells of confluent 7 day Caco-2. Following co-incubation and elimination of extracellular bacteria as described in section 2.2.2, the Caco-2 cells were lysed with 100 µl PBS + 1% (v/v) Triton X-100 and the lysate was added to a flask containing 100 ml LB broth + chloramphenicol and cultured overnight at 37°C with shaking. A further 2 wells of Caco-2 were used for enumeration of library invasion efficiency.

For the second round of selection, a 1 ml aliquot was removed from the overnight culture of library clones isolated from invasion selection round 1, and was prepared for co-incubation. Isolation of invasive clones was repeated as described above and the lysate from this second invasion selection round was used to inoculate a fresh overnight culture in 100 ml LB broth + chloramphenicol.

The invasion selection procedure was repeated for 4 rounds in total. For the final round of invasion selection, a total of 16 clones were isolated from 4 wells of Caco-2. Glycerol stocks were prepared and labelled D1 to D16.

2.3.4 Profiling of D series clones by restriction digest.

Minipreps of all 16 clones were carried out with the Qiaprep Spin Miniprep kit. Preps were digested using a mix of *Bam*HI, *Sph*I and *Xba*I and electrophoresed on a 0.8% (w/v) agarose gel. 2 clones displaying each banding pattern were selected and sent for sequencing with pWEB.For and pWEB.Rev primers. 3 representative genetically distinct D series clones: D5,

D6 and D9 were used for subsequent enumeration of invasion efficiency by the gentamicin protection assay as described in section 2.2.2.

2.3.5 Selection of adherent library clones using a single round of selection.

The genomic library was prepared for co-incubation as per section 2.1.1b. Following 1 h of co-incubation in quadruplicate wells of Caco-2, the medium was removed and the monolayers were washed as per adherence assay described in section 2.2.1. The total number of adherent clones enumerated from 4 replicate wells was 4.3 X 10^4 cfu. 40 clones were selected from isolated colonies and streaked on LB agar + chloramphenicol. The clones were labelled E1 to E40. The clones were screened by adherence assay on duplicate wells of Caco-2 as described in methods section 2.2.1, to identify any clones exhibiting increased levels of adherence.

2.3.6 Selection of adherent library clones using multiple rounds of selection.

In order to optimise selection of adherent library clones, the selection process was adapted. The lysate from a single round of selection (4 X 1 ml aliquots) was added to 40 ml of LB broth + chloramphenicol. The flask was incubated at 37°C with shaking overnight. 1 ml overnight culture was taken and centrifuged at 10,000 X *g* for 2 min. Supernatant was discarded and the pellet was washed with 1 ml PBS. Centrifugation was repeated and the pellet was resuspended in 1 ml PBS. The OD_{600} of the cell suspension was adjusted to 0.2 in 1 ml. 45 µl aliquots were then added to quadruplicate wells of 7 day cultured Caco-2 (MOI = 10). The adherence assay was repeated as per section 2.2.1. The lysate from the second round of selection was used to inoculate a fresh 40 ml aliquot of LB broth + chloramphenicol. The flask was incubated at 37°C with shaking overnight and selection was repeated. In total selection was carried out 4 times, at which point the total number of cfu of adherent clones from 4 replicate wells was 2.4 X 10^5. Again 40 clones were selected from isolated colonies

and streaked on LB agar + chloramphenicol. The clones were labelled F1 to F40. Finally, the clones were screened by adherence assay on duplicate wells of Caco-2 as described in methods section 2.2.1, to identify any clones exhibiting increased levels of adherence.

2.3.7 Library validation by antibiotic selection.

The pWEB-TNC based genomic library was validated by carrying out selection for norfloxacin resistance mechanisms. Glycerol stocks of the genomic library were diluted by tenfold serial dilution and spread plated on LB agar and LB agar + 0.1 μg ml^{-1} norfloxacin. 8 resistant clones were selected and sent for sequencing with pWEB.For and pWEB.Rev primers. Minimum inhibitory concentrations (MICs) were determined for each of the norfloxacin resistant clones by incubation in LB broth with doubling dilutions of norfloxacin concentrations from 0.3 μg ml^{-1} to 0.02 μg ml^{-1} and monitoring growth over 24 h using the Tecan Sunrise Absorbance Reader.

2.3.8 Bioinformatic analysis

Following functional analysis, clones of interest were chosen for identification of the insert DNA. Cosmid DNA was prepared using the Qiaprep Spin Miniprep kit and the extremities of the cosmid inserts were sequenced using pWEB.For and pWEB.Rev primers. These sequences were aligned to the genomic sequence of *V. parahaemolyticus* RIMD2210633 using NCBI BLAST to identify DNA region contained in each insert. The genes within this region were identified using CMR and EMBL databases.

Each gene contained within insert DNA was then analysed using a range of bioinformatic tools including BLAST analysis, Pfam motif analysis, pSORTb analysis to determine subcellular localisation, Transmembrane Hidden Markov Model analysis (TmHMM)

(Comprehensive Microbial Resource), and putative operon assignment coupled with literature analysis.

2.4 Generation of genetic constructs and *V. parahaemolyticus* mutants to investigate putative adhesins, invasins and antimicrobial resistance mechanisms.

2.4.1 Generation of a knock-out mutation in *V. parahaemolyticus.*

2.4.1a Construction of a mutated allele by overlap extension PCR.

First, a mutated allele of *ompA* with an inactivating in-frame deletion was constructed. This mutated *ompA* allele was generated using the process of overlap extension PCR (See Fig 5.7, page 197). The accuzyme proof reading polymerase mix was used for all PCR reactions (Bioline). Briefly, a region of DNA containing 7 codons of *ompA* and 557 bp of upstream DNA was amplified from *V. parahaemolyticus* RIMD2210633 genomic DNA by PCR using primers VPA0248.DelA and VPA0248.DelB. The resulting PCR product was denoted VPA0248.DelAB. The reverse primer VPA0248.DelB was designed such that its 5' end contained a 9 bp overlap which was complementary to the VPA0248.DelCD product. VPA0248.DelCD was produced by PCR amplification of the 3 terminal codons of *ompA* and 610 bp of DNA downstream of *ompA* using primers VPA0248.DelC and VPA0248.DelD. The forward primer VPA0248.DelC was designed with a 7 bp overhang at its 5' end which was complementary to the terminal region of the VPA0248.AB product. AB and CD products were isolated by agarose gel electrophoresis and purified.

25 ng purified VPA0248.AB and VPA0248.CD templates were added to 25 µl of 2X Accuzyme mix and the reaction volume was completed to 46 µl with PCR water. 5 PCR cycles were carried out with an annealing temperature of 50°C, to allow for fusion of the AB

template to the CD template *via* complementary over hangs on the Del.B and Del.C primers. 0.4 pmol μl^{-1} of primers VPA0248.A and VPA0248.D was then added and PCR was carried out for 30 cycles with an annealing temperature of 68°C. The resulting product was a truncated form of *ompA* with only the first 7 and last 3 codons remaining.

2.4.1b Topo TA cloning of mutated allele into pCR2.1.

The next step was to insert the mutated *ompA* allele into the pCR2.1 cloning vector by TA cloning. As 3' adenylation was required in order to carry out TA cloning into pCR2.1, 1 U of BIOTAQ Taq polymerase (Bioline) was added to the PCR reaction and the mix was heated to 72°C for 10 min. Positive clones were identified by plasmid miniprep followed by restriction digest and sequences were verified by sequencing with M13.For and M13.Rev primers.

2.4.1c Cloning of mutated allele into pDS132.

Following sequence confirmation, the *ompA* deletion allele was excised from the pCR2.1-derived plasmid using restriction enzymes *Xba*I and *Sac*I (section 2.1.8), isolated by agarose gel electrophoresis, purified and ligated into pDS132 suicide vector (section 2.1.10).

pDS132 contains a Π-dependent origin of replication and thus cannot replicate in *E. coli* lacking the Π protein (Reyrat *et al.*, 1998). As such, recombinant pDS132 containing the *ompA* deletion construct was transformed into One Shot Competent Pir1 *E. coli* (Invitrogen). Positive clones were identified by miniprep followed by restriction digest and labelled *E. coli* PIR1 (pDS-*ompA*).

2.4.1d Introduction of mutated allele into *V. parahaemolyticus* by triparental conjugation.

The plasmid pDS-*ompA* was conjugated into *V. parahaemolyticus* by triparental conjugation. Briefly, 1 ml aliquots of *V. parahaemolyticus*, *E. coli* PIR1 (pDS-*ompA*) and *E. coli* CC118 *λ*

pir (pEVS104) overnight cultures were centrifuged at 5,000 X *g* for 5 min. The supernatants were discarded and the pellets were washed with 1 ml LB broth. Centrifugation was repeated and the pellets were resuspended in 500 µl LB broth. 250 µl of each *E. coli* strain was added to a tube containing 100 µl *V. parahaemolyticus*. Centrifugation was repeated, the supernatants were again discarded and the pellet was placed on an LB agar plate. The triparental conjugation was incubated at 37°C for 5 h. The bacteria were scraped from the plate and resuspended in 500 µl LB. 100 µl of the resuspended pellet was then spread on LBN agar + chloramphenicol to select for ex-conjugants. The plate was incubated at 37°C overnight. Large ex-conjugant colonies were streaked on TCBS + chloramphenicol to confirm conjugation.

As *V. parahaemolyticus* does not possess the Π protein, and therefore cannot replicate pDS132 extra-chromosomally, any ex-conjugant colonies can be considered first recombinants. Either the AB or the CD region of the deletion cassette has recombined with its homologous locus on the chromosome and the entire vector has integrated upstream or downstream of the site of recombination (Fig 5.8). In Fig 5.8, first recombination via the AB or upstream region is shown, however recombination can also occur via the CD or downstream homologous region. The *sacB* gene on pDS132 codes for levansucrase which produces toxic byproducts in the hydrolysis of sucrose (Gay *et al.*, 1983). In order to encourage plasmid loss by secondary recombination, the first recombinants were grown in the absence of selection. A first recombinant colony was inoculated in 2 ml LBN broth and incubated overnight at 37°C with shaking. 20 µl overnight culture was used to inoculate a second 2 ml aliquot of LBN broth, which was incubated at 37°C with shaking for 6 h. Finally, 20 µl from the 6 h culture was used to inoculate 2 ml LBN broth which was again incubated at 37°C with shaking overnight. Tenfold serial dilutions of the overnight culture were carried out and plated on LBN agar + 10% (w/v) sucrose to select for recombinants

lacking *sacB* and therefore pDS132. The absence of pDS132 was confirmed by replica plating in LBN broth alone and LBN broth containing chloramphenicol. Only chloramphenicol sensitive recombinants were used in further analysis. Second recombinants at this point must be either *ompA* knock out mutants or wild type *V. parahaemolyticus* (Fig 5.8).

Final confirmation of *ompA* knockout was confirmed by PCR amplification of regions flanking the *ompA* deletion. PCR with the primers VPA0248.DelA and VPA0248.DelD resulted in a 2,145 bp product for the wild type *ompA* allele and a product of 1,196 bp for the truncated knockout form. Wells from the replica plate which yielded positive bands for Δ*ompA* were streaked on LBN agar and colony PCR was carried out with primers VPA0248.DelA and VPA0248.DelD to confirm the presence of the deletion (Fig 5.9A).

2.4.1e Construction of type IV pilus (TFP) deletion mutants.

The genes *mshE*, *mshL*, *mshA*1, *mshA*2, *mshA3* and *pilA* which are encoded on loci: *VP2701*, *VP2704*, *VP2698*, *VP2697*, *VPA0747* and *VP2523* respectively, were selected for analysis of involvement in *V. parahaemolyticus* pathogenicity. Single, double and triple deletion mutants were constructed as described in methods section 2.4.1a - 2.4.1d. For *mshA*2, *mshA3* and *pilA*, deletion constructs were produced by overlap PCR of homologous loci upstream and downstream of the gene of interest, as shown in Fig 5.7, using the primers listed in Table 2.3. For *mshE*, *mshL* and *mshA*1, deletion alleles were produced using Eurofins gene synthesis and were cloned into pCR2.1. Vector constructions, conjugations and recombinant selections were carried out as described in section 2.4.1b - 2.4.1d. Second recombinants were screened using the primers listed in Table 2.3.

2.4.2 Complementation of deletions in *V. parahaemolyticus*.

2.4.2a Complementation of *ompA*.

In order to confirm any phenotype associated with Δ*ompA*, the wild type form of the gene was re-introduced into the deletion background. *ompA* was amplified by PCR using the VPA0248.For and VPA0248.Rev primers. VPA0248.For binds 48 bp upstream of the *ompA* start codon, so as to include the native promoter. VPA0248.Rev binds 34 bp downstream of the *ompA* stop codon. Accuzyme PCR was carried out and products were TOPO cloned into pCR2.1. *ompA* was excised from the pCR2.1 derivative by restriction digest with *Sac*I and *Sph*I and subcloned into the shuttle vector pVSV105, to make the recombinant vector pVSV-*ompA*. pVSV105 contains an R6Kγ origin of replication, which similar to the Π-dependent origin of replication from pDS132 also requires a *pir* background of *E. coli*. It has however been shown to replicate at low levels in *Vibrio* (Dunn *et al.*, 2006). pVSV-*ompA* was transformed into One Shot Pir1 and subsequently conjugated into *V. parahaemolyticus* Δ*ompA* as described in methods section 2.4.1d.

2.4.2b Construction of TFP complementation mutants.

Complementation plasmids were constructed for *mshE*, *mshL*, *mshA*1, *mshA*2 and *pilA*. Briefly, the wild type form of each gene was amplified by Accuzyme PCR with primers designed such that the forward primer annealed upstream of the start codon but downstream of the promoter and the reverse primer annealed downstream of the stop codon but not downstream of the start codon of the adjacent gene (Table 2.3 for primers). PCR products were 3' adenylated and TOPO cloned into pCR2.1. Sequences were confirmed by sequencing with M13.For and M13.Rev primers and inserts were digested from pCR2.1 with appropriate restriction endonucleases. Wild type alleles were then ligated into digested and de-phosphorylated pLM1877 (Plasmids listed in Table 2.2), as described in section 2.1.10. Each

plasmid was transformed into *E. coli* Top10. Following confirmation of correct insert orientation by restriction digest, triparental conjugations into the corresponding *V. parahaemolyticus* deletion mutant were carried out as per section 2.4.1d. Triparental conjugation was also carried out using DH5α (pLM1877) as a donor strain to create empty vector controls for each deletion background. Ex-conjugants were selected by plating on LBN containing 25 µg ml^{-1} gentamicin. See Table 2.2 for detailed description of each complementation vector.

2.4.3 Expression of OmpA in *E. coli* HB101.

The *ompA* gene was cloned into an inducible expression vector and transformed into *E. coli* HB101. This was done to allow for analysis of possible *E. coli* specific function of *V. parahaemolyticus* OmpA. pLM1877 is an expression vector with a *lac* promoter and selection markers for gentamicin and ampicillin. As it was desirable to use strains in gentamicin protection assays as described in section 2.2.2, the gentamicin resistance locus was removed. First, the vector was digested with *Sac*I and the 8,800 bp vector band was isolated by agarose gel electrophoresis, followed by gel purification. The vector was then re-ligated leaving all expression machinery intact but removing the gentamicin resistance gene. This vector was labelled pLMSAC. The *ompA* insert was directionally cloned into pLMSAC by digesting pCR2.1-*ompA* with *Sac*I and *Eco*RV, and isolating the 1,122 bp product of digestion. Digestion of pLMSAC with *Sac*I and *Sma*I allowed for directional cloning of the *ompA* gene directly downstream of the *lac* promoter. This recombinant vector was labelled pLMSAC-*ompA* and was transformed into chemically competent *E. coli* HB101. The empty vector pLMSAC was also transformed into HB101 as a control.

2.4.4 Cloning of *emrAB* into pET101.

Primers were designed for amplification and cloning of *emrAB* into the expression vector pET101 as recommended by Invitrogen. Forward primers (VPA0097.For, VPA0097.Forb and VPA0098.Forb) were designed with a CACC overhang 5' to the annealing sequence. Amplification was carried out with VPA0097.Rev, VPA0098.Rev and VPA0097.Revb as reverse primers (See Table 2.3 for primers used to generate each construct). Forward primers were designed to amplify from the ATG start codon of the gene to be amplified. Insert DNA was amplified by Accuzyme PCR, gel purified and TOPO cloned into pET101. 3 µl cloning reaction mix was then transformed into One Shot Top 10 cells. Ampicillin resistant colonies were screened for insert presence by PCR using T7.For and T7.Rev primers. Minipreps of positive clones were carried out using the Qiaprep Spin Miniprep kit and preps were sent for sequencing with T7.For and T7.Rev primers. Upon confirmation of the correct insert sequence, miniprep DNA was used to transform One Shot BL21/DE3 cells.

2.5 Functional assays to investigate putative adhesins, invasins and antimicrobial resistance mechanisms

2.5.1 Growth rates of TFP deletion mutants.

As many phenotypes relating to *V. parahaemolyticus* pathogenicity are directly related to MOI, it is evident that if alterations in growth rate or fitness occur due to deletions, there may be an impact on pathogenic effects on the host cell. Growth rates were analysed using a 96 well plate based growth assay. Briefly, bacteria were prepared as outlined in section 2.1.1b. Each culture was diluted to an OD_{600} of 0.1 in triplicate 250 µl volumes of LBN broth. LBN alone was used as a blank. The plate was incubated at 37°C overnight with shaking and the

OD_{595} was measured every 30 min, using Tecan Sunrise Absorbance Reader. The OD_{595} of bacterial samples at each timepoint was calculated by subtracting the blank OD_{595} from the sample OD_{595} and taking the average of 3 sample wells per strain.

2.5.2 Transmission electron microscopy of *V. parahaemolyticus* wild type and Δ*mshA*1.

Bacteria were prepared as described in methods section 2.1.1b. 10 µl 0.1 OD_{600} culture was placed on a formvar carbon coated electron microscopy grid (Agar Scientific) and allowed to stand for 10 min. Excess PBS was drawn away with a piece of vellum paper. 10 µl 1% phosphotungstic acid (pH 7.2) was added to the grid and incubated at room temperature for 10 min. Again liquid was drawn off using vellum paper. Cells were washed with 10 µl sterile water followed by drawing off with vellum paper and allowing grids to dry for 20 min before visualisation. Stained bacteria were observed using a Hitachi H7000 transmission electron microscope.

2.5.3 Glycan binding of *V. parahaemolyticus* and TFP mutants by neoglycoconjugate (NGC) array.

Bacteria were prepared as described in methods section 2.1.1b. All centrifugation steps were carried out at 5,000 X *g* for 5 min. Following growth of exponential phase culture, bacteria were washed 3 times with tris buffered saline (TBS: 20 mM Tris, 100 mM NaCl, 1 mM Mg Cl_2, 1 mM $CaCl_2$, pH 7.2). 500 µl suspensions at an OD_{600} of 2.0 were prepared and Syto 82 dye was added to a concentration of 20 µM (All steps involving Syto 82 were carried out in the dark due to light sensitivity of stain). The tubes were wrapped in foil and incubated at 37°C for 1 h on a rotator.

Excess dye was removed by centrifuging and resuspending the pellet completely in TBS. The TBS wash was carried out 7 times. Finally, the pellets were resuspended in 300 µl TBS + 0.05% Tween 20 (TBST) and the OD_{600} of the cell suspension was corrected to 2.

50 µl stained bacteria was mixed with 20 µl TBST per subarray. 3 biological replicates were analysed per strain, with one subarray being used per replicate. 70 µl aliquots of 2 control lectins were applied to one subarray on each slide. The glycan array slide was carefully placed on top of the coverslip and sealed in place with a steel gasket. The slides were transferred to a room temperature rotator for 1 h to allow hybridisation. The gaskets and coverslips were removed from the slides. The slides were washed by six 2 min incubations in TBST, followed by two incubations in TBS for 2 min each. The slides were centrifuged at 450 X *g* for 3 min to dry.

The slides were scanned at 543 nm using Perkin Elmer Scanarray Express HT. Data was extracted using Genepix software. The values for median fluorescence intensity were derived by calculating the median value of Fluorescence at 555 nm – Background at 555 nm for 6 spots per glycan (6 spots of each NGC are printed per subarray). Mean and standard deviation of 3 biological replicates were calculated. In order to normalise subarray to subarray variation, for each strain being analysed, the sum of all fluorescences on each subarray was calculated. The values for 2 biological replicates were multiplied by a normalisation factor so that the fluorescence sum for each subarray was identical.

2.5.4 Role of TFP in *V. parahaemolyticus* induced cytotoxicity of Caco-2.

Bacteria were prepared for co-incubation as described in methods section 2.1.1b and added to triplicate wells of 7 day cultured Caco-2 at an MOI of 10. Bacteria and Caco-2 were co-incubated for 4 h. 50 µl of supernatant was removed from each well and added to a sterile 96 well plate. Negative control samples were taken from triplicate wells of uninfected Caco-2

and triplicate 50 µl volumes of sterile DMEM. Positive controls were prepared by addition of 100 µl 10X lysis solution containing 8% (v/v) Triton X-100 to triplicate wells of Caco-2 followed by incubation at 37°C, 5% CO_2 for 45 min. 50 µl reconstituted substrate mix from Promega CytoTox 96 Non-Radioactive Cytotoxicity Assay kit was added to each supernatant sample and the plate was incubated at room temperature for 20 min. 50 µl stop solution was added per well and the absorbance was read at 492 nm using a Tecan Sunrise Absorbance Reader.

Sample cytotoxicity was determined by subtracting the average OD_{492} of the DMEM control from each sample and expressing the resulting OD_{492} as a percentage of the positive control. Each sample was assayed for LDH release in duplicate.

2.5.5 Role of TFP in rounding of Caco-2.

In order to analyse cell rounding, Caco-2 were cultured for 9 days on glass coverslips as described in methods section 2.2.1c. Bacteria were prepared as described in section 2.1.1b and were added to confluent Caco-2 at an MOI of 10. Bacteria and Caco-2 were co-incubated for 2.5 h. The monolayers were fixed by incubating in 300 µl 4% paraformaldehyde for 20 min. The cells were permeabilised by incubation in 300 µl PBS + 0.1% (v/v) Triton X-100 for 5 min. Cells were stained with 165 nM phalloidin-Alexa Fluor 568, 1.6 µg ml^{-1} Hoechst 33324 in PBS + 0.1% (w/v) BSA) for 20 min. Coverslips were washed twice with PBS and mounted on 5 µl drops of polyvinyl alcohol mounting medium with DABCO.

Cells were visualised using a Leica DMI3000 B inverted microscope and a 40X objective. Filter cube D was used for hoechst and filter cube N2.1 for phalloidin-Alexa 568. Overlays were created using imageJ.

2.5.6 *V. parahaemolyticus* stimulated interleukin 8 (IL-8) induction in Caco-2.

To analyse the mechanism of *V. parahaemolyticus* IL-8 induction, Caco-2 were cultured in 24 well plates as described in methods section 2.1.2. 1 h prior to co-incubation, IL-1β was added to triplicate wells of Caco-2 to a final concentration of 20 ng ml^{-1}. IL-1β serves as a positive control for IL-8 induction. In some experiments Bay 11-7082 was incubated with Caco-2 at concentrations ranging from 6 µM to 10 µM, 1 h prior to co-incubation. Bacteria were added to triplicate wells of Caco-2 and co-incubation was carried out for 2 h. The medium was removed and the cells were washed with PBS. 1 ml DMEM + 50 µg ml^{-1} gentamicin was added per well to kill bacteria. Co-incubation was allowed to proceed for a total of 24 h with 25 µl supernatant samples being taken periodically for determination of IL-8 concentrations. Firstly, a time-course of IL-8 secretion following infection with *V. parahaemolyticus* was carried out. Samples were taken 2 h, 3 h, 4 h, 6 h, 8 h, 20 h and 24 h after addition of bacteria and stored at -20°C for enzyme linked immuno-sorbent assay (ELISA) at a later stage.

IL-8 concentrations were determined by ELISA using Human IL-8/NAP-1 Matched Antibody Pairs (Bender Medsystems). 50 µl 5 µg ml^{-1} IL-8 coating antibody solution in PBS was added per well to a 96 well ELISA plate. The plate was immediately sealed and incubated at 4°C overnight. Coating antibody solution was aspirated and discarded. The ELISA plate was washed with twice with 300 µl wash buffer (PBS + 0.05% Tween-20) per well. The plate was blocked by addition of 125 µl assay buffer (wash buffer + 5 mg ml^{-1} BSA) per well followed by 2 h incubation at room temperature on an orbital shaker. The assay buffer was discarded and the plate was washed three times with 300 µl of wash buffer per well.

Duplicate doubling dilution series of standardised IL-8 from 1,000 pg ml^{-1} to 15.6 pg ml^{-1} were prepared by addition to 50 µl volumes of sample diluent on the 96 well plate. 50 µl sample diluent was included as a blank. Duplicate 25 µl or 10 µl samples of Caco-2 supernatant were added to 50 µl sample diluent. 25 µl samples of DMEM were included as a negative control. Biotin conjugated anti-human IL-8 was diluted 1:1,000 in assay buffer before use. 25 µl diluted biotin conjugate was added per well to all samples, including standards and blanks and the plate was incubated at room temperature on an orbital shaker for 2 h. The samples were discarded and the plate was washed three times with 300 µl of wash buffer per well. Strepdavidin-HRP (horseradish peroxidase) was diluted 1:10,000 in assay buffer. 50 µl diluted strepdavidin-HRP was added per well and the plate was incubated for 1 h at room temperature with gentle shaking. The strepdavidin-HRP was discarded and the plate was again washed three times with 300 µl of wash buffer per well. 50 µl 3,3′,5,5′-Tetramethylbenzidine (TMB) ELISA substrate was added per well and the plate was wrapped in foil before incubating with gentle shaking for 30 min. The reaction was stopped by addition of 50 µl 4N H_2SO_4 per well.

Absorbance at 450 nm was recorded using a Tecan Sunrise Absorbance Reader. A standard curve was constructed using both dilution series of IL-8 concentrations. A linear trend line was fitted to the standard curve and the slope of the line was noted. IL-8 concentrations were determined by subtracting the medium control OD_{450} from the sample OD_{450} and dividing the resulting value by the slope of the standard curve. The mean values of sample replicates and standard deviations were recorded.

2.5.7 Expression of EmrAB in BL21/DE3 and assessment of involvement in norfloxacin resistance.

Colonies of BL21/DE3 (pET101) and BL21/DE3 (pET-*emrAB*) were inoculated in 2 ml LB + ampicillin. The cultures were incubated at 37°C with shaking overnight. The OD_{600} was adjusted to 0.05 in 2 ml fresh LB broth + ampicillin. The cultures were incubated at 37°C with shaking for 1.5 h. IPTG was added to a final concentration of 100 μM and the cultures were induced at 37°C with shaking for a further 1.5 h. Exponential phase cultures were used to inoculate LB broth containing doubling dilutions of norfloxacin from 0.6 μg ml^{-1} to 0.04 μg ml^{-1}. MICs were determined and recorded.

Chapter 3

The adherent and invasive properties of *V. parahaemolyticus* and the role of TTSS in each process

3.1 Introduction.

Efficient adherence and colonisation are prerequisites for a successful bacterial pathogen. The gastro-intestinal tract provides a challenging environment for bacteria in which to establish an infection. Shear forces, mucus, and the presence of commensals are a few of the many obstacles encountered in establishing an initial attachment, which can lead to effective colonisation. Successful pathogens have evolved an array of virulence mechanisms to enable their establishment in the gastro-intestinal tract. Pili are particularly useful for initiating attachment to the host cell. Once initial attachment is brought about, alterations in expression occur, leading to formation of adhesin-receptor interactions between the host cell and the pathogen, allowing for the formation of a persistent infection.

Infection of intestinal cells by the pathogen *V. parahaemolyticus* is heavily reliant on the bacterium's ability to bring about an intimate attachment with the host cell. The principal cause of *V. parahaemolyticus* cytotoxicity is the secretion of effector proteins through TTSS (Matlawska-Wasowska *et al.*, 2010). Secretion *via* TTSS leads to inflammation, enterotoxicity, morphological alterations of the host cell and ultimately host cell death (Matlawska-Wasowska *et al.*, 2010; Hiyoshi *et al.*, 2010; Burdette *et al.*, 2008). Much *V. parahaemolyticus*-related research has focused on the role played by TTSS. In order to efficiently deploy and secrete effector proteins, *V. parahaemolyticus* must first establish tight adherence to the host cell. Initial contact between bacterial adhesins and the host cell may then activate expression of further bacterial adhesins, toxins and other virulence factors.

An interesting model for TTSS involvement in adherence has been presented by Kenny *et al.* (1997) who found that enteropathogenic *E. coli* secrete an effector protein known as Tir into host cells. This protein is then translocated to the apical surface of the host cell where it behaves as a receptor for the bacterial adhesin, intimin. Such a system has not been identified

in *V. parahaemolyticus*, however assessment of the adherence of TTSS mutants compared with the wild type may help to establish a connection between TTSS activity and attachment to host cells.

It is worth noting that bacterial adhesins can often function as invasins (Oelschlaeger, 2001). The intracellular environment of intestinal epithelial cells provides a niche for bacterial survival, where the stresses of the intestinal lumen (mucus, commensals etc) are absent. The intracellular environment also provides an opportunity for immune evasion, as the threats of phagocytosis, antibodies, complement and inflammation are absent. The intracellular environment is not without risk however, as increased oxidative stress and low pH can be brought about due to lysosomal fusion. It has also been shown that intracellular bacteria can be destroyed by a form of programmed host cell death known as autophagy (Rich *et al.*, 2003).

It has been shown that manipulation of the Rho GTPases RhoA, Rac1 and Cdc42 alters the invasiveness of *V. parahaemolyticus* (Akeda *et al.,* 2002). As described in Table 1.1 and Fig 1.8, TTSS effectors such as VopS, VopC and VopQ are capable of directly or indirectly modulating Rho GTPase activity (Yarbrough *et al.*, 2009; Zhang *et al.*, 2012; Burdette *et al.*, 2009). As such the TTSS of *V. parahaemolyticus* represent attractive model systems for the regulation of *V. parahaemolyticus* uptake by host cells.

It has been shown that *S.* Typhimurium, and *S. flexneri* are both capable of using TTSS to hijack host cell machinery involved in entry and vesicular trafficking, allowing induction of invasion into the intracellular environment (Cossart and Sansonetti, 2004; Fig 1.7). Following invasion, the strategies of these pathogens diverge, as *S. flexneri* escapes the endocytic vacuole favouring cell to cell spread, while *S.* Typhimurium persists within a *Salmonella* containing vacuole (SCV) (Cossart and Sansonetti, 2004). Interestingly persistence and

proliferation in the SCV is brought about by secretion of effector proteins through a second secretion system which prevents phago-lysosomal maturation and subsequent intracellular killing of *S.* Typhimurium (Brumell and Grinstein, 2004). Intracellular survival and replication of wild type *V. parahaemolyticus* in Caco-2 cells has not been studied. The following chapter will investigate the strategy employed by this pathogen in the intracellular environment.

A role for *V. parahaemolyticus* TTSS in adherence to Caco-2 cells has not yet been investigated. The following chapter will investigate the efficiency of adherence and invasion of the pandemic clone of *V. parahaemolyticus*, RIMD2210633. This strain was originally isolated in 1996 and is a member of the highly virulent O3:K6 serogroup, a clade which has since disseminated globally (Boyd *et al.*, 2008). RIMD2210633 possesses both TTSS1 and TTSS2 and since 1996, researchers have been studying this strain in order to understand the molecular mechanisms underlying its pronounced virulence (Boyd *et al.*, 2008). Assessment of adherence and invasiveness was made using comparison to a positive control for invasion: *Salmonella* Dublin, which like *Salmonella* Typhimurium is also invasive and has the ability to persist intracellularly (Wood *et al.*, 1996). Non-pathogenic lab strains of *E. coli* XL-1 blue and *E. coli* HB101 were used as negative controls for invasion and adherence.

The relative roles of TTSS1 and TTSS2 were analysed using mutants possessing inactivating deletions of the TTSS-associated ATPases *vscN*1 and *vscN*2. Deletion of the gene coding for the ATPase prevents formation of the needle complex and hence prevents secretion of effector proteins by the TTSS (Kubori *et al.*, 2000).

A cancerous human intestinal epithelial cell model was used for adherence and invasion assays. *V. parahaemolyticus* causes infection of the gastro-intestinal tract and as such, intestinal cell lines are most appropriate for use in the study of *V. parahaemolyticus*

pathogenicity. The Caco-2 cell line has the ability to differentiate, forming cells which are a good representation of the cells of the gastro-intestinal tract (Darfreuille-Michaud *et al.*, 1990; Everest *et al.*, 1992). For all experiments involving Caco-2, the cells were grown for 7 days to allow confluency to be reached and to allow for differentiation. The cell line has also been used in assessment of *V. parahaemolyticus* adherence and invasion, using methods similar to those employed in this study (Yu *et al.*, 2012; Akeda *et al.*, 2002).

3.2 Role of TTSS in adherence and invasion of *V. parahaemolyticus* to Caco-2.

In order to gain a general understanding of the adherence and invasion properties of *V. parahaemolyticus*, a number of experiments were carried out. These included the adherence assay (section 2.2.1a), the gentamicin protection assay (section 2.2.2) and an intracellular proliferation assay (section 2.2.3). These assays were carried out with the *V. parahaemolyticus* RIMD2210633 wild type, lab strains of *E. coli* with low rates of adherence and invasion, and a positive control for invasion, *S.* Dublin. TTSS deletion mutants were also included in order to gain an insight into the relative roles of TTSS in the processes of adherence, invasion and intracellular persistence.

Adherence and invasion assays were carried out by incubating Caco-2 cells with exponential phase bacteria at an MOI of 10 for 1 h. Exponential phase bacteria were used as high levels of protein are produced during this growth phase and also to ensure a high ratio of live:dead bacterial cells. An MOI of 10 was used as higher MOIs were found to cause rapid cell lysis and lower MOIs resulted in poor activation of MAPKs, a phenotype associated with *V. parahaemolyticus* infection (Boyd lab, unpublished data). At an MOI of ten, cell rounding was evident at time points later than 1 h and it was believed that this may indirectly affect the enumerable counts of adherent/invasive bacteria. As such, co-incubation times of 1 h were

routinely employed. Adherent/invasive bacteria were selected as outlined in section 2.2.1a and 2.2.2 and were enumerated by spread plating.

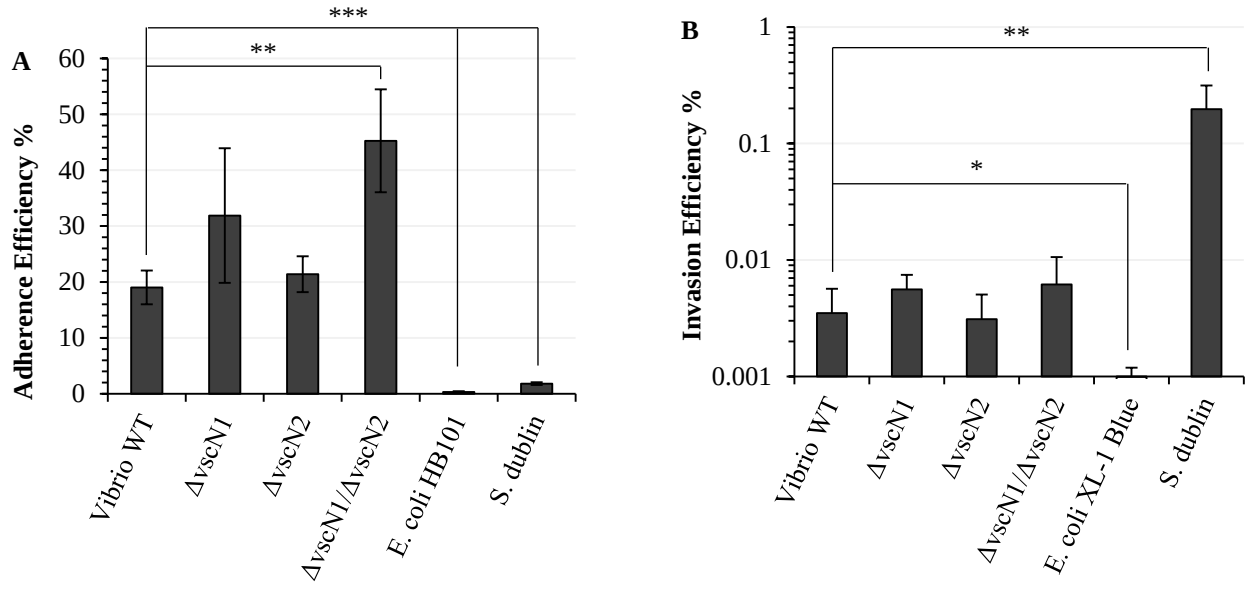

Fig 3.1 *V. parahaemolyticus* TTSS do not play a significant role in adherence or invasion. (**A**) Adherence efficiency of *V. parahaemolyticus* wild type and TTSS deletion mutants. Data were generated from a single experiment with 4 replicates per strain. (**B**) Invasion efficiency of *V. parahaemolyticus* wild type and TTSS deletion mutants. Invasion data is represented as the mean plus standard deviation of at least three experiments. Adherence and invasion efficiency was calculated as a percentage of inoculum. *, $P<0.05$; **, $P<0.01$; ***, $P<0.001$.

V. parahaemolyticus displayed an adherence efficiency of 19% of the inoculum, twenty-fold higher than that of the non-adherent *E. coli* HB101 (Fig 3.1A). Adherence was also significantly higher than that of *S.* Dublin (ten-fold higher). Fig 3.1B shows the results of a gentamicin protection assay to measure the invasion efficiency of *V. parahaemolyticus* wild type and control strains. *V. parahaemolyticus* wild type yielded significantly lower invasion efficiency (0.004% of the inoculum) than the intracellular pathogen *S.* Dublin (0.2% of the inoculum). *V. parahaemolyticus* invaded Caco-2 with five times the efficiency of *E. coli* XL-1 Blue (0.0008%).

These findings demonstrate that *V. parahaemolyticus* is a highly adherent intestinal pathogen. *V. parahaemolyticus* is also invasive, however taking into consideration the high level of adherence observed on Caco-2, this invasive phenotype may have arisen due to the increased binding to Caco-2 rather than active induction of invasion by the bacterium.

A significant increase in adherence efficiency was observed between the Δ*vscN*1/Δ*vscN*2 double mutant and the *V. parahaemolyticus* wild type (Fig 3.1A). Inactivation of individual TTSS did not have a significant effect on the adherence efficiency of *V. parahaemolyticus*. A non-significant increase in adherence efficiency was seen with Δ*vscN*1. A similar increase in invasion efficiency was observed for the Δ*vscN*1 mutant although again this increase was not statistically significant ($P>0.05$). No difference in adherence or invasion efficiency was observed between the Δ*vscN*2 single deletion and the wild type. However, the double deletion of *vscN*2 and *vscN*1 resulted in further increased adherence efficiency than the Δ*vscN*1 strain. This may indicate that TTSS2 has an accessory role in inhibition of adherence by *V. parahaemolyticus*. TTSS do not appear to play a significant role in the process of invasion. Taking the 4 strains into account, a similar pattern is seen in Fig 3.1B (invasion efficiency) to that observed for Fig 3.1A (adherence efficiency) and as such, differences in invasion may be attributable to increased contact with Caco-2 cells and thereby an increased possibility of entry.

3.3 Effect of co-incubation time on invasion efficiency of *V. parahaemolyticus* and TTSS deletion mutants.

It has been shown that co-incubation time has an effect on the level of cell death induced in epithelial cells by *V. parahaemolyticus* (Matlawska-Wasowska *et al.*, 2010). In order to investigate the dynamics of *V. parahaemolyticus* infection with respect to the process of

invasion, the gentamicin protection assay was carried out with various co-incubation times being employed.

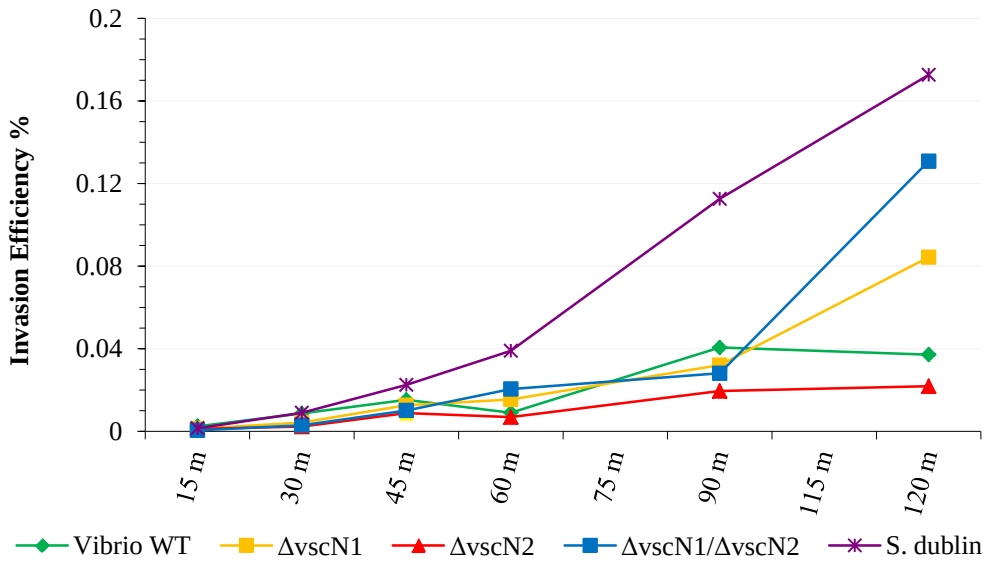

Fig 3.2 Effect of co-incubation time on invasion efficiency. Data represented are from a single representative experiment with 2 sample replicates per time point.

Invasion efficiency increased with co-incubation time for all strains analysed with *V. parahaemolyticus* wild type increasing from 0.002% of the inoculum at 30 min to 0.4% at 120 min (twenty-fold increase). The invasion efficiency of the Δ*vscN*1/Δ*vscN*2 mutant increased from 0.003% to 0.13% (forty-fold increase) over the same period.

With co-incubations up to 45 min, TTSS mutants display similar invasion efficiency to the wild type. The increased invasion efficiency exhibited by mutants lacking TTSS1 becomes evident after 45 min of co-incubation. With increased co-incubation time, this effect becomes more pronounced. Co-incubation times longer than 60 min enhance the differences observed due to presence/absence of active TTSS.

3.4 Intracellular proliferation of *V. parahaemolyticus*.

Many invasive bacteria exhibit the ability, not only to invade into host cells but also to survive and replicate in the intracellular environment. *S.* Typhimurium, *H. pylori*, *L. monocytogenes* and *S. flexneri* have all been shown to survive in intestinal epithelial cells (Brumell and Grinstein, 2004; Amieva *et al.*, 2002; Gaillard *et al.*, 1987; Ogawa and Sasakawa, 2006). As seen in Fig 3.1B, *V. parahaemolyticus* is capable of invading Caco-2 epithelial cells, and the number of invading intracellular bacteria increased with longer co-incubation times (Fig 3.2). A survival/proliferation assay was designed in order to assess whether *V. parahaemolyticus* could persist and replicate intracellularly following invasion of Caco-2. Cells were infected at an MOI of 10 for 1h. Extracellular bacteria were then killed by incubation in medium containing gentamicin and counts of intracellular bacteria were taken at the time points shown in Fig 3.3.

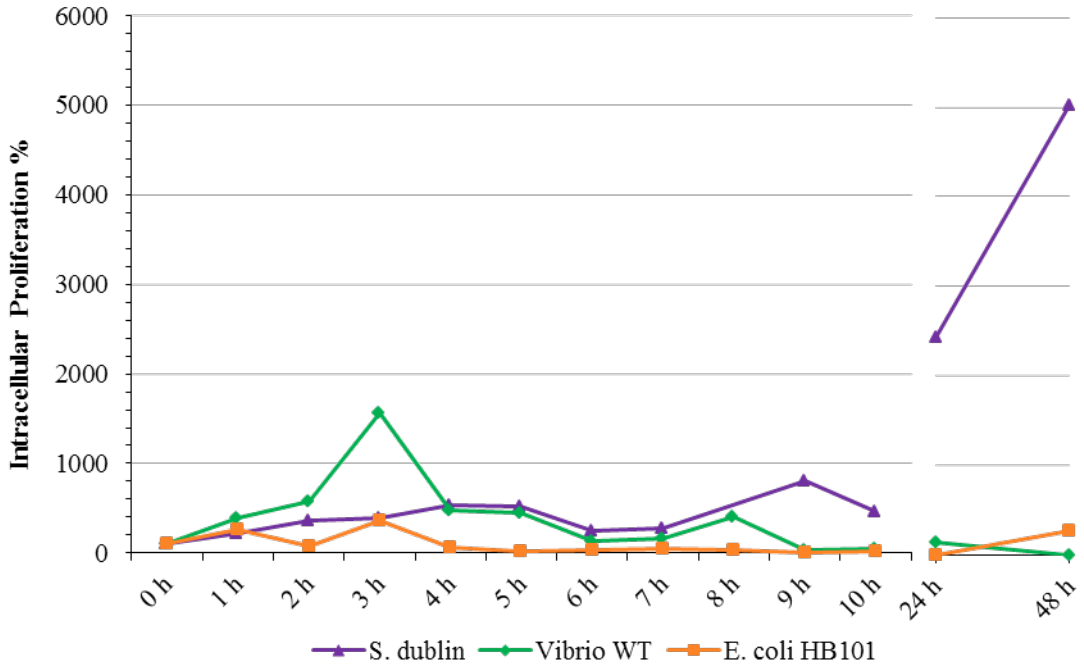

Fig 3.3 *V. parahaemolyticus* proliferates rapidly in Caco-2. Caco-2 were infected at an MOI of 10 for 1 h. Gentamicin was added at 50 µg ml^{-1} for 1 h to kill extracellular bacteria. At this time point (0 h), duplicate wells of Caco-2 were harvested to determine the number of intracellular bacteria. Gentamicin was included at 10 µg ml^{-1} for all further time points. For each time point, Caco-2 cells were lysed and intracellular cfu were recorded by plating on appropriate agars. Percentage proliferation was calculated by expressing the number of intracellular bacteria at a given time point as a percentage of the intracellular cfu at 0 h. Data shown is from one representative experiment with 2 sample replicates being tested per time point.

As seen in Fig 3.3, *V. parahaemolyticus* proliferated rapidly in Caco-2 cells. A six-fold increase in intracellular cfu was observed by 2 h. Peak numbers for the *V. parahaemolyticus* wild type were observed at 3 h (1,600% of initial intracellular cfu). This number decreased rapidly and while viable intracellular bacteria were still observed after 24 h, the levels were similar to that detected upon initial enumeration of intracellular bacteria (~100%). No viable intracellular bacteria were detected after 48 h for the *V. parahaemolyticus* wild type. Peak values for *E. coli* HB101 were significantly lower, with three times the initial intracellular levels being reached at both 3 h and 48 h of incubation. Although still present after 48 h, the numbers of intracellular *E. coli* were significantly lower than that of *V. parahaemolyticus* at

all other time points. For example, at 3 h, 25 intracellular cfu well^{-1} was observed for *E. coli* HB101, while 3.7 X 10^{3} intracellular cfu well^{-1} was observed for *V. parahaemolyticus*. The persistence of a small number of *E. coli* HB101 after 48 h of infection is likely due to its lack of cytotoxicity towards Caco-2. Cytotoxicity can be measured by determination of the secretion of lactate dehydrogenase (LDH), a cytoplasmic enzyme which is released upon cell lysis (section 2.5.4). Indeed, negligible levels of extracellular LDH were observed after 48 h of incubation with *E. coli* HB101, while *V. parahaemolyticus* caused release of LDH to levels corresponding to 32% lysis of the Caco-2 monolayer. It is unclear whether the cytotoxicity induced by *V. parahaemolyticus* was caused by delivery of TTSS effectors during the initial 1 h co-incubation or by delivery of effector proteins from within the intracellular environment.

S. Dublin exhibited considerably slower proliferation in the Caco-2 cells than *V. parahaemolyticus*, although as seen in Fig 3.1B, *S.* Dublin yields an initial intracellular count fifty-fold higher than that of *V. parahaemolyticus*. Results for *S.* Dublin were quite variable in the early stages of the incubation with proliferation levels ranging from 200 to 500% of the initial intracellular cfu during the first 8 h. After 9 h, intracellular levels approach ten times the initial intracellular count. After 24 h and 48 h, proliferation levels reached 2,400% and 5,000% respectively. Interestingly, even after 48 h of incubation, like *E. coli* HB101, *S.* Dublin did not cause cell lysis (as measured by LDH quantitation, data not shown). The peak intracellular count at 48 h for *S.* Dublin (1.4 X 10^{6} cfu well^{-1}) was four hundred fold higher than that of *V. parahaemolyticus* (3.7 X 10^{3} cfu well^{-1}).

TTSS of other gram negative pathogens have been shown not only to play a role in the process of invasion of epithelial cells but also to be involved in bringing about the persistence of invasive bacteria following invasion (Brummel and Grinstein, 2004). The role of TTSS in

the intracellular persistence and proliferation of *V. parahaemolyticus* was assessed by comparing TTSS mutants using the survival assay described in section 2.2.3.

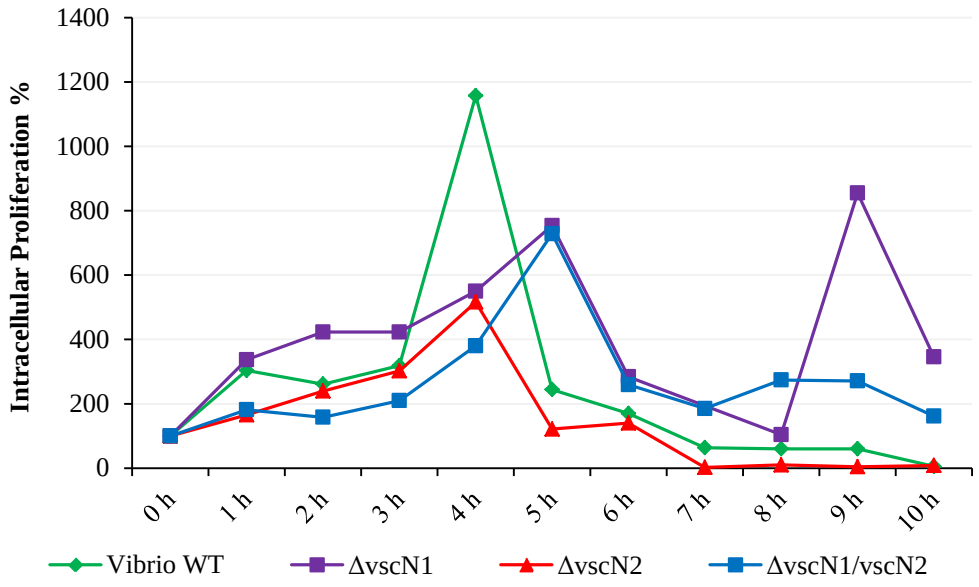

Fig 3.4 TTSS play an indirect role in the intracellular proliferation of *V. parahaemolyticus*. Caco-2 were infected at an MOI of 10 for 1 h. Gentamicin was added at 50 µg ml^{-1} for 1 h to kill extracellular bacteria. At this time point (0 h), duplicate wells of Caco-2 were harvested to determine the number of intracellular bacteria. Gentamicin was included at 10 µg ml^{-1} for all further time points. For each time point, Caco-2 cells were lysed and intracellular cfu were recorded by plating on LBN agar. Percentage proliferation was calculated by expressing the number of intracellular bacteria at a given time point as a percentage of the intracellular cfu at 0 h. Data shown is from one representative experiment with 2 sample replicates being tested per time point.

All strains tested exhibited rapid proliferation in Caco-2 with maximum levels ranging from 500% to 1,100% of the initial intracellular numbers. The wild type and Δ*vscN*2 reached maximum levels (at 4 h) before the Δ*vscN*1 and double mutant strains (5 h), a pattern which was observed across multiple experimental replicates. After the peak level of proliferation was reached, the numbers of intracellular bacteria decreased rapidly. After 6 h of incubation, the number of viable intracellular bacteria for the wild type and Δ*vscN*2 strains decreased

markedly. 10 h after initial determination of invasion efficiency, the numbers of intracellular bacteria for the wild type and Δ*vscN*2 were just above the level of detection (90 cfu well^{-1}, 6% of initial intracellular levels for the wild type; 105 cfu well^{-1}, 9% of initial intracellular levels for Δ*vscN*2), while the number of intracellular bacteria enumerated for the Δ*vscN*1 and double mutant were still greater than that of the 0 h time point (ie > 100% of initial intracellular levels).

The presence of an active TTSS2 may enhance proliferation of *V. parahaemolyticus* in Caco-2 cells. For all time points taken, the intracellular counts of Δ*vscN*2 were lower than that of the wild type. The pattern of proliferation was similar to that of the *V. parahaemolyticus* wild type. This indicates that clearance of the bacteria, either due to host cell death or bacterial cell death occurred at a similar time point. It is a distinct possibility that clearance of the bacteria occured due to the cytotoxic effects of *V. parahaemolyticus*. As the *V. parahaemolyticus* wild type and the Δ*vscN*2 strain have been shown to display similar levels of cytotoxicity towards Caco-2 cells (Matlawska-Wasowska *et al.*, 2010), it is not surprising that the pattern of proliferation of both strains is similar. This hypothesis is supported by the fact that the pattern observed for the Δ*vscN*1/Δ*vscN*2 double mutant closely resembles that of the Δ*vscN*1 single mutant. The rapid increase in wild type numbers between 3 h and 4h, and subsequent rapid decrease in numbers from 4 h to 5 h could indicate that the peak value for the Δ*vscN*2 strain fell between the time points at which samples were taken. Had the peak value been detected, the pattern of proliferation for the wild type and Δ*vscN*2 strain would have been more similar still.

It appears that the wild type invades a small number of Caco-2 (calculation of bacteria invaded per Caco-2 from a typical invasion assay yields only 1 invasive cfu per 4,500 cells, assuming one bacterium per cell and a confluent monolayer containing 450,000 Caco-2). The

invasive bacteria then proliferate intracellularly and secrete TTSS effector proteins leading to lysis of those invaded cells. Subsequently bacteria are exposed to gentamicin and are killed. This hypothesis requires that *V. parahaemolyticus* is capable of secreting effector proteins from inside the host cell. The effector proteins secreted during the first hour of co-incubation may also be responsible for host cell death, by exerting their effects after the killing of extra-cellular bacteria. In both cases, the lysis of Caco-2 cells by strains lacking TTSS1 is delayed, therefore maximum proliferation levels are reached at a later stage and bacteria are exposed to gentamicin at time points later than 10 h after initial invasion.

In order to assess whether intracellular *V. parahaemolyticus* were capable of dissemination, the invasion assay was performed, extracellular bacteria were killed with gentamicin and the medium was replaced with antibiotic free medium. This would allow any bacteria released from lysed cells to survive in the extracellular milieu. Subsequently, total cfu were enumerated and the level of Caco-2 cell lysis was recorded by LDH assay at the indicated time points (Fig 3.5, blue lines). Fig 3.5 also illustrates the cfu and LDH levels recorded from intracellular gentamicin protected bacteria for comparison (green lines).

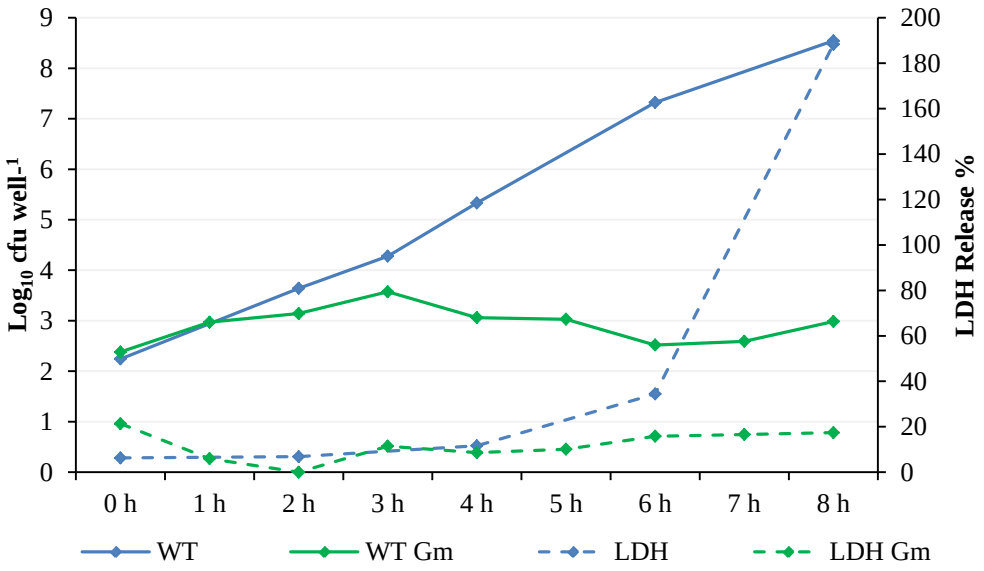

Fig 3.5 *V. parahaemolyticus* can emerge from the intracellular environment, causing complete lysis of the Caco-2 cell monolayer. Caco-2 were infected at an MOI of 10 for 1 h. Gentamicin was added at 50 µg ml^{-1} for 1 h to kill extracellular bacteria. For gentamicin protected samples (WT Gm, LDH Gm), gentamicin was included at 10 µg ml^{-1} for all further time points. To assess dissemination, following the killing of extracellular bacteria, the Caco-2 cells were washed and the medium was replaced with antibiotic free medium (WT, LDH). For each time point, Caco-2 were lysed and total cfu per well were recorded by plating on LBN agar. Supernatant samples were assessed for lysis by LDH assay using uninfected Caco-2 and detergent lysed Caco-2 as negative and positive lysis controls. Data shown is from one representative experimental replicate with 2 sample replicates being tested per time point.

Gentamicin protected intracellular cfu (solid green line) and cfu from intracellular bacteria cultured in antibiotic free medium (solid blue line) were quite similar prior to the peak proliferation level at 3 h. At this point, in the antibiotic free sample wells, the total number of bacteria per well continued to increase exponentially, while the numbers decreased in the gentamicin protected sample wells (Fig 3.5). This implies that *V. parahaemolyticus* is not killed by the Caco-2 cells after internalisation, but that it can disseminate from the Caco-2, thereby causing infection of further cells in the monolayer. The LDH levels observed further highlight the significance of this capability, as following dissemination, the Caco-2 cells were rapidly lysed by *V. parahaemolyticus* (dashed blue line), whereas after 8 h of intracellular growth, only 17% lysis was observed (dashed green line). The 188% lysis level detected after

dissemination of intracellular bacteria is likely a combination of 100% Caco-2 cell lysis and lysis of a sub-population of the bacteria, due to growth at extremely high density.

3.5 Visualisation of adherent *V. parahaemolyticus* by epifluorescence microscopy.

The colony forming unit based adherence assay described in section 2.1.3 is useful for enumerating levels of adherence, however no understanding of the pattern of adherence is obtained. As such, the pattern of adherence was visually analysed by epifluorescence microscopy using fluorescently tagged bacteria. Bacteria were fluorescently tagged by conjugal transfer of vectors which allow for constitutive expression of GFP or RFP (pVSV105 and pVSV208). GFP and RFP are particularly useful tools for detection of microorganisms as they can be easily expressed at high concentrations without affecting viability and can be detected using commonly available fluorescent filters and excitation sources. Fig 3.6 contains representative images from fluorescence based adherence analysis.

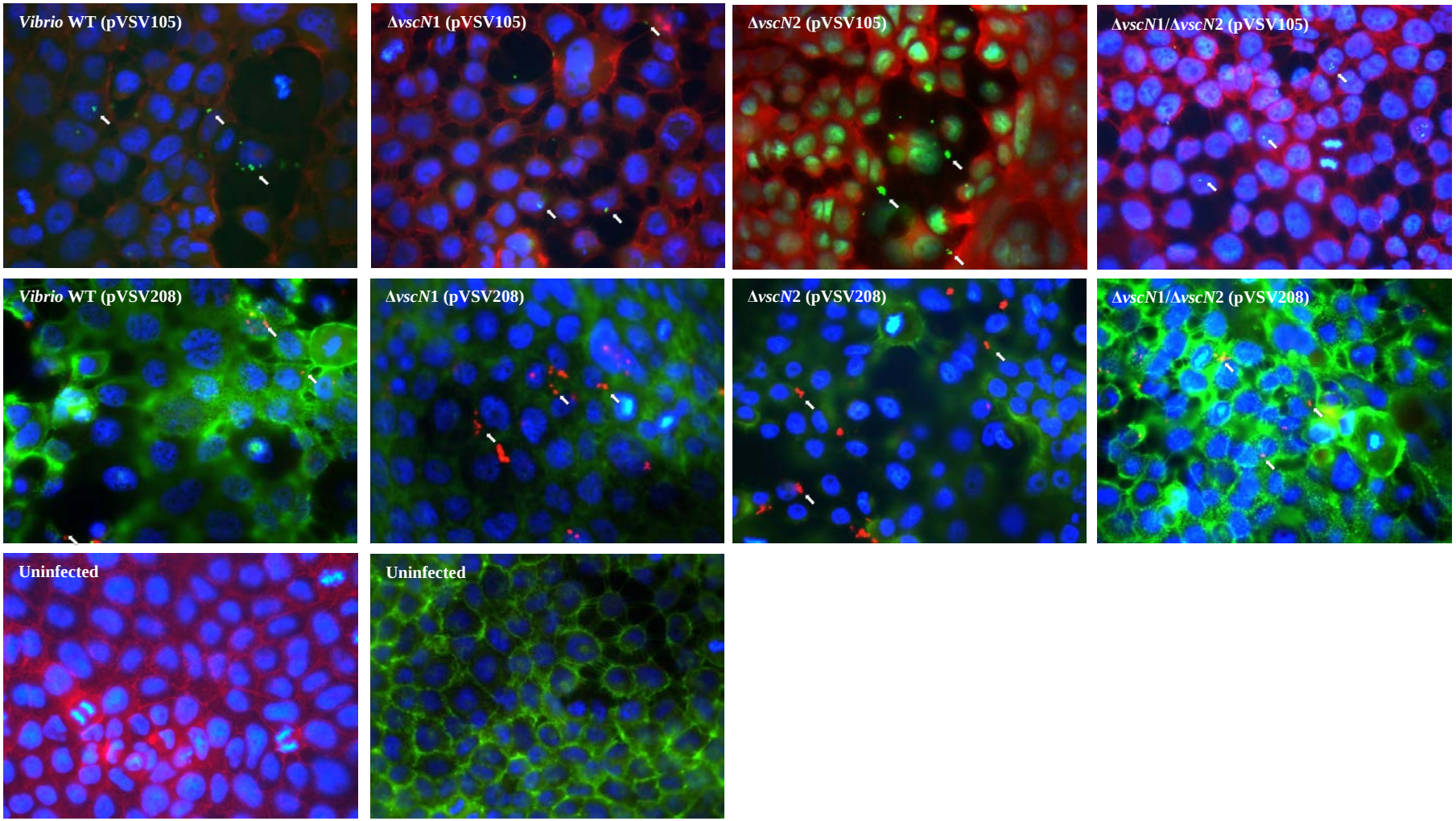

Fig 3.6 Visualisation of adherent *V. parahaemolyticus* by epifluorescence microscopy. Confluent Caco-2 cells were infected for 1 h with *V. parahaemolyticus* strains, washed 3 times with PBS, fixed in 4% paraformaldehyde and stained with Hoechst 33258 (Blue) and Phalloidin-Alexa 568 (Red) or Phalloidin-FITC (Green). pVSV105 encodes GFP (Green), pVSV208 encodes RFP (Red). Adherent bacteria are indicated by white arrows.

Phalloidin and Hoechst staining of Caco-2 allowed for greatly enhanced definition of cell morphology compared with that of light microscopy. Phalloidin was used to stain the actin cytoskeleton while Hoechst was used to stain the nuclei. Phalloidin-Alexa 568 exhibited increased photo-stability compared with the phalloidin-FITC stain, which allowed for lower exposure settings and sharper images to be taken. The Caco-2 cells which have been infected with *V. parahaemolyticus* appear less defined, as in many cases focusing on the bacteria required that the Caco-2 cells were out of focus. This was expected as the majority of *V. parahaemolyticus* were expected to be located on the apical surface rather than inside the Caco-2 (Fig 3.1). Uninfected monolayers show a dense layer of Caco-2 cells with clearly defined borders of actin filaments, indicative of the formation of tight junctions, a process which occurs during differentiation. The actin cytoskeleton and tight junctions appear disrupted in cells infected with *V. parahaemolyticus*, consistent with the findings of Lynch *et al.* (2005). Very little empty space was observed in uninfected monolayers and mitotic cells were visualised, indicating the relative health of uninfected cells compared with those infected with *V. parahaemolyticus*.

Upon comparison of RFP and GFP tagged bacteria, it can be seen that GFP tagged bacteria appear sharper than RFP tagged cells. This effect was due to rapid photo bleaching during excitation of RFP tagged bacteria. As photo bleaching occurred more slowly with GFP excitation, shorter exposure settings were employed and sharper images were obtained.

Bacteria can be seen in contact with Caco-2 for each of the strains being analysed. Bacteria are predominantly found in clusters of cells. These clusters may have arisen from cell division following binding of a single cell to the surface of the Caco-2. Clusters may also have arisen from bacteria preferentially binding to certain regions of the monolayer. *V. parahaemolyticus* wild type was found to have 0.33 +/- 0.03 cell-associated bacteria per Caco-2, a number significantly lower than that obtained from colony counts in section 3.2

(2.55 +/- 0.4, assuming 450,000 Caco-2 per confluent monolayer). This difference can be attributed to rapid photo bleaching of GFP and RFP tagged bacteria and also to differences in the numbers of cells observed at different levels of focus through the monolayer.

TTSS mutants exhibited similar numbers of cell-associated bacteria to those observed with the *V. parahaemolyticus* wild type. Δ*vscN*1 (0.41 +/- 0.39), Δ*vscN*2 (0.45 +/- 0.1), and Δ*vscN*1/Δ*vscN*2 (0.35 +/- 0.03) showed no significant differences in cell-associated bacteria per Caco-2 compared with the wild type.

3.6 Summary and Discussion

The aim of the work described in this chapter was to analyse the phenotypes of *V. parahaemolyticus* with respect to adherence, invasion and intracellular proliferation in the intestinal epithelial cell line Caco-2. It is known that *V. parahaemolyticus* exerts its principal pathogenic effects on host cells by secretion of effector proteins through TTSS and that intimate association between the bacterium and the host cell is required for efficient secretion to occur. It has also been shown that TTSS from other bacterial species can play a role in the processes of adherence, invasion and intracellular replication (Kenny *et al.*, 1997; Cossart and Sansonetti, 2004; Brumell and Grinstein, 2004). Therefore, we analysed a range of mutants carrying inactivating mutations of TTSS components for adherence, invasion and proliferation compared with the *V. parahaemolyticus* wild type.

V. parahaemolyticus research has established a link between pathogenicity and adherence. (Hackney *et al.*, 1980; Iijima *et al.*, 1981). Iijima *et al.* (1981) found that adherence to cultured epithelial cells correlated with the ability to colonise intestinal tissues in the guinea pig and with lethality in mice. Hackney *et al.* (1980) found that strains of *V.*

parahaemolyticus displaying the same serotype had much lower levels of adherence to intestinal epithelial cells if they were isolated from seafood rather than from infected individuals. Early research identified the ability of *Vibrio* species to agglutinate red blood cells and established a link between piliation and agglutination (Tweedy *et al.*, 1968). It was also found that this agglutination reaction was inhibited by incubation of *V. parahaemolyticus* in D-mannose, leading to the conclusion that a specific interaction with mannose containing oligo-saccharides was present. In 1994 it was established by Nagayama *et al.* that mannose sensitive haemagglutination of a range of *V. parahaemolyticus* isolates directly correlated with adherence to Caco-2 epithelial cells.

As seen in Fig 3.1A, *V. parahaemolyticus* adhered at a high level to Caco-2, with 20% of the inoculum being recovered. Nagayama *et al.* (1994) found a correlation between mannose sensitive haemagglutination and adherence to differentiated Caco-2 using a variety of clinical and environmental isolates. However, adherence of the recently emerged, more virulent, pandemic strain RIMD2210633 to differentiated Caco-2 has not been documented previously. Nagayama *et al.* (1994) found that between 10 and 50 bacterial cells were bound per Caco-2 for strains exhibiting mannose sensitive haemagglutination. Approximately 2.5 *V. parahaemolyticus* RIMD2210633 cells were found to attach per Caco-2 in the work presented here. A much higher inoculum (4 X 10^8 cfu) was used in Nagayama's study than that used in this work (4.5 X 10^6 cfu). As such it is difficult to draw conclusions from the results presented here with available published data. The 20% inoculum recovery obtained for *V. parahaemolyticus* in Fig 3.1A was significantly higher than the *E. coli* HB101 negative control and also significantly higher than the value obtained for *S.* Dublin. *E. coli* HB101 is used extensively as a negative control strain for adherence assays as it contains a deletion in the type I fimbrial operon, leading to low levels of adherence (Blomfjeld *et al.*, 1991). *S.* Dublin, like *V. parahaemolyticus* is an intestinal pathogen and as such, efficient colonisation

of intestinal cells is necessary for establishment of a persistent infection. Like *V. parahaemolyticus, S.* Dublin deploys TTSS once binding to the host cell has been initiated, with subsequent alterations in host cell signalling (Collazo and Galan, 1997). It is an interesting observation that with similar colonisation requirements, *V. parahaemolyticus* adheres to Caco-2 with ten-fold higher efficiency than *S.* Dublin.

We have demonstrated an effective means of visualising the adherence of *V. parahaemolyticus* to Caco-2 cells using bacteria which constitutively express fluorescent proteins (Fig 3.6). As discussed earlier, much lower counts of bacteria per Caco-2 (~0.3) were obtained using this method compared to the cfu based assay (~2.5). These differences may be attributed to rapid photo bleaching of fluorescently tagged bacteria and also to bacteria being present at different planes of focus through the Caco-2 cell monolayer. The use of a different anti-fade solution coupled with confocal scanning microscopy would lead to more accurate counts of cell-associated bacteria using this method. This use of fluorescently tagged bacteria allowed the pattern of adherence to be visualised and the *V. parahaemolyticus* were bound to the cells in clusters. These clusters may have arisen from cell division following binding of a single cell to the surface of the Caco-2 or from bacteria preferentially binding to certain regions of the monolayer.

V. parahaemolyticus was found to invade Caco-2 with significantly higher invasion efficiency than that of *E. coli* XL-1 Blue (Fig 3.1B). The mechanism of invasion used by *Salmonella* species has been extensively characterised with TTSS effector proteins playing an integral role. It is for this reason that *S.* Dublin was included as a positive control. As expected, after only one hour of co-incubation, *S.* Dublin reached a mean invasion efficiency of 0.2% of the inoculum, fifty-fold higher than that of *V. parahaemolyticus* (0.004%). *V. parahaemolyticus* may actively induce its own uptake at low levels to provide a pool of viable bacteria which can emerge from the host cell when conditions become favourable.

Conflicting information is present in published literature regarding the invasiveness of *V. parahaemolyticus*, with some publications pointing towards *V. parahaemolyticus* as an exclusively extracellular pathogen which actively inhibits cellular uptake (Burdette *et al.*, 2008) and others describing the pathogen as being invasive (Akeda *et al.*, 2002; Boutin *et al.*, 1979; Bhatarcharjee *et al.*, 2008; Zhang *et al.*, 2012). Direct comparison of the invasion efficiency of *V. parahaemolyticus* (0.004%) with that of *E. coli* XL-1 blue (0.0008%) appears to point towards an invasive phenotype, however the more likely scenario is that because of the high levels of adherence exhibited by *V. parahaemolyticus*, there is a higher possibility of uptake across the apical membrane of the host cell. Indeed, upon calculation of the percentage of cell-associated bacteria which are invasive, *V. parahaemolyticus* levels equate to 0.02%, compared with 0.25% for *E. coli*. The same calculation carried out using values for *S.* Dublin indicates that 10.8% of the cell-associated bacteria are intracellular. This indicates that *V. parahaemolyticus* can be found in the intracellular environment, and this is likely due to a pronounced ability to adhere to host cells. Therefore a proportion of the *V. parahaemolyticus* population do traverse into the intracellular environment and this may have biological relevance.

As seen in Fig 3.4, once inside the host cell, rapid proliferation occurs, with intracellular numbers reaching 10 times the initial levels after 4 h of infection. Intracellular replication of *V. parahaemolyticus* had not previously been reported in the literature. This is followed by a rapid reduction in viable cfu of intracellular bacteria. By ten hours, values for the *V. parahaemolyticus* wild type decrease to uncountable levels. One possible reason for the decrease in intracellular bacteria numbers was the lysis of the eukaryotic cells leading to efflux of the bacteria and their demise in the gentamicin-containing medium. An experiment was therefore performed to look at efflux and dissemination of intracellular bacteria. By washing the infected Caco-2 cells, following the killing of extracellular bacteria, and

replacing the gentamicin-containing medium with antibiotic-free medium, the intracellular bacteria could emerge from the infected cells after 3 h and grow exponentially in the medium (Fig 3.5). This implies that *in vivo* infections would not result in killing of the bacteria but would instead result in release of large numbers of bacteria from the lysed intestinal cells, which could subsequently infect further host cells and aid in dissemination throughout the host.

The *V. parahaemolyticus* TTSS1 causes cell lysis due to the delivery of the cytotoxic VopQ effector into host cells. The cytotoxic effects of TTSS1 can be measured by quantifying LDH release and observing cell rounding. When bacteria are added to Caco-2 cells and allowed to co-incubate without the addition of gentamicin, LDH release is observed first at 3h (20% lysis) and extensive cell lysis is observed at 4 h (90% lysis) (Matlawska-Wasowska *et al.*, 2010). Analysis of LDH release and morphology of the Caco-2 cell monolayer during intracellular proliferation assays, which were performed with the continued presence of gentamicin after the initial killing of extracellular bacteria, showed low levels of cytotoxicity and cell rounding during the first 8h of the assay (Fig 3.5). This was to be expected, as only a very small number of Caco-2 become infected with intracellular *V. parahaemolyticus* (1 invasive cfu per 4,500 cells, assuming one bacterium per cell and a confluent monolayer containing 450,000 Caco-2). The lysis of this number of cells by intracellular bacteria would not result in detectable levels of LDH in the extracellular medium. While it is possible that other non-TTSS factors are reponsible for the lysis of cells containing intracellular bacteria, this does suggests that the intracellular replicating bacteria secrete cytotoxic TTSS effectors after internalisation. Overall, these results indicate that cell to cell spread and subsequent destruction of the entire monolayer does not occur while gentamicin is maintained in the extracellular environment.

Invasive bacteria of other species can survive in the intracellular environment without causing destruction of the monolayer. *Salmonella enteritidis* has been shown to have 100% survival in Caco-2 cells after 24 h with no detectable lysis of host cells (Foster *et al.*, 2001). Wells *et al.* (1996) found that *L. monocytogenes*, *S.* Typhimurium, enteropathogenic *E. coli*, *Proteus mirabilis* and *Enterococcus faecalis* were all capable of invading and surviving in Caco-2 for 20 h with only *L. monocytogenes* causing a decrease in host cell viability. These findings are in agreement with that of Gaillard *et al.* (1987) who observed that *L. monocytogenes* proliferated to 4 times initial invasive levels after 8 hours, followed by a steady decrease in intracellular numbers to similar levels to that of initial invasion by 18 h. 18 h of infection with *L. monocytogenes* resulted in 70% cytotoxicity of the Caco-2 cell monolayer in the same experiment.

Similarly, we found during the intracellular replication experiments that after 48 h, the level of LDH release from cells infected with the *V. parahaemolyticus* wild type corresponded to 30% lysis of the monolayer. It is likely that this level of lysis is the result of secretion of cytotoxic TTSS1 effectors during the first hour of incubation. These effectors would continue to be active inside the cells even after the extracellular bacteria had been killed. The continued presence of low levels of effectors in the host cell leads to delayed cell lysis, affecting a large proportion of the monolayer. This increased lysis at 48 h corresponded to the time when intracellular *V. parahaemolyticus* were no longer detected.

The findings of this work and the work of others serves to demonstrate the complex dynamics of host cell adherence, invasion and intracellular replication, which pathogenic bacteria orchestrate in order to facilitate their establishment in a niche which allows their survival and persistence. Having observed a highly adherent phenotype for *V. parahaemolyticus* using Caco-2 and also having observed that internalised bacteria were capable of intracellular proliferation, the molecular mechanisms governing the process were investigated. TTSS were

analysed as *V. parahaemolyticus* research points towards TTSS as the principal virulence mechanism used during infection of intestinal cells (Matlawska-Wasowska *et al.*, 2010; Hiyoshi *et al.*, 2010; Ritchie *et al.*, 2012). The involvement of TTSS in binding to host cells indicates a potential role in adherence. Further evidence supporting the hypothesis that TTSS can play a role in adherence was observed by Kenny *et al.* (1997). Their work describes the TTSS of enteropathogenic *E. coli*, which translocates the Tir receptor into the host cell. Tir is subsequently inserted into the apical membrane of the host cell where it can interact with the bacterial adhesin, intimin. Indeed, the Type 6 secretion system of *V. parahaemolyticus*, which functions in a similar manner to TTSS, by binding to the host cell and secreting effector proteins, has recently been shown to play a role in adherence to Caco-2 (Yu *et al.*, 2012).

Comparison of *V. parahaemolyticus* wild type adherence with that of TTSS deletion mutants (Fig 3.1A) indicates that deletion of both *vscN*1 and *vscN*2 in the same strain leads to a significant increase in adherence. Deletion of *vscN*1 alone yielded a small increase in adherence, however this was not significantly different to the wild type. Consistent differences between TTSS mutants and *V. parahaemolyticus* wild type were not observed using the fluorescent microscopy based approach shown in Fig 3.6. A similar pattern to that observed for adherence efficiencies (Fig 3.1A) was seen in terms of invasion with inactivation of the TTSS1 ATPase VscN1, causing small increases in invasion in Δ*vscN*1 and Δ*vscN*1/Δ*vscN*2 (Fig 3.1B). These findings were not significant across three experimental replicates.

It is somewhat unusual for a strain depleted of a TTSS to display enhanced adherence and thereby potentially enhanced virulence. This effect may be explained by deletion of the surface expressed TTSS allowing more intimate contact with the host cell, thus enabling other surface expressed *V. parahaemolyticus* adhesins and invasins to come into contact with the host cell. This hypothesis is supported by the findings of Cornelis *et al.* (2006) who found

that the TTSS of *Y. enterocolitica* measured approximately 60 nm in length. As TTSS needle complexes are relatively well conserved, a similar length could be expected in *V. parahaemolyticus*, and may contribute to preventing access to adhesins which are found more proximal to the bacterial cell wall.

Alternatively, *V. parahaemolyticus* may actively reduce adherence and thereby invasion, using its TTSS as a means of persistence on the surface of the gastrointestinal mucosa, hence avoiding the intracellular environment. *V. parahaemolyticus* is known to inhibit Rho GTPases using a TTSS1 effector protein, VopS (Yarbrough *et al.*, 2009). It has also been shown using HeLa epithelial cells that a TTSS1-associated effector protein VopS inhibits each of these eukaryotic proteins by addition of adenosine 5'-monophosphate to a conserved threonine residue (Yarbrough *et al.*, 2009). These host cell proteins are involved in maintaining cellular structure and are intermediates in the process of bacterial invasion through regulation of actin polymerisation (Cossart and Sansonetti, 2004). Their inhibition may lead to reduced numbers of bacteria being internalised. Inhibition may also alter the topology of the apical membrane of the host cell, decreasing the number of available sites for bacterial attachment. Alterations in the host membrane may also lead to a decreased availability of receptors for adhesin binding. It is known that other *V. parahaemolyticus* TTSS effector proteins interact with additional cell signalling pathways in eukaryotic cells, including the MAPK pathway (Matlawska-Wasowska *et al.*, 2010). It is possible that alterations in multiple pathways may lead to modifications in apical membrane topology/composition.

Interestingly, studies carried out using phagocytic RAW 264.7 murine macrophages, found that the TTSS1 effector, VopS was responsible for upregulation of RhoB, leading to increased actin remodelling and a subsequent increase in internalisation (Bhattacharjee *et al.*, 2008). While the differences observed between the findings of Yarbrough *et al.* (2009) and

Bhattacharjee *et al.* (2008) may be attributable to intrinsic differences between the human and murine cell lines used, or specific differences in the mechanism of upregulation of RhoB, a differential role for VopS in phagocytic and non-phagocytic cells is a distinct possibility. VopQ, the effector protein which is most responsible for the cytotoxic effects of TTSS1 was found by Burdette *et al.* (2009) to have an opposite effect to VopS in terms of phagocytosis in RAW 264.7 macrophages. Here, deletion mutants of VopQ were found to display increased cellular uptake, illustrating that VopQ acts to inhibit phagocytosis in the *V. parahaemolyticus* wild type. Burdette *et al.* (2009) hypothesised that inhibition of phagocytosis may have been brought about indirectly due to VopQ redirecting cellular machinery towards autophagy.

While redirection of cellular machinery away from actin rearrangement, which facilitates the attachment and uptake of bacteria, would explain increased adherence in TTSS1 deletion mutants, another explanation lies in the fact that TTSS1 has a cytotoxic effect which causes cell rounding by actin rearrangement, monolayer destruction and cell lysis (Matlawska-Wasowska *et al.*, 2010; Burdette *et al.*, 2008). While cytotoxicity was only seen 3 h post-infection by Matlawska-Wasowska *et al.* (2010), cell rounding occurs earlier during the disruption of the host cell by *V. parahaemolyticus* (Burdette *et al.*, 2008). Indeed, Fig 3.6 shows evidence of actin cytoskeleton disruption and increased amounts of empty space (cells have become detached), when Caco-2 cells were infected with *V. parahaemolyticus*. Removal of rounded cells from the monolayer and lysis of infected Caco-2 cells, during incubation with gentamicin, may occur with infection with the *V. parahaemolyticus* wild type, leading to a reduction in enumerable cell-associated cfu. Cytotoxicity is markedly delayed in cells lacking TTSS1 (Matlawska-Wasowska *et al.*, 2010), therefore more viable Caco-2 cells are present following co-incubation and hence a higher viable adherent cfu count may be obtained. This theory is supported by the data in Fig 3.2 which shows that as co-incubation time proceeds and cytotoxicity takes effect, the differences observed in invasion efficiency

between *V. parahaemolyticus* wild type and TTSS mutants becomes greater. In support of this hypothesis, analysis of phalloidin stained Caco-2 following 2.5 h of infection with *V. parahaemolyticus* (Fig 5.17), showed that much of the monolayer had been disrupted and empty space was visible where rounded cells had been detached.

Upon analysis of intracellular proliferation/survival it was seen that inactivation of TTSS1 led to maximum levels of intracellular bacteria being reached at a later time point and a delay in clearance from Caco-2 (Fig 3.4). For the delay in clearance, it may be the case that TTSS1 is specifically recognised by Caco-2 cells and this has the effect of inducing lysosomal fusion and bacterial killing. A more likely scenario is that the cytotoxic effects of TTSS1 influence the viability of the cells which have been invaded by *V. parahaemolyticus*. TTSS1 effector proteins may continue to be secreted in cells invaded by the wild type, leading to cell rounding and detachment of invaded cells from the monolayer. This loss of cells from the monolayer does not occur with *V. parahaemolyticus* strains lacking TTSS1. As with the adherence and invasion assays, this may result in a lower intracellular wild type cfu count at later timepoints, than that observed with strains lacking TTSS1.

The kinetics of intracellular Δv*scN*2 closely resembled that of the *V. parahaemolyticus* wild type throughout the period of measurement. However, the numbers of intracellular Δv*scN*2 bacteria were lower than wt throughout the time course. Peak values were reached at a similar time point and reductions in intracellular cfu occurred at a similar rate for each strain. Similarly, Δ*vscN*1/Δ*vscN*2 closely followed the pattern observed in the Δ*vscN*1 single mutant, but with lower numbers detected during the early stages of infection. As such it is likely that TTSS2 does play a role in the survival/proliferation of *V. parahaemolyticus* in the intracellular environment of Caco-2 cells. We did not detect any role for TTSS2 in the invasion of *V. parahaemolyticus* into host cells. This finding is in direct contrast to that of a study published after we had performed our experiments. Zhang *et al.* (2012) found that

TTSS2, and specifically the effector protein VopC, were required for invasion and proliferation in HeLa cells by RIMD2210633-derived strain CAB2. It is worth noting that the CAB2 strain used by Zhang *et al.* (2012) lacked the transcriptional regulator ExsA which is required for expression of TTSS1 and therefore should resemble Δ*vscN*1 in terms of TTSS activity. In our study, the double mutant Δ*vscN*1/Δ*vscN*2 had the same invasion efficiency (0.006%) as the Δ*vscN*1 mutant (Fig 3.1B). The Δ*vscN*2 single mutant also had similar invasion efficiency (0.003%) to the *Vibrio* WT (0.0035%). This implies that TTSS2 is not involved in the invasion of Caco-2. These findings point towards tissue specificity of TTSS in relation to involvement in the process of invasion and highlight the necessity for the use of appropriate cell lines in analysis of such traits.

In this chapter, we have described the adhesive and invasive properties of *V. parahaemolyticus*. This pathogen displays high levels of adherence, with adherence efficiency tenfold higher than that of *S.* Dublin. This is the first study to comprehensively illustrate the pronounced adhesiveness of *V. parahaemolyticus* RIMD2210633 by comparison with another enteric pathogen. The use of a human intestinal cell line to demonstrate this phenotype further highlights the relevance of this trait with respect to human infections.

V. parahaemolyticus is also capable of entering Caco-2 cells and surviving over a period of 8 h. During this period, *V. parahaemolyticus* proliferates rapidly, before a rapid reduction in viable intracellular cfu. This study and the study carried out by Zhang *et al.* (2012) are the first reports of intracellular survival and replication of *V. parahaemolyticus*. These findings illustrate that *V. parahaemolyticus* should not be considered an exclusively extracellular pathogen and that even low levels of cellular invasion could result in the dissemination of large populations of bacteria from the intracellular environment. This has important consequences for our understanding of *V. parahaemolyticus* infection and may have implications for the design of effective therapeutics.

TTSS appear to play an indirect role in the processes of attachment, invasion and intracellular proliferation. The differences observed between TTSS deletion mutants and the wild type are likely the result of the cytotoxic effects, altered cell signalling and morphological alterations which these systems induce in host cells. As deletion of TTSS components did not lead to a decrease in adherence or invasion, the secretion systems should not be considered adhesins or invasins. Their relevance in the processes of cellular attachment, invasion and proliferation should however, not be underestimated. Having observed interesting phenotypes for *V. parahaemolyticus*, particularly in terms of adherence, an investigation was undertaken to attempt to identify the molecular mechanisms governing these virulence-associated traits.

Chapter 4

Preparation, selection and validation of a genomic library for the identification of novel *V. parahaemolyticus* adhesins and invasins

4.1 Introduction.

As shown in Chapter 3, *V. parahaemolyticus* displays significantly higher adherence and invasion compared with the control *E. coli* strains tested (Fig 3.2). While some work had been carried out investigating adherence of *V. parahaemolyticus* to host cells, the specific proteins (adhesins) involved have not been identified or characterised. Therefore in this study we aimed to identify at a molecular level the adhesins of *V. parahaemolyticus*.

Functional screening of heterologous proteins from pathogenic organisms provides a means of identifying previously uncharacterised hypothetical proteins with roles in pathogenicity. As the number of sequenced genomes continues to grow, molecular biologists are faced with the prospect of assigning annotations to a vast number of hypothetical proteins. Here we describe a rapid, unbiased means of identifying adhesins and invasins which involves the introduction of random fragments of *V. parahaemolyticus* genomic DNA into a weakly-adherent, non-invasive strain of *E. coli*, HB101. The pWEB-TNC cosmid cloning vector was employed for this procedure as it allows for incorporation of large insert fragments (up to 45 kb). In order to avoid the introduction of bias, genomic DNA from *V. parahaemolyticus* was randomly sheared, rather than shearing by restriction digest, which may exclude potential adhesins/invasins containing restriction sites for the endo-nucleases used. Hirono *et al.* (1998) describe an effective means of screening for functional chitinases from two *Vibrio* species, *V. parahaemolyticus* and *Vibrio anguillarum* using a cosmid library. This work involved the introduction of 2-16 kb fragments of *Vibrio* DNA into *E. coli* DH1. Detection of functional chitinases from the *E. coli* based library illustrates that *E. coli* serves as an effective host for expression of *Vibrio* genes from native promoters and highlights the potential for use of *E. coli* based libraries for detection of uncharacterised proteins from gram negative species.

Cosmids offer an increased likelihood of expression as they are retained in multiple copies, unlike other high capacity vectors such as fosmids, bacterial artificial chromosomes and yeast artificial chromosomes (Shashikant *et al.*, 1998). However, retention of multiple copies of a large foreign DNA molecule, coupled with high levels of expression increase the likelihood of toxicity in heterologous hosts. It is also worth noting that expression in the heterologous host is reliant on recognition of native promoters, as pWEB-TNC does not carry a promoter to direct expression. Differential codon usage between the source organism and the host organism may also lead to poor levels of expression. In order to combat these issues, a high level of coverage was employed and alternatives to genomic library selection were also investigated for adhesin and invasin identification. *E. coli* HB101 was chosen as a heterologous host as it possesses a deletion in the Type I fimbrial operon which is present in *E. coli* K12 (Blomfjeld *et al.*, 1991), rendering the organism non-adherent and non-invasive. *E. coli* HB101 is also deficient in restriction endonucleases and recombinases making it an effective host for retention of heterologous DNA (Boyer and Roulland-Doussoix, 1969). The strain has been used as a negative control strain for adherence and as a host for expression of heterologous adhesins by groups including Nicholls *et al.*, (2002) and Pallesen *et al.*, (1995). *E. coli* HB101 was used as a negative control for invasion and was successfully used to identify a *S.* Typhi invasion locus from a cosmid library by Elsinghorst *et al.*, (1989). *E. coli* HB101 has been used as a negative control in gentamicin protection assays by many groups, including Monack *et al.* (1996), and Elsinghorst and Weist (1994).

Following preparation of the genomic library, a range of selections were carried out in order to isolate clones expressing functional *V. parahaemolyticus* adhesins and invasins. Selection of invasive clones was carried out by use of the gentamicin protection assay. This method involved the incubation of the genomic library with Caco-2 cells and the killing of extracellular bacteria by incubation in medium containing gentamicin. Subsequently,

intracellular invasive clones were released by lysis and plating. Selection of adherent clones was carried out by incubating the library with Caco-2 cells, washing Caco-2 to remove non-adherent clones and lysing Caco-2 to allow plating of adherent clones within the lysate. A summary of the selection process using an invasion assay for initial selection is illustrated in Fig 4.1. Expression of functional adhesins by *E. coli* HB101 would increase the likelihood of internalisation by Caco-2. Similarly, clones expressing functional invasins may have increased adherence to Caco-2 by virtue of invasins binding to host cell receptors. For this reason both invasion and adherence selections were carried out and following these selections, clones with consistently elevated invasion were also tested for elevated adherence and *vice versa*. Clones which displayed high levels of adherence or invasion in pure culture experiments were chosen for further experimental replicates. Clones with consistently increased adherence or invasion were selected for sequencing of insert DNA extremities, followed by bioinformatic analysis to reveal potential adhesins/invasins.

As in chapter 3, Caco-2 cells were grown for 7 days prior to carrying out library selections. This resulted in the formation of a polarised differentiated Caco-2 cell monolayer. This polarisation, coupled with the formation of tight junctions, a process which occurs during differentiation, leads to establishment of a monolayer which is highly representative of the human intestinal epithelium.

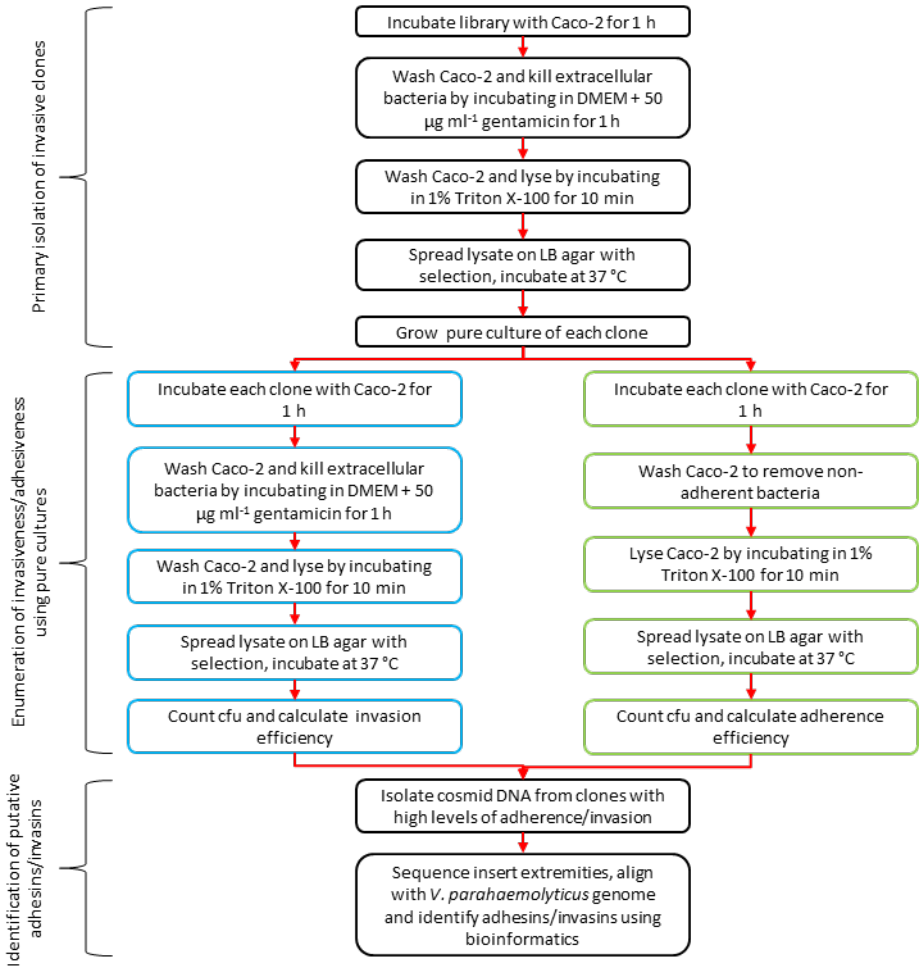

Fig 4.1 Flow diagram illustrating the process of isolation and characterisation of clones selected using the adherence assay or the gentamicin protection assay.

A similar library screening approach to that discussed here was undertaken by Waterfield *et al.* (2008), also using the pWEB cosmid vector for library preparation. Waterfield *et al.* (2008) screened a pWEB library for the presence of insert sequences which led to a "gain of toxicity" (GOT) in a non-toxic strain of *E. coli* against a number of invertebrate hosts and/or murine macrophages. A total of 21 loci were identified from the 5.0 Mb genome of *Photorhabdus asymbiotica* which conferred the GOT phenotype upon infection of either macrophages or invertebrate hosts. Interestingly, the putative virulence-associated loci included: putative haemagglutinins; a putative invasin; TTSS genes and effectors; fimbrial

operons; and type VI secretion system operons, all of which have been associated with adherence and/or invasion in gram-negative pathogens. This work demonstrated that proteins from pathogenic microorganisms can be functionally expressed and selected for using an avirulent *E. coli* host.

Since the *V. parahaemolyticus* genome was sequenced in 2003 by Makino *et al.*, a wealth of bioinformatic information has been generated pertaining to potential virulence proteins possessed by the organism. In case of poor isolation of adherent/invasive library clones, a bioinformatic mining approach was also undertaken in an attempt to identify adhesins and invasins. This involved the use of a cross-referencing database (The Virulence Factors of Pathogenic Bacteria Database [VFDB]) in order to identify *V. parahaemolyticus* protein sequences bearing homology to virulence-associated protein sequences from the better studied pathogen, *V. cholerae*.

The following chapter will describe the preparation of a genomic library of *V. parahaemolyticus* DNA, and investigate its use in selecting potential adhesins and invasins, sequencing and alignment to reveal adherence/invasion loci and bioinformatic analysis of inserts to assign putative adhesin/invasin function. The alternative bioinformatics based approach used to identify putative adhesins and invasins will also be described.

4.2 Optimisation of shearing of *V. parahaemolyticus* genomic DNA.

In order to isolate random fragments of *V. parahaemolyticus* genomic DNA which were of a suitable size for cloning into pWEB-TNC, purified chromosomal DNA was sheared as described in section 2.3.1, with a variable number of passages through a syringe with a narrow bore needle. As seen in Fig 4.2A, the size of the DNA fragments reduced as the

solution was drawn up and expelled an increasing number of times. After 4 passages, the majority of the DNA was less than 48.5 kb in size, which was deemed suitable for library preparation.

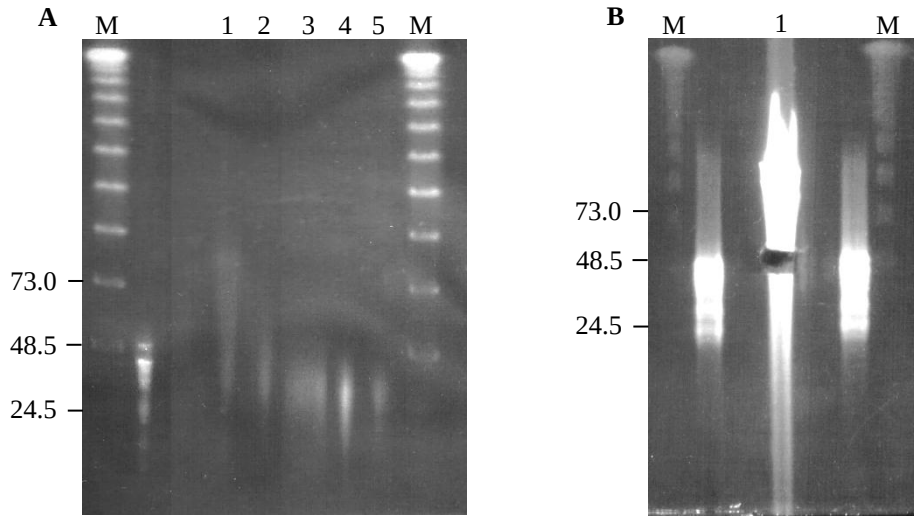

Fig 4.2 Optimisation of DNA shearing and isolation of ~40 kb fragments of *V. parahaemolyticus* genomic DNA. (**A**) Optimisation of DNA shearing, Lane 1: DNA passed through the syringe once, Lane 2: DNA passed through the syringe twice, Lane 3: DNA passed through the syringe three times, Lane 4: DNA passed through the syringe four times, Lane 5: DNA passed through the syringe 5 times. (**B**) Isolation and excision of 40 kb fragments of genomic DNA following four passages through the syringe, Lane 1: 50 µg sheared genomic DNA with ~40 kb region excised from the gel. Samples were separated by PFGE, stained with SYBR Gold and visualised under blue light. Molecular weight marker (M) sizes shown are in kb.

4.3 Genomic library Preparation.

Genomic DNA of a high concentration was prepared and sheared using 4 passages through a 51 µm bore needle. This DNA sample was then isolated by PFGE as shown in Fig 4.2A. The gel was stained with SYBR gold and visualised using blue light in order to maximise cloning efficiencies. Hartman *et al.* (1991) found that exposure of a variety of plasmids to UV trans-illumination for as little as 1 minute resulted in up to 100 fold decreased transformation efficiency. Unlike conventional ethidium bromide stain, SYBR gold nucleic acid stain is excitable in the blue light wavelength, eliminating the requirement for exposing DNA

samples to damaging UV light. A region corresponding to ~40 kb was excised from the gel as shown in Fig 4.2B. The DNA was purified from the gel excision, ligated into pWEB-TNC, packaged into phage and transformed into *E. coli* HB101 as outlined in section 2.3.1. A library titer of 2.8 X 10^4 cfu ml^{-1} was obtained. This allowed for production of a library with 5X coverage of the *V. parahaemolyticus* genome and a 99.9% probability of containing a given sequence.

In order to rapidly confirm insert size and randomness of the prepared genomic library, three clones were selected from library titering. Clones were cultured with selection for the pWEB-TNC cosmid and cosmids were purified from overnight cultures as described in section 2.1.5. The extremities of the insert DNA from the three random clones was sequenced using pWEB.For and pWEB.Rev primers and sequences were aligned with the *V. parahaemolyticus* genome sequence using NCBI BLAST. The following co-ordinates and corresponding insert sizes were obtained:

- C1 (1938862-1972129, Chromosome 1, 33.27 kb)
- C2 (982321-1020235, Chromosome 2, 37.91 kb)
- C3 (2870641-2899260, Chromosome 1, 28.6 kb)

As seen by the sequencing results from clones C1, C2 and C3, insert fragments have been derived from distinct chromosomal loci. Insert DNA from clones C1 and C3 originate from loci 899 kb apart on chromosome 1, while the insert contained within clone C2 originates from chromosome 2. Insert sizes are in the expected range as observed from the gel excision in Fig 4.2B and should therefore be sufficient to allow for co-expression of multiple genes within the same region. The sequencing results from clone C1, C2 and C3 therefore confirm the randomness of the genomic library and also serve to illustrate that inserts contained within the library are of the desired size for use in selection experiments.

4.4 Selection of invasive library clones with a single round of selection.

The genomic library was selected for invasive phenotypes by gentamicin protection assay as described in section 2.2.2. This involved incubating the genomic library with Caco-2 epithelial cells and selectively killing the extracellular bacteria with gentamicin. Clones which invaded were protected from the gentamicin, and were plated by lysing the Caco-2 and spreading on agar containing selection for the pWEB-TNC vector (See Fig 4.1). Selection was carried out on two separate days, with 37 clones being isolated on the first day (A1 to A37) and 18 clones being isolated on the second day (B1 to B18). The inoculum cfu count was also enumerated on the days of selection in order to calculate the invasion efficiency of the library during each selection. The A series selection resulted in an invasion efficiency of 0.0004% of the inoculum, while B series selection resulted in invasion efficiency of 0.0002%. Both values are similar to the background levels which are typically observed for the *E. coli* HB101 control strain. Although low levels of invasion were observed for the genomic library as a population, we expected that there would have been individual clones selected, which possessed a stable invasive phenotype due to the expression of *V. parahaemolyticus* invasins.

As a result it was subsequently necessary to enumerate the invasion efficiency of each clone, using a pure culture in order to confirm the establishment of an invasive phenotype. In order to screen a large number of clones in a high throughput manner, each clone was tested on two replicate wells of Caco-2 cells. Results for mean invasion efficiency for the first test of each library clone are shown in Fig 4.3. These results are expressed as invasion efficiency, where the value displayed corresponds to the number of intracellular bacteria expressed as a

percentage of the inoculum. Clone A13 failed to grow in liquid culture and as such is not shown in Fig 4.3.

Inter-experimental variation was quite high. This can be seen by comparing the values obtained for *E. coli* HB101 in each experiment. In the second experiment (quantifying invasion of clones A11 to A20) a value of 0.0001% invasion efficiency was obtained for *E. coli* HB101, while in the fifth experiment (quantifying invasion of clones B5 to B13), a value of 0.015% was obtained (>100-fold increase). Variation from experiment to experiment also occurred with the clones being tested, such that experiments where the control strain had high levels of invasion (>0.001%) also resulted in high invasion of clones being tested. Comparison of the values obtained for clone A16 (0.001%) and clone B8 (0.006%) seem to indicate that clone B8 is more invasive, however all clones (and the *E. coli* HB101 control) tested in parallel with clone B8 displayed high invasion efficiency (>0.001%). Clone B8 had much lower invasion efficiency than *E. coli* HB101 (0.015%) for the same experiment and was therefore not used in further analysis. These findings highlighted that it was important not to select clones for further analysis based upon comparisons between results obtained from different experiments, but to compare the values obtained within a single experiment.

The 2 clones yielding the highest levels of invasion for a given experiment were tested in further experiments on quadruplicate wells of Caco-2 cells (A4, A6, A9, A15, A16, A19, A26, A34, A36, B1, B9, and B14). Increasing from two sample wells to four resulted in a more accurate assessment of the mean invasion efficiency and a greater ability to establish the significance of differences between clones and the control strain. It was also important to ensure that the level of invasion exhibited by clones considered for further analysis was higher than that obtained for *E. coli* HB101 in the same experiment. The invasion efficiency of *E. coli* HB101 was ten-fold higher in the fifth and sixth experiments (Fig 4.3) than in previous experiments. This resulted in values for all clones tested being similar to *E. coli*

HB101. As such, it was difficult to select clones for further analysis from these experiments. Clones A9 and A15 were selected as representatives from these 2 experiments and were used in further analyses to enumerate their invasion efficiencies.

Fig 4.4 shows the invasion efficiency enumerated from individual sample wells of Caco-2 expressed as a ratio of the average *E. coli* HB101 invasion efficiency for a given experiment (relative invasion efficiency). Values for each clone are separated by X-axis tick marks. Columns representing each clone have also been coloured differentially. The first 2 columns for each clone in Fig 4.4 represent the invasion efficiency enumerated from each of the two individual replicate wells of Caco-2 which were used in the first experiment. The mean invasion efficiency from each of these two sample replicates was plotted in Fig 4.3. Clones which were selected for further analysis have more than two columns in Fig 4.4. As further experiments involved the use of at least 4 sample wells of Caco-2, those clones which were re-tested have a minimum of 6 columns representing the 6 sample wells of Caco-2 used for enumeration of invasion efficiency for that clone. For example, for clone A16, the first two columns represent the relative invasion for experiment 1 (mean invasion efficiency plotted in Fig 4.3), the next 4 columns for clone A16 represent the values obtained from each sample well of Caco-2 in experiment 2, etc.

In many cases where clones exhibited higher levels of invasion than *E. coli* HB101 in the first experiment (mean value, Fig 4.3; first two columns for each strain, Fig 4.4), repeat experiments showed significantly lower levels (third and subsequent columns for each strain Fig 4.4). See clones A4, A6, A9, A15, A19, A26, A36 and B14. For example clone A6 had an invasion efficiency of 0.0018% for the first experiment compared with 0.0002% for *E. coli* HB101 in the same experiment (relative invasion = 10). In the repeat experiment, A6 displayed a mean invasion efficiency of 0.0001% of the inoculum, while *E. coli* HB101 exhibited an invasion efficiency of 0.002% (relative invasion = 0.05). As a result of low

mean invasion efficiency in the second experimental test, further analysis was not carried out on any of these clones. Only clones displaying relative invasion levels higher than the control strain in both experiments were used in a third experiment (Clones A16, A34 and B1).

For clone A16, invasion efficiency from 19 out of 22 sample wells of Caco-2 tested across 5 experiments resulted in higher invasion efficiencies than that of HB101 for the same experiment, with 16 of those having at least two-fold increased invasion efficiency compared with HB101. For clone A34, 7 out of 10 sample replicates across 3 experiments showed higher levels of invasion compared with HB101. Clone B1 yielded higher levels of invasion than HB101 in 8 out of 10 sample replicates. Clone A16 showed the highest and most consistent levels of increased invasion compared with the *E. coli* HB101 control, and was therefore sequenced and analysed bioinformatically as described in section 2.3.8. Mean invasion efficiency across all experiments carried out is displayed in Fig 4.6A, with corresponding invasion relative to *E. coli* HB101 shown in Fig 4.6B. Paired student's *t* test analysis of relative invasion values confirmed the significance of the increased invasion exhibited by clone A16 ($P<0.05$). Comparison of the mean plus standard deviation of relative invasion for clone A34 and clone B1 with the control strain did not yield a statistically significant difference. Therefore further analysis was not carried out with these clones.

During analysis of clone A16, it was observed that inoculum cfu counts for this clone (Mean = 3.8×10^5 cfu per well) were consistently lower than that observed for *E. coli* HB101 (Mean = 2.5×10^6 cfu per well) in the same experiment, even though the OD_{600} of the suspension used for each was identical. As invasion efficiencies were derived as a function of the inoculum count, this may have had an influence on the results observed. It appears that under the growth conditions used, clone A16 grows to a similar OD_{600} to *E. coli* HB101, however fewer cfu are present in the cell suspension. This could be explained by accumulation of dead cells, an increase in cell size or formation of clusters or aggregates of bacterial cells, each of

which having the ability to form a single colony forming unit. Analysis of carbol fuschine stained bacteria by light microscopy failed to yield significant differences in morphology or aggregation between *E. coli* HB101 (pWEB) and clone A16 (Data not shown), however it is possible that while cells present in the suspension of clone A16 were intact, their viability may have been compromised. The aforementioned phenotypes may be explained by the presence and/or expression of large fragments of heterologous DNA inducing high levels of stress on clone A16. It is also possible that expression of a single foreign protein in *E. coli* HB101, such as an integral membrane protein, could lead to compromised membrane integrity and/or viability of the heterologous host. It is worth considering that each of these phenotypes may be indirectly affecting the numbers of invasive cfu being obtained by the gentamicin protection assay.

Taken together, the results for invasion efficiencies were highly variable (Fig 4.3 and Fig 4.4). This occurred for 3 reasons: Firstly, inoculum plate counts for many strains yielded significantly fewer cfu than the *E. coli* HB101 control. This may have been the result of decreased viability of library clones, increased cell size or altered cell morphology leading to a higher OD_{600} with fewer viable cells or formation of clusters or chains of bacterial cells, each of which yielding only one countable colony when plated. As invasion efficiency is a function of the inoculum count, low inoculum counts in some cases resulted in overestimation of invasion efficiency. The second reason for high variability in enumerated invasion efficiencies was that sensitivity of the enumeration method was low. *E. coli* HB101 yields a very low level of background invasion, with approximately 20 cfu of invasive bacteria being obtained from an entire well of Caco-2. Many clones yielded fewer than 5 adherent cfu from a single well of Caco-2. As a result, resolution between strains was poor and repeat experiments were required. Finally, while invasins may have been expressed in the initial selection process, the growth of a pure culture of such strains may have resulted in the

bacteria adapting so as to reduce expression of a potentially deleterious protein. This would result in selection of clones which do indeed carry *V. parahaemolyticus* invasins but which have become incapable of expressing such proteins.

As mentioned previously, the process of selection using the gentamicin protection assay resulted in the isolation of clones which became internalised due to increased contact with the Caco-2 cells, which may have been facilitated by the expression of *V. parahaemolyticus* adhesins. The adherence efficiency of the three clones with suspected elevated levels of invasion was therefore enumerated as described in section 2.2.1. Fig 4.6C and Fig 4.6D show the adherence efficiency and relative adherence of clones A16, A34 and B1 across 3 experimental replicates. Although increased adherence was observed for all 3 clones, the difference was not statistically significant.

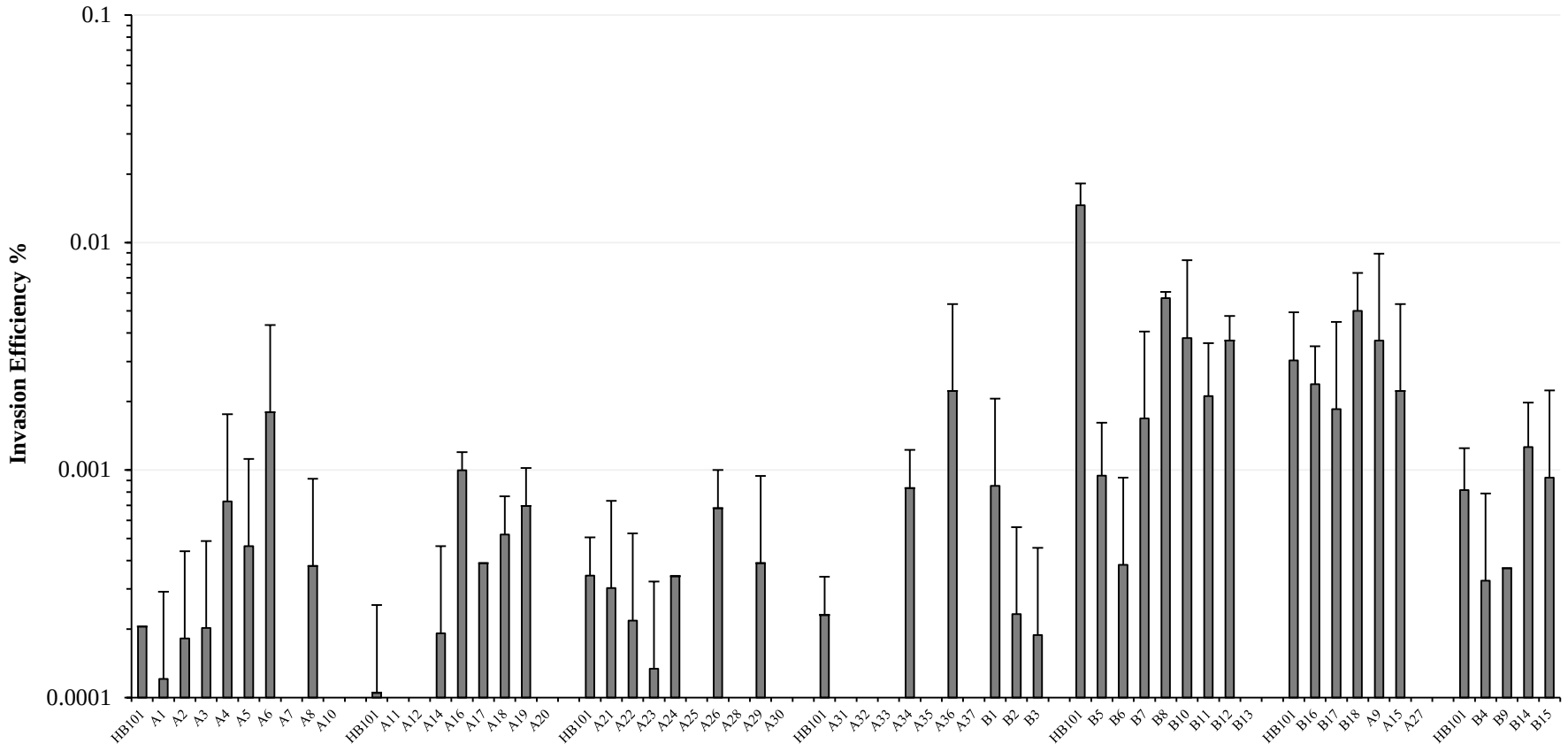

Fig 4.3 Invasion efficiency of library clones isolated by a single round of selection for invasion. Mean plus standard deviation invasion efficiency for two sample replicates is shown for each strain. Individual experiments are separated by blank columns.

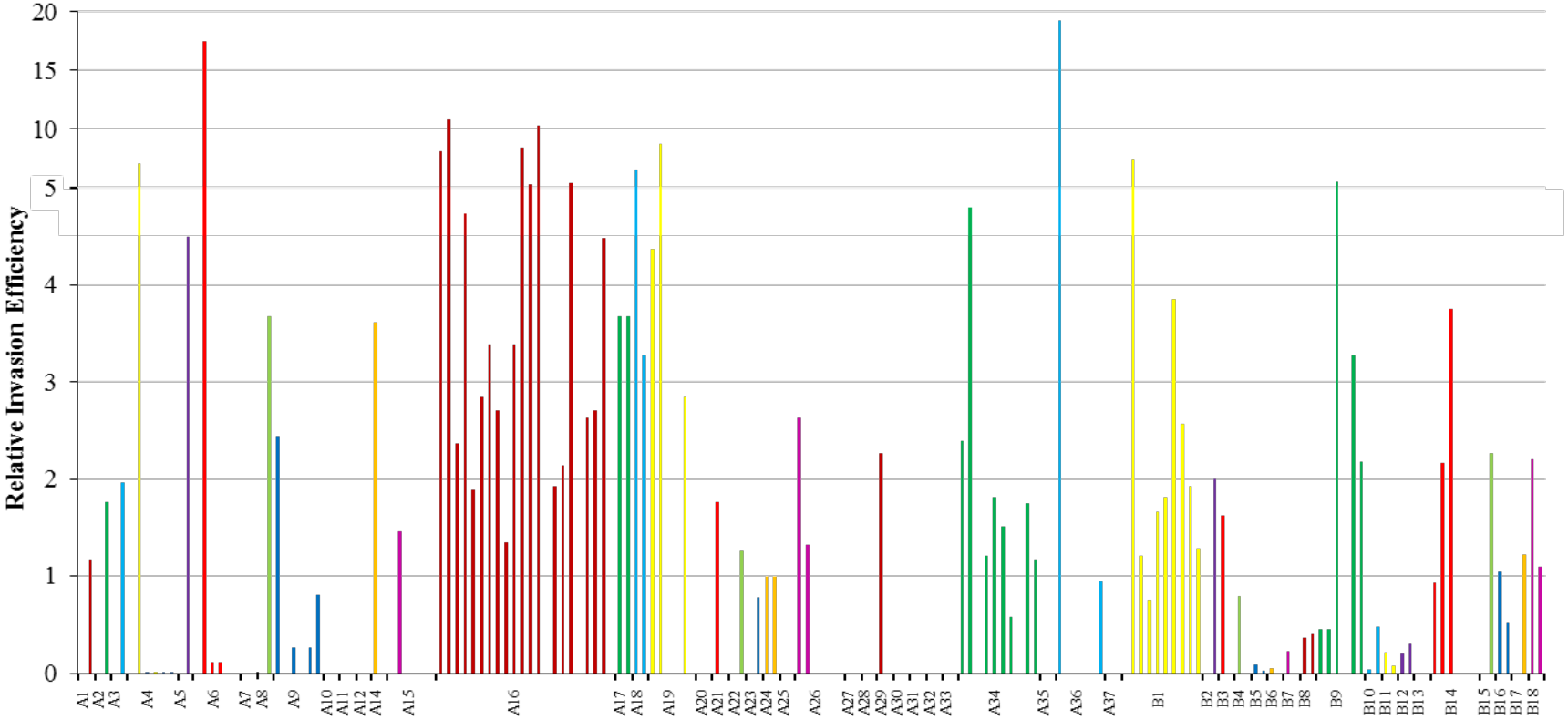

Fig 4.4 Relative invasion efficiency of library clones for all sample replicates tested. X-axis tick marks separate replicates of each library clones. Values plotted indicate the fold change in invasion comparing invasion efficiency from each sample well of Caco-2 to the average *E. coli* HB101 invasion efficiency for the same experiment. The first two columns for each clone represent the values obtained for each sample well used in the first experiment. The mean plus standard deviation of the corresponding invasion efficiencies from the first experiment are also represented in Fig 4.3. Repeat experiments used at least 4 sample wells of Caco-2. Clone A16 was tested in 5 experimental replicates (22 sample wells [2 for the first experiment, 4 for each subsequent experiment]), clones A34 and B1 were tested in 3 experimental replicates (10 sample wells), clones A4, A6, A9, A15, A19, A26, A36, B9 and B14 were tested in 2 experimental replicates (6 sample wells). Blank columns indicate that no invasive bacteria were detected from the corresponding Caco-2 sample well.

4.5 Selection of invasive library clones with four rounds of selection, restriction profiling and sequencing of insert DNA.

Four successive rounds of selection were then carried out in order to optimise selection towards invasive clones by culturing the lysate from one selection overnight and incubating an aliquot with quadruplicate wells of Caco-2 the following day. The gentamicin protection assay was repeated in order to isolate invasive clones from the second round. Again intracellular clones were cultured overnight and the selection process was carried out a total of four times. An aliquot of the lysate, which contained the intracellular clones was plated each day in order to enumerate the library invasion efficiency.

The following invasion efficiencies were obtained: Round 1: 0.0006%; Round 2: 0.0014%; Round 3: 0.0001%; Round 4: 0.0003%. It was expected that the use of four rounds of selection would amplify the selection of invasive clones, however after four rounds of selection the invasion efficiency of the genomic library was lower than that observed after a single round. It is also of note that the invasion efficiency observed (0.0003%) after 4 rounds of selection is typical of that observed for *E. coli* HB101 upon selection with a single gentamicin protection assay. Invasion efficiency did increase with 2 rounds of selection. It may be the case that selection of invasive clones was indeed amplified over two rounds of selection, but that subsequent rounds of selection resulted in out-growth of truly invasive clones, by clones which were not actively invasive but exhibited a more rapid growth rate than the invasive population. Higher rates of bacterial growth would lead to a greater possibility of uptake by Caco-2 due to higher prevalence in the inoculum. Culturing of the lysate overnight may also have led to out-growth of rapidly growing clones and subsequent bias towards those clones during library selection. Therefore it was necessary to enumerate the invasion efficiency of the clones isolated in order to establish whether or not a truly invasive phenotype had been selected for.

16 clones were obtained from a total of 4 sample wells of Caco-2 following the four rounds of selection. This number is lower than that obtained from the first selection using the genomic library (36 A series clones) but similar to that observed for the second library selection (18 B series clones), both of which were carried out using a single round selection.

In order to analyse the diversity of insert sequences contained within the cosmids from D series clones, cosmid DNA from each clone was purified and analysed by restriction digest. Results are shown in Fig 4.5. 3 distinct banding patterns were obtained, indicating the presence of 3 genetically distinct clones. Clones D1 and D5 fell into the first clonal type, clones D2, D3, D6, D8, D10, D12, D13, D14, D15 and D16 formed the second clonal group and clones D4, D7, D9 and D11 formed the third clonal group. 2 representatives from each clonal type were end-sequenced. As expected, clones with similar banding patterns contained identical inserts. Sequencing of the extremities of the insert DNA from clones D6 and D14 revealed 2 loci 356.7 kb apart. It is likely that these clones contain two 40 kb fragments which ligated to one another during ligation with the pWEB-TNC vector.

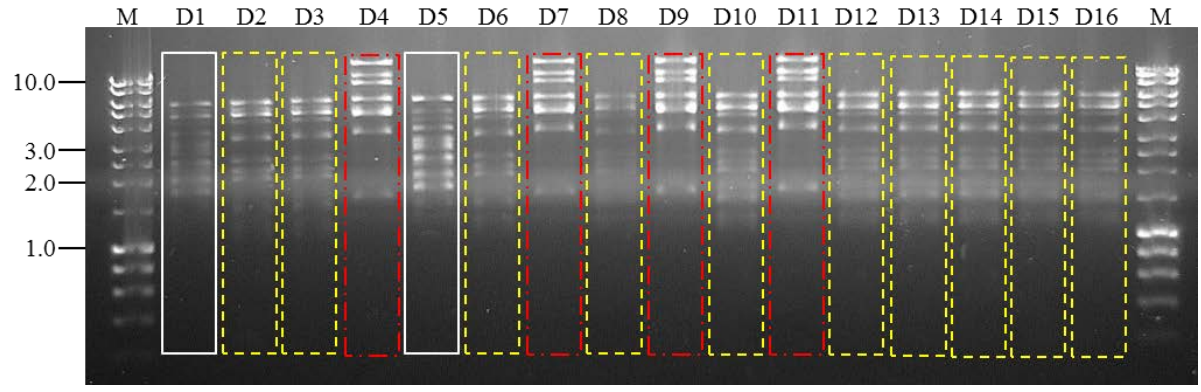

Fig 4.5 Four rounds of invasion selection resulted in selection of 3 genetically distinct clonal types. Cosmid DNA was purified and digested with *Bam*HI, *Sph*I and *Xba*I. Clones displaying similar banding patterns are surrounded by similar boxes. Genetic similarities were confirmed by sequencing a pair of preps from each clonal type. Molecular weight marker (M) sizes are in kb.

As observed in the gel image, profiling by restriction digest represents a rapid, inexpensive means of comparing library clones in order to identify genetically distinct clones from a population. The result of the restriction analysis and sequencing of the D series clones show that selection has occurred towards three genetically distinct clones. In order to assess whether selection towards invasive and/or adherent clones had occurred, pure cultures from one of each genetically distinct clonal type were tested by adherence and invasion assay.

4.6 Enumeration of invasion and adherence efficiency of D series clones.

As seen in Fig 4.6A and Fig 4.6B, no significant differences were observed in invasion efficiencies between HB101 and clones D5, D6 and D9. Adherence assays were also carried out in order to assess whether increased ability to bind to Caco-2 was displayed by these clones in spite of their low levels of invasion. As seen in Fig 4.6C and Fig 4.6D adherence efficiency of these clones, in a similar manner to invasion efficiency was not significantly different to that of *E. coli* HB101.

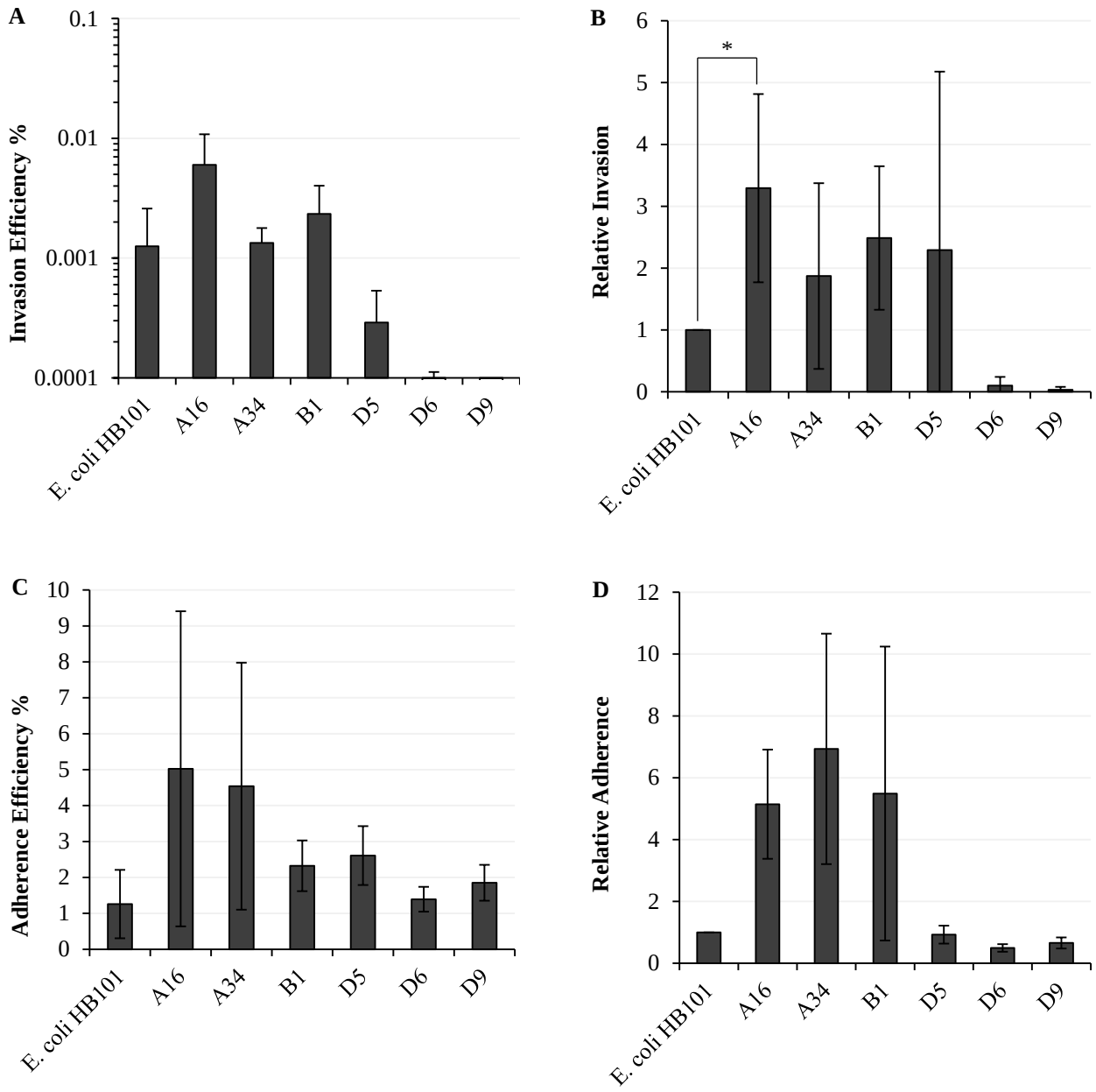

Fig 4.6 Clone A16 displays significantly increased invasion efficiency compared with *E. coli* HB101. (**A**) Mean plus standard deviation invasion efficiencies for A, B and D series clones of interest. (**B**) Mean plus standard deviation invasion efficiencies expressed relative *to E. coli* HB101 invasion efficiency. (**C**) Mean plus standard deviation adherence efficiencies for A, B and D series clones of interest. (**D**) Mean plus standard deviation adherence efficiencies expressed relative *to E. coli* HB101 adherence efficiency. Data for A and B series clones are from at least 3 replicate experiments. Replicates were not carried out for D series clones as invasion and adherence efficiencies were not significantly different to *E. coli* HB101 in first experiments. * $P<0.05$, calculated using paired student's *t* test.

Taken together, the selection of the *V. parahaemolyticus* genomic library for invasion in the heterologous host *E. coli* HB101, led to the isolation of a single clone with elevated levels of

adherence. Invasion efficiencies of 0.0004% (A series), 0.0002% (B series) and 0.0003% (D series) were obtained for each selection. These values are typical of those observed for the library host *E. coli* HB101 using the gentamicin protection assay. The use of multiple rounds of selection (D series) did not lead to an amplified selection towards invasive library clones, likely due to introduction of bias towards rapidly growing clones which were internalised by the Caco-2 cells. The problems encountered in the selection of invasive library clones may have been the result of unsuitability of the *E. coli* HB101 strain as a host for expression of *V. parahaemolyticus* DNA. As mentioned in chapter 3, while *V. parahaemolyticus* (invasion efficiency = 0.004%) does become internalised at a higher rate than *E. coli* (invasion efficiency = 0.0008%), this may be due to *V. parahaemolyticus'* pronounced adherence capacity (fifty-fold more adherent than *E. coli* HB101). This is further highlighted by consideration of the number of cell-associated *V. parahaemolyticus* which become internalised (0.02%), compared with that of *E. coli* XL-1 blue (0.25%). In any case, expression of *V. parahaemolyticus* adhesins by the *E. coli* HB101 genomic library would lead to an increased likelihood of uptake by Caco-2 and therefore selection via the gentamicin protection assay. It is therefore likely that the poor level of isolation of invasive clones resulted from poor expression, toxicity or improper functionality of *V. parahaemolyticus* proteins produced by *E. coli* HB101, a hypothesis which will be further investigated in the coming sections of this chapter.

Clone A16 represents the only library clone which displays truly enhanced invasion compared with the control strain. As such it was the only clone selected for end-sequencing and bioinformatic analysis of its insert in order to identify putative invasins encoded therein. Sequencing and bioinformatic analysis of this clone will be described in section 4.8.

4.7 Selection of adherent library clones.

Selection of adherent clones was carried out by library-Caco-2 co-incubation for 1 h to allow bacteria to adhere to the cells. The Caco-2 cells were then washed to remove non-adherent clones. Finally, the cell-associated clones were recovered by lysing the Caco-2, serially diluting the lysate and plating out appropriate dilutions. The total number of cell-associated clones enumerated from 4 replicate wells was 4.3 X 10^4 cfu. Selection by the gentamicin protection assay yielded only 37 invasive clones from 4 sample wells of Caco-2 cells (section 4.4). This indicated that an insignificant proportion of the total cell-associated bacteria isolated were invasive. As the adherence based selection yielded >1,000-fold more clones than the gentamicin protection assay, all clones could not be analysed for possession of a stable adherent phenotype. As such, 40 clones were selected at random and were labelled E1 to E40.

As with the invasion selection, adherence selection was also carried out using 4 rounds of selection (section 2.3.6) in order to enhance selection towards clones with high levels of adherence. A total of 2.4 X 10^5 cfu of cell-associated bacteria were isolated from 4 wells of Caco-2 (five-fold higher than the adherence efficiency of library selection from a single round of selection). The improved recovery of library clones following four rounds of selection may have occurred due to removal of non-adherent clones by the selection process. The improved recovery however, could also be attributed to the removal of slow growing library clones by four successive rounds of growth. Again 40 clones were selected at random and labelled F1 to F40.

To assess for a stable adherent phenotype, clones were initially tested for adherence efficiency on 2 replicate wells of Caco-2. In Fig 4.7, results are expressed as the mean adherence efficiency (percentage of inoculum) plus standard deviation from two sample wells

of Caco-2. Individual experiments are separated by blank columns. A large degree of variation is observed in the results in Fig 4.7. This is seen both in terms of the large degree of standard deviation between adherence efficiency of each strain from the two sample wells of Caco-2 used for enumeration and in strain to strain variation. Results for adherence efficiency of *E. coli* HB101 (pWEB) also varied up to 400% with the lowest value being obtained in the second experiment (0.9%) and the highest being obtained in the first experiment (3.9%). For E and F series clones, a number of clones had markedly reduced inoculum counts compared with *E. coli* HB101 (pWEB). E3, E25, E32, E35, E38 and E39 had inoculum counts greater than five-fold lower than *E. coli* HB101 (pWEB). As adherence efficiency is determined as a percentage of the inoculum, these clones exhibited high adherence efficiency (Fig 4.7). Although E32 stands out as having the greatest invasion efficiency in Fig 4.7 at 47% of the inoculum, the inoculum cfu count for this strain was just 1.4×10^5 cfu, while the inoculum cfu count for *E. coli* HB101 in the same experiment was 4.2×10^6 cfu. Further tests were not carried out with these clones as low inoculum was the principal reason for high adherence efficiency rather than high levels of binding to Caco-2.

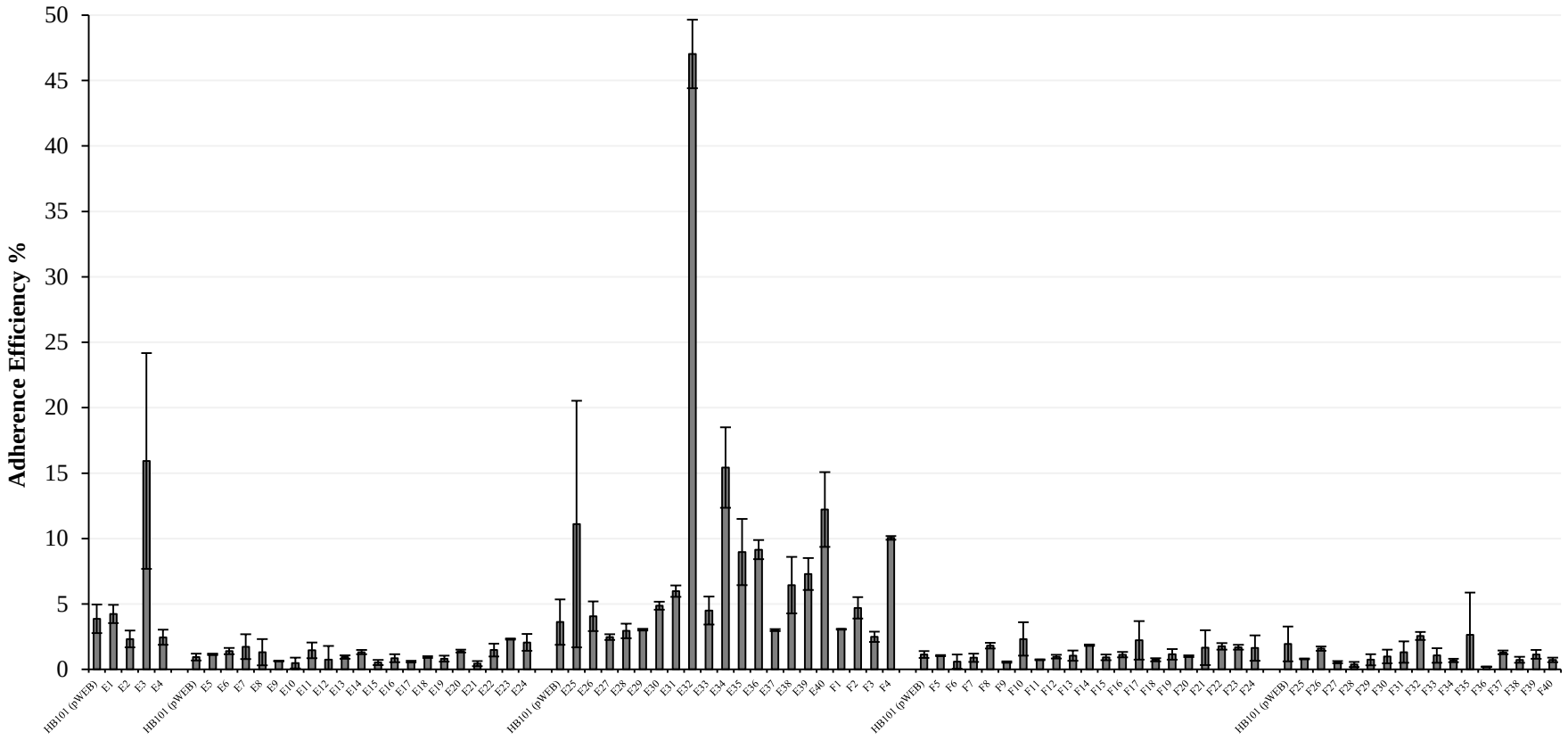

Fig 4.7 Adherence efficiency of library clones (isolated by adherence selection) from first experiments. Individual experiments are separated by blank columns. Adherence efficiency was derived from two sample replicates and is represented as the adherent cfu expressed as a percentage of the inoculum cfu.

Clones displaying higher levels of adherence than *E. coli* HB101 (pWEB) were tested for adherence efficiency on a further 4 wells of Caco-2. A cut-off was set at two-fold higher adherence efficiency than the control strain so as to reduce the numbers of clones analysed in further experiments. Due to the inherent variation between sample wells as seen by the high standard deviation in Fig 4.7, clones where one or both wells led to two-fold higher adherence efficiency than the control were re-tested in a further experiment. The use of a greater number of sample wells to enumerate the adherence efficiency of each clone led to a more accurate evaluation of the mean adherence efficiency. Also, as the adherence efficiency of *E. coli* HB101 (pWEB) varied from experiment to experiment (Fig 4.7), it was necessary to assess adherence efficiency using multiple experiments. Adherence efficiency expressed relative to the *E. coli* HB101 (pWEB) value for the same experiment from all sample wells of Caco-2 tested is shown in Fig 4.8. Values for each clone are coloured differentially and separated by X-axis tick marks. For each clone, the first two columns represent the values obtained for the first experiment. All clones shown in Fig 4.8 either showed higher levels of adherence than the control strain, for one or both of the sample wells used in the first experiment (relative adherence >2, Fig 4.8). The next four columns for each clone are from the second experiment.

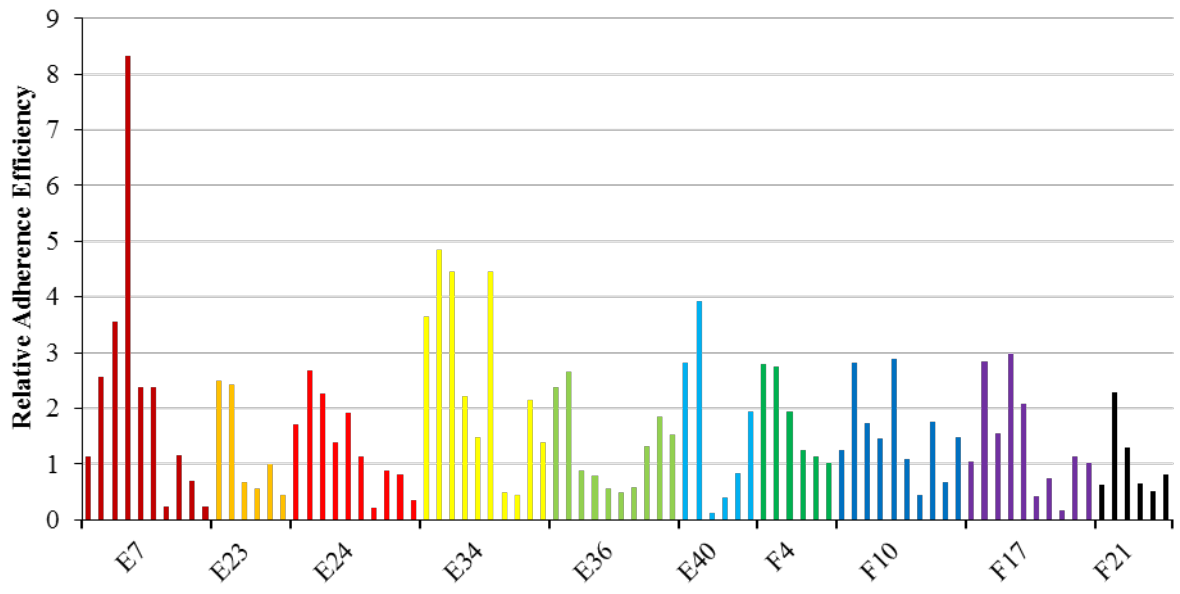

Fig 4.8 Relative adherence efficiency of library clones for all sample replicates tested. X-axis tick marks separate replicates of each library clone. Values plotted indicate the fold change in adherence comparing each sample replicate to the average *E. coli* HB101 adherence efficiency for the same experiment.

Clones E7, E24, E34, E36, F10 and F17 exhibited higher levels of adherence (relative adherence >1) than the control strain for the majority of sample wells used in the first two experiments and were therefore tested in a final experiment on a further four wells of Caco-2 (10 columns in total).

Clones E7, E34 and F10 exhibited the most consistently increased levels of adherence efficiency compared with *E. coli* HB101 (pWEB) across the 3 experiments. Although, 7 out of 10 replicate wells for E7, 8 out of 10 replicates for E34 and 8 out of 10 replicates for F10 had higher levels of adherence than *E. coli* HB101 (pWEB) (ie relative adherence >1), the levels of adherence for the majority of sample replicates across the three experiments showed less than a two-fold increase compared with the control strain. Also some sample wells for every clone tested showed levels of adherence lower than the *E. coli* value for the same experiment, with E7 having one sample well with a relative adherence of only 0.2 (One fifth

of the *E. coli* efficiency). This highlights the inherent variability of the colony counting method with respect to enumeration of bacterial adherence and also emphasises the requirement for a consistent, two-fold or greater increase in adherence efficiency before drawing conclusions about expression of heterologous adhesins. Indeed a paired student's *t* test, taking the mean relative adherence for each experiment with any of the E and F series clones compared with the *E. coli* adherence expressed as 1 failed to yield significant differences ($P<0.05$).

As such it was decided that the adherence efficiency of E and F series clones was not significantly increased and therefore, sequencing and bioinformatic analysis was not warranted.

4.8 Bioinformatic analysis of clone A16.

Having seen significantly increased levels of invasion in clone A16 (Fig 4.6), the cosmid DNA was purified from this clone and end-sequenced with pWEB.For and pWEB.Rev primers. Sequence alignment using NCBI BLASTn to align sequence data with the *V. parahaemolyticus* RIMD2210633 genome sequence allowed identification of two fragments of *V. parahaemolyticus* DNA 33.1 kb apart. This confirmed the presence of DNA of the expected size (from isolation of the gel fragment, Fig 4.2B) and confirmed that no ligation mishaps or contaminants had been introduced during preparation of clone A16.

The 33.1 kb locus between the sequenced extremities of the A16 insert was viewed in the CMR database using chromosomal co-ordinates obtained from BLAST analysis. Each of the 36 genes contained within the insert DNA of clone A16 was then analysed individually using a variety of bioinformatic search utilities, databases and *in silico* analysis tools, including the

CMR database. The CMR website consists of a comprehensive bank of prokaryotic genomic data, which includes the raw genome sequences, primary and JCVI annotations for predicted coding regions, predicted DNA and mRNA features, together with a variety of search tools for use in genome mining applications. Conserved amino acid motifs/domains were viewed using the Pfam database and the conserved domains feature of the NCBI BLASTp database. The Pfam or protein families database makes use of multiple sequence alignments and hidden Markov models in order to assign motifs to regions within both characterised and uncharacterised proteins. NCBI BLASTp is a search utility which allows cross referencing of protein sequences of interest against those contained within the database by alignment of similar amino acid sequences. This search utility also detects conserved domains within the protein of interest and provides information pertaining to the possible activities/functions of the protein based on the functionality of conserved domains in homologous proteins from other species. A schematic representation of the DNA contained within the insert of clone A16 is shown in Fig 4.9. Putative open reading frames, functional category assignments and putative operon structures were analysed using CMR. The pSORTb subcellular localisation prediction software was used as a means of determining the localisation of the proteins of interest. pSORTb provides its predictions of cellular localisation by using BLAST against proteins of known localisation, analysis of hidden Markov models for transmembrane helices (TmHMM) and motif analysis. A summary of the information derived from bioinformatic analysis of each gene within the insert DNA of clone A16 is shown in Table 4.1.

A number of proteins were disregarded as potential adhesins/invasins based on predicted functions in cellular metabolism or regulation of transcription (VPA0227, VPA0232, VPA0233, VPA0234, VPA0235, VPA0237, VPA0240, VPA0243, VPA0244, VPA0246, VPA0249, VPA0250, VPA0251, and VPA0254). A number of proteins were predicted to be involved in transport of substrates across the cell wall (VPA0228, VPA0229, VPA0230,

VPA0231, VPA0236, VPA0238, VPA0239, VPA0241, and VPA0253), all of which were predicted to be located in the cytoplasmic membrane, with the exception of VPA0228, VPA0230 and VPA0236, whose subcellular localisation could not be determined by pSORTb analysis. As such, these proteins were also disregarded as possible adhesins/invasins.

A number of small (< 78 amino acids) hypothetical proteins were analysed, which contained no conserved domains and whose subcellular localisation could not be determined (VPA0245, VPA0247, VPA0252 and VPA0259). Due to the small size, lack of conserved features and lack of detection of transmembrane helices or signal peptides which would allow for secretion, these coding regions were unlikely to code for adhesins or invasins. One other hypothetical protein was observed during bioinformatic analysis (VPA0256). This protein was predicted by TmHMM analysis to contain five transmembrane helices, however pSORTb predicted a cytoplasmic membrane localisation with a confidence score of 10.0. This indicated that the protein would likely be hidden from any potential receptors on the host cell, therefore VPA0256 was not investigated further as a potential invasin.

A number of proteins were analysed which were predicted to have putative functions in cellular processes such as flagellar biosynthesis (VPA0261 and VPA0262) and cell wall synthesis (VPA0260). As a result, further analysis was not carried out on these proteins. The remaining proteins included a hypothetical protein with cytoplasmic localisation and putative enzymatic activity (VPA0255), a putative haemolysin (VPA0257) and a putative NUDIX family DNA repair protein (VPA0258). These were also considered unlikely to possess functionality as adhesins or invasins and were not studied further.

The remaining proteins from Table 4.1 include VPA0242 and VPA0248, both of which were found to contain outer membrane protein A (OmpA) domains.

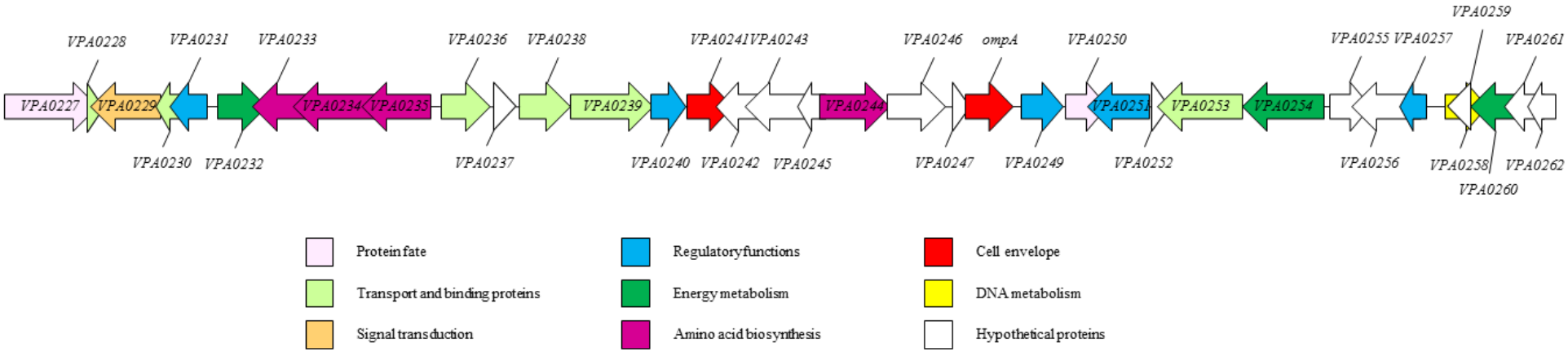

Fig 4.9 Putative coding regions contained within clone A16. Predicted functional categories listed in the key below Fig 4.9 were obtained from the CMR database and are derived from primary annotations.

Table 4.1 Summary of bioinformatic analysis carried out on the coding regions contained within the insert DNA of clone A16.

Gene	Putative operon	Functional Category	JCVI annotation	Pfam domains	Localisation (Score)
VPA0227	*VPA0027, VPA0228*	Protein fate	Cold active alkaline serine protease	1. Signal peptide: Signal for secretion through the CM. 2. I9 Inhibitor domain: Inhibits the protease by blocking the active site. 3. S8 Peptidase domain: Subtilisin like protease domain containing a conserved Asp/Ser/His catalytic triad. 4. Proprotein convertase domain: Necessary for correct folding of the protein.	$EC^{1.}$ (6.27)
VPA0228	*VPA0227, VPA0228*	Transport and binding	ATPase of the AAA+ class	1. Signal peptide: Signal for secretion through the CM.	Unknown, Non-cytoplasmic
VPA0229	*VPA0229, VPA0230, VPA0231*	Signal transduction	PTS system, enzyme IIC	1. Phosphotransferase system, enzyme IIC: Catalyses the phosphorylation of sugars during transport across the CM.	$CM^{2.}$ (10.0)
VPA0230	*VPA0229, VPA0230, VPA0231*	Transport and binding	PTS system, enzyme IIB	1. Phosphotransferase system, enzyme IIB: L-ascorbate specific PTS component. Phosphorylated by enzyme IIA.	Unknown, multiple
VPA0231	*VPA0229, VPA0230, VPA0231*	Regulatory functions	PTS system, enzyme IIA	1. Phosphotransferase system, enzyme IIA: Phosphorylated at conserved His residue by Hpr. Transfers phosphate to His or Cys on enzyme IIB. Possible fructose, mannitol or L-ascorbate specificity.	$CM^{2.}$ (9.82)
VPA0232	None	Energy metabolism	Putative transcriptional regulator	1. LacI: Helix turn helix domain of regulatory proteins which confers DNA binding. 2. Periplasmic binding protein: Domain which binds sugars, changing conformation of the LacI region, activating the transcriptional repressor.	$C^{3.}$ (9.26)
VPA0233	*VPA0233, VPA0234, VPA0235*	Amino acid biosynthesis	Phosphono-acetylaldehyde phosphono-hydrolase	1. Haloacid dehalogenase like hydrolase: Converts phosphono-acetaldehyde into phosphate and acetaldehyde. Major importance in phosphate degredation.	$C^{3.}$ (9.97)
VPA0234	*VPA0233, VPA0234, VPA0235*	Amino acid biosynthesis	Class III amino-transferase	1. Class III AT: Pyridoxal phosphate-dependent amino-transferase domain. Possible acetyl-ornithine specificity. Conversion of N-acetylornithine and αketoglutarate to L-glutamate, N-acetyl L-glutamate 5-semialdehyde.	$C^{3.}$ (9.97)
VPA0235	*VPA0233, VPA0234, VPA0235*	Amino acid biosynthesis	2-AEP phosphonate pyruvate amino-transferase	1. Class V AT: Pyridoxal phosphate-dependent amino transferase. Converts pyruvate and 2-aminoethylphosphonate to L-alanine and phosphonoacetaldehyde. Phosphate degredation.	$C^{3.}$ (9.97)

Table 4.1 continued.

VPA0236	*VPA0236, VPA0237, VPA0238, VPA0239, VPA0240*	Transport and binding	ABC transporter, periplasmic substrate binding protein	1. Bacterial extracellular solute binding protein: Contains a hit for LysR type transcriptional regulator, which binds solutes resulting in changed conformation and activity of helix turn helix. Possible 2-AEP or Fe^{3+} binding specificity.	Unknown, Non-cytoplasmic
VPA0237	*VPA0236, VPA0237, VPA0238, VPA0239, VPA0240*	Hypothetical protein	GNAT family acetyltransferase	1. GNAT family acetyltransferase: Members are involved in transcription/DNA repair. Acetyl-CoA binds to GNAT, then substrate binds to the complex, the acyl group is transferred to the substrate, the product and CoA are released.	Unknown
VPA0238	*VPA0236, VPA0237, VPA0238, VPA0239, VPA0240*	Transport and binding	ABC transporter, ATP binding protein	1. ABC transporter domain: Highly conserved domain from ATP binding cassette (ABC) transporter proteins. Contains phosphate (ATP) binding P-loop. 2. TOBE: Transport-associated domain found downstream of ATP binding region of ABC transport proteins. Binds small molecules (AEP, Fe^{3+}, sulphates etc).	$CM^{2.}$ (10.0)
VPA0239	*VPA0236, VPA0237, VPA0238, VPA0239, VPA0240*	Transport and binding	ABC permease, unknown substrate	1. Binding protein-dependent transport system, inner membrane component: Translocates substrate across the inner membrane. C-terminal region conserved region which forms a cytoplasmic loop between two transmembrane domains.	$CM^{2.}$ (10.0)
VPA0240	*VPA0236, VPA0237, VPA0238, VPA0239, VPA0240*	Regulatory functions	Gluconate repressor (GntR) family transcriptional regulator	1. GntR: This domain contains a conserved N-terminal winged helix turn helix motif, consistent with DNA binding. 2. UTRA: UbiC family transcriptional regulator-associated domain. Ligand binding domain which binds small solutes, changing activity of the regulator. Multi-hit for PhnR. A repressor which regulates degredation of AEP.	$C^{3.}$ (9.97)
VPA0241	None	Cell envelope	Permease of the DMT superfamily	1. 10 transmembrane helices. 2. EamA like transporter domain: Commonly found adjacent to AEP catabolism operons.	$CM^{2.}$ (10.0)
VPA0242	*VPA0242, VPA0243, VPA0245*	Hypothetical protein	OmpA like transmembrane protein	1. Signal peptide: Signal for secretion through the CM. 2. OmpA domain: N-terminal domain found in many outer membrane proteins. This protein does not contain the OmpA C-terminal conserved domain. OmpA domains play a role in aggregation, phage binding and porin function	Unknown, Non-cytoplasmic
VPA0243	*VPA0242, VPA0243, VPA0245*	Hypothetical protein	Putative VirK regulatory protein	1. DUF535: This domain is found in VirK like regulators. *S. flexneri* VirK regulates expression and surface localisation of IcsA, a protein involved in intracellular motility.	$C^{3.}$ (8.96)

Table 4.1 continued.

VPA0244	*VPA0244, VPA0246*	Amino acid biosynthesis	Glycine/D-amino acid oxidase	1. FAD-dependent D-amino acid oxidase domain: Oxidation of neutral and basic amino acids into keto acids. Hit for AEP oxidoreductase PhnW. Converts AEP to ammonia and phosphonoacetaldehyde. Alternative to AEP transaminase VPA0235.	$C^{3.}$ (9.26)
VPA0245	*VPA0242, VPA0243, VPA0245*	Hypothetical protein	Putative protein	None.	Unknown
VPA0246	*VPA0244, VPA0246*	Hypothetical protein	Zinc Carboxypeptidase	1. Signal peptide: Signal for secretion through the CM. 2. M14 peptidase domain: Binds Zinc at His/Glu/X/X/His activating the catalytic C-terminal Glu residue. Hydrolyses C-terminal amino acids from polypeptides.	Unknown
VPA0247	None	Hypothetical protein	Putative protein	None.	Unknown
VPA0248	None	Cell envelope	OmpA, homology with VC2213	1. Signal peptide: Signal for secretion through the CM. 2. OmpA domain: Transmembrane domain consisting of 8 stranded anti-parallel β barrel. 3. OmpA C-terminal domain: Covalently interacts with peptidoglycan in the periplasm.	$OM^{4.}$ (9.93)
VPA0249	*VPA0249, VPA0250*	Regulatory functions	LysR family transcriptional regulator	1. HTH1: DNA binding helix turn helix domain. Members include resistance regulators AmpR and CatM. 2. PBP2: Periplasmic binding protein domain. This domain can bind small solutes.	$C^{3.}$ (9.26)
VPA0250	*VPA0249, VPA0250*	Protein fate	Trifolitoxin immunity protein	1. APH: Amino glycoside phosphotransferase. Resistance protein which phosphorylates glycosidic antibiotics such as kanamycin. Can also be used in fatty acid biosynthesis by phosphorylation of choline and ethanolamine.	Unknown
VPA0251	None	Regulatory functions	LysR family transcriptional regulator	1. HTH1: DNA binding helix turn helix domain. Members include resistance regulators AmpR and CatM. 2. PBP2-LTTR: Periplasmic binding protein domain of LysR type transcriptional regulator. This domain can bind small solutes.	$C^{3.}$ (9.97)
VPA0252	None	Hypothetical protein	Conserved hypothetical protein	None.	Unknown, Non-cytoplasmic
VPA0253	*VPA0253, VPA0254*	Transport and binding	Putative proton/peptide symporter	1. MFS: Major facilitator superfamily domain. Members transport small solutes in response to chemi-osmotic gradients. Bacterial members function primarily in antibiotic resistance	$CM^{2.}$ (10.0)
VPA0254	*VPA0253, VPA0254*	Energy metabolism	L-serine dehydratase SdaA	1. SDHβ: Found in heterodimeric Sdh proteins. Require iron and dithiotreitol. 2. SDHα: Sdh removes an amino group from serine yielding pyruvate and ammonia. Forms an early part of the TCA cycle.	$C^{3.}$ (9.97)

Table 4.1 continued.

VPA0255	None	Hypothetical protein	Conserved hypothetical protein	1. DUF218: Conserved domain containing several highly charged amino acids, suggestive of enzymatic activity. Family members include SanA which confers vancomycin resistance and proteins involved in peptidoglycan synthesis.	C[3.] (8.96)
VPA0256	*VPA0256, VPA0257*	Hypothetical protein	Conserved hypothetical protein	1. 5 transmembrane helices.	CM[2.] (10.0)
VPA0257	*VPA0256, VPA0257*	Hypothetical protein	Putative Hlx haemolysin	1. DUF333: Found in many uncharacterised bacterial proteins. 2. Multi-domain hit for Hlx, a putative haemolysin domain. No homology with TdhI (VP1378), TdhII (VP1314) or Tlh (VPA0226)	Unknown
VPA0258	None	Regulatory functions	MutT, NUDIX family protein	1. NUDIX: NUcleoside DI-phosphate linked to some other moiety, "X". Hydrolase which degrades oxidatively damaged forms of guanine, ADP-ribose, NADPH, dNTP or NTP.	C[3.] (8.96)
VPA0259	None	Hypothetical protein	Putative uncharacterised protein	None.	Unknown
VPA0260	*VPA0260, VPA0261, VPA0262*	Energy metabolism	Membrane bound lytic murein transglycosylase D	1. Signal peptide: Signal for secretion through the CM. 2. SLT: Soluble lytic transglycosylase. A domain found in both soluble and membrane bound lytic transglycosylases. This domain is catalytically active and cleaves the β1-4 glycosidic bond between N-acetylmuraminic acid and N-acetylglucosamine in peptidoglycan. Role in cell division.	Unknown, Non-cytoplasmic
VPA0261	*VPA0260, VPA0261, VPA0262*	Hypothetical protein	LfgN related protein	1. FlgN: Involved in flagellar biosytnthesis. Both FlgN and its chaperone contain the FlgN domain.	Unknown
VPA0262	*VPA0260, VPA0261, VPA0262*	Hypothetical protein	LfgM/FlgM	1. FlgM: Flagellar biosynthesis regulator which binds to and inhibits σ^{28}. Exported through the basal body and hook structure, once produced, which releases σ^{28} to activate transcription of other flagellar genes.	P[5.] (9.83)

Gene names and functional categories were derived from primary annotations in the CMR database. Putative operons were predicted by analysing terminator/promoter positions, ribosomal binding sites and directions of transcription using region view and gene graphic features on the CMR database. Predicted annotations were derived from JCVI annotations in the CMR database. Conserved protein domains were analysed using the Pfam, protein families database and the NCBI BLASTp conserved domains feature. Signal peptides and transmembrane helices were detected using the Pfam database and the CMR TmHMM analysis feature. Subcellular localisation was predicted using the pSORTb computational analysis tool. Abbreviations: [1.] EC, Extracellular; [2.] CM, Cytoplasmic Membrane; [3.] C, Cytoplasm; [4.] OM, Outer Membrane; [5.] P, Periplasm.

VPA0242 was found to code for a protein with a primary annotation as a hypothetical protein and a JCVI annotation as an OmpA-like transmembrane domain protein. TmHMM analysis failed to detect trans-membrane helices. pSORTb analysis also failed to identify the subcellular localisation of the protein coded for by *VPA0242*, however an N-terminal signal peptide was identified, leading to the conclusion that the protein was non-cytoplasmic. Pfam analysis confirmed the presence of the OmpA beta barrel transmembrane domain and also the N-terminal signal peptide. Pfam domain description indicated that many members of the OmpA-like family also possess a C-terminal conserved domain. This domain was not detected in *VPA0242*. A BLAST search for homologous proteins found 38 homologous hypothetical proteins and OmpA domain containing proteins from *Vibrio* and *Shewanella* species with E values for similarity <0.001. Literature analysis revealed roles for OmpA-like proteins in phage interactions, formation of aggregates and invasion into host cells (Schweizer and Henning, 1977; Prasadarao *et al.*, 1996). The findings of Prasdarao *et al.* (1996) demonstrated that attachment of *E. coli* K1 to brain microvascular endothelial cells is facilitated by S-fimbriae attaching to NeuAcα2,3-Gal containing glycoproteins, a process which is followed by OmpA binding to GlcNAcβ1-4GlcNAc residues which promotes traversal across the apical membrane.

VPA0248 was found to code for an OmpA-like protein with homology to VC2213 from *V. cholerae*. An upstream promoter and downstream terminator were detected in the CMR database, lending to the likelihood that OmpA is coded for in a single gene transcriptional unit. TmHMM analysis detected a possible signal peptide and no trans-membrane helices. It appears that the outer membrane beta barrel is not recognised by conventional TmHMM analysis. pSORTb analysis predicted an outer membrane localisation with a confidence score of 9.93. Pfam analysis detected an N-terminal OmpA domain similar to that detected in VPA0242. A C-terminal OmpA domain was also detected, as is common in many OmpA

proteins. Conserved domains were also viewed in NCBI BLAST. The N-terminal OmpA domain contains a motif consistent with the OmpA trans-membrane beta barrel which is predicted to have 8 membrane spanning regions. It was found that the C-terminal domain commonly interacts with peptidoglycan in the gram negative periplasm and is found in many outer-membrane proteins such as the *Vibrio* flagellar motor proteins PomB and MotY. OmpA proteins commonly possess hydrophilic loops which are exposed on the cell surface. It is these loops which play a role in the interaction of OmpA proteins with phage and host cell receptors (Prasadarao *et al.*, 1996; Pautsch and Schulz, 2000). The *V. parahaemolyticus* OmpA protein was found by BLAST analysis to have 30% amino acid identity to the *E. coli* K1 OmpA, which was described by Prasadarao *et al.* (1996) as being involved in the invasion of brain micro-vascular endothelial cells (BMECs). As seen in Fig 4.11, homology between VPA0242, VPA0248 and *E. coli* K1 OmpA is scattered throughout the protein. All 4 of the extracellular loops exhibit pronounced variability and as such it is likely that the proteins may have diverse functionality. As *E. coli* K1 OmpA is involved in invasion of BMECs, the variability within these exposed extracellular loops may confer intestinal tissue specificity to the *V. parahaemolyticus* OmpA proteins, thereby allowing *V. parahaemolyticus* (and library clones expressing *V. parahaemolyticus* OmpA, such as clone A16) to invade intestinal cells.

Fig 4.10 High resolution 3D structure of *E. coli* OmpA. Hydrophilic extracellular loops are labelled L1 to L4. The conserved OmpA β barrel domain, consisting of 8 anti-paralell β strands is indicated by green regions. The C-terminal periplasmic binding domain is labelled T3. Black circles indicate well characterised regions where mutations lead to phage resistance. Figure adapted from Pautsch and Schulz, 2000.

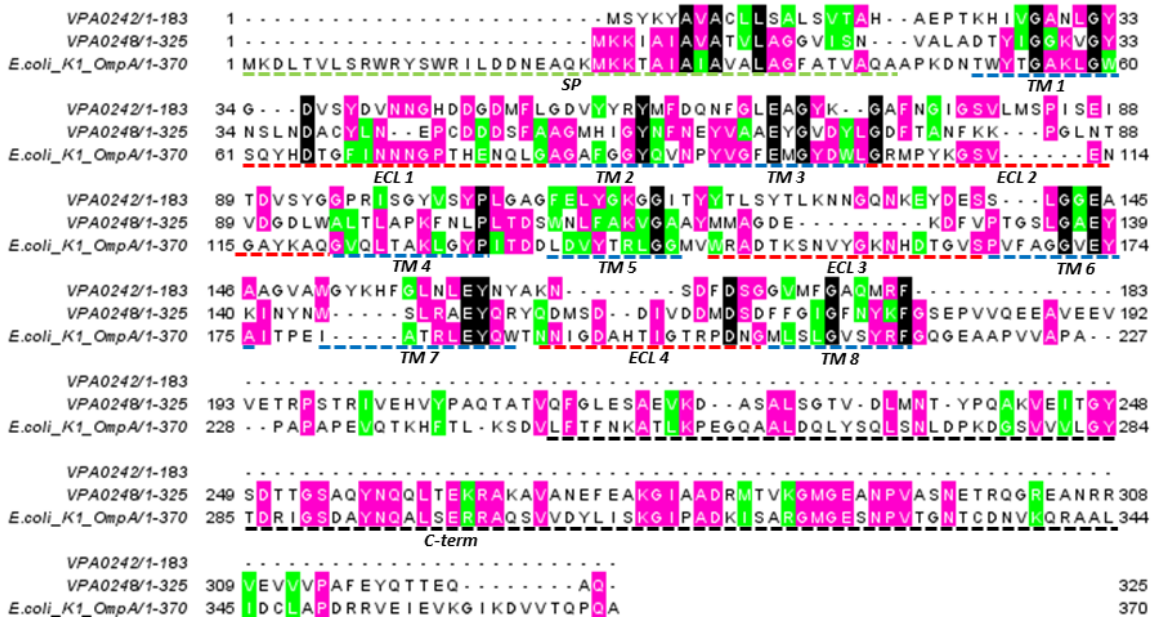

Fig 4.11 Multiple sequence alignment of VPA0242, VPA0248 and *E. coli* K1 OmpA. Multiple sequence alignment was generated using EMBL-EBI Clustal Omega alignment tool. Editing was carried out using the Jalview editor. Black residues are conserved across all three proteins, pink residues are conserved between two of the three proteins and amino acids with similar properties are indicated by green shading. The β helical transmembrane domains are indicated by blue dashed lines with labels *TM 1-TM 8*. The extracellular loops are indicated by red dashed lines and labels *ECL 1-ECL 4*. The signal peptide is indicated by the green dashed line, labelled *SP*. The C-terminal conserved OmpA domain is indicated by the black dashed line, labelled *C-term*.

VPA0242 was found by BLASTp analysis to possess 22% identity across 197 residues of the *E. coli* K1 OmpA protein, compared with 30% identity across the entire protein for VPA0248. VPA0242 is also lacking the periplasmic C-terminal conserved OmpA domain and as such, functionality may be quite diverse compared with the *E. coli* K1 OmpA protein. It was decided that OmpA encoded by *VPA0248* (based on its surface localisation, possession of exposed extracellular loops with binding ability and similarity to a previously studied protein, illustrating a role in the process of attachment and invasion), was the most likely invasin contained within the insert DNA of clone A16 (Fig 4.9, Table 4.1). Further investigations into the role of this OmpA protein in the processes of attachment and invasion of *V. parahaemolyticus* will be provided in the proceeding chapter.

4.9 Library validation by antibiotic selection.

Due to limited detection of strongly invasive/adherent clones from library selections (Fig 4.3, Fig 4.7), an antibiotic selection was carried out in order to confirm that the genomic library was of sufficient quality and coverage. *V. parahaemolyticus* possesses a range of antibiotic resistance mechanisms including the efflux pumps VmrA (Chen *et al.*, 2002) and NorM (Morita *et al.*, 1998). VmrA was shown by Chen *et al.* (2002) to play a role in resistance of *V. parahaemolyticus* to multiple antimicrobials, including acriflavine and ethidium bromide *via* a sodium-coupled efflux mechanism. NorM has been shown by Morita *et al.* (1998), to confer resistance to the fluoroquinolone family of antimicrobials including ciprofloxacin and norfloxacin. Detection of NorM by selection and sequencing of norfloxacin resistant clones would serve to confirm that expression of *V. parahaemolyticus* inserts was possible in the *E. coli* HB101 genomic library. Detection of multiple genetically distinct inserts harbouring the same resistance locus would confirm that an appropriate coverage had been attained.

Spread plating of serial dilutions of the *V. parahaemolyticus* genomic library on agar containing norfloxacin at inhibitory concentrations for *E. coli* HB101, yielded a norfloxacin resistant count of 1.6 X 10^5 cfu ml^{-1} from a total of 3.1 X 10^7 cfu ml^{-1} (0.5%). The *V. parahaemolyticus* genome consists of 5.8 Mb on two separate chromosomes. Assuming an insert size of 30 kb, the 0.5% norfloxacin resistance observed in the genomic library corresponds to 1 resistant clone per unit coverage of 6 Mb of DNA. This indicates that one norfloxacin resistance locus was likely selected. 8 representative colonies were selected and the extremities of the insert DNA from each were sequenced.

All 8 clones were found to contain similar DNA fragments with an identical locus being found in each (Fig 4.12). This was a strong indication of a role for the selected locus in norfloxacin resistance and hence an indication that expression of *V. parahaemolyticus* DNA within this region was possible. Only 3 clones contained identical inserts (N2, N3 and N6, Fig 4.12). This indicates that growth of the recipient strain during phage adsorption and library selection did not result in bias towards a small number of rapidly growing clones. The isolation of 6 genetically distinct clones from the 8 clones sequenced served to confirm that a good level of library coverage was attained.

Interestingly, the known norfloxacin resistance pump NorM was not detected by library selection, indicating that although coverage and quality of the genomic library was appropriate, expression/functionality/correct localisation of *V. parahaemolyticus* proteins in *E. coli* HB101 was not maintained universally. Morita *et al.* (1998) successfully expressed functional NorM in *E. coli* from the native promoter using pBR322 as a shuttle vector. It is worth noting however that a hypersensitive strain of *E. coli,* KAM3 was used in the work of Morita *et al.* (1998). This strain was made sensitive to a variety of antimicrobials by mutation of the *acrAB* multi-drug resistance locus by introduction of Mu phage, which may have increased the sensitivity of detection of norfloxacin resistant recombinant clones. Indeed,

KAM3 displayed a norfloxacin MIC of 0.03 µg ml^{-1} compared with 0.08 µg ml^{-1} observed for *E. coli* HB101 (pWEB) during this work (Fig 4.13).

In any case, functional heterologous expression from native promoter sequences was obtained by Morita *et al.* (1998) and as such, one would expect that functional expression from the cosmid library used in this work would have occurred. This has implications for use of the library not only in screening for antibiotic resistance mechanisms but also in screening for adhesins and invasins. Many adhesins and invasins require expression of multiple proteins. If expression of all components is not possible in *E. coli* HB101, this could explain the poor levels of adherent/invasive clone identification observed in Fig 4.3 and Fig 4.7. Another explanation for the lack of detection of NorM in the library screen is differing codon usage and/or promoter recognition between *V. parahaemolyticus* and *E. coli* HB101.

In order to identify the specific locus responsible for resistance to norfloxacin in the clones isolated, bioinformatic analysis was focused on the common region (Fig 4.12I) observed in all clones isolated. A summary of the bioinformatic analysis carried out on the common DNA locus from the norfloxacin resistant clones is illustrated in Table 4.2. CMR annotations of each of the genes revealed an Emr efflux pump encoded by VPA0097 and VPA0098. EmrAB is a member of the major facilitator superfamily multi-drug efflux pumps and is usually composed of an inner membrane component (EmrB), which confers substrate specificity of the pump, a periplasmic component (EmrA) and an outer membrane pore protein (TolC), which may be found in a different locus to the EmrAB complex (Piddock, 2006). A number of proteins were excluded as potential norfloxacin resistance factors based on bioinformatic analysis. For example, the cell envelope protein encoded by *VPA0102* was found to be a putative isomerase lipoprotein with a domain for α-glucosidase activity by CMR annotations and BLAST analysis of conserved domains. As such, activity in quinolone resistance was ruled out for *VPA0102* and further work was focused on the EmrAB efflux mechanism.

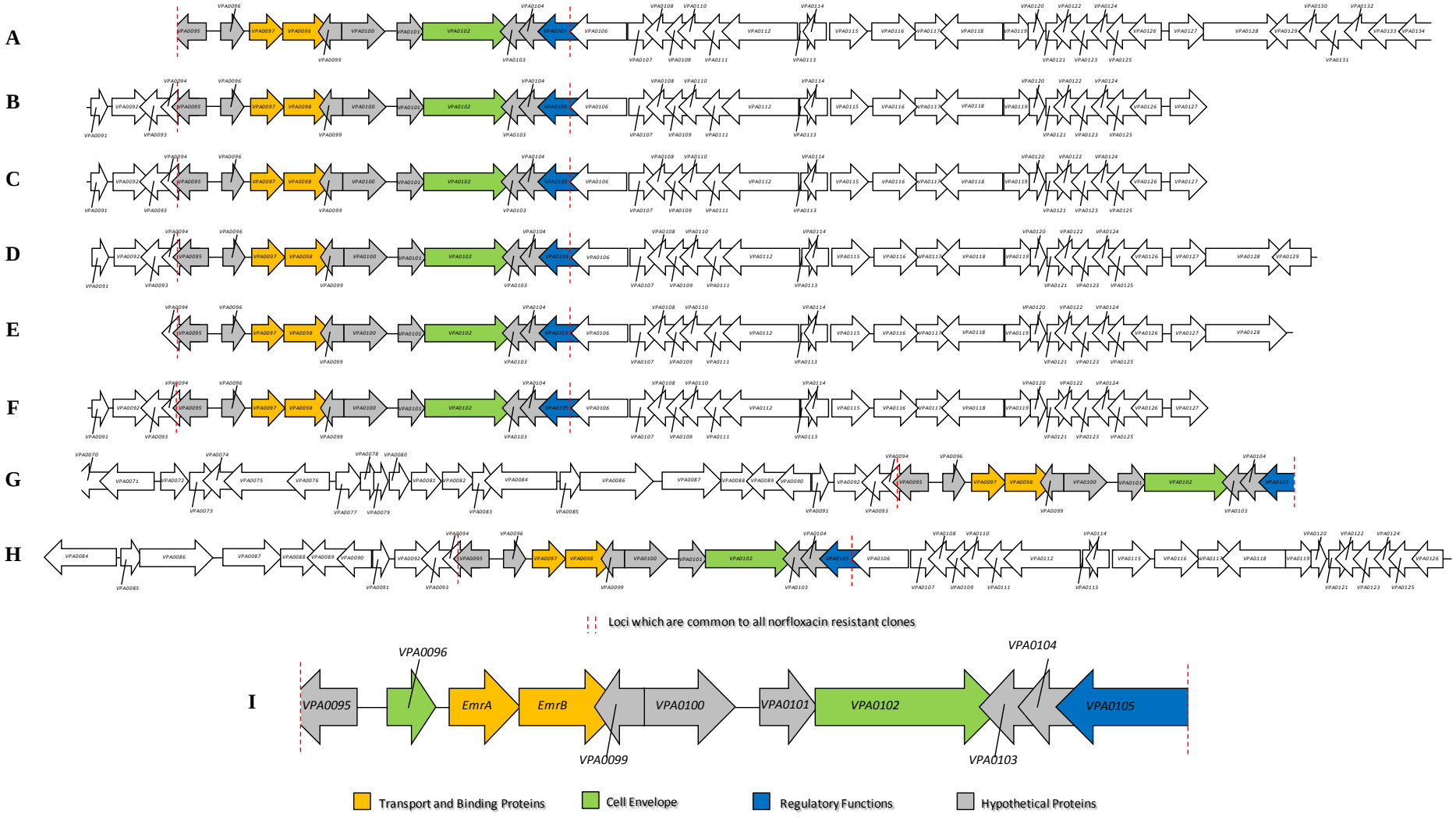

Fig 4.12 Insert DNA contained with norfloxacin resistant library clones. (**A**) N1, (**B**) N2, (**C**) N3, (**D**) N4, (**E**) N5, (**F**) N6, (**G**) N7, (**H**) N10, (**I**) Expanded view of the common locus contained within all 8 clones.

Table 4.2 Summary of bioinformatic analysis carried out on the common region contained within the insert DNA of norfloxacin resistant clones.

Gene	Putative operon	Functional Category	JCVI annotation	Pfam domains	Localisation (Score)
VPA0095	None	Hypothetical protein	Putative pentapeptide repeat protein	1. 3 pentapeptide repeat domains: Domains which mimic the structure of DNA. Family member MfpA binds to and inhibits DNA gyrase.	EC[1.] (9.45)
VPA0096	*VPA0096, VPA0097, VPA0098*	Cell envelope	Outer membrane protein OprG	1. Signal peptide: Signal for secretion through the CM. 2. OmpW: Family of outer membrane proteins. The receptor for colicins in *E. coli*. May also form an outer membrane channel or be involved in cell wall biogenesis.	OM[4.] (10.0)
VPA0097	*VPA0096, VPA0097, VPA0098*	Transport and binding	HlyD family secretion protein	1. HlyD: Bacterial secretion protein. Members include proteins which translocate bacterial haemolysins. Multi-domain hit for the multi-drug efflux domain EmrA. Also contains 2 catalytic biotinyl/lipoyl-dependent carboxylase domains	CM[2.] (9.82)
VPA0098	*VPA0096, VPA0097, VPA0098*	Transport and binding	Putative EmrB/QacA family efflux protein	1. MFS1: Major facilitator superfamily efflux protein domain. Transport a wide variety of substrates. Multi-domain hit for EmrB. Commonly encoded in the same locus as EmrA. Multi-drug resistance. Family members confer resistance to quaternary ammonium compounds, fatty acids and tetracenomycin C.	CM[2.] (10.0)
VPA0099	None	Hypothetical protein	Conserved hypothetical protein	1. ROF: Modulator of Rho-dependent transcription termination. ROF binds to Rho and inhibits Rho-dependent termination.	Unknown
VPA0100	None	Hypothetical protein	Metallo-β-lactamase protein	1. Lactamase B2: Part of the β lactamase superfamily. Predicted Zinc-dependent β lactam specific hydrolase.	C[3.] (8.96)
VPA0101	*VPA0101, VPA0102*	Hypothetical protein	Conserved hypothetical protein	None	C[3.] (8.96)
VPA0102	*VPA0101, VPA0102*	Hypothetical protein	Putative lipoprotein	1. PRK10137: α glucosidase domain. Also domain for trehalase activity. Recycles trehalose to glucose. Trehalose is a glucose dimer which can be broken down under conditions of stress.	Unknown
VPA0103	*VPA0103, VPA0104, VPA0105*	Hypothetical protein	Expressed protein	1. Macro: ADP ribose binding domain. In *E. coli*, family member YmdB downregulates RNAse III activity by interacting with the region of the protein required for dimerization/activation.	Unknown
VPA0104	*VPA0103, VPA0104, VPA0105*	Hypothetical protein	Ring cleaving di-oxygenase	1. Glyoxalase: Domain found in bleomycin resistance proteins, glyoxalase I and ring cleaving di-oxygenase, which incorporate both atoms of O_2 into substrates using metal ions as co-factors.	C[3.] (9.97)

Table 4.2 continued.

VPA0105	*VPA0103, VPA0104, VPA0105*	Regulatory functions	PutativeLysR transcriptional regulator	1. HTH1: DNA binding helix turn helix domain. Members include resistance regulators AmpR and CatM. 2. LysR: Substrate binding domain. LeuO type domain. LeuO activates leucine synthesis and biofilm formation in *V. cholerae*.	C[3.] (9.97)

Gene names and functional categories were derived from primary annotations in the CMR database. Putative operons were predicted by analysing terminator/promoter positions, ribosomal binding sites and directions of transcription using region view and gene graphic features on the CMR database. Predicted annotations were derived from JCVI annotations in the CMR database. Conserved protein domains were analysed using the Pfam, protein families database and the NCBI BLASTp conserved domains feature. Signal peptides and transmembrane helices were detected using the Pfam database and the CMR TmHMM analysis feature. Subcellular localisation was predicted using the pSORTb computational analysis tool. Abbreviations: [1.] EC, Extracellular; [2.] CM, Cytoplasmic Membrane; [3.] C, Cytoplasm; [4.] OM, Outer Membrane.

4.10 Norfloxacin MIC of resistant clones.

The 8 clones shown in Fig 4.12 were found to be norfloxacin resistant by plating on LB agar + 0.1 µg ml^{-1} norfloxacin. In order to quantify the resistance of each clone, an MIC was carried out by incubation of library clones in a doubling dilution series of norfloxacin concentrations in LB broth as described in section 2.3.7. Results are shown in Fig 4.13. A four-fold increase in norfloxacin MIC was observed in all of the clones selected by plating on LB agar + 0.1 µg ml^{-1}(Fig 4.13B). Fig 4.13A illustrates growth curve analysis of clones grown in medium containing 0.08 µg ml^{-1} norfloxacin. No effect on growth rate was seen for any of the clones analysed. Growth of *E. coli* HB101 however was completely inhibited at this concentration.

A

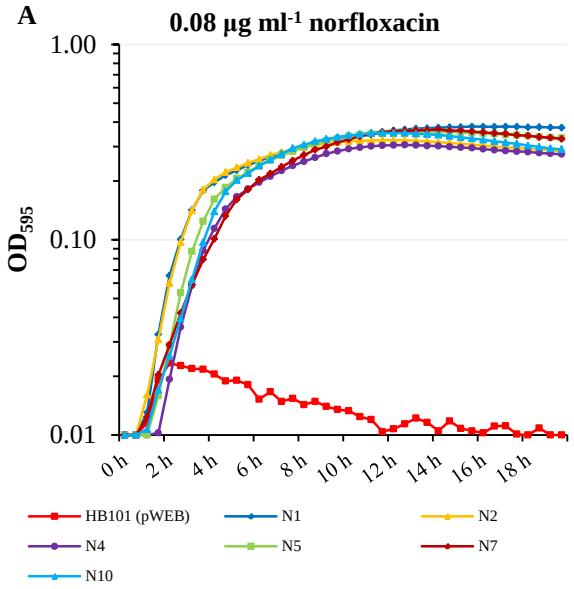

B

Strain	MIC of norfloxacin (µg ml^{-1})
E. coli HB101 (pWEB)	0.08
N1	0.3
N2	0.3
N4	0.3
N5	0.3
N7	0.3
N10	0.3

Fig 4.13 Library clones isolated by selection on LB agar + norfloxacin display elevated norfloxacin MIC compared with *E. coli* HB101. (**A**) Growth curve analysis of genetically distinct library clones cultured in LB + 0.08 g ml^{-1} norfloxacin. Each data point is the mean OD595 for 2 sample replicates. (**B**) Summary of norfloxacin MICs for genetically distinct library clones. The MIC value shown was observed in at least 2 of 3 experimental replicates.

4.11 Expression of EmrAB in *E. coli* BL21.

In order to ascertain if EmrAB was responsible for the increased norfloxacin resistance observed in the clones isolated by antibiotic selection (Fig 4.13), the *emr* genes were cloned into pET101. In order to analyse the role of each component, *emrA* and *emrB* were cloned independently into pET101. A third construct was prepared, containing the full *emrAB* locus. The strains were compared by MIC with BL21/DE3 harbouring the empty pET101 vector. *E. coli* BL21 was used due to its ability to stably maintain vectors during high levels of expression. Expression via the T7 promoter was induced in exponential phase cultures for 1.5 h prior to exposure to norfloxacin. Expression was maintained throughout growth curve analyses by including IPTG during overnight incubation at the same concentration as that used for initial induction.

IPTG concentrations of 50 mM, 100 mM, 500 mM and 1 M were employed. No resistance to norfloxacin was observed in any of the strains tested, even at concentrations as low as 0.04 μg ml^{-1} (data not shown). Plate count MICs were also attempted at concentrations ranging from 0.04 to 0.3 μg ml^{-1} on LB agar, again no differences were observed between *E. coli* BL21 carrying the empty pET101 vector and BL21 expressing EmrAB. When carrying out plate count MICs, it was noted that all strains (including the empty pET101 control) displayed lower viable cfu with induction levels higher than 50 mM IPTG. It is unclear why this sensitivity to IPTG occurred, particularly in the empty vector control strain.

These findings demonstrated that efflux *via* EmrAB is not the reason for resistance of the clones tested in Fig 4.13 to norfloxacin. It was decided to carry out further bioinformatic analysis of the hypothetical proteins contained within the common locus. *VPA0095* was found to encode a protein with a pentapeptide repeat domain, a domain which is commonly involved in DNA binding (Table 4.2). *VPA0096* was found to encode a putative OmpW

family porin protein.*VPA0099* was found to encode a putative inhibitor of Rho-dependent transcriptional termination. *VPA0100* was found to possess a conserved metallo-β-lactamase domain, which could indicate a role in resistance to β-lactam antimicrobials but not members of the quinolone family. *VPA0103* was found to possess an ADP-ribose binding domain which is found in many unrelated proteins. *VPA0104* was found to encode a putative ring cleaving dioxygenase. No annotations or conserved domains were detected in the CMR database, Pfam or NCBI BLAST for *VPA0101*.

Literature analysis of the hypothetical pentapeptide repeat protein encoded by *VPA0095* resulted in the finding that *VPA0095* encodes a Qnr (quinolone resistance) protein (Poirel *et al.*, 2005; Saga *et al.*, 2005). Poirel *et al.* (2005) found that expression of *V. parahaemolyticus* Qnr in *E. coli* Top10 increased norfloxacin MIC from 0.032 μg ml^{-1} to 0.38 μg ml^{-1}. While the precise mechanism of Qnr proteins has yet to be described, it has been suggested that the protein prevents the formation of the gyrase-DNA-quinolone complex thereby interfering with quinolone activity (Tran *et al.*, 2005).

The above findings demonstrate that *VPA0095* encodes a previously identified and characterised quinolone resistance mechanism. This confirms that expression of *V. parahaemolyticus* insert sequences from the genomic library was possible. It has also been shown that library coverage should be sufficient, as 6 genetically distinct loci possessing *VPA0095* were isolated from the norfloxacin screen. The lack of detection of the known norfloxacin efflux pump NorM illustrates that expression of *V. parahaemolyticus* sequences was not occurring universally in the genomic library, thus highlighting the difficulties which were encountered during selection of adhesins and invasins from the genomic library. Functional assessment of the role of the EmrAB efflux pump is now being undertaken by analysis of MICs for various antimicrobial compounds using *E. coli* BL21 expressing EmrAB from the pET101 vector. A knockout deletion mutant of *emrAB* in *V. parahaemolyticus* will

also be screened for sensitivity to a range of antimicrobial compounds in order to confirm the role of EmrAB.

4.12 Alternative means of adhesin identification.

Library selection for invasion resulted in identification of one clone from 55 tested which exhibited significantly increased invasion (3 fold higher than the control strain). As *V. parahaemolyticus* displays markedly higher adherence than the control strain *E. coli* HB101 (fifty-fold increase) and only a five-fold increase in invasion, an attempt to identify adhesins was undertaken. Adherence selection failed to retrieve clones with consistently elevated levels of adherence from 80 clones tested. Due to the low numbers of clones obtained and also the low relative adherence of all clones analysed, an alternative method to library selection was investigated in order to identify putative adhesins.

The VFDB (Virulence Factors of Pathogenic Bacteria Database) was consulted in order to identify putative *V. parahaemolyticus* adhesins based on homology with adhesins from the more studied organism, *V. cholerae*. The VFDB is a comprehensive, comparative pathogenomics database, which makes use of the vast amounts of sequence data which has been derived from bacterial pathogens and allows for a variety of comparative analyses in order to predict the presence of virulence factors in a variety of bacterial species. A summary of the information retrieved from the VFDB search, coupled with BLASTp results for homologous proteins in *V. parahaemolyticus* is shown in Table 4.3.

The *V. cholerae* accessory colonisation factor locus contains four genes: *acfA*, *acfB*, *acfC* and *acfD* in a single poly-cistronic unit. Peterson and Mekalanos (1988), found that transposon insertions in any of the four *acf* genes resulted in a reduced colonisation capacity during *in*

vivo infections of CD1 mice. While the precise mechanism of action of the accessory colonisation factor has yet to be determined, the *acf* locus is found adjacent to the toxin co-regulated pilus locus and transcription of both *acf* and *tcp* genes is regulated by the transcription factor ToxR (Kovach *et al.*, 1996). Of the four genes, greater than 40% amino acid identity with *V. parahaemolyticus* proteins was only found to AcfA using BLAST analysis. Also, no other coding regions with *acf* annotations were identified in the vicinity of the *V. parahaemolyticus acfA* gene. As only *acfA* was found in *V. parahaemolyticus* and *acfA* itself had only 41% homology to the *V. cholerae* protein, further analysis of the *acf* locus was not carried out.

The MSHA locus containing 13 genes involved in production of a type IV pilus was found to be present in both *V. cholerae* and *V. parahaemolyticus*. Primary annotations in the CMR database assigned VP2697 as the major pilin subunit, MshA in *V. parahaemolyticus*. JCVI annotation however, assigned VP2698 as the major pilin due to homology with VC0409 (*V. cholerae* MshA) with VP2697 also assigned as an MshA major pilin subunit. BLAST analysis confirmed VP2698 as the MshA major pilin subunit with 59% amino acid identity to *V. cholerae* MshA over 57% of the sequence. Another MshA homologue (VPA0747) was found on chromosome 2 of *V. parahaemolyticus* bearing 50% identity over 67% of the *V. cholerae* MshA amino acid sequence. VP2697 did not bear significant homology to any *V. cholerae* proteins but homologues from other *Vibrio* species were found by BLAST analysis. MshA proteins VP2698, VPA0747 and VP2697 were labelled MshA1, MshA2 and MshA3 respectively for convenience.

A third TFP locus, which exhibited homology to the *pilABCD* locus of *V. cholerae* was identified in *V. parahaemolyticus*. The major pilin subunit, PilA of *V. parahaemolyticus* was found to have 42% amino acid homology across 96% of the *V. cholerae* PilA protein sequence.

Mutants of both *mshA*1 and *pilA* have been constructed in *V. parahaemolyticus* RIMD2210633 and have been studied for involvement in biofilm production by Shime-Hattori *et al.* (2006). It was found that MshA1 played a role in initial attachment to abiotic surfaces, while PilA played a role in formation of bacterial aggregates. It was found that *pilA* transcription was induced by a mixture of monomeric GlcNAc and chitooligosaccharide. This finding was consistent with reports that *V. cholerae pilA* is the major pilin subunit of a chitin regulated pilus (Meibom *et al.*, 2003). A correlation between adherence of clinical and environmental *V. parahaemolyticus* strains to Caco-2 and their ability to agglutinate human erythrocytes was observed by Nagayama *et al.* (1994). In addition to OmpA (section 4.8), it was decided to analyse the relative roles of PilA and the putative mannose sensitive haemagglutinins MshA1, MshA2 and MshA3 in adherence of the pandemic clone of *V. parahaemolyticus* RIMD2210633 to Caco-2.

In order to gain a better understanding of the construction of the MSHA, it was decided to also construct inactivating mutations of the putative MSHA ATPase encoded by *mshE* and the outer membrane secretin protein encoded by *mshL*.

Table 4.3 VFDB, BLASTp comparison of adherence-related virulence genes from *V. cholerae* and *V. parahaemolyticus*.

Virulence factors	Related genes	*V. cholerae* N16961 (O1 biovar eltor)	*V. parahaemolyticus* RIMD 2210633	Coverage	E value	Identity
Accessory colonization factor	*acfA*	*VC0844*	*VPA0695**	100%	2×10^{-68}	41%
	acfB	*VC0840*	*VPA0511**	100%	3×10^{-102}	33%
			*VP1904**	99%	8×10^{-68}	29%
			*VP2827**	80%	1×10^{-66}	31%
			*VP1651**	83%	5×10^{-60}	30%
	acfC	*VC0841*	None			
	acfD	*VC0845*	*VPA1376**	99%	0	60%
Mannose-sensitive hemagglutinin (MSHA type IV pilus)	*mshH*	*VC0398*	*VP2708**	99%	0	62%
	mshI	*VC0399*	*VP2707**	100%	5×10^{-137}	42%
	mshJ	*VC0400*	*VP2706**	100%	2×10^{-75}	49%
	mshK	*VC0401*	*VP2705*	95%	4×10^{-28}	46%
	mshL	*VC0402*	*VP2704**	100%	0	68%
	mshM	*VC0403*	*VP2703**	100%	9×10^{-131}	62%
			VP0415	98%	3×10^{-51}	38%
	mshN	*VC0404*	*VP2702**	98%	3×10^{-93}	43%
	mshE	*VC0405*	*VP2701**	99%	0	78%
			*VP0134**	73%	9×10^{-116}	43%
			*VP2524**	96%	3×10^{-103}	36%
	mshG	*VC0406*	*VP2700**	100%	0	71%
			VP0135	100%	3×10^{-59}	25%
			VP2525	99%	3×10^{-55}	29%
	mshF	*VC0407*	*VP2699*	88%	3×10^{-13}	24%
	mshB	*VC0408*	*VPA0747*	29%	1×10^{-14}	52%
			VP2698	59%	4×10^{-14}	31%
			VP1434	42%	1×10^{-8}	29%
			VP2523	16%	4×10^{-8}	53%
	mshA	*VC0409*	*VP2698*	57%	1×10^{-34}	59%
			VPA0747	67%	3×10^{-34}	50%
			VP1434	38%	9×10^{-15}	45%
			VP2523	17%	1×10^{-7}	55%
	mshC	*VC0410*	*VP2696*	94%	3×10^{-18}	33%
	mshD	*VC0411*	*VP2695*	96%	3×10^{-35}	37%

Table 4.3 continued.

Virulence factors	Related genes	*V. cholerae* N16961 (O1 biovar eltor)	*V. parahaemolyticus* RIMD 2210633	Coverage	E value	Identity
Toxin-coregulated pilus (type IVB pilus)	*tcpA*	*VC0828*	None			
	tcpB	*VC0829*	None			
	tcpQ	*VC0830*	None			
	tcpC	*VC0831*	None			
	tcpR	*VC0832*	None			
	tcpD	*VC0833*	None			
	tcpS	*VC0834*	None			
	tcpT	*VC0835*	*VP0134*	66%	9×10^{-48}	30%
			VP2524	67%	5×10^{-45}	33%
			VP2701	66%	5×10^{-37}	28%
			VP2615	30%	8×10^{-23}	34%
	tcpE	*VC0836*	*VP0135*	77%	1×10^{-9}	32%
			VP2700	77%	9×10^{-7}	22%
	tcpF	*VC0837*	None			
	tcpN/toxT	*VC0838*	None			
	tcpJ	*VC0839*	*VP2526*	85%	3×10^{-29}	31%
	tcpI	*VC0825*	*VPA1462*	54%	2×10^{-50}	34%
			VPA1492	54%	1×10^{-47}	36%
			VP0963	64%	5×10^{-44}	34%
			VPA0511	81%	1×10^{-39}	28%
	tcpP	*VC0826*	*VPA1332*	41%	8×10^{-8}	29%
			VPA1076	31%	4×10^{-7}	34%
	tcpH	*VC0827*	None			
Type IV pilus	*pilA*	*VC2423*	*VP2523*	96%	3×10^{-25}	42%
			VP0656	37%	7×10^{-13}	43%
			VP0136	54%	5×10^{-11}	30%
			VP2698	20%	1×10^{-7}	52%
	pilB	*VC2424*	*VP2524**	100%	0	74%
			*VP0134**	69%	3×10^{-125}	47%
			*VP2701**	97%	2×10^{-104}	36%
			VP2615	51%	2×10^{-30}	31%
	pilC	*VC2425*	*VP2525**	99%	0	74%
			VP0135	96%	1×10^{-59}	29%
			VP2700	97%	5×10^{-58}	28%
	pilD	*VC2426*	*VP2526**	98%	5×10^{-156}	73%
			VP2422	39%	1×10^{-6}	31%

This table illustrates the results of a VFDB search for adherence-related genes in *V. cholerae*, coupled with the results of BLASTp analysis to detect homologous proteins in *V. parahaemolyticus*. Adherence-related virulence genes from *V. cholerae* were observed using the VFDB. The presence of homologous genes in *V. parahaemolyticus* was confirmed by BLASTp alignment of the amino acid sequence of each *V. cholerae* protein with the *V. parahaemolyticus* proteome (sequences obtained from CMR). Up to four homologous proteins were included in the results for each BLASTp search, with a cut-off alignment score of >40 being employed for inclusion of a given homolog. * denotes *V. parahaemolyticus* proteins with high levels of homology to the corresponding *V. cholerae* protein (alignment score >200).

4.13 Summary and Discussion.

Genomic library screening led to the isolation of a single library clone with elevated invasion. A total of 54 clones were isolated by selection using the gentamicin protection assay. In order to ascertain whether the selected clones were obtained due to increased invasiveness conferred by *V. parahaemolyticus* insert DNA or due to background invasion of *E. coli* HB101, pure cultures of each clone were analysed. Of the 54, only clone A16 exhibited significantly increased invasion compared with the *E. coli* HB101 control. 80 library clones were selected by adherence assay and tested for elevated levels of adherence using pure cultures. No clone showed significantly elevated adherence compared with the *E. coli* HB101 (pWEB) control strain. Although *E. coli* HB101 is considered non-adherent and non-invasive (Blomfjeld *et al.*, 1991), background levels of adherence and invasion may still have a major influence on selection of library clones. Background adherence is of particular concern as ~ 4 X 10^4 (1% of the inoculum) cell-associated *E. coli* HB101 were recovered from a typical adherence assay.

Although background levels of adherence may explain to some extent the poor recovery of truly adherent/invasive clones, expression of *V. parahaemolyticus* adhesins/invasins should have increased the likelihood of recovery with the selection methods described in this chapter. The increased likelihood of recovery should have been amplified by using multiple rounds of selection. As seen by the low invasion efficiencies exhibited in D series clones (Fig 4.6A) and the low adherence efficiencies exhibited by F series clones (Fig 4.7), this was not the case. As demonstrated in Fig 4.5, selection for invasion with multiple rounds did result in recovery of 3 clonal types. It is likely that selection of these clones resulted from bias towards fast growing clones which may have outgrown other clones within Caco-2 cell lysates from previous selections. Having taken steps to ensure that background adherence/invasion would not interfere with selection of adherent/invasive clones, it appears that other issues may have

caused poor recovery rates, such as incompatibility between the *V. parahaemolyticus*-derived cosmid library and the heterologous *E. coli* host.

Cosmid libraries have been used extensively for functional metagenomic analysis by groups such as Gloux *et al.* (2007), Brady *et al.* (2007) and Craig *et al.* (2010). In the case of metagenomics, DNA is extracted from highly diverse microbial populations such as those residing in soil or in the human intestinal tract. Such libraries represent a rich source of highly variable insert sequences, coding for a myriad of proteins with wide ranging functional characteristics. Brady *et al.* (2007) have described "hit rates" of as low as 1 in 100,000 clones for the phenotypes of antibiotic activity and pigmentation. Low hit rates in metagenomic libraries commonly result as a result of incompatibility between the source DNA and the heterologous host. The complexity inferred on metagenomic libraries as a result of their diversity also requires that a large number of clones must be screened to detect a functionally active clone. This has the effect of limiting functional analysis to simple traits such as pigmentation and antimicrobial activity.

The choice of a heterologous host for expression is of key importance in construction of heterologous libraries which require functional screening. Craig *et al.* (2010) describe the functional screening of a soil DNA library in six different species of bacteria. *E. coli* yielded 2 antibacterially active clones and no pigmented clones, while *Ralstonia metallidurans* yielded 4 clones positive for antimicrobial activity and >18 clones which tested positive for at least 3 different types of pigmentation. As *E. coli* is derived from the *gammaproteobacteria* and *R. metallidurans* is derived from the *betaproteobacteria*, it is clear that selecting a range of diverse hosts represents the best possible solution for expression of heterologous DNA from environmental sources. While the use of diverse hosts is an important consideration for functional metagenomic analysis, it is likely that *E. coli* represents the most suitable host for

heterologous expression of *V. parahaemolyticus* DNA, as both organisms are closely related members of the *gammaproteobacteria*.

Many of the issues with lack of expression occur as a result of differential codon usage between the source organism and the expression host. Codon usage of *E. coli* and *V. parahaemolyticus* is quite similar. Codons which are commonly problematic for heterologous expression in *E. coli* due to low frequency of occurrence include: arginine (AGG); arginine (AGA); leucine (CUA); isoleucine (AUA); proline (CCC); glycine (GGA) (Terpe, 2006). All of these occur at similarly low frequencies in *V. parahaemolyticus* RIMD2210633, with the exception of leucine (CUA) which occurs at a frequency of 1.51% of the total codon usage in *V. parahaemolyticus* and 0.39% in *E. coli* K12. Terpe (2006) suggests that codon usage of greater than 1.5% in any of the six rare codons listed above may yield problems in high level expression in *E. coli*. Although CUA usage is higher in *V. parahaemolyticus*, than *E. coli*, CUA only represents 15% of the total leucine codon frequency. For these reasons, it is unlikely that differential codon usage would have led to significant decreases in functional expression of adhesins and invasins from the genomic library.

Differential GC content between the source organism and the heterologous host has been presented as a reason for low expression and/or functionality upon screening of genomic libraries (Waterfield *et al.*, 2008; Gustafsson *et al.*, 2004). Knight *et al.* (2001) state that codon usage corresponds to the GC content of an organism and is in part influenced by the mutation and selection equilibrium of the different synonymous codons for each amino acid. *E. coli* K12 has a genome GC content of 51%, while *V. parahaemolyticus* has a lower genome GC content of 45%. Waterfield *et al.* (2008) were capable of isolating *E. coli* clones expressing multiple functionally active virulence proteins from a genomic library derived from *Photorhabdus asymbiotica*, even though *P. asymbiotica* has a GC content of 42%. While expression of insert sequences from this library was not problematic, it was found that

correct sub-cellular localisation of one heterologous protein, the toxin Mcf1 did not occur. Mcf1 is secreted by *P. asymbiotica* and induces toxicity in insects. Daborn *et al.* (2002) showed that Mcf1 is accumulated in the cytoplasm when expressed in *E. coli*, however the protein remains functional and *E. coli* cells possessing cytoplasmic Mcf1 are capable of causing insect cytotoxicity. These findings indicate that adhesins or invasins from the *V. parahaemolyticus* genomic library described in this chapter, may be expressed *in E. coli*, however without the correct secretion machinery and subsequent cell surface localisation, the functionality of such proteins may be lost.

The presence of appropriate secretion machinery in the heterologous host represents one bottleneck for functional expression. Difficulties may also be encountered in terms of basic expression machinery and regulatory elements required for transcription, translation and post-translational modifications. For example, many virulence-associated traits are regulated by transcription factors and sigma factors in the native environment. Without the presence of such transcription factors, adequate expression at functional levels may not occur. *Pseudomonas syringae* has been shown to possess such a sigma factor, HrpL. This sigma factor was shown by Xiao and Hutchenson (1994) to direct transcription of six operons involved in pathogenicity. Klose and Mekalanos (2002) found that *V. cholerae* mutants lacking *rpoN* which codes for σ^{54} were defective for colonisation of mice and were also non-motile. The findings of these two groups demonstrate that possession of virulence genes alone, without the appropriate regulatory elements may not be sufficient to enable functional expression from a genomic library. The use of large inserts such as those described in this work (~40 kb) may increase the likelihood of co-expression of adhesins/invasins with their corresponding transcription factors, however this would require localisation within the same genetic region.

Post-translational modifications are of key importance to protein functionality. The glycosylation of the type IV pilus of *Neisseria meningitidis*, which is involved in attachment to host cells and is a key virulence factor, has been extensively characterised. Stimson *et al.* (1995) showed that the pilus is glycosylated at serine 63 by the tri-saccharide Gal (β1-4) Gal (α1-3) 2,4-diacetimido-2,4,6-trideoxyhexose and that the galactosyltransferase PglA plays a role in the *O*-glycosylation process. It has also been shown that the genes *pglB*, *pglC*, *pglD* and *galE* are required for biosynthesis of the tri-saccharide structure (Power *et al.*, 2000). While Marceau *et al.* (1998) showed that glycosylation of the *N. meningitidis* type IV pilus was not required for adherence to epithelial cells, this may not be the case for adhesins from other bacterial species. Should glycosylation be a requirement for *V. parahaemolyticus* adhesin function, it would be necessary for all of the biosynthetic genes and the glycosyltransferases to be co-expressed in the same strain. While the known adhesin MAM7 was successfully expressed in *E. coli* without the need for co-expression of glycosylation factors by Krachler *et al.* (2011), co-expression of proteins involved in glycosylation may be a requirement for functionality of *V. parahaemolyticus* TFP. This may explain the lack of detection of TFP by the selection methods employed in this work.

Although detection levels for library screening were low, a single clone of interest was obtained, clone A16. This clone has significantly elevated invasion compared with the background *E. coli* strain. Sequencing and subsequent bioinformatic analysis of each of the coding regions from this clone led to the selection of OmpA, encoded by *VPA0248* as the most likely invasin within the insert DNA from clone A16. Literature analysis strengthened the prediction that OmpA may have functionality as an invasin, as it has been shown to play a role in the invasion of *E. coli* K1 into brain micro-vascular endothelial cells (Prasadarao *et al.*, 1996). The protein has also been shown to play a role in binding to a range of ligands including colicin, bacteriophage, the glycoprotein EcgP and the complement protein C4BP

(Morona *et al.*, 1984; Prasadarao *et al.*, 1996; Prasadarao *et al.*, 2002). The flexibility of binding displayed by OmpA is believed to be brought about by virtue of its 4 exposed extracellular loops. The diversity of receptors to which OmpA can bind has led to roles being extablished in immune evasion, aggregate stabilisation, adherence, invasion, membrane stabilisation, phage resistance and antimicrobial resistance (Smith *et al.*, 2007). It is for this reason that Smith *et al.* (2007) termed OmpA, "A molecular Swiss army knife".

While clone A16 did yield significantly elevated invasion, there was evidence of indirect effects of heterologous expression on this clone. Significantly lower inoculum counts were obtained for clone A16 than that of the background *E. coli* strain, even when OD_{600} measurements were similar. Possible explanations for this include increased cell size, presence of unviable cells in the suspension or formation of clumps or aggregates of cells. Each of these factors has the ability to lower the enumerable inoculum count, thereby increasing the apparent invasion efficiency. It is also possible that increased cell size, or formation of aggregates could lead to an increased rate of attachment to the Caco-2 cell monoloayer. As OmpA is also involved in membrane stabilisation, expression of the *V. parahaemolyticus* OmpA in *E. coli* HB101 could conceivably have a dramatic impact on the integrity of the membrane and therefore result in altered cell morphology. Deletion of *ompA* in *V. parahaemolyticus* and/or directed expression of OmpA in *E. coli* HB101 will determine whether the increased adherence exhibited by clone A16 is due to expression of an invasin – OmpA or due to the indirect stresses incurred on clone A16 due to the expression/presence of heterologous *V. parahaemolyticus* sequences.

The stresses induced in *E. coli* during production of recombinant proteins have been well documented. Gill *et al.* (2000) found that a wide range of stress response genes were induced during recombinant expression of chloramphenicol acetyl-transferase, human interleukin-2, an anti-botulinum toxin antibody fragment (btFab), the coat protein of the tobacco mosaic

virus (TMVCP) and viral protein 5 (VP5) from segment A of double stranded RNA infectious bursal disease virus. Up-regulation of heat shock (*ftsH*, *clpP*, *lon*, *ompT*, *degP*, *groEL*, *aceA*, *ibpA*), SOS/DNA damage (*recA*, *lon*, *IS5 transposase*), stationary phase (*rpoS*, *aceA*), and bacteriophage lifecycle (*ftsH*, *recA*) genes was observed by DNA microarray and northern blot analysis. In the work carried out by Gill *et al.* (2000), single recombinant proteins were expressed. Although expression was induced to high levels, one can imagine the burden induced in *E. coli* by the presence of 40 kb (~35 genes) of foreign DNA and the subsequent alterations in expression of stress response systems. Gill *et al.* (2000) also saw reduced growth rates and increased cell lysis upon expression of each of the proteins tested. The stresses encountered during expression of foreign protein may explain the altered phenotypes exhibited by clone A16 and may also be explain the low rate of adherent/invasive clone detection from the genomic library screen. Increased expression of proteases, loss of cosmid stability and even lysis of clones may have occurred during expression of *V. parahaemolyticus* insert DNA.

Taking into account the difficulties listed above which may be encountered during heterologous expression, it was deemed necessary to validate the genomic library, to show that expression of *V. parahaemolyticus* insert DNA was possible and also to show that low coverage levels were not responsible for the low levels of detection of adherent/invasive library clones. It has been shown that *V. parahaemolyticus* is resistant to fluoroquinolones, including norfloxacin by virtue of an efflux pump NorM, encoded by *VP1479* (Morita *et al.*, 1998). A simple antibiotic selection assay led to isolation of 1.6×10^5 cfu ml^{-1} of norfloxacin resistant clones. 8 clones were selected at random and the extremities of the insert DNA from each clone were sequenced and aligned with the *V. parahaemolyticus* genome. As seen in Fig 4.12, all 8 clones contained a similar locus. Interestingly, NorM was not present within this locus, indicating an alternate resistance mechanism. Bioinformatic analysis of each of the

genes within the common locus led to the identification of an EmrAB efflux mechanism. This EmrAB locus was cloned into the inducible pET101 vector and expressed in *E. coli* BL21/DE3. No increase in norfloxacin resistance was observed upon expression of EmrAB, therefore the hypothetical proteins encoded in the common locus were analysed in greater detail.

The hypothetical protein encoded by VPA0095 was found to encode a Qnr like protein. This protein has previously been studied and characterised by Poirel *et al.* (2005) and Saga *et al.* (2005). Poirel *et al.* (2005) found that expression of *V. parahaemolyticus* Qnr in *E. coli* Top10 increased norfloxacin MIC from 0.032 μg ml^{-1} to 0.38 μg ml^{-1}. Expression of Qnr also significantly increased the MICs of *E. coli* Top10 to sparfloxacin, ciprofloxacin, moxifloxacin, ofloxacin, enrofloxacin, flumequine and nalidixic acid. The precise mechanism of action of this Qnr protein is unknown, however it has been shown that QnrA from *Klebsiella pneumoniae* inhibits formation of the gyrase-DNA-quinolone complex by binding to GyrA, GyrB or the DNA gyrase holoenzyme early in the gyrase catalytic cycle (Tran *et al.*, 2005). *K. pneumoniae* QnrA shares 58% amino acid identity with the Qnr encoded by *VPA0095* and as such the mechanism of action of *V. parahaemolyticus* Qnr may be similar to that of QnrA. Successful selection of a *V. parahaemolyticus* norfloxacin resistance mechanism demonstrated that expression of *V. parahaemolyticus* inserts from the cosmid library was possible in *E. coli* HB101. The lack of detection of NorM strengthened the hypothesis that many *V. parahaemolyticus* proteins may not be expressed optimally or translocated to the correct cellular location for functionality as an adhesin or invasin. This may explain the low levels of detection in adherence and invasion based library selections. The isolation of six genetically distinct clones from 8 clones analysed indicates that coverage of the library should be sufficient and that bias due to out-growth of slow growing clones should not have occurred during the library construction process.

Due to concerns arising from low detection levels of adherent/invasive clones from the genomic library screen, alternative means of adhesin/invasin identification were investigated. The modern day biologist has a wealth of bioinformatic tools and databases available to facilitate the automated analysis and mining of genomes for coding regions of interest. The VFDB was consulted in order to identify potential virulence genes with a role in adherence or invasion. Literature analysis was subsequently carried out in order to identify gaps in current understanding and to gain further information about the properties of the adhesins and invasins selected from the VFDB consultation. Analysis was focused on the type IV pili, two of which have been shown to play a role in biofilm formation in *V. parahaemolyticus* RIMD2210633. The type IV pilus composed of PilA subunits has been shown to be induced by the presence of chitin and is involved in formation of bacterial aggregates, whereas the MshA1 pilus is expressed under normal growth conditions and is involved in attachment to solid surfaces (Shime-Hattori *et al.*, 2006). Deletion mutants of both major pilin subunits were found to be defective for adsorption to chitin, a molecule which is found in abundance in the commensal environment of *V. parahaemolyticus*. The use of multiple pili with different expression and binding profiles may represent a refined strategy for the colonisation and survival of *V. parahaemolyticus* in multiple environments. While the correlation of mannose sensitive haemagglutination and binding to Caco-2 cells has been investigated using a variety of environmental and infectious isolates of *V. parahaemolyticus*, it has not been studied using the recently emerged pandemic clone RIMD2210633 (Nagayama *et al.*, 1994). As *V. parahaemolyticus* possesses 3 mannose sensitive haemagglutinin major subunit homologues (MshA1, MshA2, MshA3, coded for by *VP2698*, *VPA0747* and *VP2697* respectively), deletion of the genes coding for each individual protein will allow for a more comprehensive analysis of the roles played by each protein/pilus.

The work described in this chapter has led to the identification of four potential adhesins (PilA, MshA1, MshA2 and MshA3), by a bioinformatic mining approach. A novel genomic library screening based approach led to the identification of one potential invasin (OmpA). As these proteins have not been analysed for a role in cellular adherence or invasion of the pandemic *V. parahaemolyticus* clone, they offer significant opportunity to develop understanding of the molecular mechanisms governing these processes.

The issues encountered during library selections led to detailed critical analysis of the selection process and highlighted a number of factors which may be taken into consideration during the preparation of future genomic libraries for the identification of surface expressed heterologous proteins. We have demonstrated an effective means of rapidly profiling library clones by restriction digestion of cosmid DNA. We have also demonstrated a rapid library validation technique, through the use of antibiotic selection, followed by sequencing and alignment of insert DNA. The application of these techniques will enable rapid assessment of the suitability of heterologous library hosts and allow for improved turnaround times in the genetic profiling of library clones. Such applications may prove useful not only in the preparation of *V. parahaemolyticus* genomic libraries, but in genomic libraries from diverse organisms and for the screening of proteins with diverse functionalities.

The following chapter will deal with the construction of inactivating deletions of each adhesin/invasin identified and the use of deletion mutants to analyse the relative roles of these proteins in adherence, invasion and subsequent TTSS function. This will yield detailed characterisation of the roles of each adhesin/invasin being analysed as well as an understanding of the involvement of each protein in the pathogenesis of *V. parahaemolyticus*.

Chapter 5

Confirmation of adhesin and invasin functionality and investigation into involvement in *V. parahaemolyticus* pathogenicity

5.1 Introduction.

Chapter 4 detailed attempts to identify novel adhesins and invasins from *V. parahaemolyticus* using a genomic library selection technique. One invasive clone was obtained from library selections. Bioinformatic analysis of the *Vibrio* DNA insert contained within that clone led to the selection of *ompA* for further investigation as a putative invasin encoding gene. An alternative adhesin/invasin identification method was employed by *in silico* comparative analysis of virulence factors shared between *V. parahaemolyticus* and the more well studied organism *V. cholerae* (Table 4.3). A number of genetic regions encoding type IV pili (TFP) were identified in both organisms. *V. parahaemolyticus* was found to have 4 genes annotated as coding for major pilin subunits in comparison to *V. cholerae* which possessed 3. The TcpA pilin of *V. cholerae* plays a major role in pathogenesis by mediating adherence and colonisation of the organism, as described in the mouse model and by infection of human volunteers (Attridge *et al.*, 1996; Thelin and Taylor, 1996). This pilin is absent in *V. parahaemolyticus*, as is its biosynthetic operon. The possession of different pilins and the variability exhibited in the amino acid sequences of the two shared pilins (PilA and MshA1, Table 4.3) offered an interesting avenue for investigation into the differential roles of TFP in the adherence and pathogenicity of these two related organisms.

TFP have been studied extensively in many bacterial pathogens including *S.* Typhi, *V. cholerae*, *E. coli*, and *P. aeruginosa*. These filamentous structures can play a key role in virulence by initiating colonisation of the host cell through attachment to cell surface receptors. Type IV pilins are commonly identified during annotation of sequenced genomes due to the presence of a conserved N-terminal amino acid motif (GFxxxE) contained within the major pilin subunit protein. As described in Chapter 4, a total of four putative major structural subunit genes are contained within the *V. parahaemolyticus* genome, including 3 mannose sensitive haemagglutinin genes and a *pilA* gene (Table 4.3). The homologue search

summarised in Table 4.3 identified a number of *V. parahaemolyticus* genes with pilin homology, including *VP0136* which codes for GspG, a pseudopilin of the general secretory pathway. As such, a cut-off E value of 1 X 10^{-20} was employed in order to identify the genes with the highest likelihood of coding for pilins. Although the roles played in biofilm formation by two of the proteins coded for by these genes has been assessed by Shime-Hattori *et al.* (2006), using strain RIMD2210633, the role of each pilin in attachment to the host cell and subsequent infection has not been elucidated.

A number of TFP have been extensively characterised. Typically TFP are approximately 7 nm in diameter and are formed by the helical assembly of major and minor pilin subunits to form a rod/filament which can measure several microns in length (Craig *et al.*, 2004). Pilin subunits are termed major or minor due to their relative abundance in the pilus filament (Helaine *et al.*, 2007). Fig 5.1A provides a schematic representation of a type IV pilus, using the example of the *Neisseria meningitidis* type IVa pilus. The pilus contains a number of membrane-associated proteins, which are required for assembly and disassembly of the pilus filament. The pilus shown in Fig 5.1A is used in the uptake of foreign DNA for homologous recombination and is partly responsible for the high level of genetic diversity exhibited in the meningococcal *Neisseria* species (Davidsen and Tonjum, 2006). The high resolution scanning electron micrograph shown in Fig 5.1B illustrates the complex network of type IVa pili which are expressed on the surface of *Neisseria gonorrhoeae*. These long (several µm) pili interact with host cells and other cells within the *Neisseria* population to form aggregative microcolonies, which establish a highly successful infection in the urito-genital tract (Craig *et al.*, 2006). Fig 5.1C shows a negatively stained transmission electron micrograph containing *V. cholerae* expressing the toxin co-regulated pilus which is a member of the type IVb family. These pili have a tendancy to form bundles through interactions with

neighbouring pili. This pilus is so called due to its co-expression with cholera toxin and is required for colonisation and lethality in the infant mouse model (Attridge *et al.*, 1996).

Fig 5.1 Type IV pilus structure. (**A**) Schematic representation of the type IV pilus of *N. meningitidis* including the inner membrane ATPase PilF, the pre-pilin peptidase PilD and outer membrane secretin PilQ. Pre-pilin (PilE) subunits are cleaved by the peptidase PilD, allowing for secretion into the periplasm. Subunits are then secreted through the outer membrane via the secretin protein PilQ to form a helical filament. The process is powered by the ATPase PilF. The filament can be assembled and disassembled as required. *N. meningitidis* uses its type IV pilus to take up exogenous DNA by allowing DNA to bind to the pilus, then retracting the pilus together with the DNA, thus allowing the DNA to enter into the cytosol where homologous recombination can occur with the native DNA molecule. Figure adapted from Davidsen and Tonjum, (2006) (**B**) Type IVa pili of *N. gonorrhoeae* by high resolution scanning microscopy and negatively stained transmission electron microscopy (inset). Pili form long (> 1 µm), independent filaments which are ~ 6 nm in diameter. Figure adapted from Craig *et al.* (2006). (**C**) Large bundle of *V. cholerae* type IVb toxin co-regulated pili. Type IVb pili have a propensity to form bundles through anti-paralell interactions, as seen by the looping of individual pili (inset). Figure adapted from Craig *et al.* (2004).

In order to fully understand the functionality of the various TFP possessed by pathogenic bacteria, it is necessary to analyse the dynamics of major pilin structure in detail. Crystal structures from a number of pilin proteins, such as the *N. gonorrhoeae* gonococcal pilin (GC pilin), the *P. aeruginosa* strain K pilin (PAK pilin), the *E. coli* longus pilin (LngA pilin) and the *V. cholerae* toxin co-regulated pilin (TcpA pilin) have been resolved, leading to new

insights into pilus assembly and function (Parge *et al.*, 1995; Craig *et al.*, 2003; Kolappan *et al.*, 2012). A ribbon diagram of the mature PAK pilin, following removal of the signal peptide is illustrated in Fig 5.2A.

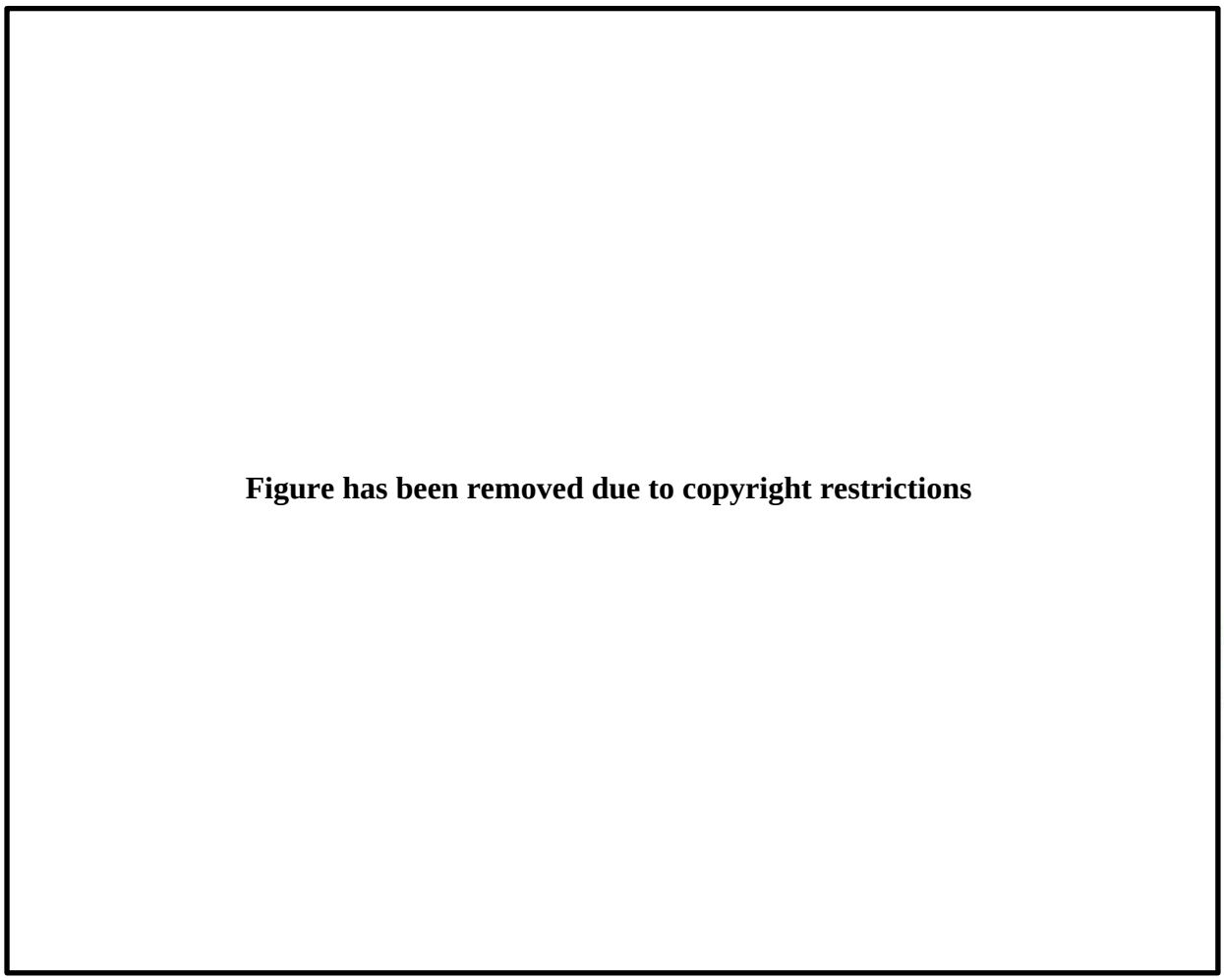

Fig 5.2 Assembly of the *P. aeruginosa* strain K pilus (PAK pilus). Models for PAK pilus assembly derived from X-ray crystallographic analysis. (**A**) A single PAK pilin subunit with hydrophobic N-terminal alpha helix (silver helix), alpha-beta loop (green), beta sheet domain (silver arrows) and receptor binding D domain located between di-sulphide bonds (magenta). (**B**) Filamentous assembly of PAK pilin subunits. In the PAK pilin, the receptor binding D domain is buried within the pilus filament but is exposed at the tip of the pilus (**C**) Detailed view of the interaction between the PAK alpha-beta loop and D domain. The green asterisk indicates the position of a di-saccharide in the homologous *N. gonnorhoeae* GC pilin. (**D**) End view of the assembled PAK pilus with subunits arranged at 90° to one another. Figure adapted from Craig *et al.* (2004).

The protein is composed of two distinct domains. The N-terminal region of the protein forms an alpha helical structure (silver helix) which is connected to the globular head domain via an

alpha-beta loop (green). The loop domain possesses a small beta sheet composed of three anti-paralell beta strands. The majority of the head region consists of a four stranded beta sheet which contains a di-sulphide bond between two conserved cysteine residues at the distal C-terminal. The alpha helical region of pilin proteins is conserved across all type IV pili, with pilin proteins belonging to the type IVa class bearing higher levels of identity to one another than to that of their type IVb counterparts (Aagesen and Häse, 2012). The head region exhibits pronounced variability both in amino acid composition and secondary structure with the distal D region (magenta), located between the conserved cysteine residues displaying the most pronounced levels of variability (Craig *et al.,* 2004). In the case of the PAK pilin, this D region forms a loop which binds to the gangliosidic epithelial cell receptors asialo-GM1 and asialo-GM2 (Krivan *et al.*, 1988). Despite the marked differences in amino acid composition between the PAK pilin (type IVa) and the TcpA pilin (type IVb), the alpha helical spine and beta sheet containing globular head pattern is retained (Craig *et al.,* 2003).

The crystal structure of the PAK pilus yields interesting insights into the formation of the pilus filament as it appears that during assembly, the alpha-beta loop of one pilin interacts directly with the D region of the subsequent pilin being added to the helix (Fig 5.2B, C). Pilin subunits are layered in a helical manner at 90° to one another, such that the hydrophobic alpha helices remain buried in the pilus fiber (Fig 5.2D). This has the effect of producing a hydrophobic core and maximising contact between the head domains of individual pilins (Craig *et al.*, 2004). As indicated in Fig 5.2C, the GC pilin is glycosylated at Ser63 in the alpha-beta loop and it appears likely that interaction of the carbohydrate with the D region may stabilise the pilus (Craig *et al.*, 2004). In the PAK pilin (Fig 5.2B) the receptor binding D domain appears to be buried within the pilus, except at the distal end of the filament and as such Craig *et al.* (2004) hypothesise that binding to the host cell receptor asialo-GM1 is likely brought about through interactions with the pilus tip.

5.2 Bioinformatic and phylogenetic analysis of *V. parahaemolyticus* type IV pili.

5.2.1 Genetic organisation of *V. parahaemolyticus* TFP loci.

The chromosomal loci in which the TFP major pilin genes are located commonly contain a number of genes encoding proteins involved in pilus biogenesis, including: ATPases, signal peptidases and pore proteins/secretins. The biogenesis machinery required for the production of type IV pili is generally conserved (Craig *et al.*, 2003). Homologous gene sets for type IVa pili have been found in most bacterial species. They are typically flanked by similar housekeeping genes and are not located on any identifiable pathogenicity island or mobile genetic element, indicating that they are unlikely to have been acquired by horizontal transfer (Aagesen and Häse, 2012). These factors imply that such pili are ancient to the bacterial species in which they are found (Aagesen and Häse, 2012). Marsh and Taylor (1999) describe a deviation from this hypothesis with respect to the *V. cholerae* MSHA locus. This locus was found to be flanked by a direct 7 bp repeat sequence and was situated between the genes *ydhA* and *mreB* which are found adjacent to one another in *E. coli* (Marsh and Taylor, 1999). Both of these points indicate horizontal acquisition and as such, imply that the MSHA pilus may differ from other type IVa pili. As the MSHA pilus is not implicated in virulence of *V. cholerae*, Marsh and Taylor (1999) labelled the locus as an environmental persistence island due to its role in biofilm formation (Watnick *et al.*, 1999). Amino acid BLAST comparison of *V. parahaemolyticus* MshA1 with its *V. cholerae* counterpart revealed 59% identity across 57% of the protein and as such a role in virulence of *V. parahaemolyticus* was considered (Table 4.3).

In order to observe the organisation of the pilin loci and predict possible features of regulation and biosynthesis, a genetic organisation schematic was constructed using sequence

data from the CMR database. Fig 5.3 shows the genetic loci in which the type IV pilin genes of *V. parahaemolyticus* are found and the corresponding loci in *V. cholerae*.

As seen in Fig 5.3 the genetic loci in which the type IV pilin genes are located are quite similar in *V. parahaemolyticus* and *V. cholerae*. The *mshA* locus on chromosome 1 contains ten pilus biogenesis genes, followed by five pilin genes and a further two biogenesis genes. The *pilA* locus is also quite similar in both organisms, with the major pilin subunit PilA being encoded upstream of an ATPase and a pre-pilin peptidase. The flanking genes of the TFP loci are also similar. A DNA repair protein and a transcriptional regulator are encoded upstream of the *mshA* locus and various genes involved in cell wall and cell shape regulation located downstream, including the *mreBCD* complex. In the *pilA* locus, two cytoplasmic enzymes are encoded upstream, with a NadC Quinolinate phosphoribosyl transferase, which is involved in $NADP^+$ biosynthesis located proximally to *pilA*. Downstream of *pilA* in both organisms, a de-phospho CoA kinase is encoded, which is involved in production of CoA, a key co-factor in the biosynthesis of fatty acids. As commonly observed for type IVa pili, the major PilA pilin, corresponding biosynthetic genes and minor pilins are scattered throughout the genome (Pelicic, 2008; Fig 5.3).

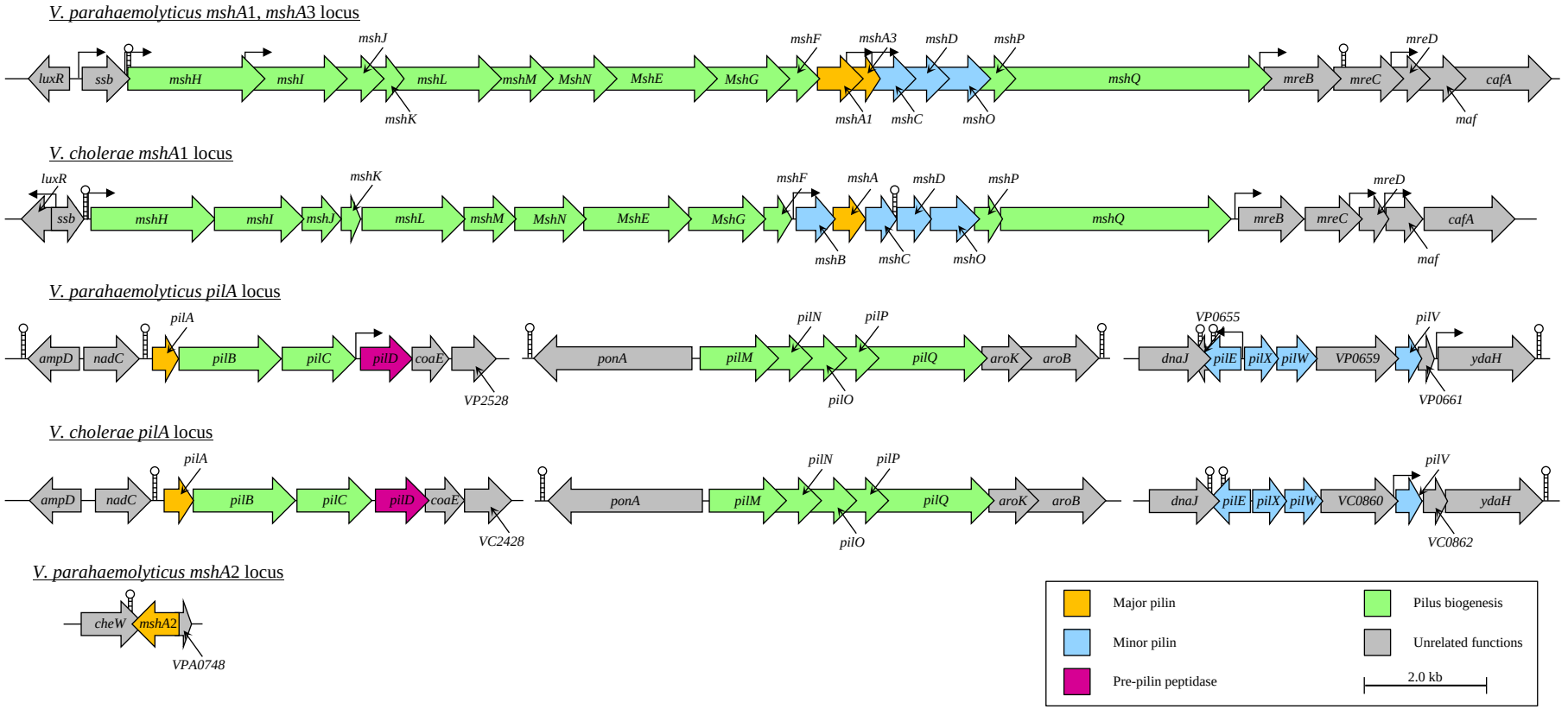

Fig 5.3 The arrangement of type IVa pilus biogenesis components is conserved between *V. parahaemolyticus* and *V. cholerae*, while major pilin components differ between the species. The schematic shown above illustrates the organisation of type IVa pilin loci in *V. parahaemolyticus* and *V. cholerae*. Promoter positions are indicated by arrows, pointing in the direction of transcription. Terminators are indicated by stem-loops. Sequence data, open reading frame positions and putative annotations were obtained from the CMR database. Promoter locations were predicted using the Soft Berry BPROM sigma70 promoter prediction tool with a cut off of < -4.0 LDF (Linear discriminant function) and a threshold distance of < 100 bp from the start codon of a given open reading frame. Terminator positions were predicted using the ARNold Rho-independent terminator prediction tool with a stem-loop free energy threshold of < -11.0 kcal mol^{-1} being employed.

V. parahaemolyticus posseses a third pilin locus which is not found in *V. cholerae*. The *mshA*2 locus on chromosome 2 contains a single pilin gene and no pilus biogenesis genes. It is flanked downstream by a small gene coding for a hypothetical protein and upstream by a chemotaxis signal accepting protein CheW. As both of these genes are encoded on the opposite strand to *mshA*2, it is unlikely that they would be co-expressed. It is an interesting observation, that although the *mshA*1 locus in both strains contains 17 genes with functions pertaining to pilus production, no signal peptidase is contained in this region. As secretion of pilin subunits involves cleavage of the hydrophilic N-terminal signal peptide (Marsh and Taylor, 2009), it is likely that formation of the pilus filament requires co-expression of genes from multiple chromosomal loci. Marsh and Taylor (2009) state that the genes for secretion and synthesis of type IVb pili are commonly located in a single locus and may be associated with pathogenicity islands and/or plasmids, while the genes required for type IVa pilus production are commonly carried in multiple genetic loci. In the case of PilA and MshA2 this requirement is especially true as the *pilA* locus possesses only an ATPase, a signal peptidase and an inner membrane pore protein, while the *mshA*2 locus contains no biogenesis genes. As such it is likely that the basal structures (membrane components) of PilA and MshA2 pili are composed, at least in part, of proteins produced from other genetic regions.

The genetic loci involved in production of the *N. meningitidis* TFP have been extensively characterised. The screening of a collection of transpositional mutants by Carbonnelle *et al.* (2005) identified a total of 15 genes which were critical for either production or functionality of the *N. meningitidis* TFP. A BLAST search was carried out in order to identify homologous *V. parahaemolyticus* proteins to those identified by Carbonnelle *et al.* (2005). A second biosynthetic operon containing the *pilMNOPQ* operon was identified in the *VP2746-VP2750* locus of chromosome 1 (Fig 5.3). Carbonnelle *et al.* (2006) further characterised these biogenesis proteins, identifying all 5 as putative membrane-associated proteins, with *pilQ*

encoding a putative outer membrane secretin. This indicates that the PilA TFP is likely self-sufficient and would not require co-expression of genes from the MSHA locus. Interestingly, two proteins bearing high degrees of similarity (66% and 40% amino acid identity) to PilT, which plays a role in pilus retraction in *N. meningitidis* (Pujol *et al.*, 1999), were found to be encoded by *VP2615* and *VP2614*. The ability to induce retraction of the TFP may have implications for twitching motility or DNA uptake, as well as the stabilisation of bacterial aggregates (Whitchurch *et al.*, 1991; Carbonnelle *et al.*, 2006; Shime-Hattori *et al.*, 2006). A similar organisation of *pilT* alleles is observed in *N. meningitidis*, with one gene referred to as *pilT* and the other annotated as *pilU* (Pelicic, 2008).

While the general organisation of the TFP loci is similar in both organisms, key differences exist in the major pilin components encoded by each. *V. parahaemolyticus* possesses three putative MshA proteins based upon homology with the *V. cholerae* MshA protein. Most databases have annotated VP2697/MshA3 as the major pilin component, likely due to the correlation of its location in the TFP operon with that of the *V. cholerae mshA* gene (second putative pilin gene, two open reading frames downstream of *mshF*). However, MshA1 encoded by *VP2698* possesses the greatest similarity to the *V. cholerae* MshA with 59% identity across 57% of the *V. cholerae* protein. Another putative MSHA protein MshA2 is found on chromosome 2. Encoded by *VPA0747*, this protein has the second highest similarity to the *V. cholerae* MshA pilin with 50% identity across 67% of the *V. cholerae* protein. The pilin encoded by *VP2697*, MshA3 possesses only 39% identity to *V. cholerae* MshA with a 57% coverage of the *V. cholerae* MshA amino acid sequence. MshA3 is also significantly shorter than *V. cholerae* MshA (178 amino acids) at 80 amino acids, while MshA1 and MshA2 are 165 and 178 amino acids in length respectively. Taken together these findings may indicate that MshA1 and MshA2 are more likely to possess major pilin functionality, consistent with the MshA pilin of *V. cholerae*, than MshA3.

5.2.2 Phylogenetic analysis of pilin genes.

As type IV pili are found almost ubiquitously in bacteria and display a widely ranging repertoire of functionalities, their phylogenetic relationships are particularly interesting. In order to establish the evolutionary relationships between the TFP possessed by *V. parahaemolyticus* and those of other species, pilin genes from a number of species were selected for phylogenetic analysis. Pilin genes from 11 members of the *Vibrio* genus were analysed together with type IVa and type IVb major pilin genes from a number of related members of the proteobacteria phylum. Two species each from two genera related to *Vibrio* were selected for analysis: *Shewanella putrefaciens* and *Shewanella violacea* from the *Shewanellaceae*, and *Photobacterium profundum* and *Photobacterium damselae* which also form part of the *Vibrionaceae* family. It was expected that species of these genera would possess similar type IV pilin genes based on the relatively close evolutionary relationships between the genera and the *Vibrio* genus. Major type IV pilin genes from a number of human pathogens including *Salmonella enterica*, entero-haemorrhagic *E. coli*, entero-toxigenic *E. coli* and *Pseudomonas aeruginosa* were also selected for comparison.

V. parahaemolyticus possesses 3 putative MshA major mannose sensitive haemagglutinin pilin proteins and a fourth type IVa pilin protein, PilA, which forms the chitin regulated pilus (Shime-Hattori *et al.*, 2006). The genomes of each organism of interest were mined for pilin genes bearing similarity to each *V. parahaemolyticus* pilin gene by BLASTn analysis. Nucleotide sequences were derived from accession numbers obtained in BLASTn analysis, or by searching the EMBL-EBI (European Molecular Biology Laboratory – European Bioinformatics Institute) database for *pilA* or *mshA* genes from each species. The EMBL-EBI database search allows simultaneous search across a vast number of databases including nucleotide collections, gene ontologies, protein sequence databases, pathways and network modelling and small molecule collections using keywords and accession numbers.

All 9 members of the *Vibrionaceae* were found to possess at least one putative *mshA* gene and a *pilA* gene, with the exception of *V. hollisae* which does not possess a *pilA* homologue. *V. alginolyticus* and *V. harveyi* possess a similar complement of type IV pilin genes to that of *V. parahaemolyticus* with *mshA*1, *mshA*2, *mshA*3 and *pilA* being found in all three strains. Other strains were found to possess homologues to *mshA*1 and *mshA*2 but not *mshA*3 (*V. fischeri*, *V. vulnificus* and *P. profundum*). *V. cholerae*, *V. anguillarum*, *V. mimicus*, *V. hollisae*, and *S. putrefaciens* were all found to possess one putative *mshA* gene. For species possessing more than one *mshA* homologue (for example, *P. damselae*), the gene bearing the greatest levels of similarity to *V. parahaemolyticus mshA*1 by BLASTn score was labelled *mshA*1. The gene most similar to *mshA*2 was labelled *mshA*2 and subsequent genes were labelled *mshA*3, *mshA*4 and *mshA*5 in order of decreasing similarity to the *V. parahaemolyticus mshA* nucleotide sequences.

In total, the nucleotide sequences for 50 pilin genes were used in phylogenetic analysis. A method adapted from Aagesen and Häse, (2012) was employed in order to compare the pilin gene sequences within the dataset. Briefly, nucleotide sequences were entered into the MEGA 5 phylogenetic analysis software package. Sequences were aligned using the ClustalW algorithm within the MEGA 5 package. A maximum likelihood (ML) tree was assembled using the Tamura-Nei model. Significance of branching was assessed by a bootstrap test employing 500 replicates. The resulting ML phylogenetic tree is shown in Fig 5.4. In Fig 5.4 it can be observed that homologues of *V. parahaemolyticus* major pilin genes form 3 distinct monophyletic clades, with homologues of *mshA*1, *mshA*2, *mshA*3 and *pilA* being found clustered on independent branches.

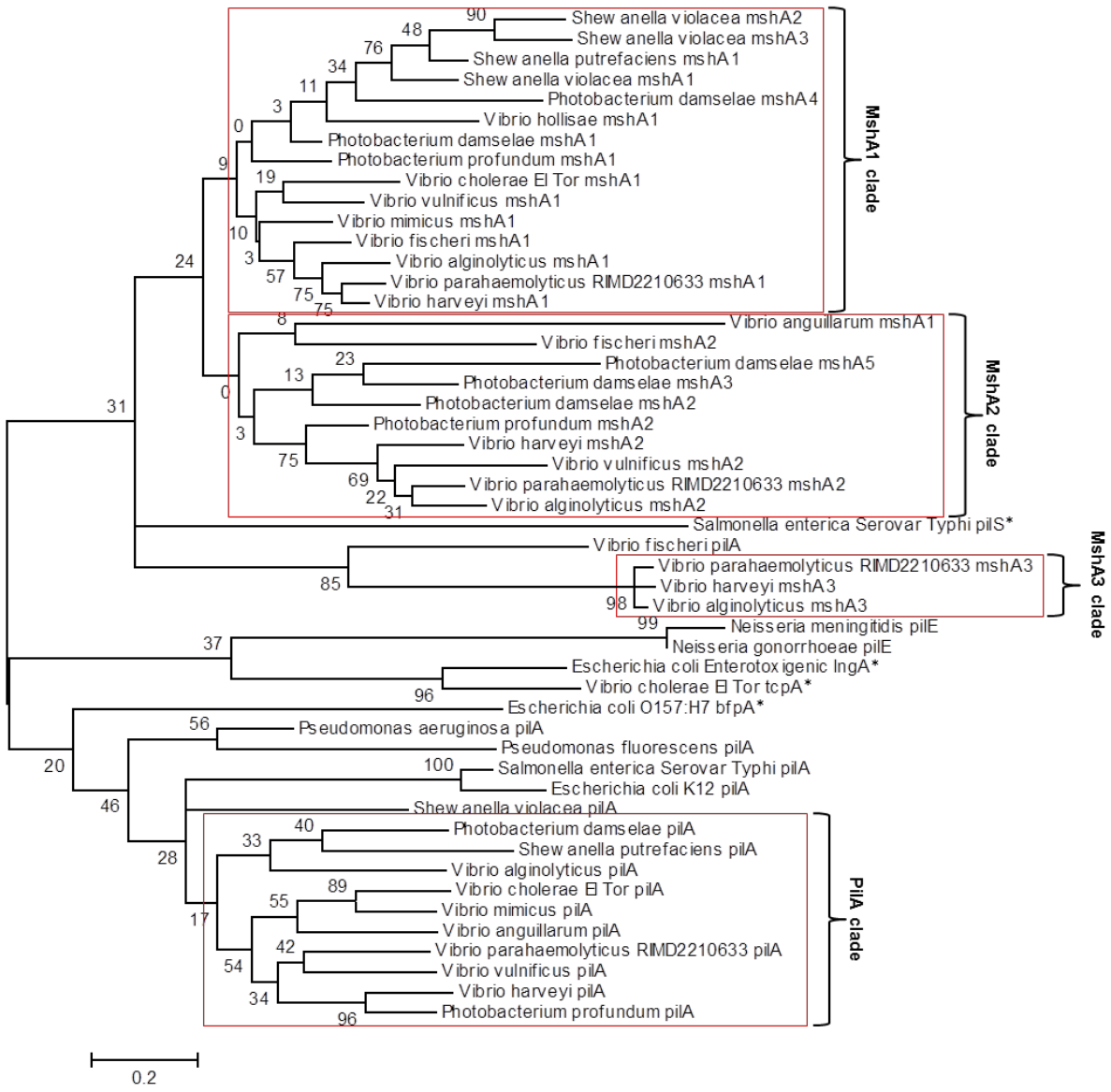

Fig 5.4 *pilA* and *mshA* pilin genes form independent clades. Maximum likelihood bootstrap tree showing the phylogenetic relationships between 50 pilin genes from a variety of bacterial species. Nucleotide sequences for pilin genes bearing sequence similarity to corresponding *V. parahaemolyticus* coding sequences were obtained by BLASTn search against the *V. parahaemolyticus* sequence. All other coding sequences were obtained from the EMBL-EBI database. Sequences were aligned using the ClustalW algorithm as part of the MEGA phylogenetic analysis package. The sequence alignment was used to construct a maximum likelihood phylogenetic tree, using the Tamura-Nei model. *mshA*1, *mshA*2, *mshA*3 and *pilA* clades are indicated by red boxes and corresponding labels. * indicates type IVb pili. Significance of branching was determined by bootstrap test with 500 replicates. All bootstrap values are shown.

The pilin genes in Fig 5.4 appear to be divided into two distinct families with *Vibrio* spp. *pilA*, *Neisseria* spp. *pilE*, and the type IVb pilin genes *E. coli bfpA*, *E. coli lngA* and, *V.*

cholerae tcpA being contained in one family. The mannose sensitive haemagglutinins make up the remainder of the phylogenetic tree. *S.* Typhi *pilS* and *V. fischeri pilA* form an exception to this grouping as they are found within the *mshA* sub-tree, although the long branch lengths exhibited by these two genes indicate that these genes exhibit a high level of variability compared with other genes within the group.

Interestingly the type IVb pilin genes fell into multiple clades, with only *V. cholerae tcpA* and *E. coli lngA* sharing common ancestry. Also, the branch lengths of the remaining type IV pilin genes, *S.* Typhi *pilS* and *E. coli bfpA*, are extremely long confirming the large degree of divergence from other pilin genes contained in the dataset. Indeed it has been suggested that the classification of the *E. coli* bundle forming pilus, which is composed of BfpA major pilin subunits is somewhat tentative and it may be the case that BfpA should be classified as a distinct TFP, outside of the type IVa and type IVb classifications (Kachlanay *et al.*, 2001). The localisation of Type IVb pilin genes in various regions within the type IVa pilin clades likely reflects the high level of diversity in the TFP in general rather than the convergent evolution of two groups of pilin genes from a common ancestor.

The separation of the *mshA* and *pilA* genes into monophyletic clades indicates that these proteins diverged early in the evolution of the TFP. It is a striking observation that the separation of the type IVa pilin families appears to be more pronounced than the separation between the type IVa and type IVb pilin gene families. This may indicate that the mannose sensitive haemagglutinins have diverged from the classical type IVa pili to such an extent that they have become an independent family of pilins.

In general, low bootstrap values were obtained for most of the branches in Fig 5.4. As described by Kachlanay *et al.* (2001), this is a common feature of phylogenetic analyses using short sequences. With pilin sequences as low as 240 nucleotides, it is clear that this

may have contributed to the low confidence of branching as assessed by bootstrap analysis. An identical method was employed by Aagesen and Häse (2012) in comparison of intra species variation of *V. parahaemolyticus* and *V. cholerae mshA* and *pilA* genes, with similarly low bootstrap values being obtained for many branches within the *V. parahaemolyticus* dataset. Aagesen and Häse (2012) found that *V. cholerae mshA* and *pilA* sequences obtained from clinical isolates were highly conserved, leading to formation of mono-phyletic clades distinct from that of the environmental isolates. *V. parahaemolyticus mshA*1 and *pilA* sequences on the other hand were highly variable outside of the N-terminal region and no discernible groupings based upon isolate source were formed upon construction of ML phylogenetic trees. Taking the finding of large degrees of intra-species diversity in pilin genes by Aagesen and Häse (2012), it is not surprising that a high level of variation is observed upon comparison of genes coding for different pilin types in a variety of bacterial species (Fig 5.4).

5.2.3 Amino acid conservation and domain organisation of *V. parahaemolyticus* major pilins.

In order to gain a detailed insight into the relationships between *V. parahaemolyticus* pilins and those of other organisms, it was decided to look not only at the genetic composition at a whole gene level as described in section 5.2.2, Fig 5.4, but to also carry out amino acid alignments with a number of pilins from other species to ascertain where the differences in pilin composition were located and to establish whether such variations could lead to variable functionality. Fig 5.5 contains the results of three amino acid alignments carried out using the Clustal Omega algorithm. The four *V. parahaemolyticus* pilins under investigation (PilA,

MshA1, MshA2 and MshA3) were included in the alignments, together with a number of pilins for which structural analysis has been carried out.

Fig 5.5 PilA, MshA and type IVb pilins exhibit differential secondary structure and domain organisation. Clustal Omega alignment of type IV pilin amino acid sequences, illustrating α helical domains (orange shading) and β strands (green shading). Conserved C-terminal domains upon which a di-sulphide linkage is formed are shaded in purple. * indicates residues which are conserved in >50% of sequences per alignment. Amino acid sequences were obtained from the EMBL-EBI database. Sequences were then aligned using Clustal Omega within the EMBL-EBI server. Alignments were edited using the Jalview alignment editor. Domain organisations for the *N. gonorrhoeae* GC pilin (*GC_pilin*), *P. aeuruginosa* K112 pilin (*K_112_pilin*), *P. aeruginosa* PAK pilin (*PAK_pilin*) and *V. cholerae* TcpA pilin (*Vc_TcpA*) were adapted from Craig *et al.* (2003). *E. coli* LngA (*Ec_LngA*) domain organisation was adapted from Kolappan *et al.* (2012). Secondary structure of *V. parahaemolyticus* pilin proteins was analysed using the I-TASSER protein structure and function prediction server (Ambrish *et al.*, 2010), followed by sequence

comparison with type IV pilins of solved structure. Individual alignments were carried out in three separate groups (**A**, **B** and **C**), with pilins bearing the greatest levels of identity by pairwise alignment being grouped together.

In order to facilitate detailed comparison of secondary structures between pilin proteins, individual alignments were carried out with pilin proteins bearing the highest levels of similarity to one another by pairwise alignment. As seen by phylogenetic comparisons (Fig 5.4) using nucleotide sequences, the MshA pilins (Fig 5.5A) formed a distinct group from the PilA type pilins (Fig 5.5B). Two IVb pilins were also included for comparison (Fig 5.5C). Within each individual alignment, the N-terminal sequences were highly conserved (asterisks indicate residues conserved in greater than 50% of pilins), particularly within the α1 helix domain. The head region of the pilins by comparison was found to be quite variable, with some conserved residues within the beta strands (green). The receptor binding D region, which is located between the conserved cysteine residues at the C-terminus of the pilin sequence, was found to be highly variable in all alignments. This highlights the adaptability of this region and provides an indication for an involvement in the diversity of TFP function in bacteria.

The domain organisation of each of the pilins contained within the alignments in Fig 5.5 is summarised in the schematic (Fig 5.6).

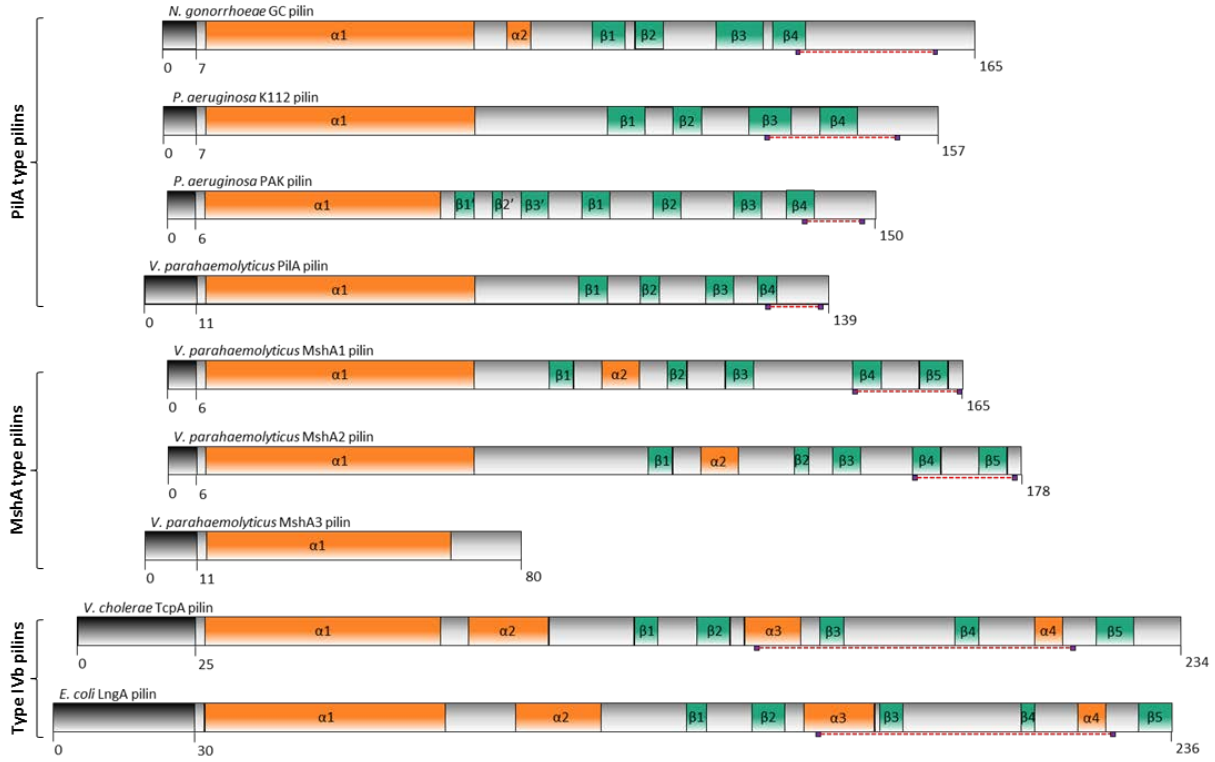

Fig 5.6 PilA, MshA and type IVb pilins exhibit differential secondary structure and domain organisation. Schematic illustrating the orgaisation of secondary structure domains within major type IV pilins. Signal peptides are shaded in black, alpha helical regions are shaded in orange, β strands are shaded in green. Conserved C-terminal cysteine residues upon which a di-sulphide bond is formed are indicated by purple boxes. The hypervariable C-terminal "D" domain, located between the conserved C-terminal cysteine residues is indicated by the dotted red line. Domain organisations for the *N. gonorrhoeae* GC pilin, *P. aeuruginosa* K112 pilin, *P. aeruginosa* PAK pilin and *V. cholerae* TcpA pilin were adapted from Craig *et al*., 2003. *E. coli* LngA domain organisation was adapted from Kolappan *et al*., 2012. Secondary structure of *V. parahaemolyticus* pilin proteins was analysed using the I-TASSER protein structure and function prediction server (Ambrish *et al*., 2010), followed by sequence comparison with type IV pilins of solved structure.

Three distinct groupings are evident in the domain organisation of the type IV pilins shown above. The type IVb pilins can be distinguished from their type IVa counterparts as they are approximately 80 amino acids longer and possess signal peptides which are at least 25 amino acids long. They also possess a second alpha helix at the N-terminal of the protein and two alpha helical domains throughout the globular head region, which are contained within the receptor binding D region (dotted red line). The D domain in the type IVb pilins is also considerably longer than that found in other pilins at 66 amino acids in TcpA, compared with

just 11 amino acids for the *V. parahaemolyticus* PilA. Type IVb pilins have only been found in bacterial pathogens which infect humans (Craig *et al.*, 2004). As such, the possession of a longer D region may offer greater potential for variation through mutation, allowing for antigenic diversity and immune evasion. The large D domain may result in exposure of a larger receptor binding area along the pilus and hence a greater affinity for receptors, including pilin proteins on adjacent pili. This may explain the bundling which occurs in type IVb pili as seen in Fig 5.1C.

The PilA type pilins GC, K112, PAK and PilA all possess four beta strands in the head region of the protein. N-terminal signal peptides within this grouping are of similar size (6 to 11 amino acids) and D domains are considerably shorter than that of the type IVb pilins, with lengths of between 11 and 29 amino acids. With the exception of the slightly longer signal peptide and shorter overall length, the *V. parahaemolyticus* pilin PilA possesses a number of features in common with one or all of the pilin proteins within this grouping. The D region is a similar size and is contained within a similar portion of the pilin to the PAK pilin. The α1 helix and beta strand pattern is quite similar to the K112 pilin with respect to both the size of the domains and the position within the protein. Taking these factors into consideration, it is likely that the PilA pilin of *V. parahaemolyticus* possesses similar tertiary structure to the characterised pilin proteins within the group.

The MshA pilins appear to form an independent group from the other type IVa pilins in Fig 5.6, based upon the possession of a second N-terminal alpha helix and an extra beta strand in the C-terminal head region in both MshA1 and MshA2. MshA3 by contrast is composed of only 80 amino acids and lacks secondary structure outside of the N-terminal alpha helix. While this suggests that consistent functionality with the *V. cholerae* MshA (178 amino acids) is unlikely, MshA3 should not be disregarded as a potential major pilin protein. A distinct class of type IV pilins has been identified which appear to form a discrete

monophyletic clade from the conventional type IV pilins. The Flp1 pilins have been described by Kachlanay *et al.* (2001) as forming an independent group, which consisted of small (~80 amino acids) pilins that could be distinguished from conventional type IV pilins. The Flp1 major pilin of *Actinobacillus actinomycetemcomitans*, which is composed of 75 amino acids, forms a helical type IV pilus which is involved in non-specific attachment to a variety of surfaces and plays a role in the establishment of juvenile periodontitis (Kachlanay *et al.*, 2001). This example serves to illustrate that small pilins such as MshA3 could still produce functional type IV pili. As sequence composition and domain architecture of the MshA pilins did not closely resemble any of the characterised pilins in Fig 5.5 and Fig 5.6, accurate prediction of three dimensional pilin assembly was not possible.

5.3 Construction of inactivating deletions of putative adhesins and invasins using splicing by overlap extension PCR.

In order to analyse the relative roles played by each of the potential adhesins and invasins identified by the work carried out in chapter 3, stable inactivating mutations were created in *V. parahaemolyticus*. The use of stable deletion mutants, rather than transposon insertions allowed for multiple deletions within the same strain and eliminated any indirect effects which may have arisen due to antibiotic selection in such mutants. To allow for the maximum likelihood of phenotype disruption, the majority of the predicted coding region for each protein was removed. Deletions were constructed in frame so as to avoid interference with transcription of downstream genes. To construct such deletions, a deletion allele was made either by overlap extension PCR or by artificial gene synthesis as outlined in methods section 2.4.1. Fig 5.7 and Fig 5.8 illustrate the process of splicing by overlap extension using deletion of *ompA* as an example. The deletion allele consisted of loci homologous to the flanking

regions of the gene to be deleted. The upstream flanking region is coloured green and the downstream region is coloured red (Fig 5.7). These regions were amplified so as to contain a small number of codons from the start of the gene and a small number of codons from the end of the gene. The intragenic primers VPA0248.DelB and VPA0248.DelC were designed with ~10 nucleotide overhangs which enabled annealing of one strand of the AB product to the complementary ~10 nucleotide region on the CD product and *vice versa*. The resulting deletion allele encoded an in-frame, truncated form of the *ompA* gene with 948 nucleotides removed.

Deletion alleles for *mshA*2, *mshA*3, *pilA* and *ompA* were produced by overlap extension PCR as outlined in Fig 5.7. For *mshA*1, *mshE* and *mshL*, similar allelic variants were produced by artificial gene synthesis. The use of artificial gene synthesis allowed greater flexibility for subcloning due to the relative ease at which restriction sites could be added to the flanking regions of the deletion allele. Difficulties arising from polymerase errors during PCR were also eliminated. In combination, these 2 alterations resulted in greatly improved turnaround time in the production of recombinant suicide vectors for construction of deletions in *V. parahaemolyticus*. *mshE* and *mshL* code for the MSHA pilus ATPase and outer membrane secretin protein respectively. Their localisation within the pilus organelle is predicted to correlate with *N. meningitidis* PilD and PilF as illustrated in Fig 5.1A. While these proteins have been shown to be critical for biosynthesis of the *V. cholerae* MSHA pilus, their roles have not been studied in *V. parahaemolyticus* (Häse *et al.*, 1994). Assessment of the importance of the biosynthetic machinery in paralell with the major pilins was carried out in order to yield new insights into *V. parahaemolyticus* TFP production.

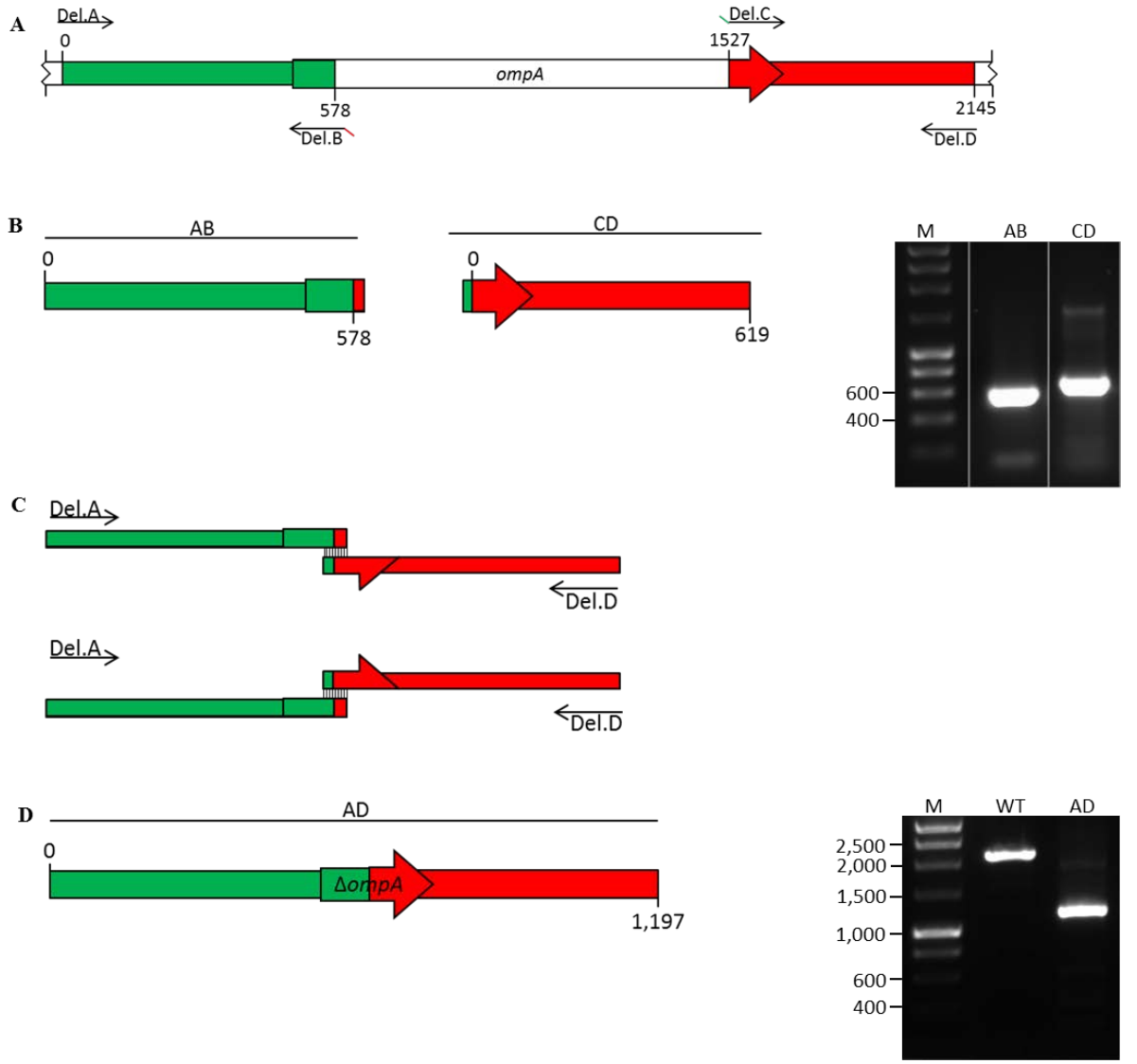

Fig 5.7 Construction of *ompA* deletion allele. (**A**) Wild type *ompA* allele with binding sites for primers required for deletion allele construction. (**B**) Schematic and gel image for amplification of AB and CD fragments which were created using primers Del.A, Del.B and Del.C, Del.D respectively. 5' overhangs on Del.B and Del.C were used to create complementary ends for overlap annealing. AB and CD products were excised, purified and used as template for overlap extension (**C**) AB and CD fragments were denatured and annealed together as described in section 2.4.1a. Primers Del.A and Del.D were added and the product was amplified to form *ompA* deletion allele. (**D**) Schematic and gel image of *ompA* deletion allele (AD product). The product of wild type allele amplification is also shown in the gel image for comparison. All molecular weights (M) are in bp. Where necessary, gel images were spliced together.

Following construction of the *ompA* deletion allele as outlined in Fig 5.7, the construct was TA cloned into pCR2.1 as described in methods section 2.4.1b. The insert was digested from pCR2.1 using *Xba*I and *Sac*I and ligated into the selectable suicide vector pDS132. This recombinant vector was then transformed into *E. coli* Pir1 and conjugated into *V.*

parahaemolyticus. As pDS132 requires the Pir protein for replication, due to the presence of the R6Kγ origin of replication, any chloramphenicol resistant *V. parahaemolyticus* ex-conjugants must be first recombinants. First recombination can occur via the upstream or the downstream homologous locus, however for convenience, only first recombination via the upstream locus is shown in Fig 5.8A. In order to select for the second recombination event, first recombinants were cultured to stationary phase three times in the absence of chloramphenicol. Loss of the chromosomally integrated vector can only occur through a second recombination event, a process which can occur via the upstream (green) or downstream (red) homologous loci. As shown in Fig 5.8C and Fig 5.8D, when dealing with first recombinants which arose from recombination of the upstream region, the second recomination event yielded the truncated form of *ompA* through downstream recombination, while upstream secondary recombination resulted in recovery of the wild type *ompA* allele. In both cases, the secondary recombinants were sucrose resistant (due to loss of *sacB*) and chloramphenicol sensitive (due to loss of *cat*).

As such, secondary recombinants were selected by plating on LBN + 10% (w/v) sucrose and confirmed by replica plating in LBN + chloramphenicol (section 2.4.1d). Final confirmation of the stable integration of the truncated allele was achieved by colony PCR of an individual chloramphenicol sensitive, sucrose resistant colony. The result of this colony PCR for *ompA* is shown in Fig 5.8C, with the wild type allele shown for comparison (Fig 5.8D).

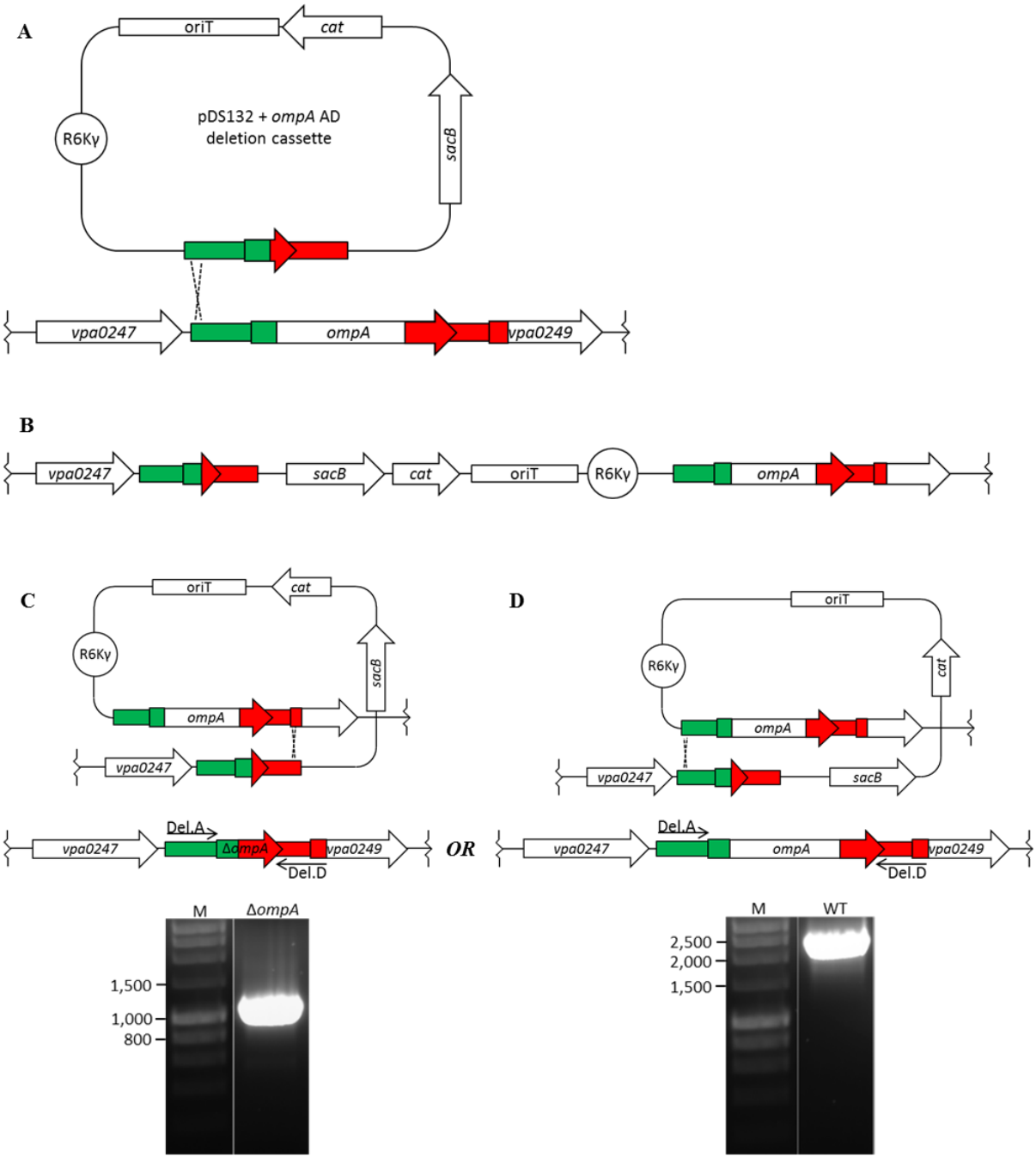

Fig 5.8 Selection of first and second recombinants for deletion of *ompA*. (**A**) The *ompA* deletion allele was cloned into the suicide vector pDS132 and transformed into *V. parahaemolyticus* by tri-parental conjugation. First recombination may occur via the upstream (green) or downstream (red) homologous region. For convenience, only upstream recombination is shown. (**B**) *V. parahaemolyticus ompA* locus after first recombination, yeilding a chloramphenicol resistant, sucrose sensitive phenotype. (**C, D**) Second recombinants were selected by growing in the absence of antibiotic selection followed by selection of sucrose resistant, chloramphenicol sensitive recombinants. (**C**) Downstream (red) recombination leads to deletion of intragenic region from *ompA*, as confirmed by PCR. (**D**) Upstream recombination (green) will result in vector excision without deletion of intragentic region from *ompA*. This results in recovery of the wild type allele as shown in the corresponding gel image. All molecular weights (M) are in bp. Where necessary, gel images were spliced together.

PCR screens for discrimination between wild type or deletion mutant alleles were carried out upon selection of sucrose resistant, chloramphenicol sensitive second recombinants. Cultures yielding mutant bands were streaked on LBN and a final colony PCR was carried out in order to confirm the presence of the truncated allele. Results of confirmatory PCRs for each knockout mutation being constructed are shown in Fig 5.9, together with a schematic representation of the binding sites and expected product sizes for the primers being used. Wild type *V. parahaemolyticus* colony PCR was carried out using the same primer pair for each mutant as a control.

PCR confirmation of single knockout mutations is shown in Fig 5.9. A number of double and triple knockout deletions were also constructed. In these cases, instead of introducing the recombinant suicide vector for a given deletion into the *V. parahaemolyticus* wild type, a knockout mutant was used as the recipient strain. Following selection of second recombinants and PCR screening to detect the presence of the truncated allele being introduced, a final confirmatory colony PCR was carried out using primers for amplification of each gene being deleted from the strain.

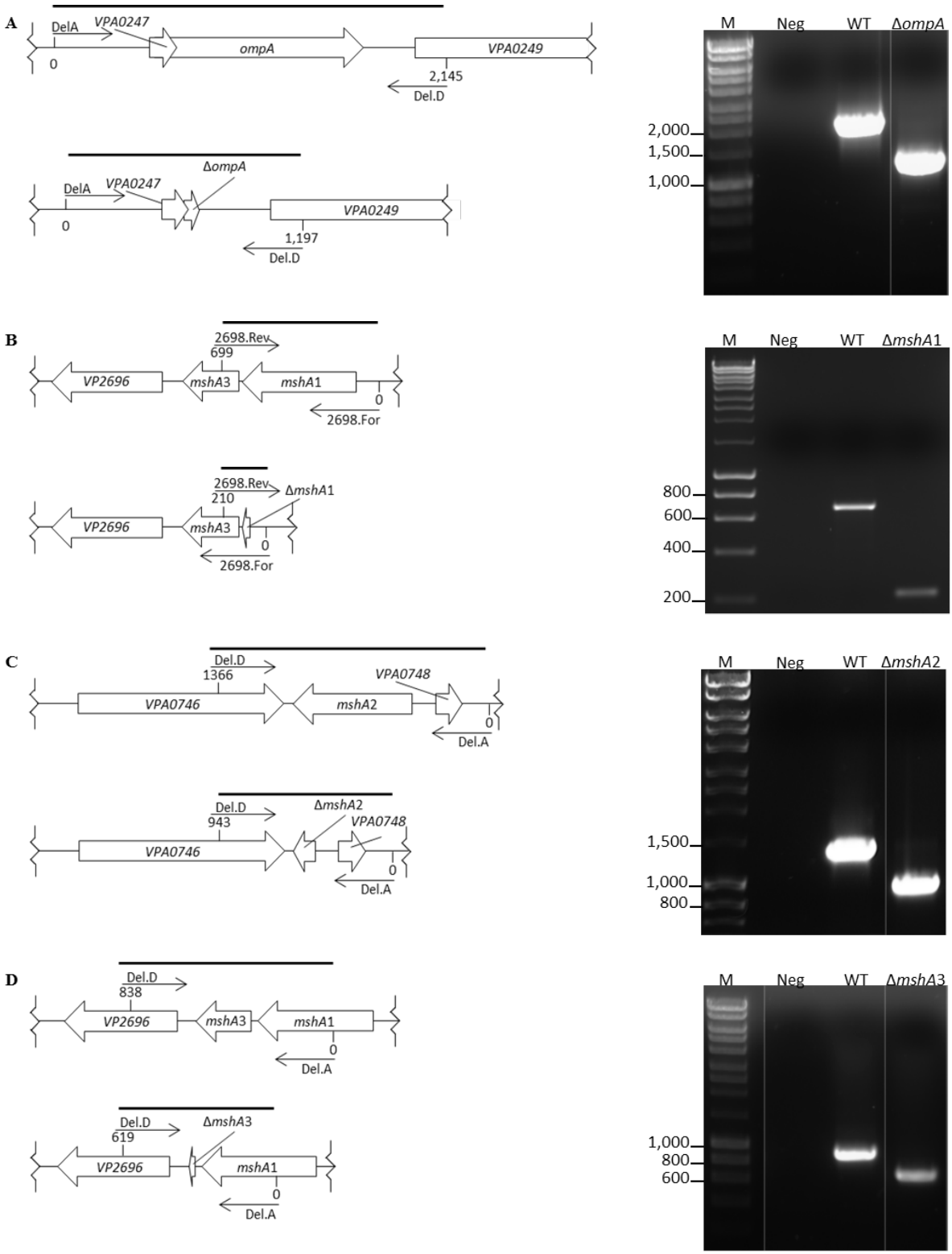
A
DelA
VPA0247
ompA
VPA0249
0
2,145
Del.D
ΔompA
1,197
B
2698.Rev
699
VP2696
mshA3
mshA1
2698.For
210
ΔmshA1
C
Del.D
1366
VPA0748
VPA0746
mshA2
Del.A
943
ΔmshA2
D
838
619
ΔmshA3
M
Neg
WT
ΔompA
ΔmshA1
ΔmshA2
ΔmshA3
2,000
1,500
1,000
800
600
400
200

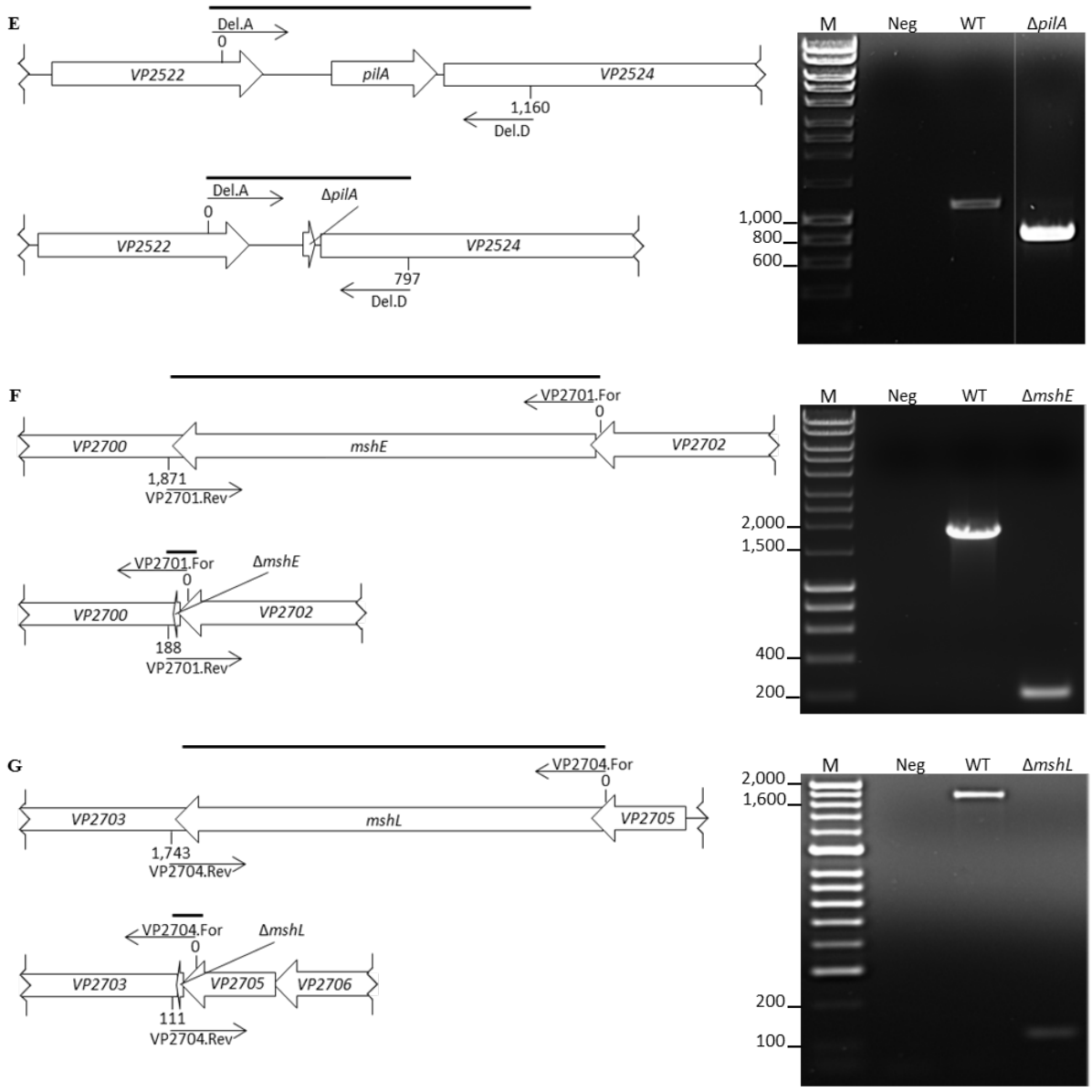

Fig 5.9 Colony PCR confirmation of *V. parahaemolyticus* putative adhesin/invasin deletions. Following selection of sucrose resistant, chloramphenicol sensitive second recombinants, isolated colonies were screened by PCR for possession of a mutated allele. Diagrams illustrate the binding positions of the primers used to test for deletions and the expected product sizes for the wild type and mutated alleles: Δ*ompA*, (**A**); Δ*mshA*1, (**B**); Δ*mshA*2, (**C**); Δ*mshA*3, (**D**); Δ*pilA*, (**E**); Δ*mshE*, (**F**); Δ*mshL*, (**G**). Gel images show the result of colony PCR using putative mutants, *V. parahaemolyticus* wild type (WT) and PCR water (Neg) as templates. See table 2.3 for a full description of the primers used. All molecular weights shown are in bp. Where necessary gel images were cropped and spliced together.

5.4 Analysis of piliation of TFP deletion mutants.

As *mshA*1, *mshA*2, *mshA*3 and *pilA* code for major subunits of the *V. parahaemolyticus* TFP, their deletion would be expected to result in diminished piliation of *V. parahaemolyticus*. In order to assess the formation of pili on the cell surface, a negative staining technique was employed in conjunction with transmission electron microscopy (TEM). The Hitachi H7000 transmission electron microscope employed for this purpose had a resolution of 1 nm and a maximum magnification of 500,000 X, compared with a resolution of 10 nm and a maximum magnification of 200,000 X for a standard scanning electron microscope (SEM). The resolving power/resolution of the microscope used determines the size of the smallest details visible by that microscope, although this also depends on the properties of the sample being visualised. As TFP are typically 5-7 nm in diameter (Craig *et al.*, 2004), SEM would not enable their visualisation, therefore TEM was employed. Negative staining with electron dense chemicals such as phosphotungstic acid also improves the resolving power of the technique being employed.

Results obtained from TEM analysis of negatively stained exponential phase cultures of *Vibrio* WT and Δ*mshA*1 are shown in Fig 5.10. Wild type and Δ*mshA*1 cells were found to be surrounded by a globular matrix, likely composed of capsular polysaccharide. In the majority of cases, flagellae had become detached from the cells, probably due to centrifugation prior to staining. Flagellae were observed, in the empty space surrounding the cells and were identified by their whip-like shape and ~60 nm diameter. Each wild type cell was found to have multiple fibres of ~5 nm in diameter protruding from the cell surface. These fibres were easily distinguishable from the flagellae seen in the empty space around the cells or attached at a single pole of some bacterial cells due to their relatively small diameter. These fibres were not observed upon analysis of Δ*mshA*1 (Fig 5.10). As such these fibres are likely to be TFP, specifically mannose sensitive haemagglutinins, composed of MshA1 major pilin

subunits. The MSHA pili observed on the surface of the *V. parahaemolyticus* wild type were found to be considerably shorter and less abundant than the *N. gonorrhoeae* TFP shown in Fig 5.1B, however, these features were consistent with previous characterisations of *V. parahaemolyticus* TFP (Nakasone and Iwanaga, 1990). A triple mutant of Δ*pilA*/Δ*mshA*1/Δ*mshA*2 was also examined by TEM (Data not shown) and like the Δ*mshA*1 single mutant, this strain was not piliated. As such it appears that under the growth conditions used, only the MshA1 TFP was expressed.

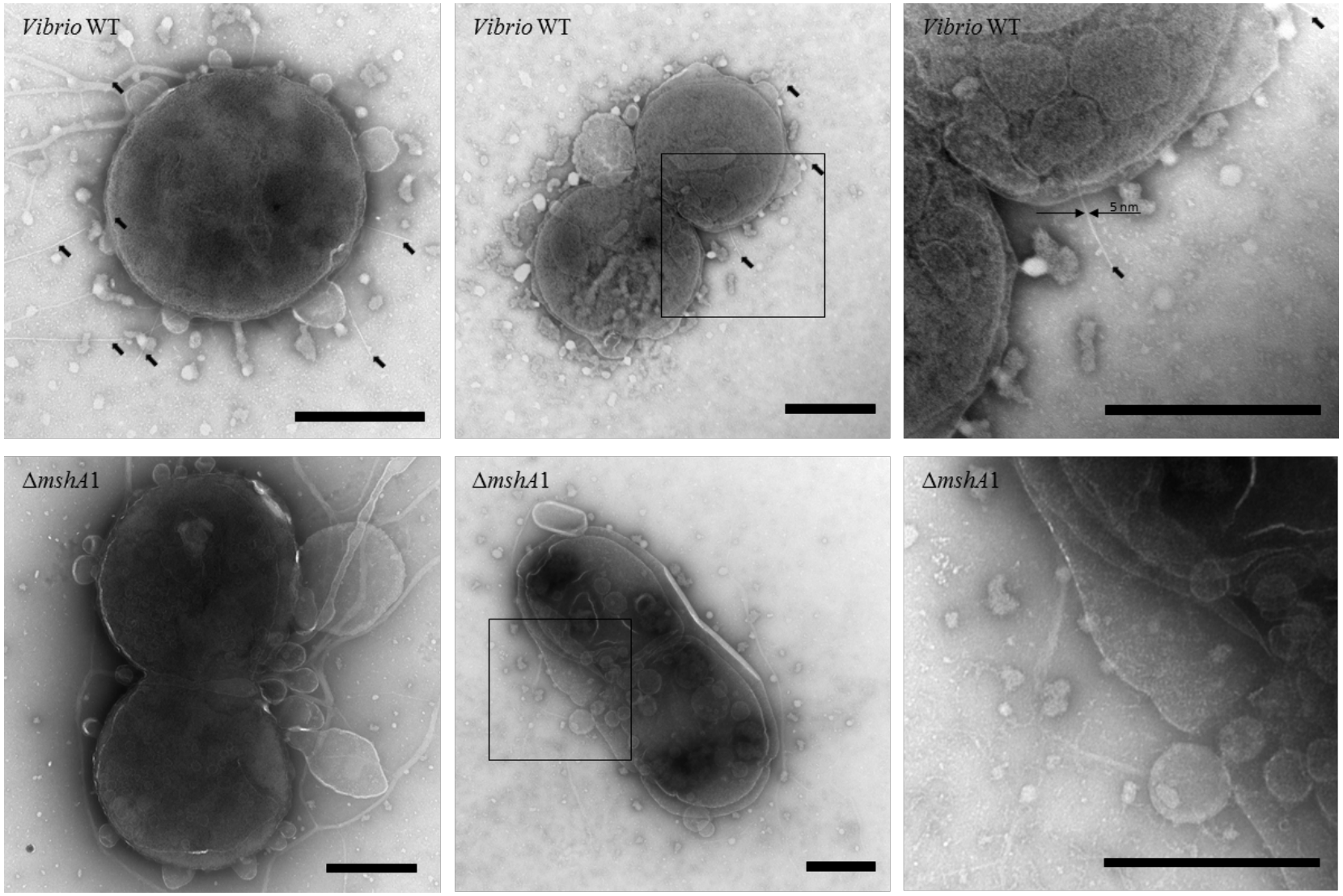

Fig 5.10 Deletion of *mshA*1 causes loss of piliation in *V. parahaemolyticus*. Exponential phase cultures of bacteria were adsorbed on to formvar carbon coated TEM grids, negatively stained with phosphotungstic acid and viewed by TEM. Scale bars represent 500 nm.

5.5 Role of TFP in the adherence of *V. parahaemolyticus* to Caco-2.

In order to assess the relative roles of each of the Type IV pilins possessed by *V. parahaemolyticus*, adherence assays were carried out on Caco-2 epithelial cells, using the *V. parahaemolyticus* wild type and type IV major pilin and pilus biogenesis deletion mutants. As mentioned in chapter 3, the Caco-2 cell line is a cancerous epithelial cell line which, when grown to confluency can form a polarised monolayer which is highly representative of the epithelial cells of the gastro-intestinal tract (Darfreuille-Michaud *et al.*, 1990; Everest *et al.*, 1992). As *V. parahaemolyticus* is a gastro-intestinal pathogen, the study of attachment, colonisation and subsequent infection of these cells is of major importance, both in terms of understanding the pathogenic mechanisms of the organism and developing therapeutics which could potentially prevent colonisation and subsequent infection.

The adherence of *V. parahaemolyticus* was assessed using two complementary assays. Both methods involved the co-incubation of bacterial strains with Caco-2 cells for 1 h, followed by extensive washing to remove any non-adherent bacteria. The number of adherent bacteria was enumerated using either a colony forming unit-based method (as described in Chapter 3) or a staining/microscopy based technique. In order to enumerate the numbers of adherent bacteria microscopically, monolayers were fixed following the removal of non-adherent bacteria by incubation in 4% paraformaldehyde. Caco-2 cells and bacteria were stained with 5% Giemsa for and visualised by phase contrast microscopy. Giemsa stain has been used extensively for the visualisation of bacteria in co-culture with eukaryotic cells as it improves the contrast between each cell type (Mohammadi-Barzelighi *et al.*, 2011; Wang and Leung, 2000).

The results of the colony forming unit based assay to enumerate the adherence efficiency of a variety of strains is shown in Fig 5.11.

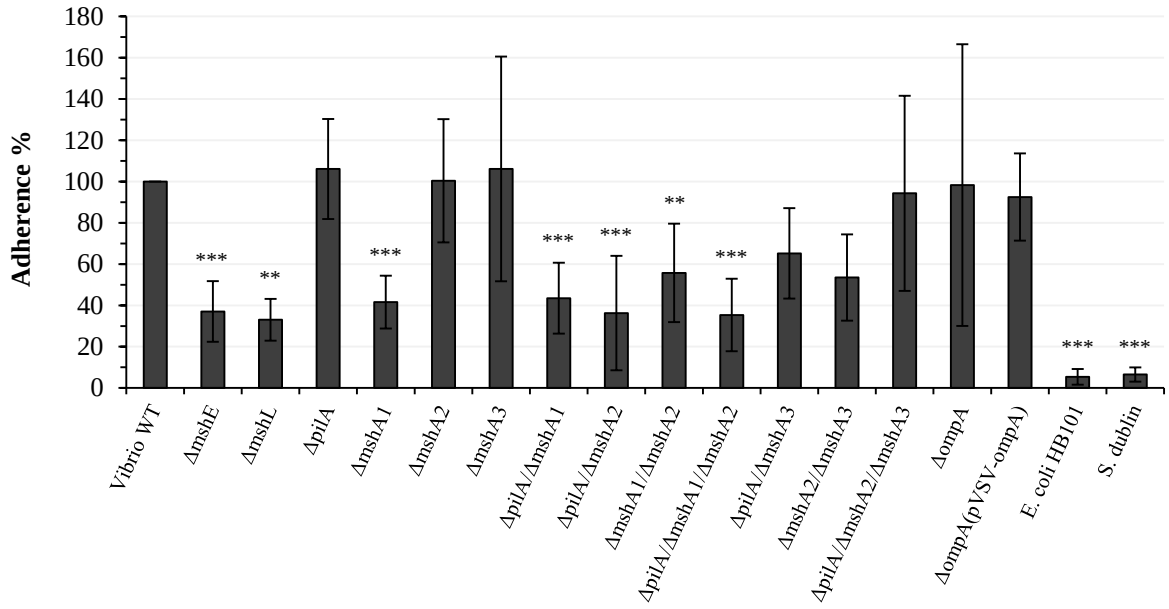

Fig 5.11 Adherence to Caco-2 is mediated by the *mshA*1 Type IV pilus. Quadruplicate wells of Confluent monolayers were infected with bacteria at an MOI of 10 for 1 h. Monolayers were washed and then lysed with 1% Triton. Cell-associated bacteria were enumerated by spread plating on the appropriate agar. Adherence of each strain is expressed as a percentage of the wild type adherence efficiency (adherent cfu as a percentage of the inoculum). Results shown are from at least three replicate experiments. *** $P<0.001$; ** $P<0.005$, calculated using paired student's *t* test to compare sample result with that of the wild type.

Mean adherence efficiencies of less than 50% of the wild type adherence efficiency were obtained for deletion mutants lacking the MSHA ATPase MshE, the outer membrane secretin MshL and the major pilin subunit MshA1. Similarly, double and triple deletion mutants lacking *mshA*1 displayed significant reductions in adherence compared with the wild type, with approximately 40% of the wild type adherence efficiency being recorded for the Δ*pilA*/Δ*mshA*1, Δ*mshA*1/Δ*mshA*2 and Δ*pilA*/Δ*mshA*1/Δ*mshA*2 strains. The reduction in adherence observed upon deletion of Δ*mshE* and Δ*mshL* illustrates that these pilus biogenesis genes are critical for pilus function. A specific role for *mshE*, *mshL* and *mshA*1 in the adherence of *V. parahaemolyticus* to Caco-2 has not been previously reported.

Single mutants lacking *pilA*, *mshA*2 or *mshA*3 did not show any attenuation of adherence to Caco-2. These results suggest that the MSHA pilus is required for adherence to Caco-2 and indicate that *mshA*1 likely encodes the major pilin subunit of the pilus, with the neighbouring gene *mshA*3 either encoding a minor pilin subunit which is not required for adherence to Caco-2 or a pilin which is expressed at levels lower than that required for functionality under the growth conditions used. As MshA1 was found to be required for piliation and subsequent adherence to Caco-2, and MshA3 was not required, further experiments were not carried out with Δ*mshA*3.

The apparent lack of involvement of *pilA* and *mshA*2 in the attachment of *V. parahaemolyticus* to Caco-2 may indicate low levels of expression under the conditions used, a hypothesis which is supported by the complete lack of piliation observed in strains possessing the *mshA*1 deletion (Fig 5.10). This hypothesis is also supported by the findings of Shime-Hattori *et al.* (2006) who found that N-acetyl glucosamine and chito-oligosaccharide were required for induction of expression of the PilA pilus. As both of these molecules are found in abundance in shellfish, which form the commensal environment of *V. parahaemolyticus*, this may be an indication that expression of PilA is specific to the commensal host. Interestingly, the double mutant of Δ*pilA*/Δ*mshA*2 did show an apparent attenuation in adherence with a similar decrease in adherence to that observed with Δ*mshA*1. Further insights into the adherence of this strain were observed by microscopic analysis of the pattern of adherence exhibited on Caco-2 (Fig 5.13) and will be dealt with in conjunction with the results from that experiment.

As observed in chapter 3, *S.* Dublin and *E. coli* HB101 adhered at a significantly lower efficiency ($P<0.001$) than *V. parahaemolyticus* (Fig 3.2A) and as such served as effective negative controls in Fig 5.11.

Chapter 4 described a genomic library screening method, to identify novel adhesins and invasins possessed by *V. parahaemolyticus*. The selection of the genomic library by gentamicin protection assay (used to isolate invasive library clones) led to the identification of a single clone with increased invasion. Clone A16 was found to invade at 3.5 times the efficiency of the *E. coli* HB101 control (Fig 4.6). Bioinformatic analysis of the DNA region contained within clone A16, including analysis of functional categories, detection of conserved domains consistent with adhesin/invasin function, literature analysis and sub-cellular localisation prediction (summarised in Table 4.1) led to the prediction of OmpA, encoded by *VPA0248* as being the most likely invasin contained within the insert DNA of clone A16. As such, a *V. parahaemolyticus* deletion was constructed in *ompA* (Fig 5.9A) and the deletion mutant was tested for adherence and invasion using Caco-2 epithelial cells. A complementation mutant was also constructed by ligating the *ompA* wild type allele, together with its native upstream sequence into the shuttle vector pVSV105. As seen in Fig 5.11, the Δ*ompA* mutant exhibited similar levels of adherence to the *V. parahaemolyticus* wild type. The complementation strain showed no apparent increase in adherence compared with the corresponding deletion mutant, Δ*ompA*. As such, it appears that under the conditions used, OmpA does not function in the adherence of *V. parahaemolyticus* to Caco-2. This is consistent with the finding that although *E. coli* HB101 clone A16, which possesses *ompA* displays significantly increased invasion compared with the *E. coli* HB101 control, it does not display a significant increase in adherence ($P>0.05$, Fig 4.6C). In order to ascertain whether *ompA* encoded a protein with specific activity as an invasin, the deletion mutant and complementation strain were tested by gentamicin protection assay (section 5.6).

In order to confirm the specificity of the phenotypes observed by deletion of major pilin components in Fig 5.11, with respect to the gene/genes being deleted, a *trans* complementation test was carried out. This involved the re-introduction of the wild type

allele into each deletion mutant, on the expression vector pLM1877. Expression was induced during exponential growth by including 100 µM IPTG in the growth medium.

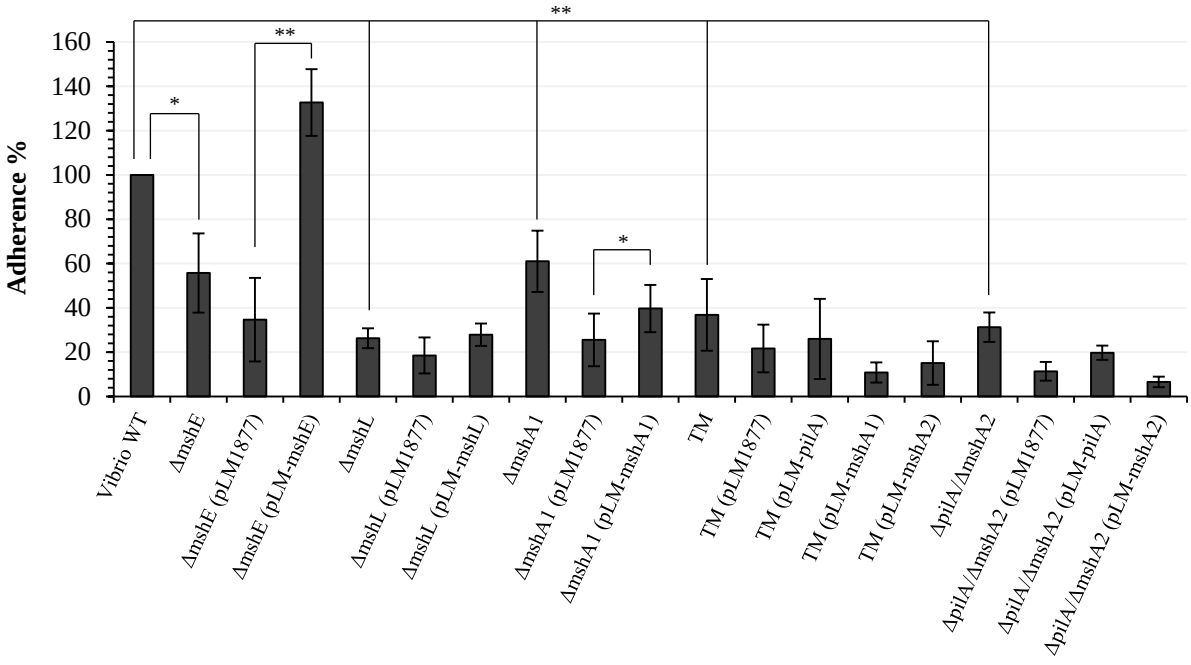

Fig 5.12 Adherence of MSHA mutant strains can be restored fully by *trans* complementation of *mshE*. Confluent Caco-2 cells were infected for 1 h with *V. parahaemolyticus* wild type and type IV pilin deletion mutants carrying either empty pLM1877 or recombinant pLM1877-derived vectors containing the gene being analysed for complementation. Strains carrying vectors were induced with IPTG for 1 h 45 min prior to co-incubation. Non-adherent bacteria were removed by washing and the monolayers were lysed with 1% Triton. Cell-associated bacteria were enumerated by spread plating on the appropriate agar. Adherence of each strain is expressed as a percentage of the wild type adherence efficiency (adherent cfu as a percentage of the inoculum). Results shown are from at least three replicate experiments. ** $P<0.01$; * $P<0.05$, calculated using paired student's *t* test to compare either mutant observations with that of the wild type or to compare empty vector controls with complemented strains as indicated by connecting lines. Δ*pilA*/Δ*mshA*1/Δ*mshA*3 is abbreviated to TM (triple mutant).

As observed in Fig 5.12, expression of *mshE* from the recombinant vector pLM-*mshE* resulted in recovery of the wild type adherence efficiency. This confirms the specificity of *mshE* function in adherence to Caco-2 cells. Although wild type levels of adherence were not attained with the *mshA*1 complementation strain, a statistically significant increase in

adherence was observed in comparison to the empty vector control ($P<0.05$). This indicates that expression of *mshA*1 can partially recover the adherence defect observed with the Δ*mshA*1 mutant.

For Δ*mshL*, Δ*pilA*/Δ*mshA*1/Δ*mshA*2 (TM), and Δ*pilA*/Δ*mshA*2, complementation did not occur, with no statistically significant increase in adherence being observed compared with the empty vector control. It is possible that expression of these MSHA components could not be achieved at appropriate levels for functionally active pili to be formed. It is also possible that expression of MSHA components led to toxicity in the deletion mutant backgrounds. It was found that at the gentamicin concentration required for vector retention (25 μg ml^{-1}) and at an IPTG concentration which is routinely employed for expression from *lac* promoters (100 μM), the strains which could not be effectively complemented showed a marked reduction in growth rate (Data not shown). This could indicate that induced expression of MSHA components could have led to compromised viability. In any case, complementation of the ATPase encoded by *mshE* and the major pilin subunit encoded by *mshA*1 confirms the specificity of the phenotypes being observed in the corresponding mutants in adherence to Caco-2. As complementation could not be achieved for Δ*mshL*, Δ*pilA*/Δ*mshA*1/Δ*mshA*2, and Δ*pilA*/Δ*mshA*2, complementation in these deletion mutant backgrounds was not studied in the analysis of the downstream pathogenic effects of *V. parahaemolyticus* infection.

As mentioned previously, a staining/microscopy based assay was performed in parallel with the colony forming unit based assays to confirm the involvement of TFP in the adherence of *V. parahaemolyticus* to Caco-2. The numbers of cell-associated bacteria cm^{-2} were enumerated by microscopically analysing giemsa-stained co-cultures of bacteria and Caco-2 following the removal of non-adherent bacteria. This technique allowed not only enumeration of the adhesive capacity of each of the strains being analysed but also allowed for visualisation of the pattern of adherence displayed by each strain on Caco-2.

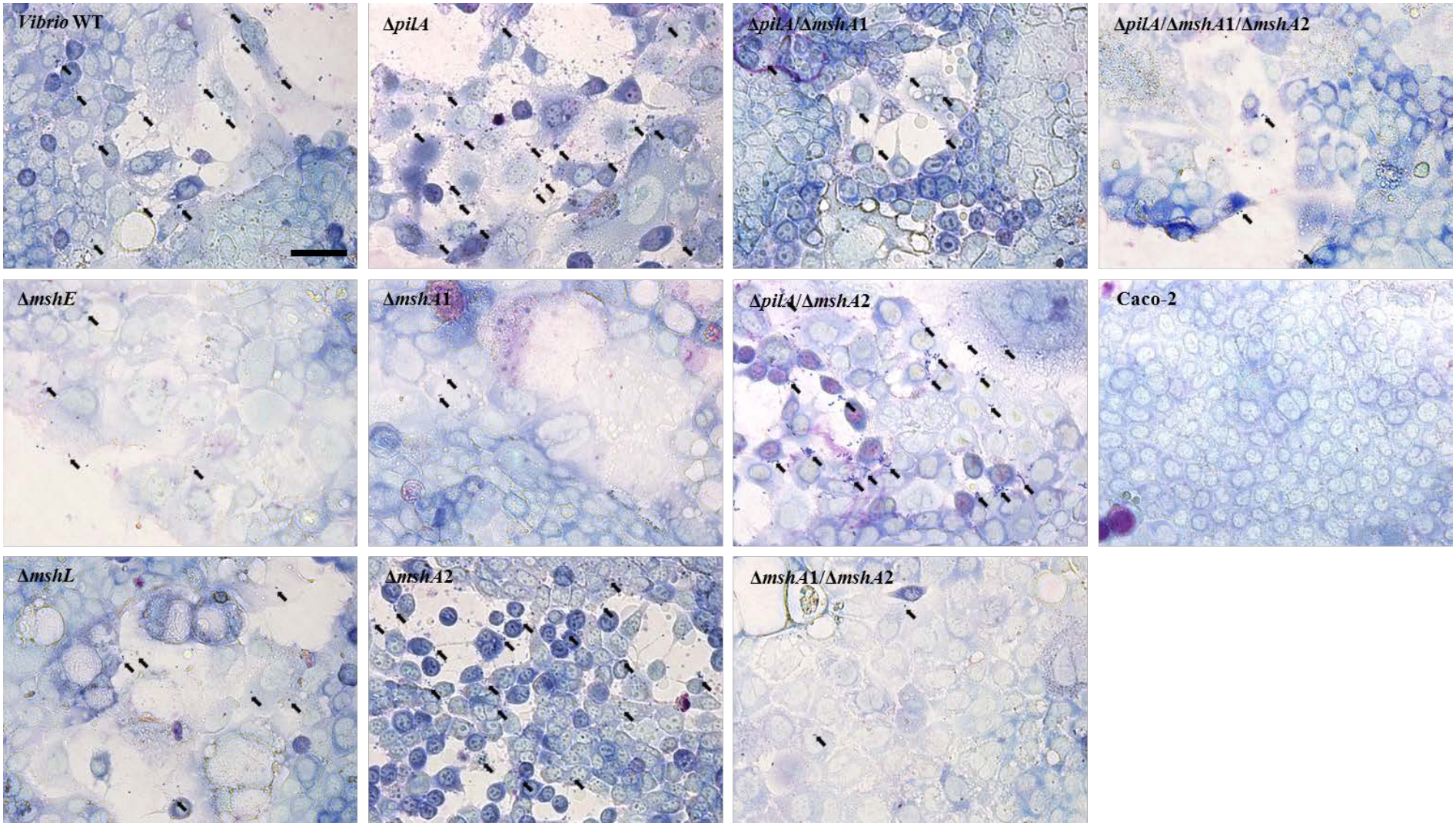

Fig 5.13 MshA1 plays a role the adherence of *V. parahaemolyticus* to Caco-2 cells. Confluent Caco-2 cells were infected for 1 h with *V. parahaemolyticus* and type IV pilin deletion mutants. Non-adherent bacteria were removed by washing, monolayers were fixed in 4% paraformaldehyde and stained with 5% giemsa. Regions of bacterial attachment are indicated by arrows. Scale bar represents 50 μm.

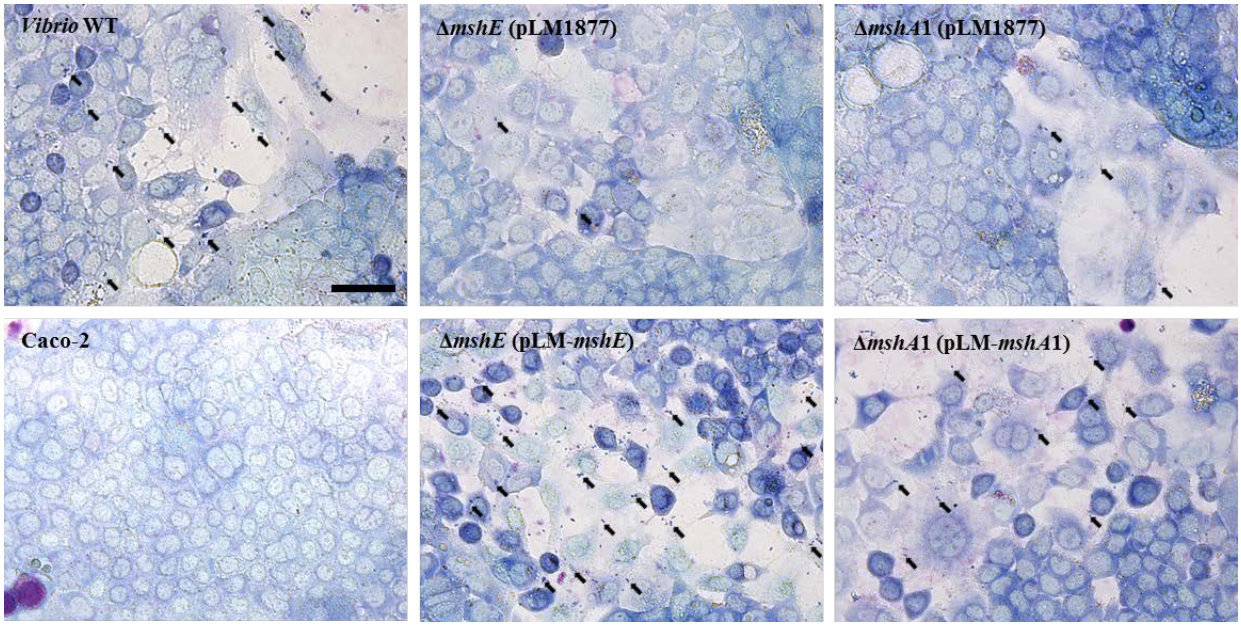

Fig 5.14 Adherence to Caco-2 can be restored by *trans* complementation of *mshE*. Confluent Caco-2 cells were infected for 1 h with *V. parahaemolyticus* wild type and type IV pilin deletion mutants carrying either empty pLM1877 or recombinant pLM1877-derived vectors containing the gene being analysed for complementation. Strains carrying vectors were induced with IPTG for 1 h 45 min prior to co-incubation. Non-adherent bacteria were removed by washing, monolayers were fixed in 4% paraformaldehyde and stained with 5% giemsa. Regions of bacterial attachment are indicated by arrows. Scale bar represents 50 μm.

Table 5.1 Log_{10} adherent bacteria cm^{-2} recorded from giemsa staining/microscopy

Strain	Log_{10} adherent cells cm^{-2}
Vibrio WT	5.73 +/- 0.19
Δ*mshE*	4.70 +/- 0.44 **
Δ*mshL*	4.90 +/- 0.36 **
Δ*pilA*	5.63 +/- 0.41
Δ*mshA*1	4.93 +/- 0.36 **
Δ*mshA*2	5.67 +/- 0.25
Δ*pilA*/Δ*mshA*1	4.93 +/- 0.32 **
Δ*pilA*/Δ*mshA*2	5.79 +/- 0.31
Δ*mshA*1/Δ*mshA*2	4.94 +/- 0.41 **
Δ*pilA*/Δ*mshA*1/Δ*mshA*2	5.03 +/- 0.52 **
Δ*mshE* (pLM1877)	4.77 +/- 0.43 **
Δ*mshE* (pLM-*mshE*)	5.66 +/- 0.26
Δ*mshA*1 (pLM1877)	4.80 +/- 0.33 **
Δ*mshA*1(pLM-*mshA*1)	5.22 +/- 0.24 *

Results were obtained by enumerating the numbers of cell-bound *V. parahaemolyticus* from ten images per experiment. Field size per image was 1.85×10^{-4} cm^{-2}. The results displayed reflect the mean plus standard deviation from 3 experimental replicates. Statistical significance was calculated using a paired student's *t* test to compare sample results with that of the wild type. ** $P<0.01$; * $P<0.05$.

As seen in Fig 5.13 and Fig 5.14, giemsa staining allows for discrimination between bacterial and eukaryotic cells, with *V. parahaemolyticus* being observed in its characteristic comma-like cell morphology and dark blue colouration. The most striking observation from the images in Fig 5.13 and Fig 5.14 is that the cell morphology of Caco-2 infected with bacteria possessing an active MSHA locus is markedly different to that of the Δ*mshE*, Δ*mshL*, Δ*mshA*1 and uninfected Caco-2. After just 1 h of co-incubation, the cells have started to detach from one another and a greater amount of empty space is visible with those bacteria expressing the MshA1 pilus (for example *Vibrio* WT). In all images, the bacteria appear to be predominantly located around the extremities of the Caco-2 cells. Bacteria are attached in small clusters of three to four cells (with the exception of the Δ*pilA*/Δ*mshA*2 strain). The regions within the monolayer which exhibit the greatest levels of cell rounding appear to have

the highest numbers of bound bacteria. This would indicate that higher numbers of bacteria can exert a more pronounced effect on Caco-2 cells, likely through delivery of a large concentration of TTSS effector proteins.

In Fig 5.11 it was observed that the double mutant Δ*pilA*/Δ*mshA*2 had significantly lower adherence than the wild type (40% of WT level, $P<0.001$). This was particularly interesting as single deletions of *pilA* and *mshA*2 did not result in lower adherence levels. Upon examination of giemsa-stained bacteria in contact with Caco-2 cells (Fig 5.13) no significant difference was observed in the pattern of adherence and the $\log_{10}$ numbers of adherent bacteria (Table 5.1) for the *Vibrio* WT, compared with the Δ*pilA* and Δ*mshA*2 single mutants. Comparison of the *Vibrio* WT and Δ*pilA*/Δ*mshA*2 double mutant in contrast, showed a distinct pattern of adherence in the Δ*pilA*/Δ*mshA*2 mutant with large aggregates of up to 30 bacterial cells being formed. The numbers of bacteria cm^{-2} were not significantly different between the two strains (Table 5.1), a finding which is in direct contrast to the numbers observed using the colony forming unit based enumeration method (Fig 5.11). It is likely that the numbers of enumerable cfu of adherent bacteria may have been significantly reduced by the formation of large aggregates each of which having the potential to form a single bacterial colony. This hypothesis may explain the discrepancy between the results obtained using each adherence efficiency enumeration method. This also serves to highlight the necessity for confirmation of any results obtained using the colony forming unit based assay, by microscopy based methods which allow for analysis of the pattern of adherence.

The giemsa staining/microscopy based technique allowed for confirmation of the phenotypes observed in Fig 5.11 and Fig 5.12 for MshE, MshL and MshA1 with respect to adherence to Caco-2. Deletion of the genes coding for each of these proteins resulted in a significant decrease in adherence to Caco-2, with mean $\log_{10}$ cm^{-2} values of 4.70, 4.90 and 4.93 being observed for Δ*mshE*, Δ*mshL* and Δ*mshA*1 respectively, in contrast to a mean $\log_{10}$ cm^{-2} of

5.73 for the *Vibrio* WT. The difference between the wild type and MSHA deletion mutants was found to be statistically significant, with *P* values <0.01 being obtained for each deletion mutant. The double and triple deletion mutants Δ*pilA*/Δ*mshA*1, Δ*mshA*1/Δ*mshA*2 and Δ*pilA*/Δ*mshA*1/Δ*mshA*2 also showed similar decreases to the Δ*mshA*1 single deletion mutant, further confirming that under the growth conditions employed, PilA and MshA2 do not play a role in adherence to Caco-2. As mentioned previously, these pilin proteins may not be expressed under the conditions used.

Results obtained for analysis of phenotype restoration by *trans* complementation (Fig 5.14), closely resembled those obtained during analysis of adherence efficiency using the colony forming unit based assay (Fig 5.12). In Fig 5.14 it can be seen that the cell rounding effects of *V. parahaemolyticus* require a functional MSHA pilus, as the *Vibrio* WT and complemented strains Δ*mshE* (pLM-*mshE*) and Δ*mshA*1 (pLM-*mshA*1) have caused cell rounding and monolayer disruption, whereas deletion mutants and empty vector controls have not.

Comparison of the numbers of adherent bacteria enumerated for each strain (Table 5.1) illustrate that the adhesiveness of the Δ*mshE* mutant can be restored to wild type levels by re-introduction and expression of the *mshE* gene. This is consistent with the results shown in Fig 5.12 and confirms that *mshE* specifically plays a role in adherence to Caco-2. By contrast, the Δ*mshA*1 (pLM-*mshA*1) strain (5.22 $\log_{10}$ cells cm^{-2}) exhibited lower levels of adherence than the wild type (5.73 $\log_{10}$ cells cm^{-2}), a difference which was found to be significant ($P<0.05$). While the results obtained for the *mshA*1 complemented strain were higher than that of the empty vector control (4.80 $\log_{10}$ cells cm^{-2}), failure to restore wild type levels of adherence indicates incomplete complementation. This is consistent with the findings in Fig 5.12 and as discussed earlier, may be a result of poor expression, toxicity as a result of expression or compromised growth due to expression.

All together these results demonstrate that the MshA1 pilus is a key determinant of *V. parahaemolyticus* attachment to human intestinal epithelial cells.

5.6 Assessment of the role of putative adhesins/invasins in the cellular uptake of *V. parahaemolyticus*.

As described in chapter 3, bacterial adhesins can function as invasins by increasing the intimacy of contact with the host cell, thereby increasing the possibility of cellular uptake. This can occur by the modification of host cell signalling pathways *via* interactions between bacterial invasins and host cell receptors or simply through sampling by the host cell through endocytosis or other related pathways. The MSHA pilus of *V. parahaemolyticus* has been shown to require the expression of MshA1 (major pilin subunit) (Fig 5.10). It has also been shown that piliation of bacterial cells with the MSHA pilus results in increased adherence to Caco-2 (Fig 5.11 and Fig 5.12). Experiments were carried out in order to assess whether the adhesive capacity of the MSHA pilus could lead to increased uptake into Caco-2.

Chapter 4 dealt with the identification of adhesins and invasins using a genomic library. As described earlier, a clone was identified with increased invasiveness in the Caco-2 cell model, as determined by gentamicin protection assay. Bioinformatic analysis of that clone led to the identification of a putative invasin OmpA, encoded by *VPA0248*. OmpA proteins of pathogenic bacteria have been shown to have the ability to bind to a variety of host cell receptors, leading to functionality in host cell adherence, invasion and immune evasion (Smith *et al.*, 2007). *E. coli* HB101 clone A16 which possesses *ompA* within a 33.1 kb *V. parahaemolyticus* cosmid insert was found to display significantly increased invasion compared with the background *E. coli* HB101 strain, without a significant increase in adherence (Fig 4.6). As seen in Fig 5.11, deletion of *ompA* in *V. parahaemolyticus* did not

affect adherence to Caco-2. Δ*ompA* was tested for a role in invasion, in parallel with putative pilin genes using the gentamicin protection assay.

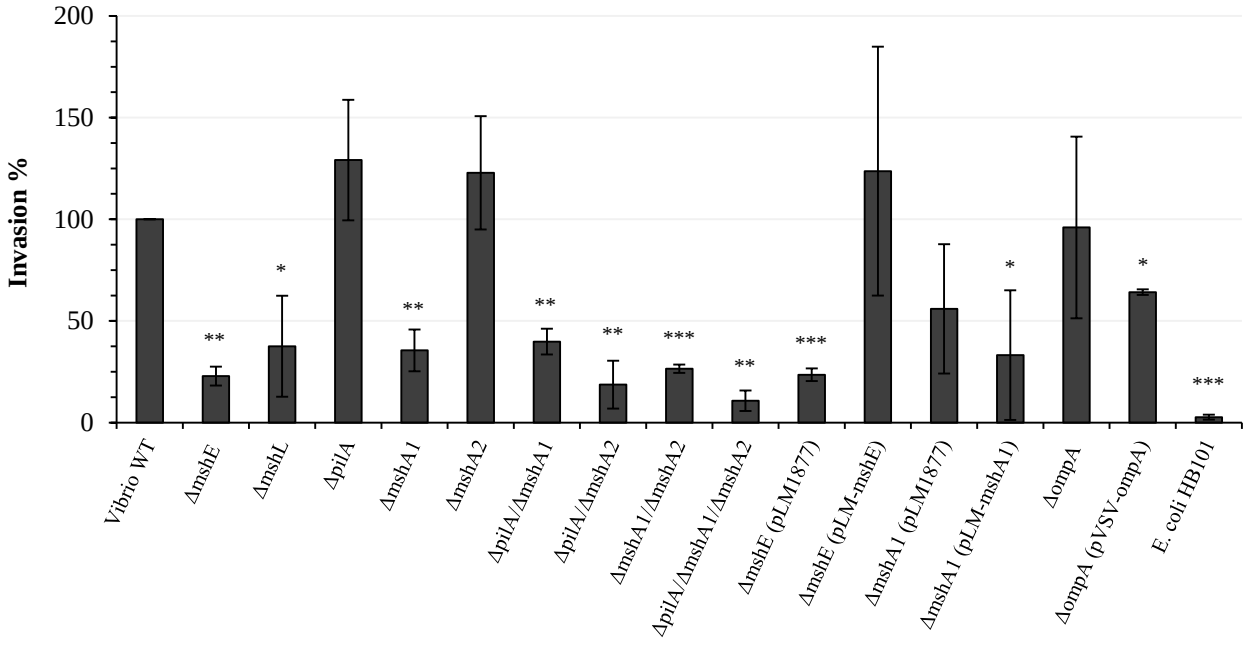

Fig 5.15 Disruption of adherence by deletion of major components of the MshA1 pilus reduces cellular uptake of *V. parahaemolyticus*. Quadruplicate wells of confluent Caco-2 were infected with bacteria at an MOI of 10 for 1 h. Monolayers were washed and extracellular bacteria were killed by incubation in 50 μg ml^{-1} gentamicin for 1 h. Intracellular bacteria were enumerated by lysing the monolayers with 1% Triton, followed by spread plating on the appropriate agar. Invasion of each strain is expressed as a percentage of the wild type invasion efficiency (intracellular cfu as a percentage of the inoculum). Results shown are from at least three replicate experiments. *** $P<0.001$; ** $P<0.01$; * $P<0.05$ calculated using paired student's *t* test to compare sample result with that of the wild type.

The results of Fig 5.15 closely resemble those observed for the adherence efficiency of *V. parahaemolyticus* deletion mutants (Fig 5.11). It appears that disruption of the MSHA by deletion of *mshE*, *mshL* or *mshA*1 reduces the adherence of *V. parahaemolyticus* to Caco-2 cells and this has the effect of reducing cellular uptake of the organism. This indicates that the MSHA components MshE (ATPase), MshL (secretin) and MshA1 (pilin) play a direct role in the process of cellular uptake of *V. parahaemolyticus*. The reduction in adherence seen in the Δ*mshA*1 mutant (40% of wild type efficiency), was almost identical to that observed

for invasion (35% of wild type invasion efficiency). The close correlation between adherence results and those observed for invasion indicate that efficient adherence is a prerequisite for cellular uptake of *V. parahaemolyticus*.

In correspondence with the results obtained with the complementation strains used for assessment of adherence efficiency, complete complementation was achieved with the Δ*mshE* (pLM-*mshE*), indicating the specific involvement of the MSHA locus in the invasion of *V. parahaemolyticus* into Caco-2 cells. Complementation was not observed with the Δ*mshA*1 (pLM-*mshA*1) strain, with lower levels of invasion being seen in the Δ*mshA*1 (pLM-*mshA*1) strain than that observed in the empty vector control Δ*mshA*1 (pLM1877). The successful phenotype restoration observed with the *trans* complementation of *mshE* illustrates the specificity of the MSHA deletions with respect to invasion and can be used to confirm such specificity relating to any other phenotypes associated with deletion of critical components of the MSHA pilus.

In Fig 5.15, similar to adherence data in Fig 5.11, the double mutant Δ*pilA*/Δ*mshA*2 displays significantly lower invasion than the wild type, while single mutants of *pilA* and *mshA*2 do not show any decrease in invasion efficiency. As mentioned previously, the double mutant Δ*pilA*/Δ*mshA*2 appears to form clusters of cells (Fig 5.13). As the gentamicin protection assay used in the enumeration of cellular uptake also relies upon enumeration of cfu, the formation of aggregates or clusters of cells may affect the results observed in a similar manner to that seen in Fig 5.11.

The putative invasin OmpA was also analysed to assess its role in the process of *V. parahaemolyticus* invasion into Caco-2. This was carried out using the deletion mutant Δ*ompA*. The specificity of any phenotype observed was assessed by the use of the complementation strain Δ*ompA* (pVSV-*ompA*). As seen in Fig 5.15, deletion of *ompA* had no

effect on the cellular uptake of *V. parahaemolyticus*, with similar levels of invasion being seen with the wild type and Δ*ompA* mutant. Similarly, re-introduction of *ompA* into the deletion mutant on a multi-copy shuttle vector pVSV105 did not result in further increased invasion compared with either the Δ*ompA* mutant or the *V. parahaemolyticus* wild type. As such, it appears OmpA does not function as an adhesin (Fig 5.11) or an invasin in *V. parahaemolyticus*.

It is possible however, that functionality as an invasin may be specific to expression of the protein within the heterologous host. Differential expression levels, protein folding or post-translational modifications could all lead to altered activity upon expression in *E. coli* HB101. As such, the wild type *ompA* allele was inserted into an inducible expression vector pLMSAC and transformed into *E. coli* HB101. Expression was induced with IPTG and the cellular uptake of the strain was analysed by gentamicin protection assay as described previously. Comparison of *E. coli* HB101 (pLM-*ompA*) invasion efficiency with *E. coli* HB101 carrying the empty expression vector pLMSAC, showed no increased levels of invasion (*E. coli* HB101 [pLMSAC] = 0.008 +/- 0.006%, *E. coli* HB101 [pLM-*ompA*] = 0.007 +/- 0.004%). As such it appears that OmpA does not function as an invasin in *V. parahaemolyticus* or *E. coli* HB101.

5.7 Adherence as a pre-requisite for *V. parahaemolyticus* pathogenicity and the involvement of TFP in the detrimental effects of *V. parahaemolyticus* on host cells.

5.7.1 Assessment of the role of TFP in the cytotoxic effect of *V. parahaemolyticus* on Caco-2 cells.

V. parahaemolyticus has been shown to induce rapid lysis of host cells through the secretion of effector proteins which modulate signalling cascades within the host cell. Burdette *et al.* (2008) showed that the TTSS-dependent cytotoxicity of *V. parahaemolyticus* is caused by a multi-faceted event involving induction of autophagy, cell rounding and eventual cell lysis and that such a process was likely the result of the secretion of multiple effector proteins. One such effector protein, VopQ encoded by *VP1680* has been shown to play a critical role in this process. Mutants which lack functional TTSS1 or *vopQ* have been shown to display marked reductions in cytotoxicity upon infection of the host cell (Matlawska-Wasowska *et al.*, 2010; Burdette *et al.*, 2009). We hypothesised that the disruption of *V. parahaemolyticus* adherence caused by deletion of TFP components would lead to decreased efficiency of TTSS effector delivery and as such, a reduction in TTSS-mediated cell lysis.

In order to assess the involvement of TFP in the cytotoxic effects of *V. parahaemolyticus*, Caco-2 cells were incubated with the *V. parahaemolyticus* wild type and TFP deletion mutants for 4 h, and the levels of the cytoplasmic enzyme lactate dehydrogenase (LDH) in the culture medium were assessed by a colorimetric assay. Matlawska-Wasowska *et al.* (2010) saw high levels of cytotoxicity with the *V. parahaemolyticus* wild type (>80% cell lysis) after 4 h of co-incubation with Caco-2. In order to yield the maximum sensitivity of differential lysis measurement between the wild type and mutant strains, it was decided to carry out LDH assays at 4 h post infection.

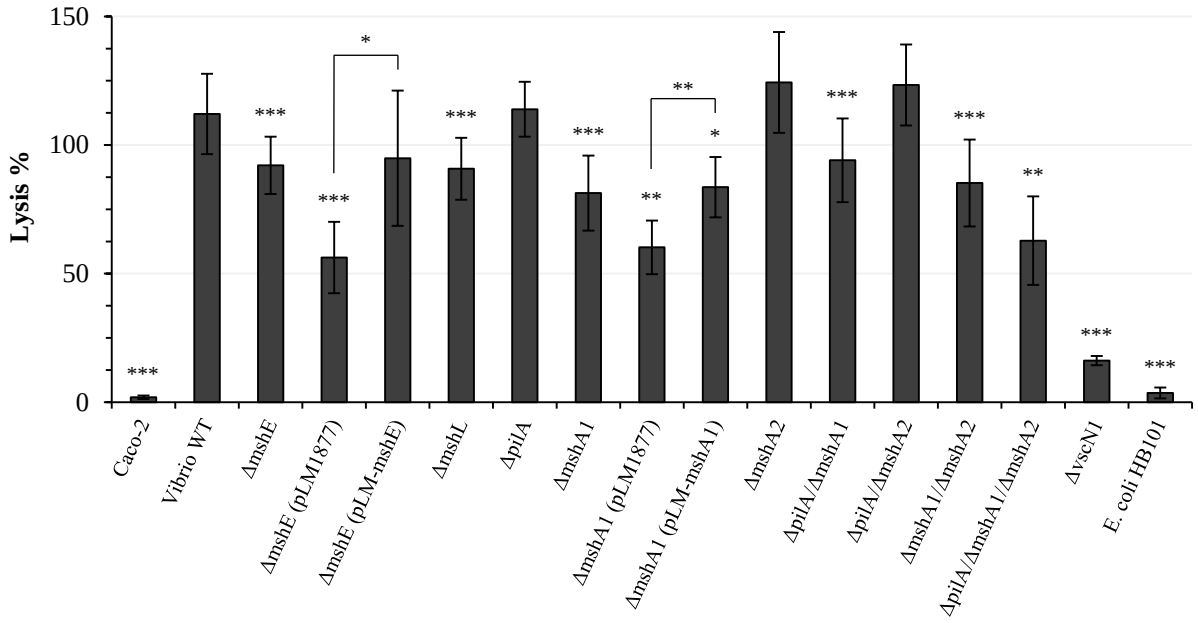

Fig 5.16 The MSHA pilus plays a role in the cytotoxicity of *V. parahaemolyticus* towards Caco-2 cells. Confluent Caco-2 cells were infected for 4 h with *V. parahaemolyticus* wild type, type IV pilin deletion mutants and mutant strains carrying either empty pLM1877 or recombinant pLM1877-derived vectors containing the gene being analysed for complementation. Strains carrying vectors were induced with IPTG for 1 h 45 min prior to co-incubation. Supernatant samples were taken from infected Caco-2 cells and were analysed for LDH release using the Promega Cytotox 96 cytotoxicity assay kit. Percentage lysis was calculated by subtracting the OD_{492} of the medium control from each sample and expressing the resulting absorbance as a percentage of that obtained for sample wells lysed by addition of detergent. The results displayed are the mean plus standard deviations from at least three experiments. *** $P<0.001$; ** $P<0.01$; * $P<0.05$ were calculated using paired student's *t* test to compare sample results with that of the wild type. Significance of phenotype restoration by complementation was assessed by paired student's *t* test comparing the empty vector control result to that of the complementation strain.

As seen in Fig 5.16, deletion of *pilA* and *mshA*2 did not affect cytotoxicity of *V. parahaemolyticus* towards Caco-2, as seen by the similar results obtained from Caco-2 infected with wild type *V. parahaemolyticus*, Δ*pilA*, Δ*mshA*2 and Δ*pilA*/Δ*mshA*2. As such under the conditions tested, PilA and MshA2 do not play a role in the cytotoxicity of *V. parahaemolyticus* in the Caco-2 cell model. This result correlated with the fact that PilA and MshA2 do not a role in the adherence of *V. parahaemolyticus* to Caco-2 (Fig 5.11 and Fig 5.13). The correlation between wild type and Δ*pilA*/Δ*mshA*2 cytotoxicity levels confirms that

although the enumerable cfu of adherent and invasive bacteria were lower for this strain (Fig 5.12 and Fig 5.10), this was due to an altered pattern of adherence, rather than altered adherence due to disruption of adhesins.

E. coli HB101 is regarded as a non-pathogenic lab strain and as such was used as a negative control for cytotoxicity. As expected both the *E. coli* HB101 control and the uninfected Caco-2 exhibited very low levels of lysis (<5%). The Δ*vscN*1 mutant, which does not produce an active TTSS1, caused low levels of lysis (16%) indicating the critical role that TTSS1 plays in the lysis of Caco-2. This finding is consistent with that of Matlawska-Wasowska *et al.* (2010).

Deletion of critical components of the MSHA pilus including MshE (ATPase), MshL (secretin) and MshA1 (major pilin) led to similar decreases in cytotoxicity, with approximately 90% lysis being observed for all strains harbouring deletions in genes coding for these proteins. By comparison, lysis levels of 110% were obtained for cells infected with *V. parahaemolyticus* wild type. Although the difference observed between the wild type and MSHA deletions was small, a difference of at least 10% of the wild type levels was observed across 6 experiments for each of these mutants. The consistency of these results is confirmed by the paired student's *t* test which allows for direct comparison of the results obtained within each experiment. As such, the significance of the differences observed between the wild type and Δ*mshE*, Δ*mshL*, Δ*mshA*1, Δ*pilA*/Δ*mshA*1, Δ*mshA*1/Δ*mshA*2, Δ*pilA*/Δ*mshA*1Δ*mshA*2 was confirmed with $P<0.01$ being obtained for each mutant. LDH concentrations leading to a lysis percentage of >100% probably occurred due to lysis of some bacterial cells within the infected sample wells, while the lysis control contained only Caco-2.

Deletion mutants carrying the empty pLM1877 vector appear to have a further decreased lytic effect on Caco-2 compared with the corresponding vectorless deletion mutants. This

could be due to the pressure of antibiotic selection resulting in either a decreased growth rate or a decrease in the expression levels of cytotoxic virulence factors due to the presence of the extra-chromosomal vector. Recovery of wild type levels of lysis was observed upon expression of MshE from pLM-*mshE* in the Δ*mshE* background, thus confirming the role of the MSHA pilus in the lysis of host cells. Partial recovery of lysis was observed with the *mshA*1 complemented strain, as observed for adherence (Fig 5.11), with a significant increase ($P<0.01$) being observed between Δ*mshA*1 (pLM1877) and Δ*mshA*1 (pLM-*mshA*1).

Therefore these results demonstrate that the MshA pilus is required for the maximal cytotoxicity of *V. parahaemolyticus*.

5.7.2 The role of TFP in the rounding of host cells caused by *V. parahaemolyticus*.

As mentioned previously, the pathogenicity of *V. parahaemolyticus* towards host cells is a dynamic process involving multiple virulence factors, which cause many independent effects on the host cell. While the TTSS1 effector VopQ has been implicated in the induction of autophagy and the eventual lysis of epithelial cells (Burdette *et al.*, 2009), independent pathogenic effects have been observed and attributed to other effector proteins. Another TTSS1 effector protein, VopS encoded by *VP1686*, has been characterised and has been identified as playing a role in the rounding of host cells. *In vitro*, this has the effect of reducing monolayer polarisation by detaching adherent cells from the substratum (Burdette *et al.*, 2008). *In vivo*, morphological disruption of host cells and eventual removal from the infected tissue could cause extreme disruption of intestinal barrier function and extensive tissue damage.

In order to observe the manner in which *V. parahaemolyticus* alters the morphology of the host cell, an epi-fluorescence microscopy based assay was carried out, employing actin staining of *V. parahaemolyticus*-infected Caco-2. Caco-2 cells were incubated with *V. parahaemolyticus* for 5 h and were examined by phase contrast microscopy at 30 min intervals in order to determine the optimal level of morphological alteration without complete monolayer disruption (Data not shown). After 2.5 h of infection, the majority of cells appeared rounded and were still attached to the monolayer. At later time points, extensive monolayer destruction was observed. For this reason it was decided to employ 2.5 h of co-incubation for examination of Caco-2. *V. parahaemolyticus* and TFP deletion mutants were incubated with Caco-2, which were grown to confluency on coverslips for 2.5 h. Coverslips were fixed by incubation in 4% paraformaldehyde for 20 min and permeabilised by incubation in PBS + 0.1% Triton for 5 min. Coverslips were then stained with a mixture of Hoechst, which binds to DNA and thus stains nuclear material blue and a phalloidin-Alexa 568 conjugate, which emits within the red spectrum. Phalloidin is a compound derived from the highly toxic *Amanita phalloides* mushroom which binds with high affinity to filamentous actin, a major component of the eukaryotic cytoskeleton (Wieland *et al.*, 1978). It is this F-actin affinity which has led to the development of a variety of phalloidin conjugates which are particularly useful in the examination of cytoskeletal modifications. Stained coverslips were mounted on slides containing a drop of polyvinyl alcohol/DABCO anti-fade reagent and were visualised by epi-fluorescence microscopy.

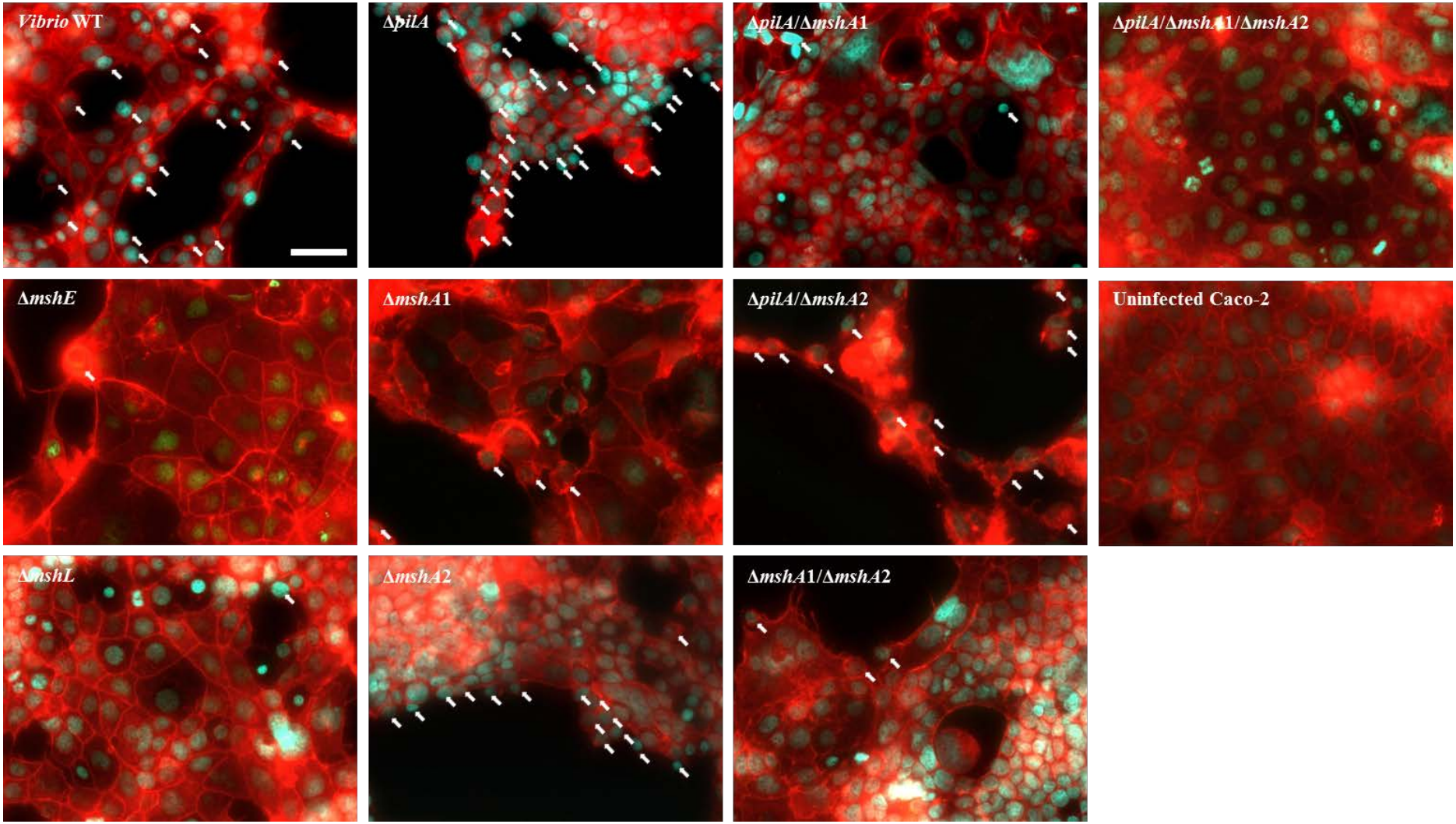

Fig 5.17 The MSHA pilus plays a role in cell rounding associated with *V. parahaemolyticus* cytotoxicity. Confluent Caco-2 cells were infected for 2.5 h with *V. parahaemolyticus* wild type and TFP mutants. Cells were fixed in 4% paraformaldehyde and stained with Hoechst 33342 (Blue) and Phalloidin-Alexa 568 (Red). Rounded cells are indicated by white arrows. Scale bar represents 50 μm.

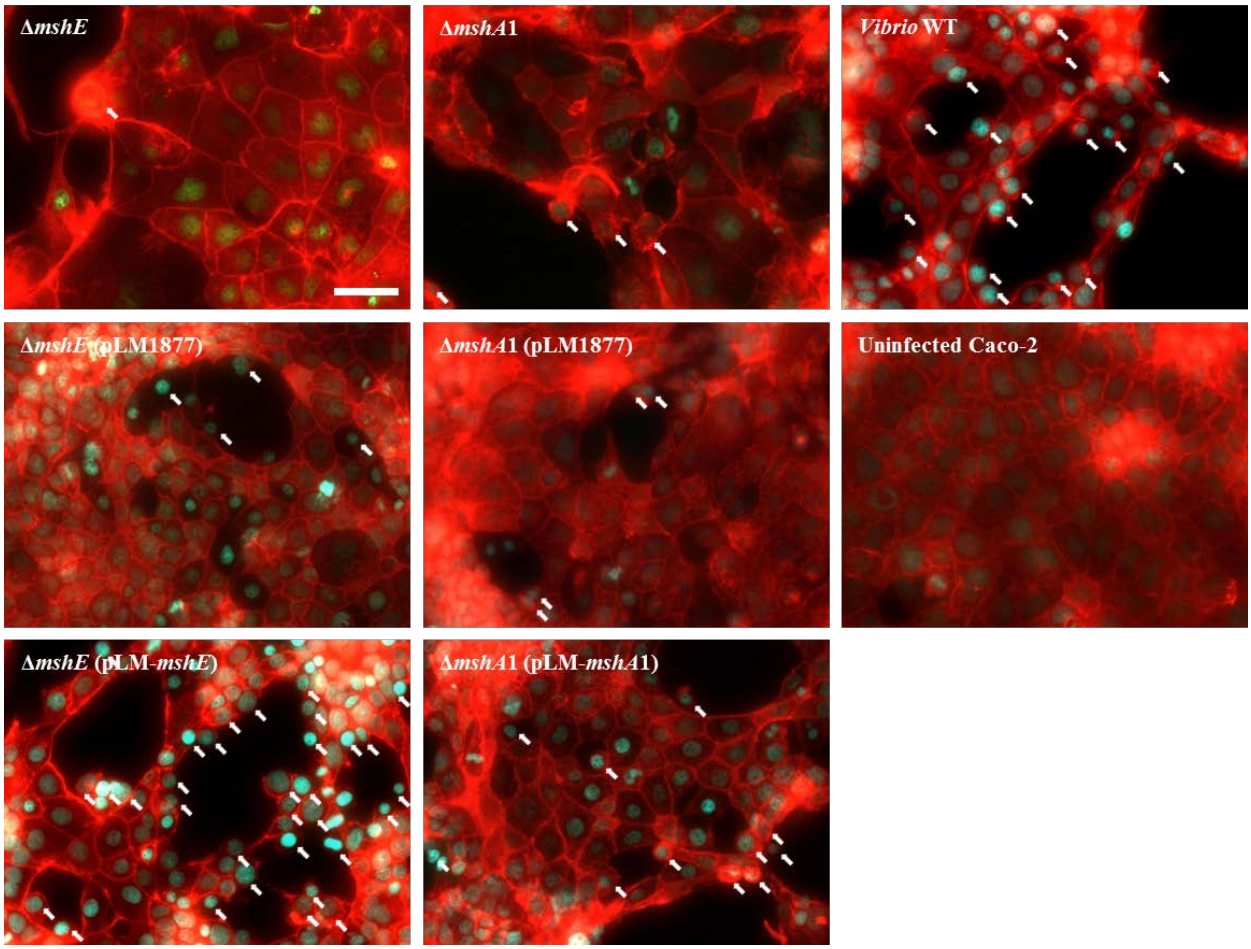

Fig 5.18 *V. parahaemolyticus*-associated cell rounding can be restored in *msh* mutants by complementation. Confluent Caco-2 cells were infected for 2.5 h with *V. parahaemolyticus*, TFP deletion mutants, empty pLM1877 controls and complementation strains. Empty vector controls and complementation strains were induced with IPTG for 1.5 h prior to infection. Cells were fixed in 4% paraformaldehyde and stained with Hoechst 33342 (Blue) and Phalloidin-Alexa 568 (Red). Rounded cells are indicated by white arrows.) Scale bar represents 50 μm.

The uninfected Caco-2 in Fig 5.17 have a regular polygonal cell shape with defined tight junctions surrounding each cell as indicated by the high levels of red fluorescence due to actin bundling. Mitotic cells were visible in the bottom left corner of the image indicating that the monolayer was actively replicating. The monolayer was also completely intact. Cells infected with the *Vibrio* WT by comparison had less defined tight junctions and the regular polygonal shape of the cells had been disrupted. A large number of cells were in the late stage of rounding as indicated by the white arrows. Shortly after rounding of infected cells, these

cells would become detached from the monolayer. This is evidenced by the fact that regions containing many rounded cells tend to border regions of empty space, where monolayer disruption has taken place due to the detachment of Caco-2 cells. No mitotic cells are visible, indicating that the normal cell cycle may have been disrupted. The density of the monolayer also seems to have been affected, as fewer cells are contained within the *Vibrio* WT image than that of the uninfected Caco-2. It is worth noting that some healthy regions were observed in monolayers infected with each *V. parahaemolyticus* strain and as such images which were representative of the state of the entire monolayer were recorded.

Again, deletion of *pilA* and *mshA*2 did not affect the results obtained in this experiment as the proportion of rounded cells and the degree of monolayer disruption closely resembled that of the *Vibrio* WT. The Δ*pilA*/Δ*mshA*2 mutant for example shows a region within the monolayer which is in the late stages of cell rounding, with very few cells remaining attached to the substratum.

Deletion of the critical MSHA genes *mshE*, *mshL* and *mshA*1 resulted in a decreased efficiency of cytoskeletal rearrangement due to *V. parahaemolyticus* infection (Fig 5.17). In mutants lacking these genes, the regular cell shape was retained and tight junctions were not disrupted to the extent observed with the *Vibrio* WT. Very few cells exhibited the characteristic rounded morphology exhibited by those infected with the *Vibrio* WT (white arrows). Monolayer disruption was also not as severe as that seen in cells infected with the *Vibrio* WT, as seen by the high density of the monolayer and the lack of significant amounts of empty space where cells had been detached. The Δ*pilA*/Δ*mshA*1/Δ*mshA*2 shows the best example of cells which have been infected but have retained their original cell morphology as these cells closely resemble that of the uninfected Caco-2.

Fig 5.18 shows the results observed for Caco-2 infected with complementation mutants and empty vector controls. As for adherence, invasion and lysis, the role of the MSHA locus in the cell rounding effect of *V. parahaemolyticus* infection was confirmed by complete recovery of the wild type result with the *mshE* complemented strain (Δ*mshE* [pLM-*mshE*]). This was seen by the marked increase in the proportion of rounded cells to healthy cells compared with the empty vector control, with similar levels of rounding being observed to that of the *Vibrio* WT. Again partial recovery was observed with the *mshA*1 complemented strain with higher levels of rounding being observed to the empty vector control but lower levels than that of the *Vibrio* WT.

These results confirm that adherence is required for efficient actin cytoskeleton rearrangements associated with *V. parahaemolyticus* infection of Caco-2. We have also shown that the MSHA pilus plays a critical role in this process as deletion of the major pilin subunit (MshA1) resulted in a marked reduction in cell rounding.

5.7.3 The role of TFP in pro-inflammatory chemokine induction.

V. parahaemolyticus infection modulates a variety of host cell signalling pathways leading to a diverse range of alterations in host cell behaviour. One such alteration is the induction of an acute pro-inflammatory response as indicated by the secretion of the pro-inflammatory chemokine IL-8. This process has been studied by Matlawska-Wasowska *et al.* (2010) and Shimohata *et al.* (2011). Both groups describe a critical role for VopQ in modulation of the ERK1/2 and p38 MAPK cell signalling cascades. It appears that this TTSS1 effector protein can phosphorylate these MAPK proteins, thereby activating downstream MAPK targets and inducing secretion of IL-8. The role of bacterial adherence in this process has not been

analysed, therefore it was decided to examine the levels of IL-8 secretion induced by the *Vibrio* WT compared with TFP mutant strains.

Matlawska-Wasowska *et al.* (2010) observed IL-8 concentrations of 600 pg ml^{-1} 6 h post-infection and 800 pg ml^{-1} 24 h post-infection with the addition of gentamicin 2 h post-infection to kill extracellular bacteria and prevent lysis of Caco-2. Shimohata *et al.* (2011) observed 60 pg ml^{-1} 6 h post-infection without the addition of gentamicin. It is worth noting that Shimohata *et al.* (2011) also used a lower MOI, with 2 X 10^4 cfu $well^{-1}$ in confluent 6 well plates containing Caco-2 cells, compared with 4.5 X 10^6 cfu $well^{-1}$ in confluent 24 well plates used by Matlawska-Wasowska *et al.* (2010). The difference in MOI was the most probable reason for the increased IL-8 concentrations observed by Matlawska-Wasowska *et al.* (2010). It is also possible that due to infection for longer than 4 h with *V. parahaemolyticus*, a significant number of Caco-2 cells may have become lysed prior to secretion of IL-8.

In a similar manner to the cytotoxicity assays described in section 5.7.1, the maximum level of IL-8 induction was assessed in order to yield the highest possibility of a difference being observed between the wild type and the TFP mutant strains. As such a method was adapted from Matlawska-Wasowska *et al.* (2010), employing a greater number of time-points to determine the optimum sampling time post-infection. 7 day old, confluent Caco-2 cells were incubated at an MOI of 10 with exponential phase *Vibrio* WT. Supernatant samples were taken 1 h and 2 h after addition of bacteria. Extracellular bacteria were killed by addition of medium containing gentamicin and supernatant samples were collected at 3 h, 4 h, 6 h, 8 h, 20 h and 24 h after the addition of bacteria. A positive control for IL-8 induction was also included by the incubation of IL-1β with Caco-2 cells for 3 h, with samples being taken in parallel with those of the *Vibrio* WT. IL-8 concentrations in the supernatant samples were determined by ELISA as described in section 2.5.6.

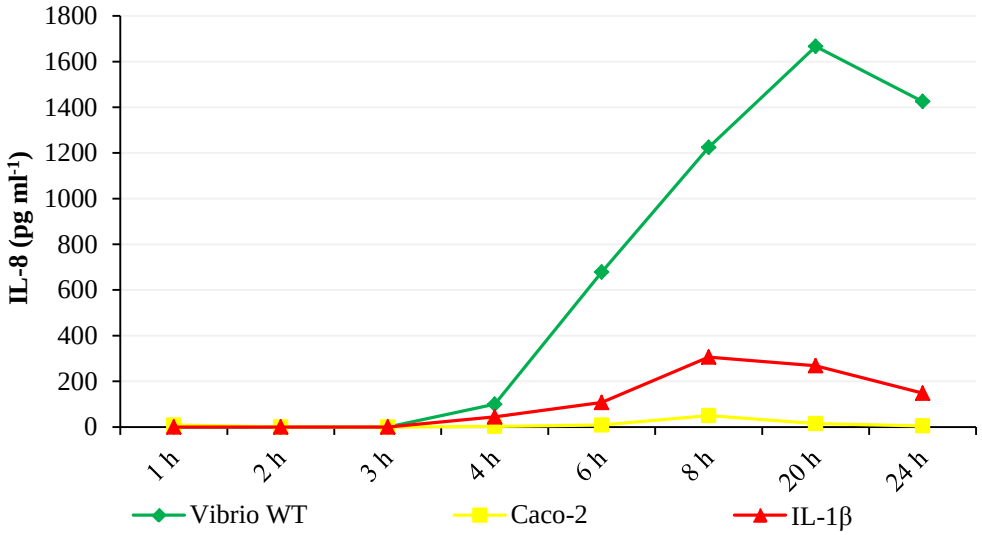

Fig 5.19 Maximum levels of IL-8 are induced 20 h post-infection with *V. parahaemolyticus*. Caco-2 cells were infected with *V. parahaemolyticus* wild type for 2 h. In separate wells IL-1β was incubated with Caco-2 cells for 3 h as a positive control for IL-8 induction. Following 2 h of infection, bacteria were killed by addition of medium containing gentamicin. Samples were taken for determination of IL-8 levels by ELISA at the indicated times post-infection. The results displayed are the mean values obtained from 3 replicate wells of Caco-2 per time point within a single representative experiment.

As seen above and in correlation with the findings of Matlawska-Wasowska *et al.* (2010), *V. parahaemolyticus* infection induces a pronounced IL-8 response in Caco-2 with approximately 600 pg ml^{-1} being detected in the medium 6 h post-infection. The induction of IL-8 by *V. parahaemolyticus* was more pronounced than that observed with stimulation by the pro-inflammatory cytokine IL-1β. Maximum levels of IL-8 (~1,700 pg ml^{-1}) were detected 20 h post-infection and as such it was decided to collect samples for future experiments at this time point.

Having optimised the sampling time for analysis of IL-8 secretion from cells infected with *V. parahaemolyticus*, it was decided to analyse which cell signalling pathways were involved in the process of IL-8 secretion. This was achieved by carrying out co-incubations and IL-8 quantitation by ELISA as described above, however Caco-2 cells were pre-incubated with inhibitors to inactivate cell signalling pathways. PD98059 prevents phosphorylation and

hence activation of MEK1, a kinase which is directly upstream of ERK in the signalling cascade. The principal function of MEK1 is the activation of the ERK complex by phosphorylation, therefore inhibition of MEK1 provides an effective means of selectively inhibiting ERK. Bay11-7082 is a selective inhibitor of NF-κB-dependent transcription. It functions by preventing the phosphorylation of IκB by the IκBK complex. IκB prevents the transcription of NF-κB-dependent genes by binding to the RelA/NF-κB complex and blocking translocation into the nucleus. Phosphorylation of IκB leads to ubiquitination and subsequent degredation by the proteasome. This leaves the RelA/NF-κB complex free to enter into the nucleus activating the transcription of NF-κB-dependent genes. As pre-treatment of Caco-2 with Bay11-7082 prevents the degradation of IκB, the NF-κB complex cannot enter the nucleus and NF-κB-dependent transcription is blocked.

Figure 5.20 shows the effect of pre-treatment of Caco-2 with the ERK inhibitor PD98059 and the NF-κB inhibitor Bay 11-7028 prior to co-incubation with *V. parahaemolyticus*.

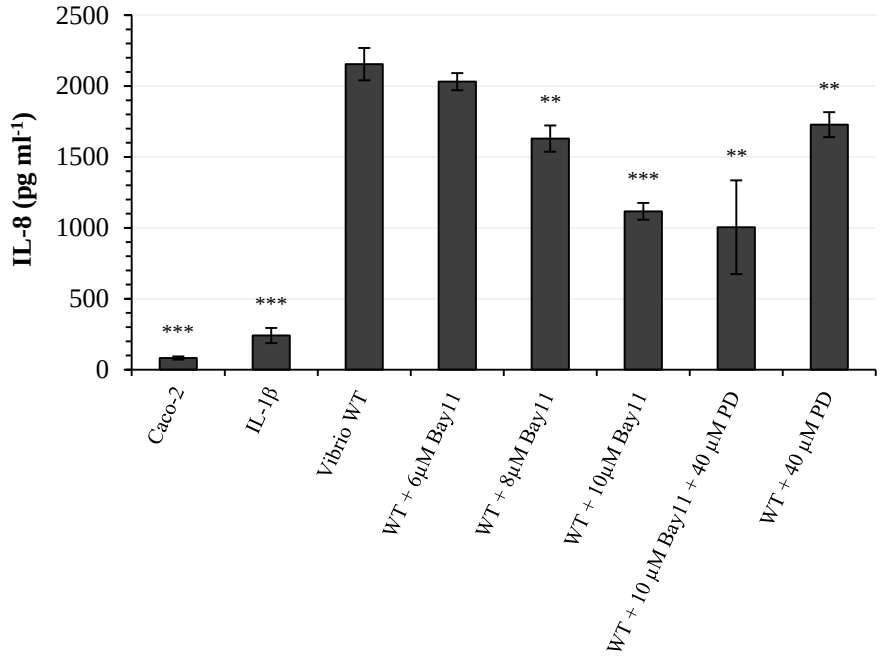

Fig 5.20 *V. parahaemolyticus* induces IL-8 secretion from Caco-2 in an NF-κB, ERK-dependent manner. Caco-2 cells were infected with *V. parahaemolyticus* wild type for 2 h. In separate wells IL-1β was incubated with Caco-2 cells for 3 h as a positive control for IL-8 induction. Inhibitors Bay11-7082 and PD98059 were incubated with the Caco-2 cells at the indicated concentrations for 1 h prior to infection and throughout the 2 h co-incubation. Following 2 h of infection, bacteria were killed by addition of medium containing gentamicin. Samples were taken for determination of IL-8 levels by ELISA 20 h post-infection. The results displayed are the mean values obtained from 3 replicate wells of Caco-2 per time point within a single representative experiment. *** $P<0.001$; ** $P<0.01$ were calculated using unpaired student's *t* test to compare sample results with that of the wild type.

As seen above, inhibition of NF-κB by pre-incubation with Caco-2 resulted in a dose-dependent decrease in IL-8 concentrations secreted upon infection with *V. parahaemolyticus*. A 50% decrease was observed at 10 μM Bay11. This indicates that NF-κB-dependent expression plays a key role in IL-8 induction by *V. parahaemolyticus*, which correlates with a transcription factor binding site with consensus for NF-κB, located upstream of the IL-8 gene (Shimohata *et al.*, 2011). A 20% decrease in *V. parahaemolyticus* stimulated IL-8 secretion was observed by pre-incubation with PD98059, indicating that the IL-8 response to *V. parahaemolyticus* infection is regulated by ERK.

Our results implicating the ERK pathway and the NF-κB pathways in the *V. parahaemolyticus* stimulated IL-8 production from Caco-2 are supported by Shimohata *et al.* (2011) in a publication which was released following the work described here. Shimohata *et al.* (2011) found that the ERK inhibitor U0126, which functions in a similar manner to PD98059 by inhibiting the activity of MEK1, reduced IL-8 induction in response to *V. parahaemolyticus* infection by 50% at a 10 μM concentration. The NF-κB inhibitor used by Shimohata *et al.* (2011), which like Bay11, prevents IκB degradation, thereby blocking translocation of the RelA/NF-κB complex to the nucleus was found to reduce *V. parahaemolyticus*-associated IL-8 induction by 30%. Shimohata *et al.* (2011) also showed by immuno-fluorescence microscopy that *V. parahaemolyticus* caused the translocation of the RelA/NF-κB complex to the nucleus of infected cells. The findings of Shimohata *et al.* (2011) correlate with those shown in Fig 5.20 and as such the involvement of the ERK pathway and NF-κB in *V. parahaemolyticus* stimulated IL-8 secretion is clearly demonstrated.

In order to assess whether adherence was required for *V. parahaemolyticus*-associated IL-8 induction and to assess the relative roles played by TFP components, IL-8 ELISA was carried out following infection with the *Vibrio* WT and TFP deletion mutants.

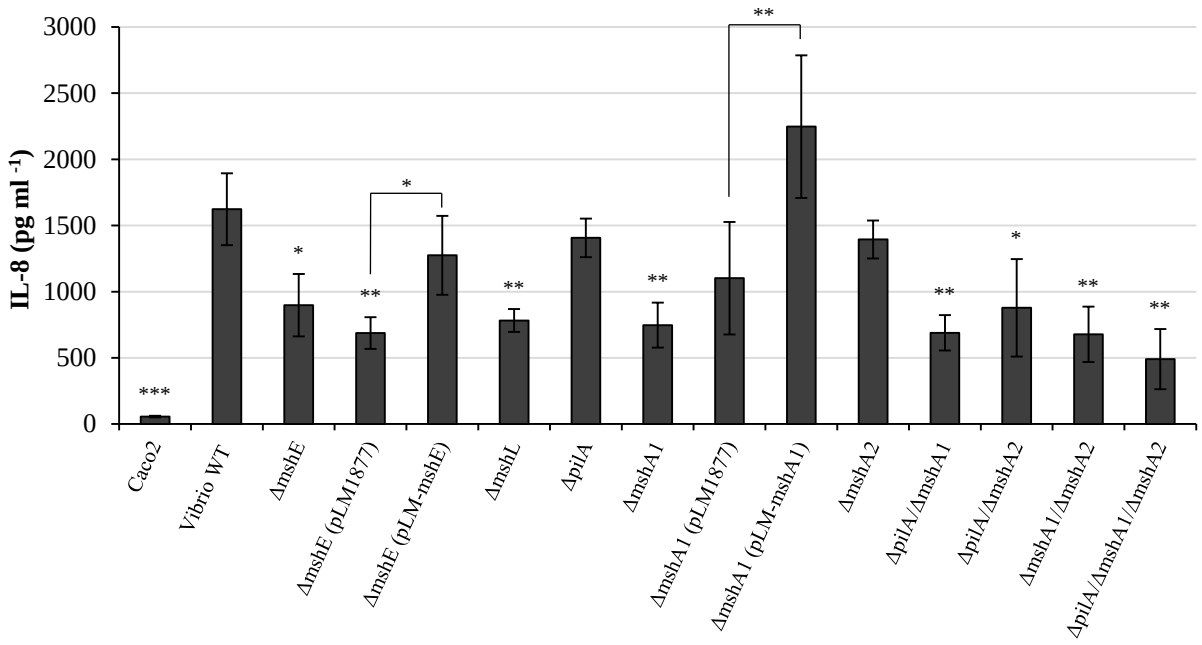

Fig 5.21 *V. parahaemolyticus* MSHA is involved in the induction of IL-8 secretion from Caco-2. Caco-2 cells were infected with *V. parahaemolyticus* wild type for 2 h. Following 2 h of infection, bacteria were killed by addition of medium containing gentamicin. Samples were taken for determination of IL-8 levels by ELISA 20 h post-infection. The results displayed are the mean values obtained from 3 replicate wells of Caco-2 per time point within a single representative experiment. *** $P<0.001$; ** $P<0.01$; * $P<0.05$ were calculated using paired student's *t* test to compare sample results with that of the wild type.

The results in Fig 5.21 show that the MSHA pilus plays a role in IL-8 secretion from Caco-2 in response to *V. parahaemolyticus* infection. Significant decreases in IL-8 induction compared to the wild type were observed with Δ*mshE*, Δ*mshL*, Δ*mshA*1, Δ*pilA*/Δ*mshA*1, Δ*mshA*1/Δ*mshA*2, Δ*pilA*/Δ*mshA*2 and Δ*pilA*/Δ*mshA*1/Δ*mshA*2. The *Vibrio* WT induced IL-8 to a concentration of 1623 pg ml^{-1} while mutants lacking critical MSHA components induced secretion of IL-8 ranging from 490 pg ml^{-1} (Δ*pilA*/Δ*mshA*1/Δ*mshA*2) to 900 pg ml^{-1} (Δ*mshE*). Restoration of IL-8 induction was observed to levels similar to that of the *Vibrio* WT for Δ*mshE* (pLM-*mshE*) and Δ*mshA*1 (pLM-*mshA*1).

Under the conditions used, deletion of *pilA* or *mshA*2 had no effect on the concentrations of IL-8 detected in the medium. A significant decrease ($P<0.05$) was observed with the

Δ*pilA*/Δ*mshA*2 mutant, with 878 pg ml^{-1} being detected for the mutant in comparison to 1,623 pg ml^{-1} for the *Vibrio* WT. This mutant exhibited an unusual pattern of binding to Caco-2 forming large aggregates of cells when in contact with Caco-2 (Fig 5.13). This may have reduced the efficiency of effector delivery during the 2 h co-incubation, leading to lower levels of IL-8 being secreted from infected cells.

The results displayed in Fig 5.21 show that adherence plays a role in *V. parahaemolyticus*-associated IL-8 induction in Caco-2 cells and that the MSHA pilus is involved in this process.

5.8 Identification of the glycan receptor for the *V. parahaemolyticus* MSHA pilus.

The work described in this chapter indicates a critical role for the MSHA pilus in the adherence of *V. parahaemolyticus* to the intestinal epithelial cell line Caco-2. A number of type IV pilins have been described as lectins, which are proteins with sugar binding activity. The PAK pilus of *P. aeruginosa* strain K and the PAO pilus from *P. aeruginosa* strain O were found to bind specifically to the GalNAcβ1-4Gal epitope which forms the carbohydrate domain of the gangliosidic receptors asialo-GM1 and asialo-GM2 (Sheth *et al.*, 1994). This is thought to aid *P. aeruginosa* in the colonisation of epithelial cells within the respiratory tract. The complement control protein CD46 which is expressed on the surface of many cell types has been identified as the receptor for the *N. gonorrhoeae* GC pilus (Källström *et al.*, 1997). Further characterisation led to the identification of 2 CD46 domains which are critical for GC pilin binding. The complement control protein repeat domain 3 (CCP-3) and a serine, threonine, proline rich domain (STP) were both found to be required for binding of the GC pilin (Källström *et al.*, 2001). The STP region is known to be *O*-glycosylated and as such glycan binding may play a role in the adherence of *N. gonorrhoeae*. Källström *et al.* (2001) also found that disruption of the *N*-glycosylation site in CD46 resulted in reduced adherence

of *N. gonorrhoeae* to cells expressing human CD46. These examples illustrate the importance of pilin-glycan interactions with respect to bacterial attachment to host tissues.

A number of technologies have been developed in recent years, with a view to unravelling the complex nature of the glycome. Carbohydrates are extremely complex molecules, with vast potential for diversity in structure, composition and function. By combining many of the technologies which have been developed for the study of proteins and nucleic acids with current knowledge of glycan structure and function, a variety of tools have become available, enabling the rapid analysis of glycan interactions. One such advancement has been the development of array based analysis techniques which can be used to study carbohydrate-receptor binding. In a similar manner to DNA microarray printing, glycan motifs can be printed onto solid surfaces and assessed for specificity of binding by fluorescently labelled lectins, viruses or bacteria.

The first glycan array was described by Fukui *et al.* in 2002 and employed the covalent attachment of glycan residues to a lipid linker molecule, followed by immobilisation on nitrocellulose membrane. One of the greatest challenges in developing glycan array technology which allows for comprehensive analysis of carbohydrate-lectin binding was the development of sufficiently diverse, biologically relevant glycan libraries. The high levels of complexity and diversity of known glycan structures does not interfere with the development of comprehensive glycan libraries, as the biologically active epitopes of oligosaccharides which take part in glycan interactions are comprised of a very finite number of structural variations (Rillahan and Paulson, 2011). Blixt *et al.* (2004) described a glycan array system comprised of 200 biologically relevant glycan structures which can be used in profiling of the carbohydrate binding specificities of lectins from plants, microbes and intact viruses. A number of advances have been made in the optimisation of ligand presentation and the

reduction of background fluorescence due to non-specific attachment of lectins by optimising slide chemistry and linker molecules (Kilcoyne *et al.*, 2012).

In order to present glycans in functional and biologically relevant conformations in array format, purified glycoproteins and lipids were printed where possible. In order to artificially construct neoglycoconjugates (NGCs) containing the desired glycan motifs for binding analysis, derivatives of glycans possessing the linker molecules 4-aminophenyl (4AP) or phenylisothiocyanate (PITC) were combined with either bovine serum albumin (BSA) or human serum albumin (HSA). The figure below describes the chemical reaction involved in constructing glucopyranoside-BSA *via* a 4AP linker (A) or a PITC linker (B).

Figure has been removed due to copyright restrictions

Fig 5.22 Construction of glucopyranoside-BSA NGCs. (**A**) Conjugation of 4-aminophenyl-β-D-glucopyranose to BSA. (**B**) Conjugation of β-D-phenylisothiocyanate glucopyranoside to BSA. Figure adapted from Mc Broom *et al.* (1972).

Following the production of NGCs, a variety of immobilisation techniques can be carried out in order to effectively print the molecules onto the microarray slide surface. The immobilisation technique used depends upon the type of slide employed and the reactivity between the functionalised slide and the NGC being printed (Rillahan and Paulson, 2011). For example, the Nexterion H slides used in this study are coated with a hydrophilic polymer which presents amine reactive N-hydroxysuccinimide ester groups on the surface of the slide for interaction with NGCs. According to Kilcoyne *et al.* (2012) the 3D hydrogel coated

Nexterion H slides provide greater reproducibility, smaller feature diameter, better spot morphology, expected ligand interaction and importantly, negligible background in comparison to the other slide chemistries analysed.

Figure has been removed due to copyright restrictions

Fig 5.23 Nexterion Slide H coating and immobilisation chemistry. Figure adapted from www.us.schott.com/nexterion.

The slides used in this study contained 52 individual spot types, including negative controls, well characterised glycoproteins and NGCs produced by conjugation of 4AP, PITC, aminophenylethyl (APE) and aminophenyldiamine (APD) glycan derivatives to either BSA or HSA. Different linker molecules were employed as it was observed by Kilcoyne *et al.* (2012) that the use of different linkers resulted in better presentation of glycan epitopes depending on the glycan being tested. The binding epitopes selected for analysis consisted of a broad range of glycans which are expressed in human tissues and have implications for human health, including pathogen binding.

In order to facilitate the detection of bound bacteria, staining was carried out using the fluorescent nucleic acid stain SYTO 82. Staining was first optimised by incubation in varying concentrations of SYTO 82 from 2.5 µM to 50 µM. Following seven washes with TBS buffer, the dye uptake from each strain was measured by excitation at 540 nm and recording of fluorescence at 560 nm. The optimal concentration as was determined to be 20 µM for all strains (Data not shown) and was used for all subsequent experiments.

Exponential phase bacteria were prepared in order to maintain consistent experimental conditions with the other experiments described in this chapter. Bacteria were stained with SYTO 82 and washed extensively as described above. Stained bacteria were then hybridised to individual subarrays on a pre-printed slide obtained from the Glycoscience Group, NCBES, NUI Galway. Tetramethyl rhodamine isothiocyanate (TRITC) tagged *Maackia amurensis* lectin and TRITC tagged *Artocarpus integrifolia* lectins were hybridised to separate subarrays on each slide as binding controls. The slides were washed thoroughly to remove unbound bacteria before scanning using a laser microarray scanner. Fig 5.24 shows a schematic representation of fluorescently tagged viral particles and fluorescently tagged lectins hybridised to two separate spots on a typical glycan array.

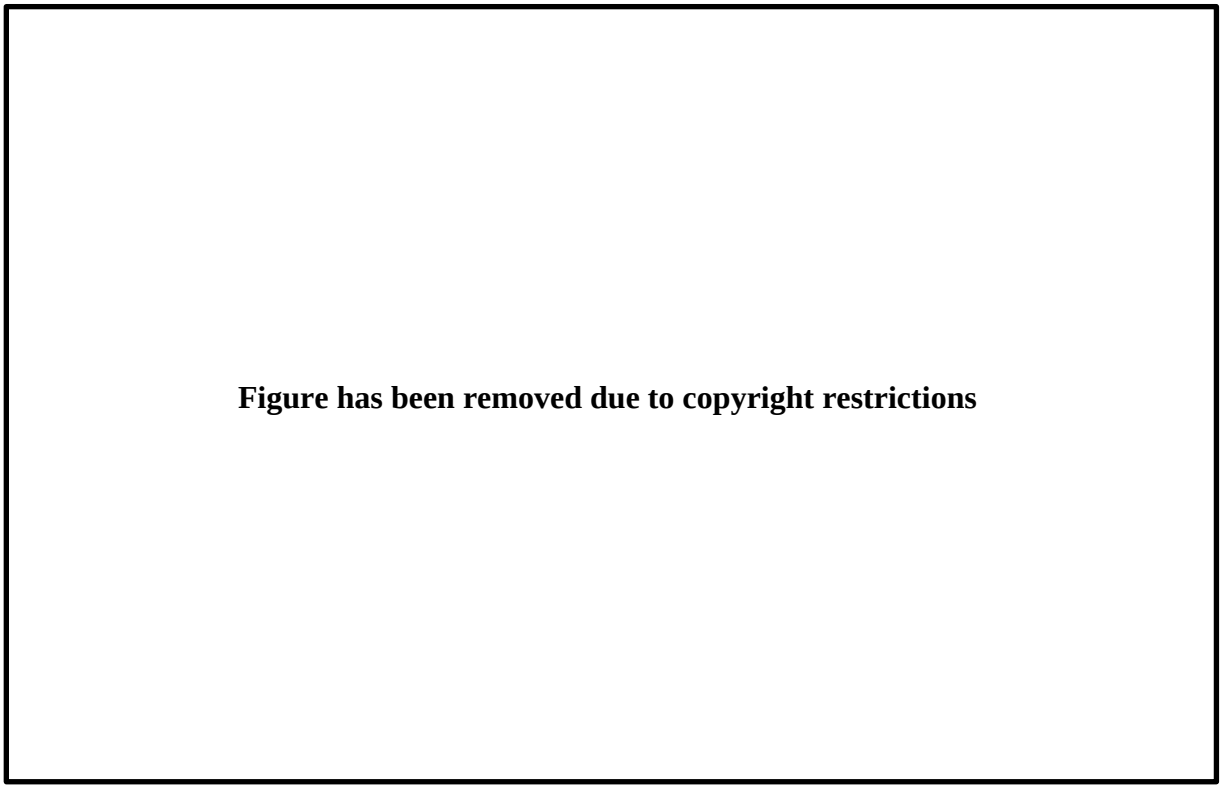

Fig 5.24 Schematic representation of the hybridisation of fluorescently tagged viral particles and fluorescently tagged lectins to a typical glycan array. Detailed images of each spot illustrate the multivalent nature of binding to glycans, which results in highly stable interactions and increases the likelihood of detection. Figure adapted from Rillahan and Paulson, (2011).

To improve the statistical robustness of the microarray platform, each spot type was printed in six replicates per subarray. At least three biological replicates were hybridised to independent subarrays for each strain being analysed. The median fluorescence intensity was calculated from the six individual spots and the mean value was calculated for the 3 subarrays used per strain. Fluorescence intensity per subarray was normalised to the mean sum of the fluorescence intensities across the 3 individual subarrays to allow for intersubarray variation. The binding profile for the fetuin/asialofetuin specific *Artocarpus integrifolia* lectin is illustrated in Fig 5.25. The data presented in Fig 5.26A, B, C and D represents the mean plus standard deviation normalised fluorescence intensity for *Vibrio* WT, Δ*mshA*1 and Δ*pilA*/Δ*mshA*1/Δ*mshA*2 across three biological replicates.

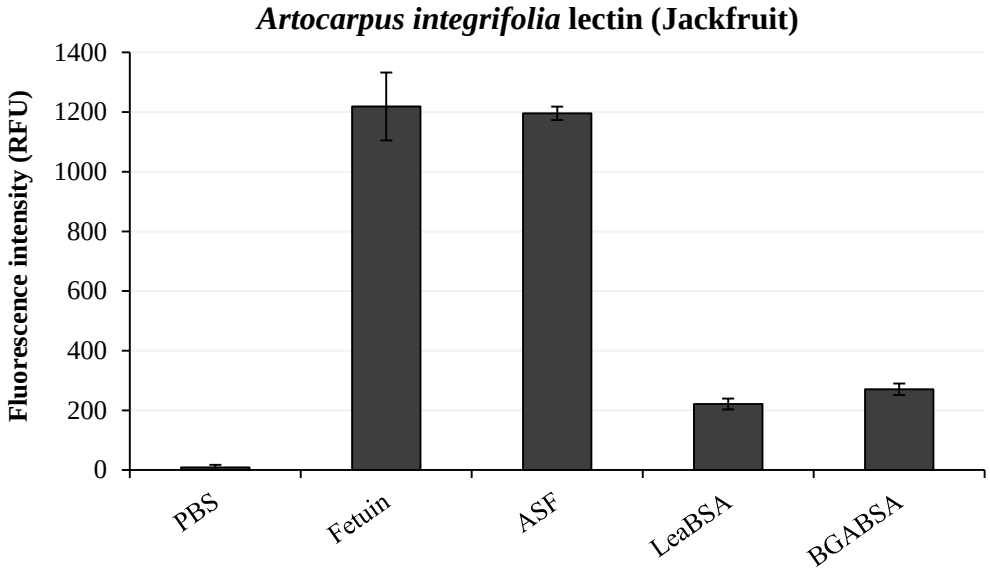

Fig 5.25 Glycan binding profile of *Artocarpus integrifolia* control lectin. Mean plus standard deviation normalised fluorescence intensity was derived from 2 experimental replicates. PBS negative control, Lewis A and blood group A NGCs were included for comparison with fetuin and asialofetuin receptors.

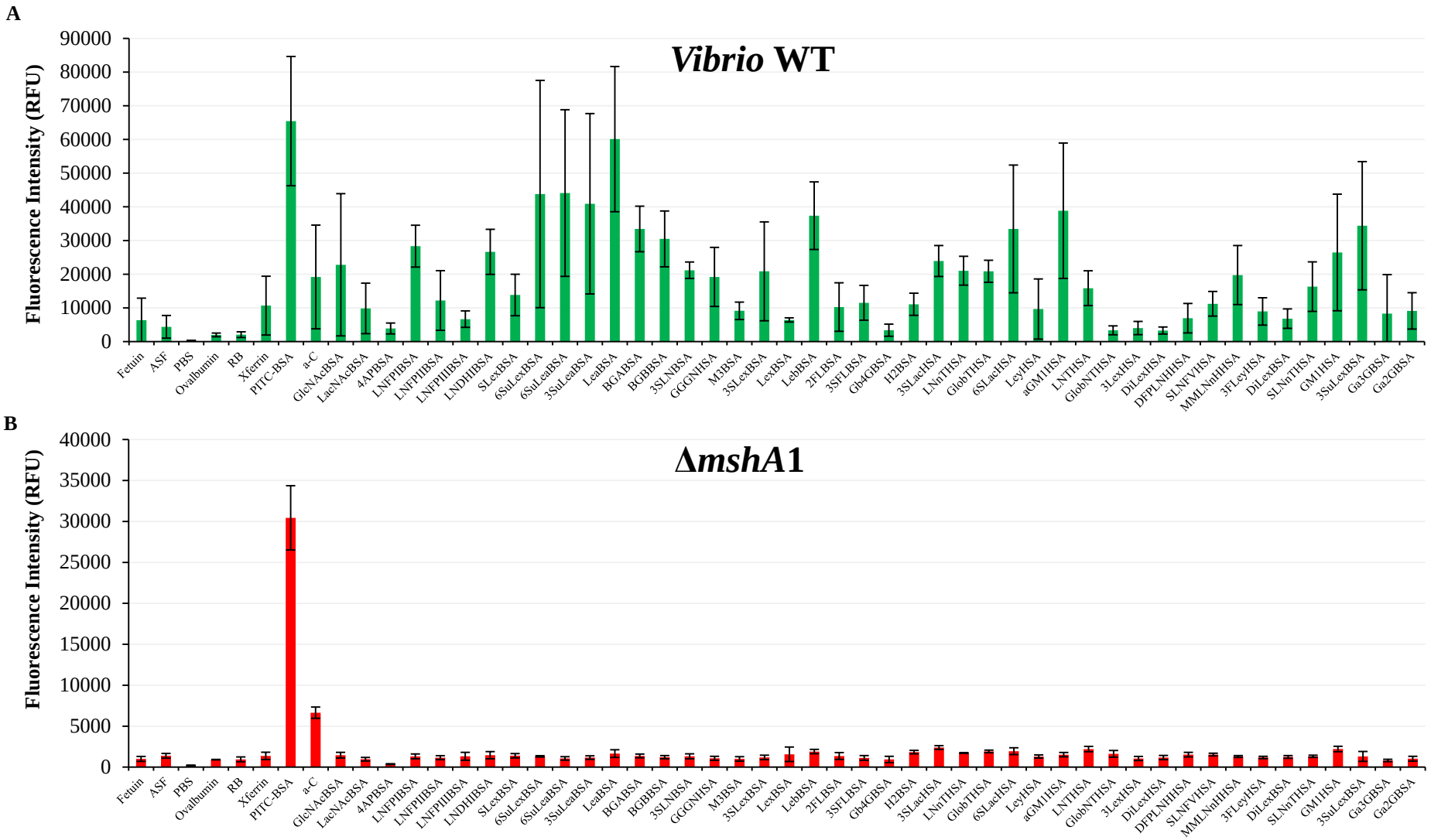

Fig 5.26 Glycan binding profiles of *Vibrio* WT, Δ*mshA*1, Δ*pilA*/Δ*mshA*1/Δ*mshA*2 and *E. coli* HB101.

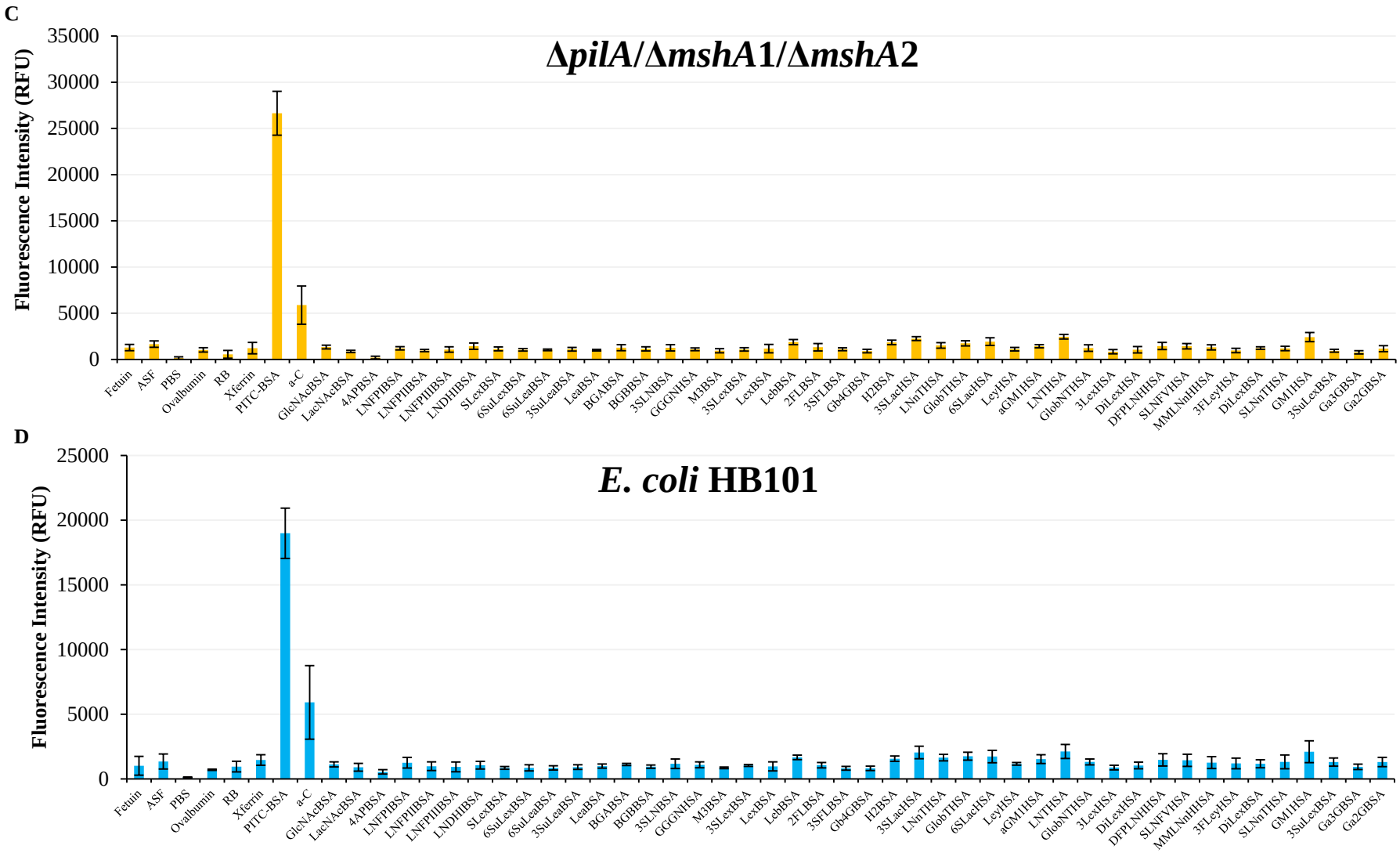

Fig 5.26 continued. Glycan binding profiles of *Vibrio* WT, Δ*mshA*1, Δ*pilA*/Δ*mshA*1/Δ*mshA*2 and *E. coli* HB101.

Table 5.2 Description of glycoproteins and NGCs contained within Fig 5.25 and Fig 5.26

ID number	X axis label	Name	Glycan Epitope
1	Fetuin	Fetuin	
2	ASF	Asialofetuin	
3	PBS	PBS	
4	Ov	Ovalbumin	
5	RB	RNAse B	
6	Xferrin	Transferrin	
7	PITCBSA	PITC-BSA	
8	a-C	α-Crystallin from bovine lens	
9	GlcNAcBSA	N-acetylglucosamine-BSA	
10	LacNAcBSA	N-acetyllactosamine-BSA	Galβ1-4GlcNAc
11	4APBSA	4AP-BSA	
12	LNFPIBSA	Lacto-N-fucopentaose I-BSA	Fucα1-2Galβ1-3GlcNAcβ1-3Galβ1-4Glc
13	LNFPIIBSA	Lacto-N-fucopentaose II-BSA	Galβ1-3(Fucα1-4)GlcNAcβ1-3Galβ1-4Glc
14	LNFPIIIBSA	Lacto-N-fucopentaose III-BSA	Galβ1-4(Fucα1-3)GlcNAcβ1-3Galβ1-4Glc
15	LNDHIBSA	Lacto-N-difucohexaose I-BSA	Fucα1-2Galβ1-3(Fucα1-4)GlcNAcβ1-3Galβ1-4Glc
16	SLexBSA	3'Sialyl Lewis X-BSA	Neu5Acα2-3Galβ1-4(Fucα1-3)GlcNAc
17	6SuLexBSA	6-Sulfo Lewis X-BSA	SO_3-6Galβ1-4(Fucα1-3)GlcNAc
18	6SuLeaBSA	6-Sulfo Lewis A-BSA	SO_3-6Galβ1-3(Fucα1-4)GlcNAc
19	3SuLeaBSA	3-Sulfo Lewis A-BSA	SO_3-3Galβ1-3(Fucα1-4)GlcNAc
20	LeaBSA	Lewis A-BSA	Galβ1-3(Fucα1-4)GlcNAc
21	BGABSA	Blood Group A-BSA	GalNAcα1-3(Fucα1-2)Gal
22	BGBBSA	Blood Group B-BSA	Galβ1-3(Fucα1-2)Gal
23	3SLNBSA	3'SialylLacNAc-BSA	Neu5Acα2-3Galβ1-4GlcNAc
24	GGGNBSA	Linear B-2 Trisaccharide-HSA	Galα1-3Galβ1-4GlcNAc
25	M3BSA	α1-3, α1-6 Mannobiose-BSA	Manα1-6(Manα1-3)Man
26	3SLexBSA	3'Sialyl Lewis X-BSA	Neu5Acα2-3Galβ1-4(Fucα1-3)GlcNAc
27	LexBSA	Lewis X-BSA	Galβ1-4(Fucα1-3)GlcNAc
28	LebBSA	LNDI-BSA/ Lewis B-BSA	Fucα1-2Galβ1-3(Fucα1-4)GlcNAc
29	2FLBSA	2'Fucosyllactose-BSA	Fucα1-2Galβ1-4Glc
30	3SFLBSA	3'Sialyl-3-fucosyllactose-BSA	Neu5Acα2-3Galβ1-4(Fucα1-3)Glc
31	Gb4GBSA	β1-4galactosyl-galactose-BSA	Galβ1-4Gal
32	H2BSA	Blood Group H Type II-APE-BSA	Fucα1-2Galβ1-3GlcNAc
33	3SLacHSA	3'Sialyllactose-APD-HSA	Neu5Acα2-3Galβ1-4Glc
34	LNnTHSA	Lacto-N-neotetraose-APD-HSA	Galβ1-4GlcNAcβ1-3Galβ1-4Glc
35	GlobTHSA	Globotriose-APE-HSA	Galα1-4Galβ1-4Glc
36	6SLacHSA	6'Sialyllactose-APD-HSA	Neu5Acα2-6Galβ1-4Glc
37	LeyHSA	Lewis Y-tetrasaccharide-APE-HSA	Fucα1-2Galβ1-4(Fucα1-3)GlcNAc
38	aGM1HSA	Asialo-GM1-pentasaccharide-APD-HSA	Galβ1-3GalNAcβ1-4Galβ1-4Glcβ-Cer
39	LNTHSA	Lacto-N-tetraose-APD-HSA	Galβ1-3GlcNAcβ1-3Galβ1-4Glc
40	GlobNTHSA	Globo-N-tetraose-APD-HSA	GalNAcβ1-3Galα1-4Galβ1-4Glc
41	3LexHSA	Tri-Lewis X-APE-HSA	Galβ1-4(Fucα1-3)GlcNAcβ1-3Galβ1-4(Fucα1-3)GlcNAcβ1-3Galβ1-4(Fucα1-3)GlcNAc
42	DFPLNHHSA	Difucosyl-para-lacto-N-hexaose-APD-HSA	Galβ1-3(Fucα1-4)GlcNAcβ1-3Galβ1-4(Fucα1-3)GlcNAcβ1-3Galβ1-4Glc
43	DiLexHSA	Di-Lewis X-APE-HSA	Galβ1-4(Fucα1-3)GlcNAcβ1-3Galβ1-4(Fucα1-3)GlcNAc
44	SLNFVHSA	Sialyl-LNF V-APD-HSA	Fucα1-2Galβ1-3(Neu5Acα2-6)GlcNAcβ1-3Galβ1-4Glc
45	MMLNnHHSA	Monofucosyl, monosialyllacto-N-neohexaose-APD-HSA	Galβ1-4(Fucα1-3)GlcNAcβ1-6(Neu5Acα2-6Galβ1-4GlcNAcβ1-3)Galβ1-4Glc
46	3FLeyHSA	Tri-fucosyl-Lewis Y-heptasaccharide-APE-HSA	Fucα1-2Galβ1-4(Fucα1-3)GlcNAcβ1-3Galβ1-4(Fucα1-3)GlcNAc
47	DiLexBSA	Di-Lewis X-APE-BSA	Galβ1-4(Fucα1-3)GlcNAcβ1-3Galβ1-4(Fucα1-3)GlcNAc
48	SLNnTHSA	Sialyl-LNnT-penta-APD-HSA	Neu5Acα2-3Galβ1-4GlcNAcβ1-3Galβ1-4Glc
49	GM1HSA	GM1-pentasaccharide-APD-HSA	Galβ1-3GalNAcβ1-4(Neu5Acα2-6)Galβ1-4Glcβ-Cer
50	3SuLexBSA	3-Sulfo Lewis X-BSA	SO_3-3Galβ1-4(Fucα1-3)GlcNAc
51	Ga3GBSA	Galα1-3-galactobiose-BSA	Galα1-3Gal
52	Ga2GBSA	Galα1-2Gal-BSA	Galα1-2Gal

Fig 5.26 and Table 5.2 Glycan binding profiles of *Vibrio* WT, Δ*mshA*1, Δ*pilA*/Δ*mshA*1/Δ*mshA*2, *E. coli* HB101. Glycan binding profiles were obtained from glycan array analysis of *Vibrio* WT (**A**), Δ*mshA*1 (**B**), Δ*pilA*/Δ*mshA*1/Δ*mshA*2 (**C**) and *E. coli* HB101 (**D**). 3 biological replicates of each strain were analysed on separate subarrays. Data represented are the mean plus standard deviation normalised median fluorescence intensity values from the three biological replicates tested. Table 5.2 contains a description of the X axis labels contained in Fig 5.25 and Fig 5.26 A, B, C, and D. Glycan epitopes for the artificially synthesised NGCs are also listed.

As observed by the Y axis scales in Fig 5.26 A, B, C and D, the *Vibrio* WT exhibited markedly higher fluorescence on many of the glycan epitopes contained within the array. Dye uptake of each strain was assessed in parallel with microarray hybridisation in order to confirm that each strain had similar fluorescence properties. No significant differences were observed between the wild type and the MSHA deletion mutants analysed (Data not shown). Therefore, any differences in fluorescence intensity on the array must be due to differential binding to the glycans contained therein.

Each strain bound to the PITC-BSA probe with the highest affinity. The PITC-BSA probe consisted of phenylisothiocyanate (the linker molecule used in the production of many of the NGCs contained within the array) bound to BSA. This probe consists of the bare linker molecule attached to the protein anchor and therefore should serve as a negative control. This however is not the case as the production of NGCs alters the chemistry of the linker molecule, changing its presentation on the surface of the probe. Kilcoyne *et al.* (2012) observed this effect with the binding of three out of four lectins tested to PITC-BSA and therefore concluded that the use of a bare linker-protein probe does not allow for estimation of the role played by the linker molecule in lectin-NGC interactions.

α-crystallin, a chaperone glycoprotein produced in the lens tissue of the eye was also found to exhibit high levels of binding to all strains tested. α-crystallin is thought to play a role in retaining the clarity of ocular lens tissue by binding other crystallin proteins in high molecular weight complexes, thereby preventing the formation of light scattering aggregates (Derham and Harding, 2002). As such, this glycoprotein may have significant and diverse binding capabilities, explaining the binding of both *E. coli* HB101 and *V. parahaemolyticus* at higher rates than many of the other glycoproteins and glycans in the array platform used.

Upon analysis of the piliation, adherence efficiency, invasion efficiency, cytotoxicity, cell rounding and IL-8 induction exhibited by Δ*pilA*/Δ*mshA*1/Δ*mshA*2, compared with the Δ*mshA*1 single mutant, little difference was observed. As such, it was hypothesised that *pilA* and *mshA*2 were either not expressed under the growth conditions used or were not playing functional roles in the phenotypes analysed on Caco-2. As seen in Fig 5.26B and C the binding pattern for Δ*pilA*/Δ*mshA*1/Δ*mshA*2 was quite similar to the single mutant Δ*mshA*1, with peaks only being observed for the PITC-BSA and α-crystallin probes. As such, it appears that *mshA*1 and hence the MSHA pilus is the key glycan binding determinant possessed by *V. parahaemolyticus*.

As deletion of *mshA*1 affects the binding of *V. parahaemolyticus* to a wide variety of glycans, it is possible that the MSHA pilus is involved in non-specific adherence. This could be brought about due to piliation altering the charge and hydrophobicity of the bacterial cell surface, leading to enhanced adherence. Another explanation for the apparent broad specificity of the MSHA pilus is that the minor pilin components MshC, MshD and MshO may all possess independent and distinct glycan binding specificity. In order to effectively analyse the role of the MSHA pilus with respect to binding to specific glycans, the fluorescence intensity of the *Vibrio* WT on each individual glycan was expressed as a ratio of the Δ*mshA*1 mutant fluorescence. Fig 5.27 shows the relative binding of the wild type against Δ*mshA*1 for each glycan together with the representative structures of the 8 glycans to which the Δ*mshA*1 mutant exhibited the greatest decrease in binding compared with the *Vibrio* WT.

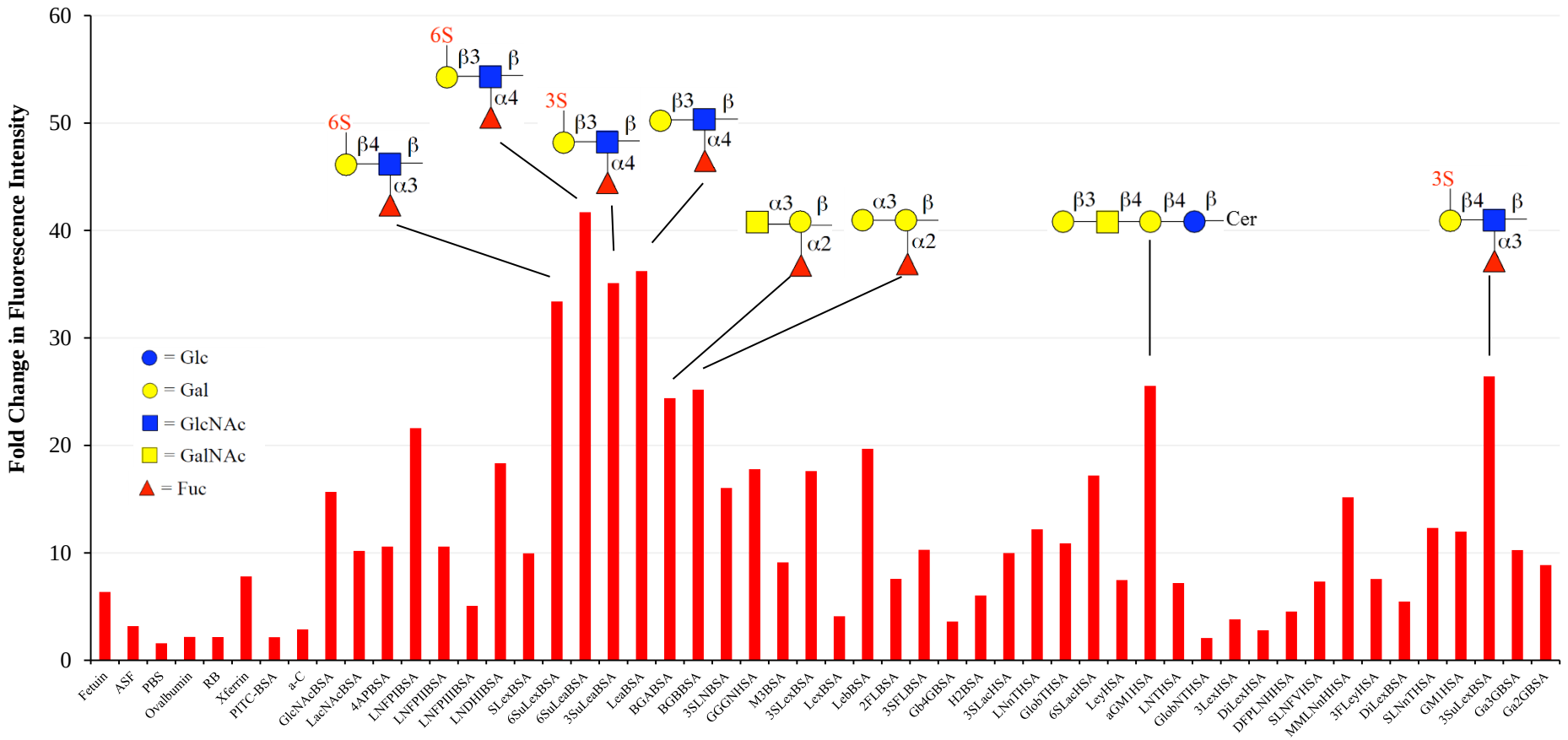

Fig 5.27 Relative fluorescence of *Vibrio* WT against Δ*mshA*1for 52 glycan epitopes. Normalised fluorescence intensity of *Vibrio* WT (Fig 5.26A) was expressed relative to the value obtained for Δ*mshA*1(Fig 5.26B) for each of the glycan epitopes being analysed. Structures of the 8 epitopes with the highest relative levels of binding are shown. Key inset indicates symbol nomenclature.

While the *Vibrio* WT exhibited greater fluorescence than the Δ*mshA*1 mutant across all 52 epitopes tested as observed by a relative fluorescence >1, setting a cut-off relative fluorescence increase of ~10 allows for more detailed assessment of glycan specificity of the MSHA pilus. Indeed the probes intended for use as controls (PBS [Probe 3] and PITC-BSA [Probe 7]) had less than two-fold increased fluorescence, comparing the wild type to the Δ*mshA*1 mutant. As the nexterion slides used in these experiments are protein reactive, differentially higher binding of the wild type to the PBS control could be explained by binding of the proteinaceous pili to the functionalised ester groups exposed on the slide surface, although blocking of slides with BSA should have minimised this effect.

The eight epitopes which exhibited the highest relative fluorescence for the wild type compared with Δ*mshA*1 and hence the highest specificity towards the MSHA pilus were 6-sulfo Lewis A (42 fold), Lewis A (36 fold), 3-sulfo Lewis A (35 fold), 6-sulfo Lewis X (34 fold), 3-sulfo Lewis X (26 fold), asialo GM1 (26 fold), blood group B (25 fold) and blood group A (24 fold).

Lewis antigens are secreted by exocrine cells and are subsequently acquired by the cells of peripheral circulation including red blood cells (Henry *et al.*, 1995). The high levels of binding to the Lewis antigens and to the blood group antigens could explain the haemagglutinating ability of piliated *V. parahaemolyticus*. This may explain the database annotation of the MSHA locus as a haemagglutinin locus. As Lewis antigens are also expressed in gastro-intestinal epithelial cells (Mollicone *et al.*, 1985), the binding of the MSHA pilus may facilitate a specific attachment in these tissues.

The gangliosidic receptor GM1 is expressed in intestinal tissues and has been implicated in the adherence of the pathogens *Shigella dysenteriae*, *H. pylori*, and *Pseudomonas aeruginosa* and the commensal bacterium *Lactobacillus reuteri* (Sai Sudha *et al.*, 2001; Saitoh *et al.*,

1991; Sheth *et al.*, 1994; Mukai *et al.*, 2002). It is therefore likely that *V. parahaemolyticus* also targets gangliosidic receptors in its attachment to the intestinal epithelium.

Common features appear in the 8 epitopes which exhibit the greatest specificity with respect to MSHA binding. 7 of the 8 epitopes contain a terminal galactose residue which is either β1-3 or β1-4 linked to the subterminal mono-saccharide. 7 of the 8 also possess a sub-terminal α fucosylted mono-saccharide. Both of these features may be critical for binding of the MSHA pilus and the similarities between the 8 epitopes bearing MSHA specificity may explain the apparent broad range of glycan binding facilitated by this pilus.

5.9 Summary and Discussion.

The TFP possessed by *V. parahaemolyticus* are of particular interest when analysing the inflammatory, diarrheagenic, pathogenic effects of the organism upon intestinal cells. While the genetic organisation of the TFP genes appears to be similar upon comparison of the related pathogens *V. parahaemolyticus* and *V. cholerae* (Fig 5.3), the major pilin genes differ both in number and sequence conservation (Fig 5.4 and Fig 5.5). Phylogenetic analysis of 50 major pilin coding sequences resulted in the clustering of MSHA type pilins in a distinct clade from that of the PilA type pilins (Fig 5.4). While the pilin genes of *V. alginolyticus* and *V. harveyi* were found clustered with the *V. parahaemolyticus* pilin genes, in general a high level of variability was observed in the 50 pilin genes used for phylogenetic comparison. Similarity between *V. parahaemolyticus*, *V. harveyi* and *V. alginolyticus* pilin genes may be attributed to the close evolutionary relatedness of the species as observed by phylogenetic analysis of 16S rRNA coding sequences (Kita-Tsukamoto *et al.*, 1993). Aagesen and Häse, (2012) observed wide ranging sequence heterogeneity at the intra-species level for *V. parahaemolyticus*, *V. vulnificus* and environmental strains of *V. cholerae*. As this heterogeneity was not observed in TCP-carrying clinical isolates of *V. cholerae*, Aagesen

and Häse, (2012) hypothesised that *Vibrio* species with broad host ranges are exposed to a selective environmental pressure which results in the retention of non-synonymous substitutions and diversity of pilin composition.

Analysis of structural domain organisation further indicated that the MSHA pilins may form a distinct family of pilins, with differential structural organisation being observed in the variable head regions of the pilins (Fig 5.5). Marsh and Taylor (1999) also observed that the genetic organisation of the MSHA gene cluster more closely resembles that of the type IVb pili than the characterised type IVa pili, with many of the pilus biogenesis genes being located upstream of the pilin cluster. The alternative organisation of the MSHA gene cluster, the diversity of pilin gene composition, the lack of conservation in the receptor binding D domain of individual pilin proteins and the differential secondary structure exhibited by the *V. parahaemolyticus* pilins compared with the other type IV pilins analysed points towards diverse functionality. This is particularly interesting as although the MSHA pilus of *V. cholerae* is not involved in host colonisation or pathogenicity (Thelin and Taylor, 1996; Tacket *et al.*, 1998), the diversity of pilin composition indicated that this may not be the case with *V. parahaemolyticus* MSHA pili.

The analysis of *V. parahaemolyticus* mutants lacking critical TFP genes provided an effective means of assessing TFP functionality with respect to adherence and subsequent pathogenesis using the intestinal epithelial cell line Caco-2. *V. parahaemolyticus* RIMD2210633 deletion mutants lacking *pilA* and *mshA*1 were produced by Shime-Hattori *et al.* (2006). Functionality in attachment to host cells was not assessed, however independent roles for each type IVa pilus were observed, with the MSHA pilus being involved in the initial attachment of *V. parahaemolyticus* to abiotic surfaces and PilA being involved in the formation of bacterial aggregates. Shime-Hattori *et al.* (2006) also observed that *pilA* transcription was regulated by chitin, a GlcNAc polymer which is present in shellfish. While this may indicate a role in

colonisation of the commensal host, GlcNAc containing oligo-saccharides are also found in the gastric epithelium (Bjork *et al.*, 1987) and as such the PilA pilus may also play a role in attachment to epithelial tissues.

During this study it was found that mutants lacking the *mshA*1 major pilin gene were non-piliated, while deletion of other putative major pilin genes *pilA*, *mshA*2 and *mshA*3 did not affect piliation. This indicated that PilA was not expressed under the conditions used, consistent with the findings of Shime-Hattori *et al.* (2006) who observed that chitin was required to induce *pilA* transcription. The formation of a functional MSHA pilus in deletion mutants lacking MshA2 and MshA3 indicates that these proteins were similarly not expressed under the growth conditions used or that the genes deleted code for minor pilin proteins which are not required for the formation of a functional MSHA pilus. The latter hypothesis is particularly likely in the case of MshA3, where the gene is encoded in a region containing five pilin genes. Characterisation of the MSHA locus in *V. cholerae* identified a single major pilin subunit and 4 minor pilins (Marsh and Taylor, 1999). If the *V. parahaemolyticus* pilin locus were to possess the same organisation, with one major and 4 minor pilin genes, that would indicate that *mshA*3 codes for a minor pilin, contrary to its database annotation as a major pilin gene. Further confirmation of this potential minor pilin role was provided by analysis of adherence (Fig 5.11) where deletion of *mshA*3 had no effect on adherence efficiency, while deletion of *mshA*1 led to a 60% decrease in adherence efficiency. While minor pilins are not required for formation of the pilus fiber, their roles in pilus functionality should not be ignored. Deletion of a predicted functional domain of the *N. meningitidis* minor pilin PilX resulted in de-stabilisation of bacterial aggregates, a phenotype which is associated with *Neisseria* TFP function (Helaine *et al.*, 2007). While this work has shown that MshA3 is not required for adherence to Caco-2, the Δ*mshA*3 mutant could be used to analyse binding to

different cell types or to glycan epitopes in order to establish the function of MshA3 in *V. parahaemolyticus*.

This work has shown that the MSHA pilus is critical for efficient attachment of *V. parahaemolyticus* to Caco-2. Deletion mutants lacking either the ATPase (MshE), the outer membrane secretin (MshL) or the major pilin subunit (MshA1) exhibited a 60% decrease in adherence compared with the *Vibrio* WT (Fig 5.11). A study involving transposon mutagenesis of *V. cholerae* also described the requirement for expression of genes corresponding to MshE and MshL in the biogenesis of the MSHA pilus (Häse *et al.*, 1994), however the *V. cholerae* pilus is not involved in adherence to host cells (Attridge *et al.*, 1996; Thelin and Taylor, 1996; Tacket *et al.*, 1998). Deletion of either the biogenesis genes *mshE* and *mshL* or the major pilin gene *mshA*1 results in complete lack of piliation, therefore MSHA function can be assessed using any of the three deletion mutants described here. In spite of difficulties encountered with reduced growth rates of many complementation strains, the specificity of the phenotypes observed in these MSHA deletion mutants could be confirmed by restoration of the wild type adherence level in the Δ*mshE* (pLM-*mshE*) complementation strain.

Similar roles for TFP in adherence to gastro-intestinal cells have been observed in other pathogenic bacteria. Deletion of the major type IVa pilin HcpA in enterohaemorrhagic *E. coli* O157:H7 resulted in an 80% decrease in adherence to Caco-2. (Xicohtencatl-Cortes *et al.*, 2007). An inactivating Ser^{129} for Cys substitution in the enteropathogenic *E. coli* bundle forming pilin BfpA resulted in a 93% decrease in adherence to Caco-2 (Cleary *et al.*, 2004). Two afimbrial *V. parahaemolyticus* RIMD2210633 adhesins have recently been characterised by comparison of wild type adherence with that of deletion mutants. The MAM7 adhesin which is possessed by a variety of gram negative pathogens was first identified in *V. parahaemolyticus* by Krachler *et al.* (2011). In that study, deletion of MAM7, encoded by

VP1611, resulted in a 50% decrease in adherence. Type VI secretion system 1 of *V. parahaemolyticus* has also been described as having a role in adherence with deletion of IcmF, the major secretion tube protein or Hcp1, a type VI secretion system translocator, led to a 50% decrease in adherence to Caco-2 (Yu *et al.*, 2012). The mechanism by which this secretion system regulates adherence to intestinal cells has not been established, however it is tempting to speculate that a similar system to the enteropathogenic *E. coli* (EPEC) Tir-intimin regulated adherence may be at play. The Tir effector protein is secreted into host cells by EPEC, where it is then translocated to the apical membrane to act as a receptor for the bacterial adhesin intimin (Kenny *et al.*, 1997). Taking into account the significant decreases observed in adherence efficiency of *V. parahaemolyticus* to Caco-2 with deletion of MAM7, IcmF and MshA1, it is evident that efficient adherence involves multiple mechanisms and disruption of any one adhesin can have a large impact on overall adhesion efficiency.

It seems that the MSHA pilus would require expression of a pre-pilin peptidase from a distinct genetic locus, as no peptidases are contained in the MSHA locus. Analysis of MSHA pilus production following deletion of *pilD* would yield interesting insight into co-expression from multiple regions during MSHA production. Similarly, expression of the PilA pilus would likely require co-expression from a distinct locus, as only four proteins are coded within the *pilA* locus. BLAST analysis identified a region distinct from the PilA pilin locus, encoding homologues to the *N. meningitidis pilMNOPQ* region. Analysis *of V. parahaemolyticus* deletion mutants lacking biogenesis components from this region, under inducing conditions for *pilA* expression, could be used to characterise PilA pilus biogenesis. Although no effects on adherence to Caco-2 were seen with deletion of *pilA* or *mshA*2 under the conditions used in this study, induction and confirmation of pilus expression prior to adherence assessment would be required in order to categorically exclude functionality in adherence to Caco-2. Use of the double and triple deletion mutants constructed during this

work would prove particularly useful in such analysis in terms of identifying the combined roles played by each major pilin in *V. parahaemolyticus* adherence.

While deletion of *pilA* or *mshA*2 had no effect on adherence of *V. parahaemolyticus*, the Δ*pilA*/Δ*mshA*2 mutant had significantly lower adherence than the *Vibrio* WT, as determined by enumeration of the cfu of cell-associated bacteria (Fig 5.11). Microscopic analysis of giemsa stained bacteria indicated that this strain exhibited an altered pattern of adherence, with large aggregates of bacteria being observed in contact with Caco-2 (Fig 5.13). This phenotype was not observed with any other *V. parahaemolyticus* strains used in this study. It is unclear why this strain exhibited an altered adherence pattern and it is particularly unusual considering that PilA is thought to play a role in aggregate stabilisation (Shime-Hattori *et al.*, 2006).

The TFP of *V. parahaemolyticus* were chosen for analysis for potential roles in adherence and invasion based upon a combination of bioinformatic analysis to detect adhesins homologous to those possessed by *V. cholerae*, published data which showed functionality in biofilm formation (Shime-Hattori *et al.*, 2006) and a correlation between pilus production and adherence to rabbit enterocytes (Nakasone *et al.*, 1990). One of the other aims of this project was to identify novel adhesins and invasins using a genomic library screening method. The selection of invasive clones from a random *V. parahaemolyticus* genomic library, heterologously expressed in *E. coli* HB101 led to the isolation of a single clone with significantly increased invasion compared with that observed for the control *E. coli* HB101 strain. Sequencing and bioinformatic analysis led to the prediction of OmpA as being the most likely invasin encoded within the insert DNA of the invasive clone A16. *VPA0248*, the gene coding for OmpA was deleted in *V. parahaemolyticus* and a complementation strain, which carried *ompA* and its native promoter on a shuttle vector was also constructed. As shown in Fig 5.11 and Fig 5.15 deletion of *ompA* in *V. parahaemolyticus* had no effect on

adherence or invasion. It is therefore apparent that OmpA does not function as an invasin in *V. parahaemolyticus*. This indicates that another putative invasin exists within the insert of clone A16 or that indirect effects of heterologous expression have led to the selection of this clone as a false positive for invasion. A number of putative reading frames were identified within the insert DNA of clone A16 (Figure 4.9, Table 4.1) which were annotated as hypothetical proteins. As little information could be obtained by bioinformatic analysis of these regions due to the absence of conserved domains with characterised functionality, it is possible that one of these regions codes for a protein which is involved in the invasion of Caco-2 cells. A second *ompA* homologue was also identified within the insert DNA of clone A16 and although this gene was found to lack the conserved 3' *ompA* sequence, which codes for the periplasmic OmpA domain, invasin functionality is still a possibility.

Low inoculum counts were observed for many of the clones being analysed, in spite of standardising the OD_{600} of cell suspensions of each clone. This would indicate altered cell morphology, cell size, formation of aggregates or alterations in cell surface properties with respect to light absorbance. As invasion efficiencies for each clone were calculated as a percentage of the inoculum, the decreased counts observed for clone A16 caused an increased estimation of invasion efficiency. This could explain the possible representation of clone A16 as a false positive for invasion. In order to reduce any indirect effects resulting from carriage of large heterologous fragments of *V. parahaemolyticus* DNA and to focus analysis of putative invasins on smaller genetic loci, the creation of sub-clones could be employed. This could be carried out by restriction digest of the insert DNA from clone A16 and subsequent ligation of smaller fragments of DNA into shuttle vectors for independent analysis of smaller loci. Due to time constraints and the possibility of indirect phenotypic alterations being responsible for the traits observed in clone A16, this was not carried out in this study and focus was directed towards developing a more complete understanding of the TFP of *V.*

parahaemolyticus and their role in pathogenesis. OmpA proteins also have functions in binding of phage, survival within macrophages, complement resistance and biofilm formation (Morona *et al.*, 1984; Sukumaran *et al.*, 2003; Prasadarao *et al.*, 2002; Barrios *et al.*, 2006). The *V. parahaemolyticus* Δ*ompA* mutant will be tested for functionality in each of these processes with a view to understanding the role of OmpA in *V. parahaemolyticus*.

An interesting facet of bacterial pathogenicity is the ability of certain pathogens to establish infection in the intracellular environment. A number of bacteria invade into host cells in order to evade the immune system or to disseminate throughout infected tissues by undergoing cell to cell spread. Adhesins of pathogenic bacteria can often function as invasins (Oelschlaeger, 2001). As such the MSHA pilus was investigated for a potential role in facilitating an increased rate of cellular uptake in Caco-2. The results of enumeration of invasion efficiency of the *Vibrio* WT compared to mutants lacking a functional MSHA pilus closely correlated with adherence data. A 65% decrease in cellular uptake was observed in Δ*mshE*, Δ*mshL* and Δ*mshA*1 indicating that the MSHA pilus plays a key role in this process. The close correlation between the 60% decrease in adherence and the 65% decrease in cellular uptake observed with MSHA mutants indicates that adherence is likely the principal factor in determining whether or not *V. parahaemolyticus* is translocated into the host cell. This has implications for whether or not *V. parahaemolyticus* should be considered a truly invasive pathogen, a point which was discussed in chapter 3, where it was observed that only 0.02% of cell-associated *V. parahaemolyticus* became internalised, compared with 0.25% for *E. coli* and 10.8% for *S.* Dublin. The intracellular localisation of *V. parahaemolyticus* may be of biological importance as even small amounts of intracellular bacteria could replicate and emerge from infected tissues allowing for a more persistent infection.

While the assessment of adherence to Caco-2 provides interesting insights into the pathogenicity of the organism, detailed conclusions of the importance of adhesins for

virulence can only be drawn by directly analysing how downstream pathogenic responses in the host cell are affected by deletion of the adhesins in question. The principal virulence-associated responses induced in Caco-2 by infection with *V. parahaemolyticus* are cell rounding, monolayer destruction, secretion of inflammatory cytokines such as IL-8 and eventual cell lysis. Each of these effects of *V. parahaemolyticus* infection was analysed individually to ascertain the importance of TFP in the pathogenticity of *V. parahaemolyticus*.

Cytotoxicity was assessed by LDH assay on supernatants from Caco-2 cells following 4 h of infection with *V. parahaemolyticus*. *V. parahaemolyticus* has been shown to induce lysis of >90% of Caco-2 and RAW 264.7 macrophage cell lines within 4 h (Matlawska-Wasowska *et al.*, 2010; Burdette *et al.*, 2008). Burdette *et al.* (2008) carried out extensive characterisation of the cytotoxic effects of *V. parahaemolyticus*, illustrating a key role for TTSS1 in the induction of autophagy, followed by cell rounding and eventual cell lysis. Further to these findings, Burdette *et al.* (2009) observed that deletion of the TTSS1 effector protein VopQ resulted in a significant reduction in host cell lysis and a marked reduction in the conversion of microtubule-associated protein light chain 3I (LC3I) to LC3II, a marker of autophagy. Chemical inhibition of PI3-kinase did not affect VopQ-associated LC3 activation or association with autophagosomal membranes, and as such VopQ was described as a PI3-kinase-independent inducer of autophagy. The recruitment of autophagy and subsequent degredation of cellular components was hypothesised by Burdette *et al.* (2009) to provide a means of sequestering nutrients and preventing the phagocytosis of extracellular bacteria.

Deletion of MSHA components resulted in a 15 to 20% decrease in lysis of Caco-2 cells following 4 h of infection. Although small, a decrease compared to the wild type was observed in all experiments carried out and as such the difference was found to be statistically significant by paired student's *t* test. Upon deletion of the MAM7 adhesin, Krachler *et al.*, (2011) observed a slight decrease of approximately 10% in *V.*

parahaemolyticus-associated cytotoxicity of Caco-2 after 4h of infection, however this decrease was not found to be statistically significant. A 30% reduction in cytotoxicity towards 3T3 fibroblasts was observed with deletion of MAM7 after a similar co-incubation period. As such, assessment of the role of the MSHA pilus in cytotoxicity of a variety of cell types would prove useful. The reduction in adherence-associated cytotoxicity observed with inactivation of the MSHA pilus and MAM7 indicates that adherence is required for efficient secretion of VopQ *via* TTSS1.

In parallel with the lytic effects of VopQ which are brought about by the recruitment of autophagy, TTSS1 induces modifications in the actin cytoskeleton of infected cells, leading to cell rounding and eventual removal from the monolayer. Another effector protein, VopS has been implicated in this process. VopS was described by Yarbrough *et al.* (2009) to cause a novel post-translational modification by the addition of adenosine mono-phosphate (AMP) to a conserved threonine residue of the Rho GTPase family of regulatory proteins. Rho, Rac and Cdc42 play critical roles in the regulation of the cell cycle, intracellular trafficking and cytoskeletal organisation by initiating signal transduction cascades when in their active GTP bound state (Casselli *et al.*, 2008). AMPylation of Rho, Rac and Cdc42 by VopS blocks GTP binding and prevents downstream signalling, resulting in severe disruption of the actin cytoskeleton and pronounced rounding of infected cells (Yarbrough *et al.*, 2009).

The results shown in Fig 5.17 indicate that disruption of adherence by deletion of *mshE*, *mshL* or *mshA*1, which are required for MSHA pilus production results in decreased rounding of Caco-2 cells after 2.5 h of infection. Strains producing an active MSHA pilus caused the rounding of a greater proportion of cells in the monolayer and as a result caused greater monolayer disruption (as seen by empty space where cells became dislodged). As VopQ and VopS are produced via the same secretion system, the importance of the MSHA pilus in the induction of actin cytoskeletal rearrangements further indicates that TTSS1 function may be

impaired by the reduction in adherence. While cytoskeletal disruption was not analysed with respect to MAM7 functionality by Krachler *et al.* (2011), a complementary toxicity assay was carried out in order to confirm the relevance of the reductions in lysis of various cell lines by deletion of MAM7. Upon feeding of *Caenorhabditis elegans* nematodes, Krachler *et al.* (2011) observed that mutants lacking MAM7 did not affect life expectancy or cause significant alterations in growth rate, or intestinal integrity. Wild type bacteria by contrast caused more rapid lethality, severe growth retardation and intestinal rupture. The findings of Krachler *et al.* (2011) demonstrate the *in vivo* confirmation of how disruption of bacterial adherence can diminish pathogenicity. The successful establishment of an animal model for *V. parahaemolyticus* infection also provides interesting possibilities for confirmation of the *in vitro* phenotypes observed for MSHA deficient strains in an *in vivo* context.

One of the prominent effects of *V. parahaemolyticus* infection is the induction of a systemic inflammatory immune response, with the presence of anti-LPS and anti-TDH antibodies, increased C-reactive protein, increased nitric oxide, TNF-α and lactoferrin being detected in the serum of infected individuals (Qadri *et al.*, 2003). *V. parahaemolyticus* is known to induce secretion of the pro-inflammatory chemokine IL-8 through a MAPK-dependent mechanism (Matlawska-Wasowska *et al.*, 2010; Shimohata *et al.*, 2011). As shown by the use of chemical inhibitors in Fig 5.20 and by Shimohata *et al.* (2011), NF-κB also plays a role in the regulation of IL-8 production by Caco-2 cells in response to *V. parahaemolyticus* infection. Successful optimisation of infections prior to quantitation of IL-8 production was achieved by altering the period of post-infection incubation (after killing extracellular bacteria). This led to maximal *V. parahaemolyticus*-associated IL-8 concentrations of 1,660 pg ml^{-1} (Fig 5.19) being detected, compared with 800 pg ml^{-1} detected by Matlawska-Wasowska *et al.* (2010) and 60 pg ml^{-1} detected by Shimohata *et al.* (2011). Establishment of the optimal infection conditions for IL-8 induction allows for greater sensitivity in the

assessment of factors which influence *V. parahaemolyticus*-associated IL-8 activation in Caco-2.

The effector protein VopQ has been described as playing a central role in modifying host cell signalling, resulting in secretion of IL-8 (Matlawska-Wasowska *et al.*, 2010; Shimohata *et al.*, 2011). As deletion of MSHA components led to a decrease in VopQ-associated cell lysis, indicating that secretion of VopQ may require efficient adherence to the host cell, it was expected that IL-8 induction may also be impaired in *mshE*, *mshL* and *mshA*1 deletion mutants. As shown in Fig 5.21, that was indeed the case with disruption of the MSHA pilus leading to approximately a 50% reduction in IL-8 20 h post infection. This further establishes the essential role of the MSHA pilus in TTSS-associated pathogenicity of Caco-2 cells.

The correlation between adherence and pathogen-associated inflammation has been observed by many groups. *L. monocytogenes* has been shown to induce IL-8 in a similar manner to that of *V. parahaemolyticus*, involving the activation of MAPK and NF-κB (Opitz *et al.*, 2005). Deletion of the internalin gene *inlB*, which has a critical role in adherence and invasion of *L. monocytogenes*, by binding to host cell E-cadherin, resulted in a 60% decrease in IL-8 secretion from endothelial cells (Opitz *et al.*, 2005). Prinz *et al.* (2001) observed that PCR detection of the *H. pylori babA*2 gene, which encodes a blood group binding adhesin, correlated directly with the severity and chronicity of inflammatory gastritis induced in infected individuals. A *peb1*A insertional mutant strain of *C. jejuni*, which displayed 50% reduced adherence compared with wild type *C. jejuni*, was found by Hickey *et al.* (1999) to induce 80% lower levels of IL-8 than the wild type following 24 h of infection of intestinal INT407 cells. A study involving the infection of INT407 with a variety of hyperadherent and non-adherent strains of toxigenic *V. cholerae* from the O395 serogroup, found a direct correlation between adherence, IL-8 transcription and secretion (Sarkar and Chaudhuri, 2004). As such Sarkar and Chaudhuri (2004) hypothesised that adherence provides a trigger

for IL-8 mRNA expression by *V. cholerae*. Interestingly, the non-pathogenic bacterium *Bifidobacterium bifidum* possesses an adhesin BopA, which functions in adherence to Caco-2 and also plays a role in IL-8 production. Treatment of Caco-2 cells with 20 μg ml^{-1} purified BopA overnight resulted in the secretion of 2,000 pg ml^{-1} IL-8 (Guglielmetti *et al.*, 2008). While it is unusual for a probiotic bacterium to possess pro-inflammatory features, the induction of IL-8 and recruitment of bactericidal leukocytes may enhance the probiotic capabilities of this organism by facilitating the removal of undesirable pathogenic species. These examples illustrate the importance of bacterial adherence with respect to initiation of IL-8 secretion from host cells.

In order to better understand the mechanism governing the adherence of *V. parahaemolyticus* and the role played by the MSHA pilus, a glycan binding profile was constructed by hybridisation to a NGC/glycoprotein array. High levels of binding to a variety of glycan motifs was observed in the *V. parahaemolyticus* wild type. Binding to all epitopes analysed was greatly inhibited by deletion of *mshA*1. It appears therefore that some redundancy exists in glycan binding of the MSHA pilus, likely due to pilus production having an effect on the charge or hydrophobicity of the cell surface. Magnusson *et al.* (1980) observed that the hydrophobicity of *E. coli*, *S.* Typhimurium and *N. gonorrhoeae* correlated with adherence to both polymorphonuclear leukocytes and HeLa cells. It was also observed that piliated *N. gonnorhoeae* were more negatively charged than non-piliated strains (Magnusson *et al.*, 1980). Pili have also been described as having a non-specific role in the adherence of *S.* Typhimurium to abiotic surfaces (Stenström and Kjelleberg, 1985). The potential non-specific binding activity of the MSHA pilus has also been observed by Shime-Hattori *et al.* (2006) who observed a role in adherence to glass coverslips and subsequent biofilm formation.

While a broad spectrum of glycan epitopes appear to function as receptors for the MSHA pilus, expression of wild type fluorescence relative to the Δ*mshA*1 mutant allowed for conclusions to be drawn regarding the most specific interactions between the MSHA pilus and the epitopes displayed on the glycan array. As shown in Fig 5.27 the wild type exhibited greater than twenty-fold higher binding to the Lewis A, Lewis X, blood group A, blood group B and asialo GM1 NGCs than that observed with the Δ*mshA*1 mutant. The high levels of binding to these epitopes, together with the conserved features associated therein, indicate that the MSHA pilus may specifically target these oligosaccharides in the process of attachment to the host cell. In particular, the terminal galactose residue and sub-terminal fucosylated mono-saccharide appear to be important mediators of MSHA specificity. As Lewis and blood group antigens are presented on the surface of erythrocytes, the specific mechanism of haemagglutination by *V. parahaemolyticus* may be explained by the specificity of the MSHA pilus towards erythrocyte glycans. As these antigens are also expressed on the surface of gastro-intestinal cells (Mollicone *et al.*, 1985), they also provide a strong indication for the receptor specificity of *V. parahaemolyticus* in the colonisation of the intestinal tract. We propose that the MSHA pilus can act as both a non-specific adhesin, by altering the surface properties of the bacterial cell, while still retaining a high degree of specificity towards AB blood group and Lewis type glycan epitopes which are expressed in intestinal cells.

The Lewis antigens have been implicated in the binding of many pathogenic bacteria and as such present a promising target for therapeutics which may specifically block pathogen binding and prevent the onset of disease. *H. pylori* has been shown to bind Lewis B antigens (Fucα1-2Galβ1-3(Fucα1-4)GlcNAc) with a high degree of specificity using the adhesin BabA (Ilver *et al.*, 1998). In a study of individuals infected with *H. pylori*, the PCR detection of *babA* from biopsies correlated directly with chronicity of gastric inflammation, indicating the

critical role of BabA in the pathogenicity of *H. pylori* (Prinz *et al*., 2001). Ilver *et al.* (1998) speculated that the use of a BabA vaccine may specifically inhibit gastric colonisation by virulent *H. pylori* and therefore prevent the establishment of persistent inflammatory infections.

Saadi *et al.* (1994) successfully purified an adhesin from *Staphylococcus aureus* by affinity absorption to synthetic Lewis A coated beads. Pre-treatment of buccal epithelial cells with the purified protein prevented the adherence of *S. aureus* (Saadi *et al.*, 1994). The binding of *S. aureus* to epithelial cells is thought to play a role in the toxigenic effects of the organism, which may play a role in sudden infant death syndrome due to the expression of Lewis A antigens in the naso-pharyngeal canal in early development (Blackwell *et al.*, 1999).

The binding of bacteria to fucosylated glycans, such as the Lewis and blood group antigens detected as being receptors for the MSHA pilus, has implications not only in colonisation and pathogenesis, but also in innate immunity. Human milk oligosaccharides which are passed from mother to infant during breast feeding can be found intact and in high concentrations in infant faeces, indicating that they are not destroyed during digestion (Chaturvedi *et al.*, 2001). Many of these milk glycans are α1-2 fucosylated and can bind to bacterial lectins with α1-2 fucose specificity, thereby saturating bacterial adhesins with “decoy” receptors and preventing colonisation of the infant host (Morrow *et al.*, 2005). This process is thought to work in parallel with the protective effects of milk immunoglobulins to prevent infant diarrhea resulting from colonisation by toxigenic bacteria.

The work described in this chapter has established a role for the Lewis and AB blood group specific MSHA pilus in the attachment, colonisation and pathogenicity of *V. parahaemolyticus*. A direct role for this pilus in adherence to intestinal cells has not been established at a molecular level in strain RIMD2210633. As such, functionality as a host cell

binding adhesin for the MSHA pilus is a novel observation. Identification of the receptor specificity of this adhesin has important implications for the development of effective targeted therapeutics. The novel application of glycan array profiling in the comparison of a wild type and isogenic adhesin deletion mutant allowed for unparalleled insight into the functionality and flexibility of the adhesin in question. The application of this approach will enable rapid characterisation of bacterial lectins and expand current knowledge of pathogen-host interactions. The reduction observed in downstream pathogenic responses of the host cell by disruption of MSHA-mediated adherence including cell rounding, cell lysis and induction of pro-inflammatory IL-8 highlight the importance of adherence in the establishment of a successful infection and illustrates the central role played by the MSHA pilus in this process.

Chapter 6

Discussion

6.1 Overview

This study set out to investigate the molecular mechanisms involved in the adherence and invasion of *V. parahaemolyticus* using the intestinal epithelial cell line, Caco-2. Contradictory reports have been published regarding invasiveness of *V. parahaemolyticus* and also the mechanisms governing this potential invasive phenotype. While TTSS have been described by many groups as key virulence factors of *V. parahaemolyticus* and are known to function in a cell contact-dependent manner, little research has been directed towards developing an understanding of the adhesins used by *V. parahaemolyticus* in the colonisation of host tissues and subsequent onset of disease. *V. parahaemolyticus* TTSS had not previously been assessed for involvement in adherence to Caco-2. It was observed during this study that *V. parahaemolyticus* adhered to Caco-2 with high efficiency and that this adherence was not mediated by TTSS.

A genomic library based approach was undertaken in an attempt to identify novel, uncharacterised proteins conferring adhesion/invasion of Caco-2 cells. A number of putative adhesins were also identified by a bioinformatic mining approach. Deletion mutants were constructed based upon genomic library screening and bioinformatic mining and were tested for abrogation of *V. parahaemolyticus* adherence/invasion. The MSHA pilus was found to be involved in adherence to Caco-2 and was found to have carbohydrate binding ability with specificity towards the Lewis type glycans. A key step in developing an understanding of bacterial pathogenesis at a molecular level lies in the identification of ligand-receptor interactions which occur between the pathogen and the host. These interactions govern the process of colonisation, and therefore not only have implications for the understanding of bacterial infection, but also present vast potential for the development of therapeutics. As shown by the role of the MSHA pilus in *V. parahaemolyticus* induction of cell rounding, cell

lysis, and inflammation, disruption of adherence can lead to reduced virulence of pathogenic bacteria.

6.2 Is *V. parahaemolyticus* an invasive pathogen?

One of the most complex, yet intriguing aspects of *V. parahaemolyticus* pathogenicity at a molecular level, is the manner in which the organism disrupts a vast number of host cell signalling networks. Much *V. parahaemolyticus* research has been focused on identifying the effector proteins responsible for manipulation of such networks and developing an understanding of the benefits which these alterations may have for the pathogen.

The findings of this study in combination with others indicate that *V. parahaemolyticus* may actively regulate cellular uptake by manipulating host cell signalling using its TTSS. GTPases are one target of such manipulation. The Rho GTPases are small proteins which are associated with the plasma membrane of polarised epithelial cells (Ridley, 2006). These molecules switch between an active GTP bound state and an inactive GDP bound state. They function by activating downstream regulators which are involved in actin polymerisation and depolymerisation, maintenance of cell polarity, regulation of cell shape, endocytosis, exocytosis, formation of fillipodia (finger like protrusions) and the formation of lamellipodia (sheet like membrane protrusions) (Etienne-Manville and Hall, 2002; Ridley, 2006). Direct manipulation of host cell Rho GTPases by *V. parahaemolyticus* has been described by a number of groups (Bhattacharjee *et al.*, 2008; Casselli *et al.*, 2008; Yarbrough *et al.*, 2009; Zhang *et al.*, 2012). As such, the manipulation of GTPase signalling and subsequent cytoskeletal rearrangement infers pronounced potential for regulating the process of cellular uptake.

TTSS of *Salmonella spp* and *Shigella spp* have been implicated in the induction of cellular invasion by the activation of the Rho family of GTPases. It was observed by Yoshida *et al.* (2002) that *Shigella* mutants lacking the effector protein VirA were incapable of Rac1 activation, formation of lamellipodia and subsequent invasion. The *Salmonella* effector protein SopE stimulates the activation of Cdc42 and Rac1, resulting in membrane ruffling (formation of lamellipodia) and cellular invasion (Hardt *et al.*, 1998). *Salmonella* has developed an intriguing strategy to reduce host cell disruption following invasion by rapidly switching off Cdc42 and Rac1 through the conversion of GTP bound Rac1 and Cdc42 to inactive GDP bound isoforms, using another TTSS effector SptP (Fu and Galan, 1999). While GTPase activation by *Salmonella spp* and *Shigella spp* can promote bacterial invasion of host cells, other bacterial species have adopted an opposing approach, favouring the inhibition of GTPases and prevention of cellular uptake. The *Yersinia* effector protein YopE inhibits Rho, Rac and Cdc42 resulting in reduced phagocytosis (Rosqvist *et al.*, 1990). These examples illustrate the key role which GTPase modification by TTSS plays in both promotion and inhibition cellular uptake.

6.2.1 TTSS as inhibitors of invasion.

While this study identified a highly adherent phenotype (20% of inoculum) for *V. parahaemolyticus* on Caco-2 cells (Fig 3.2A), the proportional invasiveness of this organism was found to be significantly lower than that of *S.* Dublin or *E. coli*. Of the cell-associated bacteria, only 0.02%, of *V. parahaemolyticus* were found to invade compared with 0.25% of the adherent bacteria for *E. coli* and 10.8% for *S.* Dublin. This indicates that *V. parahaemolyticus* likely possesses mechanisms which inhibit uptake by Caco-2. A possible inhibitory role for *V. parahaemolyticus* TTSS1 in phagocytosis by Caco-2 was identified. The Δ*vscN*1 mutant exhibited a slight increase in invasion compared with the wild type, while deletion of *vscN*2 had no effect on cellular uptake (Fig 3.2B).

A role for the TTSS1 effector protein VopS in the inhibition of GTPases has been established. This protein is capable of modifying RhoA, Rac1 and Cdc42 by addition of an adenosine monophosphate (AMPylation) to a conserved region on all three proteins (Yarbrough *et al.*, 2009). GTPase inhibition led to cytoskeletal collapse of VopS transfected HeLa cells and subsequent cell rounding. As described for the *Yersinia* effector protein YopE, inhibition of these proteins can result in reduced phagocytosis (Rosqvist *et al.*, 1990). A second mechanism which may prevent phagocytosis of *V. parahaemolyticus* was described by Burdette *et al.* (2009), who observed that the TTSS1 effector protein VopQ activated a rapid autophagic response. It was found that VopQ-dependent autophagy prevented phagocytosis of *V. parahaemolyticus* and only mutants lacking VopQ were phagocytosed (Burdette *et al.*, 2009). Burdette *et al.* (2009) hypothesised that VopQ caused redirection of cellular machinery towards autophagy, thereby preventing phagocytosis. As both of these effector proteins are secreted by TTSS1, one can imagine how both proteins could function in a synergistic manner to prevent cellular uptake, while inducing the rounding and lysis of host cells. Burdette *et al.* (2009) speculate that this process may provide a pool of readily available nutrients to facilitate rapid bacterial growth. These factors may explain why inactivation of TTSS1 by deletion of *vscN*1 led to a slight increase in invasion efficiency (Fig 3.2B).

6.2.2 TTSS as inducers of invasion.

While the findings of Yarbrough *et al.* (2009) and Burdette *et al.* (2009) seem to indicate that *V. parahaemolyticus* actively inhibits its uptake into host cells, a number of groups have speculated that the organism may indeed be capable of invasion. The first identification of invasive *V. parahaemolyticus* isolates was reported by Akeda *et al.* (1997), who observed that some clinical isolates of *V. parahaemolyticus* were capable of invading Caco-2 at a similar efficiency to *S.* Typhimurium. Further to this, it was identified that inhibition of the RhoA, Rac1 and Cdc42, by expression of dominant negative allelic variants, resulted in increased

uptake of *V. parahaemolyticus* by Caco-2 (Akeda *et al.*, 2002). This seems to contradict the common theme of bacterial entry which requires activation of Rho GTPases and formation of lamellipodia or fillipodia around the bacterial cell, which lead to phagocytosis (Cossart and Sansonetti, 2004). It may however indicate that Rho GTPase regulation by TTSS effectors has variable effects in different tissue types, as the inhibitory effects of VopS (Yarbrough *et al.*, 2009) were observed in HeLa cells, which are a cervical epithelial cell line. An alternate role for VopS was also observed by Battacharjee *et al.* (2008), where deletion mutants lacking VopS caused decreased expression of RhoB and exhibited lower macrophage phagocytosis. Assessment of the role of VopS in GTPase regulation and subsequent invasion of Caco-2 cells would prove useful in establishing whether tissue specific functionality is a factor in effector activity, particularly as Caco-2 cells represent a more appropriate model for the study of intestinal pathogens than HeLa or murine macrophages.

While TTSS2 did not appear to play a role in cellular uptake by Caco-2 in this study (Fig 3.2B), the system has recently been shown to be involved in the invasion of HeLa cells by Zhang *et al.* (2012). Deletion backgrounds lacking a functional TTSS1 were used in order to circumvent the autophagic and anti-phagocytic effects observed by Burdette *et al.* (2009), thereby allowing for assessment of TTSS2 activities in isolation from TTSS1. It was found that mutants lacking functional TTSS1 were capable of invading and proliferating within HeLa cells, however deletion of the TTSS2 effector VopC abrogated this phenotype (Zhang *et al.*, 2012). Again, a correlation between GTPase activity and phagocytosis was observed with VopC being involved in the activation of Rac1 and Cdc42. The differences observed between the findings of Zhang *et al.* (2012) and those obtained in this study again indicate that TTSS activity with respect to induction of phagocytosis may be tissue specific.

Caco-2 specific results may arise from a number of intrinsic features which are not shared with HeLa cells. For example, Caco-2 cells undergo a process of differentiation, which is

characterised by the formation of tight junctions and is accompanied by a major shift in gene expression (Saaf *et al.*, 2007; Anderson *et al.*, 1989). As this process is not observed in HeLa cells, one could expect major differences in the protein compositions of HeLa cells and differentiated Caco-2. Disruption of TTSS1 allowed co-incubation times of 2 h, compared with the 1 h infections used in this study. This indicates that the differences observed between this study and that of Zhang *et al.* (2012) may have been due to VopC inducing invasion at time points after 1 h. Such an effect is unlikely, as Zhang *et al.* (2012) observed pronounced VopC-mediated Cdc42 activation within 30 min of incubation. However, 2 h co-incubations of Δ*vscN*1 and Δ*vscN*1/Δ*vscN*2 would be required in order to categorically rule out a role for TTSS2 in the invasion of Caco-2.

6.2.3 Conclusions.

V. parahaemolyticus represents an interesting example of an organism with the capability of regulating Rho GTPase signalling pathways with a view to both promotion and inhibition of cellular uptake. The difference observed in the requirement for TTSS2 in *V. parahaemolyticus* invasion of Caco-2 intestinal cells (This study), and cervical HeLa epithelial cells (Zhang *et al.*, 2012), indicate that secretion systems may have differential roles in the invasion of different tissue types. Differences were also observed between the study of Bhattacharjee *et al.* (2008) who observed VopS-dependent upregulation of Rho GTPases and phagocytosis in murine macrophages and that of Yarbrough *et al.* (2009) who observed VopS-dependent inhibition of Rho GTPases in HeLa cells. This may indicate host specific or tissue specific activity for VopS in GTPase regulation.

While *in vitro* studies have identified TTSS1 as the principal pathogenic determinant of *V. parahaemolyticus*, it has been shown to play only minor roles in *in vivo* infections (Park *et al.*, 2004; Ritchie *et al.*, 2012). As a result, the invasive potential conferred by TTSS2, and

specifically the VopC effector protein, demonstrated by Zhang *et al.* (2012) should not be underestimated. Also, as shown in this study, even a small number of intracellular bacteria can proliferate and emerge from infected cells, thereby providing a pool of bacteria for further dissemination and infection. One of the most important aspects of future *V. parahaemolyticus* research will be to establish the factors governing expression and activity of the GTPase regulating effector proteins possessed by *V. parahaemolyticus*, and to correlate these activities with *in vivo* pathogenicity of the bacterium. In summary, *V. parahaemolyticus* is a dynamic pathogen which possesses molecular mechanisms which may be capable of selectively inducing or inhibiting invasion during infection.

6.3 Intracellular proliferation.

While invasion of host cells is of great significance for the pathogenesis of enteric species, the strategy employed once within the intracellular environment is of equal importance. The intracellular lifestyles of *Salmonella enterica*, *Shigella flexneri* and *Listeria monocytogenes* have been studied in detail. Immediately following the invasion of host cells by *Salmonella spp*, recovery of normal actin homeostasis is brought about by the effector protein SptP (Fu and Galan, 1999). The normal cellular response to the presence of phagocytic vacuoles is the induction of lysosomal fusion in order to bring about rapid hydrolytic destruction of invasive materials (Ernst *et al.*, 1999). *Salmonella spp* avoid this process by redirecting cellular signalling *via* a distinct TTSS to that employed for initial invasion (Meresse *et al.*, 1999; Steele-Mortimer, 2008). This allows for the maintenance of stable *Salmonella* containing vacuoles (SCVs) in which invasive bacteria can proliferate.

While *Salmonella spp* persist within the SCV, *S. flexneri* and *L. monocytogenes* favour escape from the vacuolar compartment in order to avoid lysosomal destruction. Following

invasion, *L. monocytogenes* secretes a pore-forming protein called listeriolysin O, which digests the phospholipid membrane of the phagocytic vacuole, thereby allowing access to the cytosol (Gedde *et al.*, 2000). Vacuolar escape by *S. flexneri* has been shown to require expression of the IpaB TTSS translocation protein (High *et al.*, 1992). Once free from the phagocytic vacuole, both *S. flexneri* and *L. monocytogenes* induce intracellular motility in order to engage in cell to cell spread. *L. monocytogenes* expresses the cell surface protein ActA which directly recruits the Arp2/3 complex, thereby facilitating actin nucleation and polymerisation (Welch *et al.*, 1998). IcsA, an unrelated surface protein produced by *S. flexneri* causes recruitment of N-WASp, a host cell protein which binds globular actin and initiates filament extension through the recruitment of the Arp2/3 complex (Egile *et al.*, 1999). The net result of ActA/IcsA activity is the formation of extensive branched filaments which enable the propulsion of bacterial cells into neighbouring cells, thereby allowing extensive tissue distribution of intracellular bacteria.

Until recently, the fate of intracellular *V. parahaemolyticus* was not known. Zhang *et al.* (2012) showed for the first time that intracellular *V. parahaemolyticus* were capable of proliferating over a 4 h period in HeLa cells, with a subsequent drop in intracellular numbers, co-incident with the time normally observed for TTSS2-dependent cell lysis. Zhang *et al.* (2012) used a CAB2 strain of *V. parahaemolyticus* which contained a deletion in *exsA*, thereby inactivating TTSS1. Similar proliferative capabilities were observed for the *V. parahaemolyticus* wild type and Δ*vscN*1 mutant during this study (Fig 3.4) and while a decrease in the maximum proliferation level was observed for the Δ*vscN*2 mutant compared with the wild type, the proliferation levels for each strain were similar at all other time points. While Zhang *et al.* (2012) reported an absolute requirement for TTSS2 in the processes of invasion and proliferation, with no invasion being observed in a CAB4 (TTSS1-, TTSS2-)

mutant, the results obtained in this study indicated that all strains, regardless of TTSS functionality were capable of invasion at low levels and subsequent proliferation.

The removal of gentamicin from cells infected with intracellular bacteria and subsequent incubation in medium without gentamicin allowed the outgrowth of bacteria at exponential levels (Fig 3.5). This indicated that intracellular bacteria were capable of dissemination from the intracellular environment and re-infection of neighbouring cells. This particular intracellular lifestyle differs from that described for *L. monocytogenes*, *Salmonella spp* and *Shigella spp* in that intracellular persistence is relatively short-lived (< 10 h, Fig 3.3). The emergence from the intracellular milieu likely occurs due to TTSS1-induced autophagic cell death. This has important implications for *in vivo* pathogenicity as the invasion of even low numbers of *V. parahaemolyticus* may provide a pool of infectious bacteria for emergence from host tissues and establishment of more persistent infections.

Taken together these findings suggest that intracellular proliferation may play a key role in the pathogenesis of *V. parahaemolyticus*. These findings and those of Zhang *et al.* (2012) are the first direct reports of intracellular proliferation of *V. parahaemolyticus*. While differences were observed between this study and that of Zhang *et al.* (2012), likely due to the *V. parahaemolyticus* strains and host cell lines used, both studies highlight the importance of intracellular proliferation in the pathogenic mechanisms of *V. parahaemolyticus*.

6.4 Summary of genomic library selections.

A principal concern of modern molecular microbiology lies in deciphering the functionalities of the vast number of sequenced genes which lack annotations. During this study, a random unbiased genomic library based approach was undertaken in order to identify novel *V.*

parahaemolyticus adhesins/invasins. 40 kb fragments of *V. parahaemolyticus* DNA were delivered into a non-adherent, non-invasive heterologous host, *E. coli* HB101. The genomic library was then subjected to selections on Caco-2 cells in order to identify invasive or adherent clones from within the library population. Following selection, pure cultures of 134 clones were tested for either elevated invasion or adherence on Caco-2 cells. Of the 134, a single clone (A16, Fig 4.6B) displayed three-fold higher invasion than the *E. coli* HB101 control strain and no clones displayed significant increases in adherence. Heterologous expression of a single *V. parahaemolyticus* protein (MAM7) in *E. coli* was shown by Krachler *et al.* (2011) to confer a six-fold increase in adherence to Caco-2. As such, in hindsight it may have been expected that MAM7, in addition to other uncharacterised adhesins and invasins would be detected by the genomic library selection methods employed. MAM7 was not selected for in any library clone, indicating that expression of adhesins and invasins may have been suboptimal in the genomic library.

The isolation of a single positive clone from the 134 selected by initial isolation indicated a high background and/or the isolation of false positives for adherence/invasion. In order to counteract the effects of background invasion or adherence by *E. coli* HB101, the selection process was amplified by pooling invasive/adherent clones from a single round of library selection, culturing overnight and subjecting to a second round of selection. Following four successive rounds of selection, no significant improvement in selection of adherent or invasive clones was observed. Carbol fuschine staining and microscopy of library clones identified altered cell morphology in many clones, with the formation of filaments and/or clusters of cells being observed in some cases.

The formation of filaments in response to the stress of heterologous expression has been documented in *E. coli* (Hoffmann and Rinas, 2004; Carrió *et al.*, 2001; Cheng, 1983; Mantile *et al.*, 1993). The regulation of filamentation has been studied by a number of groups and has

been shown to be induced by the activation of stress response networks such as the SOS system, which functions in the regulation of DNA repair (Janion, 2008; Hoffmann and Rinas, 2004; Justice *et al.*, 2006; Walker, 1985). The expression of SulA, a SOS response protein which causes the arrest of the *E. coli* cell cycle, was shown by Justice *et al.* (2006) to induce the formation of filamentous cells during *in vivo* infections of murine bladders with uropathogenic *E. coli*. Justice *et al.* (2006) also observed a hyperadherent phenotype for filamentous cells compared with Δ*sulA* isogenic mutants with normal cell morphology and hypothesised that the increased adherence of filamentous cells may have been caused by an increase in available cell surface area for interaction with host cells. It is clear that induction of the SOS response and subsequent filamentation of library clones, as a result of the expression of a large number of exogenous proteins, would lead to indirect interference with library selections, due to the selection of false positives.

Many clones, including clone A16, also displayed low inoculum counts prior to infection of Caco-2, despite correction of the OD_{600} of each cell suspension to a standardised value. This could be explained by alterations in cell shape, cell size, surface characteristics, aggregation or death of a proportion of the cell suspension. These aberrant characteristics may have arisen due to the stresses induced in the heterologous host during expression, or carriage of large foreign DNA molecules. These factors indicate that clone A16 could represent a false positive for elevated invasion efficiency.

The low detection rate of adherent/invasive clones from initial library selections indicated that functional expression of *V. parahaemolyticus* proteins might not have occurred in the *E. coli* HB101 heterologous host. This could have been due to an inability to carry out post-translational modifications such as glycosylation, which could be critical for adhesin functionality. For example glycosylation of the *N. meningitidis* type IV pilus requires co-expression of the galactosyl transferase PglA and the glycan biogenesis proteins PglB, PglC,

PglD and GalE (Stimson *et al.*, 1995; Power *et al.*, 2000). Glycosylation may be critical for the functionality of *V. parahaemolyticus* adhesins and as such, expression of the adhesin without co-expression of the glycosylation machinery, which may be located in a genetically distinct location, would not allow for functionality. *V. parahaemolyticus* possesses a number of putative glycosyltransferases (GTases), encoded by *VP1463*, *VPA1411*, *VPA0230* and *VP2713* (our data). BLAST analysis confirmed that no *E. coli* GTases possessed greater than 30% amino acid identity to the aforementioned proteins, indicating that functional glycosylation would likely require parallel heterologous expression of exogenous adhesins and GTases. It should also be noted that the PilA pilus, which was shown by Shime-Hattori *et al.* (2006) to be involved in the formation of bacterial aggregates during biofilm formation, is encoded in two separate operons. The *pilABCD* operon (Fig 5.3), which encodes the major pilin is located 251 kb apart from the *pilMNOPQ* operon which encodes the majority of the pilus biogenesis genes. As such, it would be impossible for any individual clone to functionally express an intact PilA pilus.

Intrinsic differences in transcription and translation exist, even between closely related bacteria. While *E. coli* and *V. parahaemolyticus* are both members of the gamma proteobacteria, differences in GC content and codon usage exist between the organisms, a factor which can have negative implications for heterologous expression (Terpe, 2006; Waterfield *et al.*, 2008; Gustafsson *et al.*, 2004).

An integral facet of adhesin/invasin functionality is the necessity for correct sub-cellular localisation. Recognition of signal peptides, co-expression of signal peptidases, co-expression of inner and outer membrane secretins and co-expression of secretion-associated ATPases may all be required for cell surface localisation of an adhesin or invasin. Again, such proteins may be encoded in a genetically distinct region or may be under the control of alternate transcription factors in the native organism and as such may not be expressed in *E. coli*. This

effect was observed by Waterfield *et al.* (2008) who detected cytoplasmic accumulation of the *P. asymbiotica* exotoxin Mcf1, when expressed in an *E. coli* based library. Expression of adhesins such as type IV pilins, without cell surface localisation in *E. coli* would result in lack of functionality.

The study carried out by Waterfield *et al.* (2008) provides a particularly interesting comparison to this study, as a genomic library screen for virulence genes yielded the identification of a number of adhesins and invasins. The presence of *P. asymbiotica* genes coding for a number of multicomponent organelles conferred virulence of *E. coli* clones towards invertebrate hosts. These included two distinct fimbrial operons, a TTSS operon, a T6SS operon, haemagglutinin genes and a putative invasin. Similarly, Stahlhut *et al.* (2010) identified functional expression of fimbriae from a fosmid library of *Klebsiella pneumoniae* DNA expressed in *E. coli*. Both of these studies indicate that the use of an appropriate heterologous host and a complementary vector system can yield functional expression of multiple heterologous proteins, many of which require cell surface localisation.

The genomic library selections carried out during this study may have been hindered by the factors described above or may have occurred due to poor coverage of the *V. parahaemolyticus* genome. In order to assess this, a validation technique was developed by exploiting the characterised antimicrobial properties of *V. parahaemolyticus*. *V. parahaemolyticus* possess two distinct fluoroquinolone resistance mechanisms: the NorM multi-drug efflux pump (Morita *et al.*, 1998) and the Qnr quinolone resistance protein (Poirel *et al.*, 2005; Saga *et al.*, 2005). Selection of the *V. parahaemolyticus* genomic library on a concentration of norfloxacin found to inhibit *E. coli* HB101 led to the observation of resistance in 0.5% of the library population. Taking into account the 5.8 Mb genome of *V. parahaemolyticus*, this indicated the selection of a single resistance locus. Indeed end-sequencing of eight random norfloxacin resistant clones identified a common locus in all

eight, with the Qnr resistance protein from chromosome 2 being detected in all resistant clones. Involvement of the Qnr protein encoded by *VPA0095* has been documented by Poirel *et al.* (2005) and Saga *et al.* (2005). Six genetically distinct inserts, all containing *qnr* were detected from the eight sequenced clones, indicating at least six-fold coverage of the *V. parahaemolyticus* genome. As NorM is a membrane-associated efflux pump, the lack of detection of this protein using the validation technique described here may be attributed to improper membrane localisation or poor expression in *E. coli*. This further highlights the difficulties which may have been encountered with expression of surface localised adhesins/invasins. This validation technique may prove useful for assessing coverage and heterologous host suitability of *V. parahaemolyticus* genomic libraries in future studies. Resistance frequencies of ~1% within *V. parahaemolyticus*-derived libraries with similar insert sizes to those used in this study would indicate expression of both NorM and Qnr, thereby confirming the suitability of a heterologous host for expression of *V. parahaemolyticus* DNA. End-sequencing of resistant clones and confirmation of the presence of genetically distinct loci would serve to confirm coverage of such genomic libraries.

A number of steps could be undertaken to improve the possibility of functional expression and subsequent detection of adhesins and invasins. *E. coli* HB101 was used as a genomic library host due to its extensive use as a non-adherent, non-invasive control strain (Elsinghorst *et al.*, 1989; Giron *et al.*, 2002; Jostock and Dubel, 2005; Monack *et al.*, 1996; Nicholls *et al.*, 2002). *E. coli* HB101 is deficient in restriction and recombination systems, leading to its use as a general cloning strain (Boyer and Roulland-Dussoix, 1969), however the use of the EPI-100 strain provided by the cosmid cloning kit manufacturer may have yielded improved cosmid stability, expression and functionality. This benefit would however have come at the cost of increased background adherence and invasion compared with *E. coli* HB101. The use of an *E. coli* strain optimised for cosmid cloning, successfully led to the

detection of *P. asymbiotica* adhesins, invasins and secretion system proteins, by gain of toxicity against invertebrate hosts (Waterfield *et al.*, 2008). Each of these proteins would require cell surface expression for functionality and as such it appears that the use of a general cloning strain may prove more effective for detection of virulence factors in genomic libraries.

Preparation of an alternative library by transposon mutagenesis of the *V. parahaemolyticus* wild type would allow for assessment of adhesins and invasins within the organism of interest, through phenotypic analysis for loss of function in adhesion or invasion using Caco-2 cells. The disruption of single genes would lead to a reduced risk of indirect effects, such as those observed with heterologous expression during this study, which may lead to the selection of false positives. Employing a library composed of smaller inserts, coupled with driven expression may also lead to improved expression and/or functionality in a heterologous *E. coli* host, while also reducing stresses due to expression of several exogenous proteins.

6.5 The importance of efficient adherence in *V. parahaemolyticus* pathogenicity.

As seen in Fig 3.2A, *V. parahaemolyticus* RIMD2210633 displays highly efficient adherence to Caco-2 (20% of inoculum), compared with *S.* Dublin (2%) and *E. coli* HB101 (0.3%). It is likely that this level of adherence is strain specific as it has been reported that in many *V. parahaemolyticus* strains, piliation does not appear to have an influence on adhesiveness and in those cases, a cell-associated, non-pilus haemagglutinin is the primary adherence factor (Nagayama *et al.*, 1995). A previous study identified that *V. parahaemolyticus* isolates from a variety of sources adhered to Caco-2 at between 0.1% and 9.4% of the inoculum, with clinical isolates generally displaying the highest levels of adherence (Vongxay *et al.*, 2008). It

is possible that one of the contributing factors to the increased virulence of the pandemic O3:K6 clone of *V. parahaemolyticus* was the evolution of more efficient host cell adherence mechanisms. TTSS, which have been described as the principal virulence mechanisms of *V. parahaemolyticus*, function in a cell contact-dependent manner. As such there exists a significant requirement for adherence in order for *V. parahaemolyticus* to exert its effects on the host cell. It is interesting that although *S.* Dublin also utilises TTSS, the ability of this strain to adhere to Caco-2 is significantly lower than that of *V. parahaemolyticus*. Although adherence is required for TTSS function, the secretion systems themselves do not play a role in cellular attachment. This was evidenced by the observation that deletion mutants lacking each system did not display decreased adherence compared with the wild type (Fig 3.2A). It was therefore evident that other adhesins were involved in the adhesive capabilities of *V. parahaemolyticus* towards Caco-2.

One such adhesin was identified by Krachler *et al.* (2011). Outer membrane multivalent adhesion molecule 7 (MAM7) was found to engage in protein-protein interactions (binding fibronectin) and protein-lipid interactions (binding phosphatidic acid). Deletion mutants lacking MAM7 adhered to Caco-2, HeLa, RAW 264.7 macrophages and 3T3 fibroblasts with approximately 50% lower efficiency than the *V. parahaemolyticus* wild type. Decreased adherence by disruption of MAM7 resulted in decreased cytotoxicity against two of the aforementioned cell lines and reduced lethality following infection of *C. elegans* nematodes.

This study provides further evidence for the crucial role of an adhesin in the pathogenicity of *V. parahaemolyticus*. As shown in Fig 5.11, disruption of the MSHA pilus by deletion of the pilus ATPase (MshE), outer membrane secretin (MshL) or the major pilin subunit (MshA1) resulted in a 60% decrease in adherence to Caco-2. Krachler *et al.* (2011) observed a similar defect with deletion of MAM7 after the same period of incubation. It was also observed that MAM7 was constitutively expressed and exposed on the cell surface prior to infection,

thereby rendering *V. parahaemolyticus* “primed for immediate attachment when encountering a host cell” (Krachler *et al.*, 2011). For these reasons it has been speculated that MAM7 is the principal adhesin used by *V. parahaemolyticus* in establishing initial contact with the host cell and that other factors may be expressed during infection to enhance attachment at later stages (Krachler *et al.*, 2011). The work presented here contradicts this speculation as MSHA piliation was also observed under normal growth conditions in the absence of host cells (Fig 5.10) and the MSHA pilus was also found to mediate attachment in the early stages of infection (1 h, Fig 5.11). We therefore propose that the MSHA pilus and MAM7 function synergistically in the early stages of infection by establishing multivalent contact with the host cell, a process which could be analysed further by the study of a Δ*mam*7/Δ*mshA*1 double mutant. While early research by Nakasone *et al.* (1990, 1991 and 2000) identified that the pili produced by three *V. parahaemolyticus* strains were capable of adhering to rabbit enterocytes, the underlying genes were not identified and adherence to human cells was not analysed. This study has confirmed that the adhesive pili produced by strain RIMD2210633 are encoded by the MSHA gene cluster, and are indeed involved in adherence to human intestinal cells.

Many bacterial adhesins have the ability to function as invasins either by enhancing contact with the host cell and increasing the probability of uptake, or by actively triggering a host cell response by binding to a host cell receptor. Disruption of the MSHA pilus by deletion of *mshE*, *mshL* and *mshA*1 was found to have a significant impact on the uptake of *V. parahaemolyticus* by Caco-2. As shown in Fig 5.15, MSHA mutants exhibited 60% lower levels of intracellular bacteria than the wild type. The close correlation between adherence data and invasion data indicates that adherence is the major contributing factor to the uptake of *V. parahaemolyticus* by Caco-2.

Further to its integral role in adherence to Caco-2, the MSHA pilus was found to be required for a number of pathogenic effects associated with TTSS function. Burdette *et al.* (2008)

describe *V. parahaemolyticus* infection as a multi-faceted process, involving secretion of multiple effectors, which have independent parallel effects, resulting in rounding of host cells, induction of autophagy and host cell lysis. Lysis of infected cells has been attributed to a TTSS1 effector protein VopQ (Burdette *et al.*, 2009; Matlawska-Wasowska *et al.*, 2010). Disruption of the MSHA pilus led to a 20% reduction in cell lysis after 4 h of infection as measured by LDH release from infected Caco-2 (Fig 5.16). It is likely that disruption of MSHA-mediated adherence reduced the efficiency of VopQ secretion by *V. parahaemolyticus*, leading to reduced levels of lysis. Krachler *et al.* (2011) observed a similarly small reduction in Caco-2 cell lysis at this time-point upon deletion of MAM7. The involvement of MAM7 and the MSHA pilus in the early stages of *V. parahaemolyticus* may result in only minor effects being observed during longer co-incubations. This could be the result of other adhesins being induced following attachment to the host cell. A greater effect was observed in MAM7-mediated lysis of 3T3 fibroblasts (~35% reduction) (Krachler *et al.*, 2011). This indicates that the requirement for specific adhesins in the cytotoxic effects of *V. parahaemolyticus* may vary with respect to tissue type, presumably due to receptor diversity. While intestinal cell models such as Caco-2 represent the most appropriate infection models for the study of the gastro-intestinal pathogen *V. parahaemolyticus*, assessment of a role for the MSHA pilus in a variety of cell models would provide interesting insights into tissue specificity of the pathogen.

Another effect of VopQ activity in host cells is the induction of an inflammatory response, as seen by the detection of IL-8 in the medium of Caco-2 cells infected with *V. parahaemolyticus* (Matlawska-Wasowska *et al.*, 2010; Shimohata *et al.*, 2011). Activation of both p38 and ERK by VopQ leads to stabilisation of IL-8 transcript, nuclear translocation of NF-κB and subsequent expression of IL-8 (Matlawska-Wasowska *et al.*, 2010; Shimohata *et al.*, 2011). As seen by this work and that of Shimohata *et al.* (2011), inhibition of nuclear NF-

κB translocation leads to reduced IL-8 expression (Fig 5.20) following stimulation with *V. parahaemolyticus*. Disruption of adherence by deletion of the MSHA pilus had a marked effect on NF-κB-mediated IL-8 induction, with MSHA deficient strains causing 50% less IL-8 secretion than the *V. parahaemolyticus* wild type (Fig 5.21). As such, this result complements that observed for MSHA involvement in VopQ-dependent cytotoxicity, further indicating the critical role played by the MSHA pilus in the secretion of VopQ from TTSS1. *In vitro* studies have confirmed that VopQ is the major determinant of *V. parahaemolyticus* toxicity against both HeLa and Caco-2 cells (Burdette *et al.*, 2009; Matlawska-Wasowska *et al.*, 2010). The findings of this study indicate that the efficiency of VopQ in the disruption of host cells can be abrogated by interfering with MSHA-dependent adherence, thereby highlighting the importance of MSHA as a target for potential therapeutics.

The lytic effects of *V. parahaemolyticus* occur in parallel with host cell rounding, a process which is induced by VopS. VopS binds to Rho GTPases and prevents GTP phosphorylation by the addition of adenosine monophosphate to a conserved residue on RhoA, Rac1 and Cdc42, resulting in collapse of the actin cytoskeleton (Yarbrough *et al.*, 2009). The use fluorescently tagged phalloidin conjugates allow for efficient visualisation of the actin cytoskeleton due to the high affinity of phalloidin for filamentous actin (Wulf *et al.*, 1979). Phalloidin staining following 2.5 h of incubation allowed for visualisation of the morphological alterations which are characteristic of *V. parahaemolyticus* infection (Fig 5.17). VopS-dependent cell rounding was delayed in Caco-2 which were infected with Δ*mshE*, Δ*mshL* and Δ*mshA*1, indicating that binding via the MSHA pilus plays a key role in this process, presumably by enhancing the efficacy of VopS secretion *via* TTSS1. Caco-2 cells infected with MSHA mutants displayed fewer rounded cells, more intact tight junctions and fewer detached cells compared with those infected with the *V. parahaemolyticus* wild type. The results of this experiment indicate that secretion of both VopS and VopQ from

TTSS1 may be impaired by disruption of the MSHA pilus, further illustrating the role of MSHA-mediated adherence in TTSS activity.

TTSS1, and specifically the effector proteins VopS and VopQ have been described as major virulence factors of *V. parahaemolyticus*. TTSS1 was found to be the primary cause of toxicity in Caco-2 cells, HeLa cells and *in vivo* murine infections (Matlawska-Wasowska *et al.*, 2010; Burdette *et al.*, 2009; Hiyoshi *et al.*, 2010). For this reason, this study focused on TTSS1-mediated responses in infected host cells. In order to study TTSS2-mediated effects, such as actin filament formation, invasion of HeLa cells and MAPK inhibition, the *msh* deletion alleles could be introduced into a Δ*vscN*1 background, thereby eliminating the possibility of TTSS1-mediated responses masking TTSS2-associated phenotypes. Krachler *et al.* (2011) demonstrated for the first time that disruption of adhesins in *V. parahaemolyticus* could result in impairment of toxicity which is commonly associated with TTSS1. This study further highlights the importance of adherence for *V. parahaemolyticus* pathogenicity and indicates that host cell binding via multiple adhesins forms a critical step in the development of an effective infection.

6.6 Receptor specificity of the MSHA pilus.

Functionality of the MSHA type pili possessed by *V. parahaemolyticus* represents an interesting area of molecular microbiology. *In silico* analysis of pilin loci, amino acid sequences and nucleotide sequences yielded the observation that MSHA pili form a distinct grouping to the pili which have been characterised to date (Fig 5.3 - Fig 5.6). Using conserved regions for primer design, PCR analysis of 10 environmental isolates of *V. parahaemolyticus* identified that all strains encoded *mshA*1 (Boyd lab, unpublished data). However functionality as a host cell binding adhesin may not be conserved, due to the

reported hypervariability of the *V. parahaemolyticus* pilins (Aagesen and Häse, 2012). Having observed a crucial role for the MSHA pilus in binding to Caco-2 cells and allowing for downstream pathogenic effects of *V. parahaemolyticus* to be induced, an investigation was undertaken to identify the receptor for the pilus. Recently developed glycan array technology allowed for the assessment of binding to a variety of carbohydrate epitopes in a high throughput manner. The *V. parahaemolyticus* wild type was found to bind to all glycans tested with at least two-fold higher affinity than that of the Δ*mshA*1 mutant. Increased affinity of less than fivefold in the wild type compared with the Δ*mshA*1 mutant likely occurred due to alterations in cell surface charge or hydrophobicity (Fig 5.27). Piliation has been shown to cause such changes in cell surface properties by Magnusson *et al.* (1980) and Speert *et al.* (1986). An involvement for the MSHA pilus in non-specific adherence has been described by Shime-Hattori *et al.* (2006), who observed that the pilus played a role in biofilm formation by increasing the affinity of *V. parahaemolyticus* to abiotic surfaces.

While a certain redundancy was seen in the binding of the MSHA pilus to the range of glycans analysed, relative affinities for a number of glycans were markedly higher in the wild type than the Δ*mshA*1 mutant. The MSHA pilus appears to exhibit highest affinity to the blood group type glycans including: sulphated and non-sulfated Lewis X and Lewis A antigens; blood group A and blood group B antigens. All of these glycans may be found in intestinal epithelial cells (Sakamoto *et al.*, 1986; Ilver *et al.*, 1998; Marionneau *et al.*, 2001; Jahn *et al.*, 2011) and as such we propose that these glycans form host cell receptors for the pilus. Structural similarities exist between the glycans towards which the MSHA pilus displays high affinity, in particular a terminal galactose residue which was present in seven of the eight glycans with highest MSHA affinities and a sub terminal fucosylated saccharide which was also present in seven of the eight glycans with highest MSHA affinities.

While structurally similar, the capability of the MSHA pilus to bind multiple distinct glycans indicates that it may indeed function as a multivalent adhesin, a property which may enhance the affinity of host cell binding and allow for colonisation of multiple tissue types with diverse receptor expression. It has been shown that *V. parahaemolyticus* adheres with high affinity to M cells in the lymphoid follicles in both formalin fixed human intestinal tissue and rabbit intestinal tissue (Yamamoto and Yokota, 1989). Yamamoto and Yokota (1989) also observed binding to absorptive villus cells and mucus, albeit at lower levels to that observed for M cells. Differential glycosylation between M cells and enterocytes has been reported (Giannasca *et al.*, 1999), further highlighting the possibility that the MSHA pilus may play a role in the adherence of *V. parahaemolyticus* to multiple sites in the gastro-intestinal tract.

The multivalent nature of the MSHA pilus may be conferred by flexibility of the receptor binding domain of the major pilin subunit MshA1, however it remains a distinct possibility that minor pilins could play a role in the binding of the MSHA pilus to the variety of glycan epitopes analysed in this study. While deletion of *mshA*1 completely abolishes pilus production, deletion of the minor pilins *mshC*, *mshD* and *mshO* should not impede formation of the pilus filament, due to their relatively low abundance. It has been shown that the *N. meningitidis* minor pilin PilX is critical for pilus functionality (Helaine *et al.*, 2007). Minor pilin functionality has not been analysed in *V. parahaemolyticus*. Array profiling of minor pilin deletion mutants or purified minor pilins would be particularly useful in improving understanding of this process. Research in this area would further develop understanding of MSHA pilus functionality and may yield important insights into dynamic receptor binding *via* multiple adhesins within the same organelle.

In summary, the MSHA pilus represents an intriguing bacterial adhesin which facilitates both specific and non-specific attachment to a variety of surfaces, allowing for diverse activities including the formation of biofilms and the adherence to gastro-intestinal host cells.

6.7 Potential for pilin glycosylation.

The TFP produced by *N. meningitidis*, *N. gonorrhoeae* and *P. aeuriginosa* strain 1244 have been shown to be glycosylated (Stimson *et al.*, 1995; Parge *et al.*, 1995; Castric *et al.*, 2001). The *N. meningitidis* and *N. gonorrhoeae* (MC and GC) pilins have both been shown to be *O*-glycosylated at Ser63, with the MC pilin being modified with digalactosyl 2,4-diacetamido-2,4,6-trideoxyhexose (Galβ1-4Gal-DATDH) and the GC pilin possessing Galα1-3DATDH (Stimson *et al.*, 1995; Hegge *et al.*, 2004). Glycosylation of the MC or GC pilins was not found to play any role in adherence to host cells or the formation of bacterial aggregates (Marceau *et al.*, 1998). Instead, MC pilin glycosylation was shown to be required for the production of a truncated soluble pilin variant, which does not form pili (Marceau and Nassif, 1999), a feature which Craig *et al.* (2004) speculated may subvert an anti-pilus antibody response. The GC pilin glycan was shown to be responsible for the activation of the complement receptor CR3 in cultured cervical epithelial cells (Jennings *et al.*, 2011), further highlighting a role for glycosylation of neisserial pili in the regulation of host immune responses.

Importantly, the pilin glycans produced by *Neisseria spp* were shown to be variable in length due to phase variation modulating the activity of *O*-glycosyltransferases (*O*-GTases). The *O*-GTase encoding gene *pglE* was shown to contain a variable number of heptanucleotide repeats, which enabled cycling between an “on” or “off” allelic variant (Power *et al.*, 2003). Variants possessing the “on” form of *pglE* were capable of catalysing the covalent attachment of Galβ1-4 to the di-saccharide Galα1-3DATDH, whereas frame shift mutation prevented functional expression of PglE and resulted in presentation of a di-saccharide pilin glycan (Power *et al.*, 2003).

The *P. aeruginosa* strain 1244 pilin glycan was found to be an *O*-linked tri-saccharide, attached at Ser148, which displayed antigenic similarity to LPS glycans from the same strain (Castric *et al.,* 2001). *P. aeruginosa* 1244 deletion mutants which lacked pilin glycosylation were found to produce pili which were normal in appearance, however colonization of murine respiratory tracts was significantly affected (Smedley *et al.,* 2005). This indicates that some pilin glycans are involved in mediating interactions with host cells, which directly play a role in colonisation and pathogenesis.

The mechanism of MC pilin glycosylation has been extensively characterised. Power *et al.* (2006) identified that PglL was required for the translocation of the mature tri-saccharide to the Ser63 residue of PilE during pilus assembly. PglL was therefore termed an oligosaccharyl transferase (OTase). Further to this finding, it was identified that the co-expression of exogenous PglL and MC pilin in *E. coli*, together with the biosynthetic components of the *C. jejuni* glycan synthesis locus resulted in the glycosylation of MC pilin with a *C. jejuni* glycan (Faridmoayer *et al.,* 2007). This confirmed the functionality of PglL as a promiscouous, relaxed substrate specificity OTase. Recently, a PglL homologue was identified in *V. cholerae* and was subsequently termed $PglL_{VC}$. Analysis of $PglL_{VC}$ functionality by recombinant expression in *E. coli* identified that $PglL_{VC}$ was also capable of transferring mature glycan moieties to heterologously expressed MC pilin (Gebhart *et al.*, 2012).

Taking into account the OTase functionality identified for $PglL_{VC}$, we decided to carry out a BLAST seacrch in order to identify homologous proteins possessed by *V. parahaemolyticus*. A protein bearing 66% amino acid identity with $Pgl_{V}c$ was identified. Importantly, both $PglL_{VC}$ and $PglL_{VP}$ are encoded by genes which are located five open reading frames upstream of the *msh* gene clusters. While direct PglL-mediated glycosylation of the MSHA pilus has not been reported, the characterised OTase functionality of the protein, coupled with

its close chromosomal proximity to the *msh* gene cluster renders it a prime target for analysis of potential glycosylation of MSHA pilins from *Vibrio spp*.

6.8 Significance of findings.

This study provides a detailed characterisation of a *V. parahaemolyticus* adhesin, including its role in adherence and invasion of host cells, which facilitate initiation of downstream pathogenic events in Caco-2 intestinal epithelial cells. The MSHA pili possessed by the *Vibrionaceae* were until now, thought to only be involved in environmental persistence by virtue of their involvement in biofilm formation (Shime-Hattori *et al.*, 2006; Thelin and Taylor, 1996; Marsh and Taylor, 1999; Tacket *et al.*, 1998). This study has identified that the MSHA pilus possessed by *V. parahaemolyticus* is unlike that of *V. cholerae* in functionality. The MSHA pilus may therefore represent the development of a pilus-mediated means of colonisation in *Vibrio spp* lacking the TCP pilus. The identification of a role for *V. parahaemolyticus* MSHA in pathogenicity is a novel finding and expands current understanding of the molecular interactions which are required for colonisation of host tissues by *V. parahaemolyticus*.

The use of glycan array profiling for the identification of adhesin-receptor interactions is a relatively new field of molecular biological research. As adhesins from other species have been described as carbohydrate binding proteins (Sheth *et al.*, 1994; Ilver *et al.*, 1998; Mahdavi *et al.*, 2002), this technology offered a significant opportunity for rapid characterisation of potential receptors for the MSHA pilus. The approach was not only qualitative but also quantitative, with highest glycan specificities being observed for the Lewis type glycans. The observation of lectin functionality for the MSHA pilus is a novel finding. The identification of specific receptors for the MSHA pilus presents a particularly

exciting result as the development of therapeutics typically requires the targeting of highly specific sites of interaction between the host and pathogen. To our knowledge, this study provides the first example of glycan array comparison between a wild type bacterial pathogen and an isogenic adhesin deletion mutant. This technology will prove invaluable for future studies of the interactions between pathogenic species and host glycoproteins and glycolipids.

6.9 Implications of this study in the process of *V. parahaemolyticus* pathogenesis.

In order to better understand bacterial pathogenesis, it is important to consider the various molecular mechanisms which enable virulence in the context of the overall pathogenic process. The mechanism by which *V. parahaemolyticus* elicits detrimental effects upon host cells can be summarised as follows:

1. Colonisation: *V. parahaemolyticus* constitutively expresses adhesins such as MAM7 and MSHA, thereby priming bacterial cells for attachment to host cells *via* receptors such as fibronectin, phosphatidic acid and Lewis antigen expressing membrane glycoproteins (Krachler *et al.*, 2011; Fig 5.27). Initial adherence may trigger the expression of additional colonisation factors, such as the PilA pilus, to enhance attachment to the host cell.

2. Translocation of effectors: Following the cell surface docking of bacteria, TTSS bind to the host cell and translocate a vast array of effector proteins *via* TTSS1 and/or TTSS2. The presence of bile salts enhances transcription of TTSS2-related genes, while low concentrations of lumenal calcium enhance TTSS1 transcription (Kodama *et al.*, 2010; Gotoh *et al.*, 2010). The activity of both secretion systems results in disruption of intestinal barrier function, induction of inflammation and localised cell lysis, all of which contribute to a secretory diarrheal response from the host (Park *et al.*, 2004; Ritchie *et al.*, 2012).

3. Invasion and dissemination: Importantly, during infection a small number of bacteria invade into host epithelial cells and rapidly proliferate (Zhang *et al.*, 2012; Fig 3.1B; Fig 3.3). This facilitates a brief period of evasion from immune attack and provides a pool of bacteria which emerge from infected cells and re-colonise the epithelial lining (Fig 3.5).

4. Recovery of the host: The above cycle may be repeated a number of times over 2-3 days (Nair *et al.*, 2007). The majority of infected individuals recover completely within this period, likely by immune clearance of the pathogen. In some cases however, intestinal tissue damage may be sufficient to allow traversal of *V. parahaemolyticus* into the bloodstream (Broberg *et al.*, 2011). This can result in severe septicaemia, which in many cases may be lethal.

The findings of this study have enhanced current understanding of the initial attachment phase of *V. parahaemolyticus* infection. Krachler *et al.* (2011) speculated that MAM7 may be the key adhesin used by *V. parahaemolyticus* during the early phases of infection, due to cell contact-independent expression, with other adhesins being expressed after contact with the host cell. We have successfully identified another adhesin, which like MAM7 is expressed prior to cell contact and enables attachment to Caco-2 intestinal cells. We have also expanded the receptor repertoire for *V. parahaemolyticus* adhesins, with the identification of Lewis glycan binding by the MSHA pilus.

We have provided further evidence that *V. parahaemolyticus* is capable of invading host cells, a trait which was observed previously (Akeda *et al.*, 1997; Zhang *et al.*, 2012; Fig 3.1B). The significance of this invasive phenotype was confirmed by the observation that intracellular bacteria could persist within Caco-2 cells and even proliferate before emerging due to lysis of infected cells, thereby enabling dissemination and further infection (Fig 3.3).

Future *in vivo* studies will assist in establishing the significance of tissue invasion in the context of the overall pathogenesis of *V. parahaemolyticus*.

6.10 Implications of this study for TFP as virulence factors of bacterial pathogens.

TFP have long been known to play a role in bacterial virulence. *N. meningitidis*, *N. gonorrhoeae*, *P. aeruginosa*, *V. cholerae* and enteropathogenic *E. coli* all possess TFP which have been characterised as having central roles in pathogenesis (Craig *et al.*, 2004). The *N. meningitidis* MC pilus, *N. gonorrhoeae* GC pilus, *V. cholerae* TCP pilus and *E. coli* BFP pilus have all been associated with microcolony stabilisation, a factor which is believed to assist in colonisation of epithelia during infection (Helaine *et al.*, 2005; Virji *et al.*, 2006; Kirn *et al.*, 2002; Cleary *et al.*, 2004). TFP have also been implicated in the direct binding to host cells, with the *P. aeruginosa* PAK pilin being shown to bind to the glycosphingolipid asialo-GM1 and the GC pilin being capable of binding the host cell glycoprotein receptor CD46 (Krivan *et al.*, 1988; Kallstrom *et al.*, 1997). This study involved the characterisation of a TFP with a distinct sequence composition and structural domain organisation to that of the GC, PAK and TCP pilins (Fig 5.4, Fig 5.5, and Fig 5.6). The MSHA pilus was shown to be involved in adherence to Caco-2 intestinal cells and like the GC and PAK pilins, displayed glycan binding properties (Fig 5.27). This study therefore underlines the central role of TFP in the initial attachment of pathogens to host cells. The critical nature of the MSHA pilus in *V. parahaemolyticus* pathogenicity was further highlighted by the abrogation observed in the pathogenic responses in Caco-2 upon disruption of the MSHA pilus.

6.11 Future perspectives.

This study has investigated a variety of aspects of *V. parahaemolyticus* pathobiology with respect to the interactions of the organism with host cells. The findings of this study present a wealth of opportunities for further investigation, with a view to enhancement of current understanding of the *V. parahaemolyticus* pathogenic life cycle.

As mentioned previously, *V. parahaemolyticus* TTSS have been shown to play a role in the manipulation of a variety of host cell signalling networks which modulate cellular trafficking. While Zhang *et al.* (2012) identified for the first time, a *V. parahaemolyticus* effector protein with a definitive role in the process of invasion, the overall involvement of both TTSS is still poorly understood. The inconsistencies observed between this study and that of Zhang *et al.* (2012) may be a result of their use of Δ*exsA* and Δ*vtrA* transcription factor deletion mutants to inactivate TTSS. No involvement was observed for TTSS2 in the invasion of Caco-2 cells by *V. parahaemolyticus* during this study, a finding which is in direct contrast to that of Zhang *et al.* (2012). The introduction of a *vopC* deletion into the *V. parahaemolyticus* wild type or Δ*vscN*1 mutant background may allow for the assessment of the involvement of VopC in the invasion of Caco-2, while eliminating concern arising from indirect effects on the transcription of genes other than TTSS components.

While GTPase modulation has been observed in response to VopC and VopS (Zhang *et al.*, 2012; Yarbrough *et al.*, 2009), both studies involved the use of HeLa cervical epithelial cells. Assessment of GTPase modulation by TTSS effector proteins in Caco-2 would yield important insights into potential cell type specific responses and may offer a more relevant representation of *in vivo* intestinal infections. Understanding of the signalling events involved in *V. parahaemolyticus* invasion could be further developed by analysing alterations in the

expression or activity of downstream targets of Rho GTPase signalling, particularly the WASp family of actin binding proteins.

The observation of a role for MSHA-mediated adherence in a variety of pathogenic responses to *V. parahaemolyticus* infection of Caco-2 has significant implications for our overall understanding of *Vibrio* pathogenesis. The lytic, morphological and pro-inflammatory effects analysed in this study, with respect to MSHA functionality, can be attributed to characterised responses of host cells to the TTSS1 effector proteins VopS and VopQ. Establishment of a role for the MSHA pilus in TTSS2-related virulence would confirm the importance of the pilus for overall pathogenesis. As TTSS1 is the principal virulence factor in *V. parahaemolyticus* pathogenicity towards Caco-2 cells, the introduction of *msh* deletions into the Δ*vscN*1 background would enable the analysis of TTSS2-mediated effects in isolation from TTSS1. Phenotypes such as VopT-mediated cytotoxicity, VopL-mediated stress filament formation and VopA-mediated MAPK inhibition could all be analysed in order to confirm a role for MSHA-associated adherence in TTSS2-related responses.

While Caco-2 have been used extensively in the study of enteric pathogens, due to their isolation from colonic tissue and their ability to form polarised monolayers which are highly representative of the intestinal epithelium, *in vivo* infection models are considered the most appropriate means of assessing the importance of virulence factors for overall pathogenicity. Recent advances have been made in the development of appropriate *in vivo* infection models for *V. parahaemolyticus* research. Ritchie *et al.* (2012) recently developed a *V. parahaemolyticus* oro-gastric rabbit infection model, which produces similar diarrheal symptoms to those observed in infected humans. Comparison of the *V. parahaemolyticus* wild type with Δ*msh* mutants using this model would also prove particularly useful. Again, the introduction of *msh* deletions into Δ*vscN*1 or Δ*vscN*2 strains would allow for assessment of the importance of each secretion system in isolation from the other. Assessment of an

involvement for MSHA in adherence to human intestinal tissue explants would also prove particularly useful in establishing the significance of MSHA in human infections.

The glycan array profiling of Δ*msh* mutants carried out during this study revealed a number of potential receptors for the pilus, with the Lewis A and Lewis X glycans displaying particularly high affinity towards the pilus. Pre-treatment of bacterial suspensions with purified glycans prior to glycan array hybridisation would confirm the specificity of the interactions observed in this study. Similarly, pre-incubation of glycan array slides with Lewis antigen binding lectins and/or anti-Lewis antibodies would also confirm the specificity of the interactions observed. This technique could be further applied to *in vitro* adherence assays with Caco-2 to confirm the biological relevance of interactions with specific glycans.

While the phenotypes associated with *mshE*, *mshL* and *mshA*1 deletions have confirmed a role for the MSHA pilus in adherence and subsequent pathogenicity, all three deletions prevent the formation of the pilus organelle. As previously discussed, minor pilins may play a significant role in pilus functionality, as observed with the *N. meningitidis* PilX pilin (Helaine *et al.*, 2005; Helaine *et al.*, 2007). As putative minor pilins are encoded within the MSHA locus, they present an attractive opportunity to study potential roles in MSHA pilus production and/or functionality. Deletion mutants of *mshC*, *mshD* and *mshO* could be analysed for loss of pilus functionality. The raising of antibodies against specific pilins would prove extremely useful for pilus characterisation both in terms of structural heterogeneity and functionality. Immuno-gold labelling of pilins would reveal localisation and abundance within the pilus filament, while antibodies could also be used to inhibit any potential binding events *via* receptor recognition sites within each pilin. Antibody incubations could be included in glycan array profiling to establish sugar specificities (if any) of minor pilins.

Post-translational modifications of pilins have been shown to play a central role in functionality, with glycosylation being the most extensively characterised modification. Protein glycosylation mechanisms have not been described in *V. parahaemolyticus*. As described in section 6.7, *V. parahaemolyticus* possesses an OTase, $PglL_{VP}$ which may be involved in the glycosylation of the MSHA pilus, based on chromosomal proximity to the MSHA gene cluster and homology with a functionally confirmed OTase from *V. cholerae*. Disruption of *pglL*, followed by analysis for disrupted piliation and/or MSHA pilus functionality would yield particularly interesting insights into *Vibrio* pilus biology and the importance of protein glycosylation for *Vibrio* pathogenesis. Importantly, $PglL_{VC}$ was shown to exhibit promiscuous substrate specificity, being capable of glycosylating 3 exogenous proteins, including the *N. meningitidis* pilin when expressed in *E. coli* (Gebhart *et al.*, 2012). Therefore, $PglL_{VP}$ may have similarly diverse substrate specificity and play a role in diverse protein glycosylation systems.

6.12 Applications of this research.

While the genomic library approach used during this project was limited in its capability of isolating adherent/invasive clones, the exhaustive methods employed have highlighted a number of issues which could be avoided in future genomic library based approaches for detection of surface proteins. The low rates of adherence and invasion observed for *E. coli* HB101 compared with a range of other *E. coli* strains (data not shown) led to its selection for use in preparation of the genomic library. It seems however that *E. coli* HB101 may not have been an optimal strain for use in selection for surface expressed adhesins and invasins from *V. parahaemolyticus*, likely due to issues arising from a lack of post-translational modifications, poor secretion, low expression rates and indirect effects of stress due to the

presence and expression of a large foreign DNA element. As functional expression of fimbriae, TTSS, T6SS and other multi-protein cell surface organelles was achieved by Waterfield *et al.* (2008) using *E. coli* EPI305 as a host for a pWEB library, the use of this or a similar strain may result in improved functional expression from *V. parahaemolyticus* libraries in future.

The difficulties encountered during library selections led to the development of a validation technique to assess the randomness, coverage and expression potential of the genomic library. Selection of norfloxacin resistant clones from the library population provided a rapid means of assessing the quality and suitability of the genomic library. In future, the use of this rapid validation technique, following the construction of *V. parahaemolyticus* libraries could confirm coverage and randomness, while detection of both NorM and Qnr would serve to indicate functional expression and secretion of *V. parahaemolyticus* proteins. This technique could be further applied to a wide range of antibiotic selection assays in an attempt to identify novel antimicrobial resistance mechanisms possessed by *V. parahaemolyticus*.

The role identified for MSHA not only in adherence to a human intestinal cell line, but also in the downstream pathogenesis of *V. parahaemolyticus*, indicates that MSHA represents an attractive target for the development of therapeutics. As observed by the deletion of critical MSHA components, MSHA binding has a marked effect on virulence-associated responses in Caco-2. A number of TFP which function in adherence to human tissues have been shown to exhibit vaccine potential. The *V. cholerae* TcpA pili, *N. gonorrhoeae* GC pili and enterotoxigenic *E. coli* pili were all found to be immunogenic and polyclonal anti-sera produced by vaccination were found to prevent colonisation of epithelial tissues upon infection (Sun *et al.*, 1990; Tramont, 1989; Nagy *et al.*, 1978). Nakasone *et al.* (2000) showed that purified pili from an O3:K6 derivative of *V. parahaemolyticus* were immunogenic in rabbits and that anti-pilus antibodies were effective in preventing colonisation of rabbit

intestinal tissue by *V. parahaemolyticus*. At the time of study, the protein composition of the purified pili analysed by Nakasone *et al.* (2000) was not known. The findings of this study may eventually allow for the development of highly specific vaccines for the purpose of raising antibodies which target receptor binding domains of the major and/or minor pilins of the MSHA pilus.

Despite extensive characterisation of the *Neisseria* MC and GC pili, an effective broad specificity vaccine for neisserial disease remains elusive. The PilE major pilin subunit has been shown to display significant antigenic variability due to phase variation in the pilin transglycosylase genes and a highly variable amino acid composition (Power *et al.*, 2003; Criss *et al.*, 2005). For this reason clinical trials using purified pili as a vaccine prior to gonococcal infection were largely unsuccessful (Boslego *et al.*, 1991). Glycosylation of *V. parahaemolyticus* pili has not been reported, however it is known that the amino acid composition of MSHA pili is highly variable at intra-species level (Aagesen and Häse, 2012). As such, similar difficulties may be encountered with the use of whole *V. parahaemolyticus* pili as immuno-therapeutics.

In order to counteract such issues and to develop a system which would generate antibodies with broad strain specificity, Cehovin *et al.* (2011) investigated the efficacy of minor pilins in eliciting a protective antibody response. The sera of patients convalescent from infections with *N. meningitidis* were found to contain antibodies against the minor pilins pilX, PilV and ComP (Cehovin *et al.*, 2011). In comparison to major pilins, minor pilins were found to be highly conserved and rabbit polyclonal sera generated against some minor pilins were capable of disrupting MC pilus function (Cehovin *et al.*, 2010; Cehovin *et al.*, 2011). The application of a similar approach in the development of pilin vaccines for *V. parahaemolyticus* would prove extremely valuable in prevention of disease from a wide range of strains and serotypes.

The glycan array profiling technique provided a rapid high throughput means of screening a broad range of biologically relevant glycan epitopes as potential receptors for the MSHA pilus. A number of other bacterial adhesins have been found to exhibit lectin functionality (Mahdavi *et al.*, 2002; Ilver *et al.*, 1998; Sheth *et al.*, 1994; Källström *et al.*, 2001). Comparison of multiple bacterial species with isogenic adhesin deletion mutants would provide fresh insight into the mechanisms of adhesin function and would expand the already recognised importance of adhesin-glycan interactions in bacterial pathogenesis.

Finally, although the *V. cholerae* MSHA pilus has been reported to play no role in adherence to human tissues or *in vivo* colonisation during human and murine infections (Thelin and Taylor, 1996; Tacket *et al.*, 1998), the pronounced variability observed between major pilins (Fig 5.4; Aagesen and Häse, 2012) in the *Vibrionaceae* appears sufficient to confer differential functionality. The observations of this study indicate that the MSHA pili may indeed play a role in virulence of *Vibrio spp* other than *V. cholerae.* As such, the analysis of MSHA function in *V. alginolyticus* and *V. vulnificus*, two human pathogens which are closely related to *V. parahaemolyticus*, may provide important insight into colonisation and subsequent pathogenesis in those species.

6.13 Summary and conclusions.

This study aimed to further current understanding regarding the molecular interactions between *V. parahaemolyticus* and host cells, using the established intestinal epithelial cell model of Caco-2. In chapter 3, it was observed that *V. parahaemolyticus* was capable of adhering to Caco-2 cells with ten-fold higher efficiency than *E. coli* HB101 or *S.* Dublin. This high level of adherence led to uptake of a small number of *V. parahaemolyticus* cells which were then capable of rapid intracellular proliferation. TTSS1 appears to play an inhibitory

role in the interactions of *V. parahaemolyticus* with Caco-2 cells, with deletion mutants exhibiting higher levels of adherence and invasion than the wild type.

As TTSS do not appear to function as adhesins or invasins, a genomic library screening approach was undertaken in order to identify novel adhesin/invasin genes in *V. parahaemolyticus*. The selection of adherent/invasive *E. coli* clones carrying *V. parahaemolyticus* DNA resulted in the isolation of a single clone with higher invasion efficiency than that of the library host *E. coli* HB101. Bioinformatic analysis of the insert sequence within the invasive clone A16, led to the prediction of OmpA as a putative invasin, however deletion of *ompA* in *V. parahaemolyticus* did not affect invasiveness. Clone A16 displayed reduced colony counts at standardised absorbance and this may have led to detection as a false positive for elevated invasion efficiency. Successful validation of the genomic library was achieved by antibiotic selection, a method which may be used to confirm coverage and expression of *V. parahaemolyticus* DNA in other genomic libraries.

The MSHA pilus which has been shown to play a role in biofilm formation was found to be involved in adherence to Caco-2. Deletion mutants lacking the pilus displayed fifty percent lower adherence than the wild type. MSHA-mediated adherence was then shown to be required for a number of pathogenic effects of *V. parahaemolyticus* on Caco-2 cells including: cell lysis, cell rounding and secretion of IL-8. Glycan array profiling of mutants lacking the MSHA pilus identified a broad range of potential receptors indicating that the pilus may be a multivalent adhesin. Highest binding specificity was observed for the Lewis type glycans and we therefore hypothesise that these glycans may function as receptors for the MSHA pilus in attachment to the gastro-intestinal epithelium.

In conclusion, this study has furthered current knowledge of how *V. parahaemolyticus* interacts with host cells. The involvement of TTSS in the invasion and intracellular

proliferation of Caco-2 was found to differ from that observed with HeLa cells (Zhang *et al.*, 2012). This is the first study to extensively analyse the adherence and invasion phenotypes of the pandemic RIMD2210633 strain of *V. parahaemolyticus* using intestinal epithelial cells. The MSHA pilus, previously described as playing a role in biofilm formation was found to function in adherence to Caco-2, thereby facilitating downstream pathogenesis. Glycan array profiling identified that the Lewis type glycans may function as receptors for the MSHA pilus. This data has implications not only in our understanding of *V. parahaemolyticus* pathogenesis at a molecular level, but also provides an indication of the suitability of bacterial adhesins such as the MSHA pilus as targets for the development of future therapeutics to prevent colonisation and infection by bacterial pathogens.

References

1. Aagesen, A. M. & Häse, C. C. (2012). Sequence Analyses of Type IV Pili from *Vibrio cholerae*, *Vibrio parahaemolyticus*, and *Vibrio vulnificus*. *Microbial Ecology*, 1-16.
2. Akeda, Y., Kodama, T., Kashimoto, T., Cantarelli, V., Horiguchi, Y., Nagayama, K., Iida, T. & Honda, T. (2002). Dominant-negative Rho, Rac, and Cdc42 facilitate the invasion process of *Vibrio parahaemolyticus* into Caco-2 cells. *Infection and Immunity* **70**, 970-973.
3. Akeda, Y., Nagayama, K., Yamamoto, K. & Honda, T. (1997). Invasive Phenotype of *Vibrio parahaemolyticus*. *Journal of Infectious Diseases* **176**, 822-824.
4. Allen, W. J., Phan, G. & Waksman, G. (2012). Pilus biogenesis at the outer membrane of Gram-negative bacterial pathogens. *Current Opinion in Structural Biology* **22**, 500-506.
5. Alrutz, M. A. & Isberg, R. R. (1998). Involvement of focal adhesion kinase in invasin-mediated uptake. *Proceedings of the National Academy of Sciences* **95**, 13658-13663.
6. Alrutz, M. A., Srivastava, A., Wong, K.-W., D'Souza-Schorey, C., Tang, M., Ch'Ng, L.-E., Snapper, S. B. & Isberg, R. R. (2001). Efficient uptake of *Yersinia pseudotuberculosis* via integrin receptors involves a Rac1–Arp 2/3 pathway that bypasses N-WASP function. *Molecular Microbiology* **42**, 689-703.
7. Ambrish, R., Alper, K. & Yang, Z. (2010). I-TASSER: a unified platform for automated protein structure and function prediction. *Nat. Protocols* **5**, 725-738.
8. Amieva, M. R., Salama, N. R., Tompkins, L. S. & Falkow, S. (2002). *Helicobacter pylori* enter and survive within multivesicular vacuoles of epithelial cells. *Cellular Microbiology* **4**, 677-690.
9. Anderson, J. M., Van Itallie, C. M., Peterson, M. D., Stevenson, B. R., Carew, E. A. & Mooseker, M. S. (1989). ZO-1 mRNA and protein expression during tight junction assembly in Caco-2 cells. *The Journal of cell biology* **109**, 1047-1056.
10. Ansaruzzaman, M., Lucas, M., Deen, J. L., Bhuiyan, N. A., Wang, X.-Y., Safa, A., Sultana, M., Chowdhury, A., Nair, G. B., Sack, D. A., von Seidlein, L., Puri, M. K., Ali, M., Chaignat, C.-L., Clemens, J. D. & Barreto, A. (2005). Pandemic Serovars (O3:K6 and O4:K68) of *Vibrio parahaemolyticus* Associated with Diarrhea in Mozambique: Spread of the Pandemic into the African Continent. *Journal of Clinical Microbiology* **43**, 2559-2562.

11. Attridge, S. R., Manning, P. A., Holmgren, J. & Jonson, G. (1996). Relative significance of mannose-sensitive hemagglutinin and toxin-coregulated pili in colonization of infant mice by *Vibrio cholerae* El Tor. *Infection and Immunity* **64**, 3369-73.
12. Barrios, A. F. G., Zuo, R., Ren, D. & Wood, T. K. (2006). Hha, YbaJ, and OmpA regulate *Escherichia coli* K12 biofilm formation and conjugation plasmids abolish motility. *Biotechnology and Bioengineering* **93**, 188-200.
13. Bhattacharjee, R. N., Park, K., Chen, X., Iida, T., Honda, T., Takeuchi, O. & Akira, S. (2008). Translocation of VP1686 upregulates RhoB and accelerates phagocytic activity of macrophage through actin remodeling. *J Microbiol Biotechnol* **18**, 171-175.
14. Björk, S., Breimer, M. E., Hansson, G. C., Karlsson, K. A. & Leffler, H. (1987). Structures of blood group glycosphingolipids of human small intestine. A relation between the expression of fucolipids of epithelial cells and the ABO, Le and Se phenotype of the donor. *Journal of Biological Chemistry* **262**, 6758-6765.
15. Blackwell, C. C., MacKenzie, D. A. C., James, V. S., Elton, R. A., Zorgani, A. A., Weir, D. M. & Busuttil, A. (1999). Toxigenic bacteria and sudden infant death syndrome (SIDS): nasopharyngeal flora during the first year of life. *FEMS Immunology & Medical Microbiology* **25**, 51-58.
16. Blake, P. A., Weaver, R. E. & Hollis, D. G. (1980). Diseases of humans (other than cholera) caused by vibrios. *Annual Reviews in Microbiology* **34**, 341-367.
17. Blixt, O., Head, S., Mondala, T., Scanlan, C., Huflejt, M. E., Alvarez, R., Bryan, M. C., Fazio, F., Calarese, D., Stevens, J., Razi, N., Stevens, D. J., Skehel, J. J., van Die, I., Burton, D. R., Wilson, I. A., Cummings, R., Bovin, N., Wong, C.-H. & Paulson, J. C. (2004). Printed covalent glycan array for ligand profiling of diverse glycan binding proteins. *Proceedings of the National Academy of Sciences of the United States of America* **101**, 17033-17038.
18. Blomfjeld, I. C., McClain, M. S. & Eisenstein, B. I. (1991). Type 1 fimbriae mutants of *Escherichia coli* K12: characterization of recognized afimbriate strains and construction of new fim deletion mutants. *Molecular Microbiology* **5**, 1439-1445.
19. Boettcher, K. J. & Ruby, E. G. (1990). Depressed light emission by symbiotic *Vibrio fischeri* of the sepiolid squid Euprymna scolopes. *Journal of Bacteriology* **172**, 3701-3706.

20. Bolton, A., Osborne, M. & Stephen, J. (2000). Comparative study of the invasiveness of *Salmonella* serotypes Typhimurium, Choleraesuis and Dublin for Caco-2 cells, HEp-2 cells and rabbit ileal epithelia. *Journal of Medical Microbiology* **49**, 503.

21. Bonazzi, M., Veiga, E., Pizarro-Cerdá, J. & Cossart, P. (2008). Successive post-translational modifications of E-cadherin are required for InlA-mediated internalization of *Listeria monocytogenes*. *Cellular Microbiology* **10**, 2208-2222.

22. Boslego, J. W., Tramont, E. C., Chung, R. C., McChesney, D. G., Ciak, J., Sadoff, J. C., Piziak, M. V., Brown, J. D., Brinton, C. C. & Wood, S. W. (1991). Efficacy trial of a parenteral gonococcal pilus vaccine in men. *Vaccine* **9**, 154-162.

23. Bourdet-Sicard, R., Rudiger, M., Jockusch, B. M., Gounon, P., Sansonetti, P. J. & Tran Van Nhieu, G. (1999). Binding of the *Shigella* protein IpaA to vinculin induces F-actin depolymerization. *EMBO J* **18**, 5853-5862.

24. Boutin, B. K., Townsend, S. F., Scarpino, P. V. & Twedt, R. M. (1979). Demonstration of invasiveness of *Vibrio parahaemolyticus* in adult rabbits by immunofluorescence. *Applied and Environmental Microbiology* **37**, 647-653.

25. Boyd, E. F., Cohen, A. L. V., Naughton, L. M., Ussery, D. W., Binnewies, T. T., Stine, O. C. & Parent, M. A. (2008). Molecular analysis of the emergence of pandemic *Vibrio parahaemolyticus*. *BMC Microbiology* **8**, 110.

26. Boyer, H. W. & Roulland-dussoix, D. (1969). A complementation analysis of the restriction and modification of DNA in *Escherichia coli*. *Journal of Molecular Biology* **41**, 459-472.

27. Brady, S. F. (2007). Construction of soil environmental DNA cosmid libraries and screening for clones that produce biologically active small molecules. *Nat. Protocols* **2**, 1297-1305.

28. Braun, V. & Focareta, T. (1991). Pore-forming bacterial protein hemolysins (cytolysins). *Critical Reviews in Microbiology* **18**, 115-158.

29. Broberg, C., Calder, T. & Orth, K. (2011). *Vibrio parahaemolyticus* cell biology and pathogenicity determinants. *Microbes and infection/Institut Pasteur* **13**, 992.

30. Broberg, C. A., Zhang, L., Gonzalez, H., Laskowski-Arce, M. A. & Orth, K. (2010). A *Vibrio* Effector Protein Is an Inositol Phosphatase and Disrupts Host Cell Membrane Integrity. *Science* **329**, 1660-1662.

31. Brock, T. D. (1988). Robert Koch: a life in medicine and bacteriology.

32. Brown, K. N. & Percival, A. (1978). Penetration of antimicrobials into tissue culture cells and leucocytes. *Scandinavian journal of infectious diseases. Supplementum*, 251-260.

33. Brumell, J. H. & Grinstein, S. (2004). *Salmonella* redirects phagosomal maturation. *Current Opinion in Microbiology* **7**, 78-84.

34. Burdette, D. L., Seemann, J. & Orth, K. (2009). *Vibrio* VopQ induces PI3-kinase-independent autophagy and antagonizes phagocytosis. *Molecular Microbiology* **73**, 639-649.

35. Burdette, D. L., Yarbrough, M. L. & Orth, K. (2009b). Not without cause: *Vibrio parahaemolyticus* induces acute autophagy and cell death. *Autophagy* **5**, 100-102.

36. Burdette, D. L., Yarbrough, M. L., Orvedahl, A., Gilpin, C. J. & Orth, K. (2008). *Vibrio parahaemolyticus* orchestrates a multifaceted host cell infection by induction of autophagy, cell rounding, and then cell lysis. *Proceedings of the National Academy of Sciences* **105**, 12497-12502.

37. Cabello, F. C., Espejo, R., Hernandez, M. C., Rioseco, M. L., Ulloa, J. & Vergara, J. A. (2007). *Vibrio parahaemolyticus* O3: K6 epidemic diarrhea, Chile, 2005. *Emerging infectious diseases* **13**, 655.

38. Carbonnelle, E., Helaine, S., Nassif, X. & Pelicic, V. (2006). A systematic genetic analysis in *Neisseria meningitidis* defines the Pil proteins required for assembly, functionality, stabilization and export of type IV pili. *Molecular Microbiology* **61**, 1510-1522.

39. Carbonnelle, E., Hélaine, S., Prouvensier, L., Nassif, X. & Pelicic, V. (2005). Type IV pilus biogenesis in *Neisseria meningitidis*: PilW is involved in a step occurring after pilus assembly, essential for fibre stability and function. *Molecular Microbiology* **55**, 54-64.

40. Carrió, M. M. & Villaverde, A. (2001). Protein aggregation as bacterial inclusion bodies is reversible. *FEBS Letters* **489**, 29-33.

41. Casselli, T., Lynch, T., Southward, C. M., Jones, B. W. & DeVinney, R. (2008). *Vibrio parahaemolyticus* Inhibition of Rho Family GTPase Activation Requires a Functional Chromosome I Type III Secretion System. *Infection and Immunity* **76**, 2202-2211.

42. Castric, P., Cassels, F. J. & Carlson, R. W. (2001). Structural Characterization of the *Pseudomonas aeruginosa* 1244 Pilin Glycan. *Journal of Biological Chemistry* **276**, 26479-26485.

43. Cehovin, A., Kroll, J. S. & Pelicic, V. (2011). Testing the vaccine potential of PilV, PilX and ComP, minor subunits of *Neisseria meningitidis* type IV pili. *Vaccine* **29**, 6858-6865.

44. Cehovin, A., Winterbotham, M., Lucidarme, J., Borrow, R., Tang, C. M., Exley, R. M. & Pelicic, V. (2010). Sequence conservation of pilus subunits in *Neisseria meningitidis*. *Vaccine* **28**, 4817-4826.

45. Chaturvedi, P., Warren, C. D., Buescher, C. R., Pickering, L. K. & Newburg, D. S. (2001). Survival of human milk oligosaccharides in the intestine of infants. *Advances in experimental medicine and biology* **501**, 315-323.

46. Chen, J., Morita, Y., Huda, M. N., Kuroda, T., Mizushima, T. & Tsuchiya, T. (2002). VmrA, a Member of a Novel Class of Na+-Coupled Multidrug Efflux Pumps from *Vibrio parahaemolyticus*. *Journal of Bacteriology* **184**, 572-576.

47. Chen, Y., Stine, O. C., Badger, J., Gil, A., Nair, G. B., Nishibuchi, M. & Fouts, D. (2011). Comparative genomic analysis of *Vibrio parahaemolyticus*: serotype conversion and virulence. *BMC genomics* **12**, 294.

48. Cheng, Y. S. E. (1983). Increased cell buoyant densities of protein overproducing *Escherichia coli* cells. *Biochemical and Biophysical Research Communications* **111**, 104-111.

49. Chiavelli, D. A., Marsh, J. W. & Taylor, R. K. (2001). The Mannose-Sensitive Hemagglutinin of *Vibrio cholerae* Promotes Adherence to Zooplankton. *Applied and Environmental Microbiology* **67**, 3220-3225.

50. Clamp, M., Cuff, J., Searle, S. M. & Barton, G. J. (2004). The Jalview Java alignment editor. *Bioinformatics* **20**, 426-427.

51. Cleary, J., Lai, L.-C., Shaw, R. K., Straatman-Iwanowska, A., Donnenberg, M. S., Frankel, G. & Knutton, S. (2004). Enteropathogenic *Escherichia coli* (EPEC) adhesion to intestinal epithelial cells: role of bundle-forming pili (BFP), EspA filaments and intimin. *Microbiology* **150**, 527-538.

52. Collazo, C. M. & Galán, J. E. (1997). The invasion-associated type-III protein secretion system in *Salmonella*–a review. *Gene* **192**, 51-59.

53. Cornelis, G. R. (2006). The type III secretion injectisome. *Nat Rev Micro* **4**, 811-825.

54. Cossart, P. & Sansonetti, P. J. (2004). Bacterial invasion: the paradigms of enteroinvasive pathogens. *Science* **304**, 242-248.

55. Craig, J. W., Chang, F.-Y., Kim, J. H., Obiajulu, S. C. & Brady, S. F. (2010). Expanding Small-Molecule Functional Metagenomics through Parallel Screening of

Broad-Host-Range Cosmid Environmental DNA Libraries in Diverse Proteobacteria. *Applied and Environmental Microbiology* **76**, 1633-1641.

56. Craig, L., Pique, M. E. & Tainer, J. A. (2004). Type IV pilus structure and bacterial pathogenicity. *Nat Rev Micro* **2**, 363-378.
57. Craig, L., Taylor, R. K., Pique, M. E., Adair, B. D., Arvai, A. S., Singh, M., Lloyd, S. J., Shin, D. S., Getzoff, E. D., Yeager, M., Forest, K. T. & Tainer, J. A. (2003). Type IV Pilin Structure and Assembly: X-Ray and EM Analyses of *Vibrio cholerae* Toxin-Coregulated Pilus and *Pseudomonas aeruginosa* PAK Pilin. *Molecular Cell* **11**, 1139-1150.
58. Craig, L., Volkmann, N., Arvai, A. S., Pique, M. E., Yeager, M., Egelman, Edward H. & Tainer, J. A. (2006). Type IV Pilus Structure by Cryo-Electron Microscopy and Crystallography: Implications for Pilus Assembly and Functions. *Molecular Cell* **23**, 651-662.
59. Daborn, P., Waterfield, N., Silva, C., Au, C. & Sharma, S. (2002). A single Photorhabdus gene, makes caterpillars floppy (mcf), allows *Escherichia coli* to persist within and kill insects. *Proceedings of the National Academy of Sciences* **99**, 10742-10747.
60. Daniels, N. A., MacKinnon, L., Bishop, R., Altekruse, S., Ray, B., Hammond, R. M., Thompson, S., Wilson, S., Bean, N. H., Griffin, P. M. & Slutsker, L. (2000). *Vibrio parahaemolyticus* Infections in the United States, 1973–1998. *Journal of Infectious Diseases* **181**, 1661-1666.
61. Daniels, N. A. & Shafaie, A. (2000). A review of pathogenic *Vibrio* infections for clinicians. *Infections in Medicine* **17**, 665-685.
62. Darfeuille-Michaud, A., Aubel, D., Chauviere, G., Rich, C., Bourges, M., Servin, A. & Joly, B. (1990). Adhesion of enterotoxigenic *Escherichia coli* to the human colon carcinoma cell line Caco-2 in culture. *Infection and Immunity* **58**, 893-902.
63. Davidsen, T., Beck, E., Ganapathy, A., Montgomery, R., Zafar, N., Yang, Q., Madupu, R., Goetz, P., Galinsky, K., White, O. & Sutton, G. (2010). The comprehensive microbial resource. *Nucleic Acids Research* **38**, D340-D345.
64. Davidsen, T. & Tonjum, T. (2006). Meningococcal genome dynamics. *Nat Rev Micro* **4**, 11-22.
65. DePaola, A., Kaysner, C. A., Bowers, J. & Cook, D. W. (2000). Environmental Investigations of *Vibrio parahaemolyticus* in Oysters after Outbreaks in Washington,

Texas, and New York (1997 and 1998). *Applied and Environmental Microbiology* **66**, 4649-4654.

66. Derham, B. K. & Harding, J. J. (2002). Effects of modifications of alpha-crystallin on its chaperone and other properties. *Biochemical Journal* **364**, 711.
67. Dryselius, R., Kurokawa, K. & Iida, T. (2007). *Vibrionaceae*, a versatile bacterial family with evolutionarily conserved variability. *Research in Microbiology* **158**, 479-486.
68. Dunn, A. K., Millikan, D. S., Adin, D. M., Bose, J. L. & Stabb, E. V. (2006). New rfp- and pES213-Derived Tools for Analyzing Symbiotic *Vibrio fischeri* Reveal Patterns of Infection and lux Expression In Situ. *Applied and Environmental Microbiology* **72**, 802-810.
69. Edwards, N. J., Monteiro, M. A., Faller, G., Walsh, E. J., Moran, A. P., Roberts, I. S. & High, N. J. (2000). Lewis X structures in the O antigen side-chain promote adhesion of *Helicobacter pylori* to the gastric epithelium. *Molecular Microbiology* **35**, 1530-1539.
70. Egan, E. S. & Waldor, M. K. (2003). Distinct Replication Requirements for the Two *Vibrio cholerae* Chromosomes. *Cell* **114**, 521-530.
71. Egile, C., Loisel, T. P., Laurent, V., Li, R., Pantaloni, D., Sansonetti, P. J. & Carlier, M. F. (1999). Activation of the CDC42 effector N-WASP by the *Shigella flexneri* IcsA protein promotes actin nucleation by Arp2/3 complex and bacterial actin-based motility. *The Journal of cell biology* **146**, 1319-1332.
72. Elsinghorst, E. A., Baron, L. S. & Kopecko, D. J. (1989). Penetration of human intestinal epithelial cells by *Salmonella*: molecular cloning and expression of *Salmonella* typhi invasion determinants in *Escherichia coli*. *Proceedings of the National Academy of Sciences* **86**, 5173-5177.
73. Elsinghorst, E. A. & Weitz, J. A. (1994). Epithelial cell invasion and adherence directed by the enterotoxigenic *Escherichia coli tib* locus is associated with a 104-kilodalton outer membrane protein. *Infection and Immunity* **62**, 3463-3471.
74. Ernst, R. K., Guina, T. & Miller, S. I. (1999). How Intracellular Bacteria Survive: Surface Modifications That Promote Resistance to Host Innate Immune Responses. *Journal of Infectious Diseases* **179**, S326-S330.
75. Etienne-Manneville, S. & Hall, A. (2002). Rho GTPases in cell biology. *Nature* **420**, 629-635.

76. Evans, D. J. & Evans, D. G. (2000). *Helicobacter pylori* Adhesins: Review and Perspectives. *Helicobacter* **5**, 183-195.

77. Everest, P. H., Goossens, H., Butzler, J. P., Lloyd, D., Knutton, S., Ketley, J. M. & Williams, P. H. (1992). Differentiated Caco-2 cells as a model for enteric invasion by *Campylobacter jejuni* and *C. coli*. *Journal of Medical Microbiology* **37**, 319-325.

78. Faridmoayer, A., Fentabil, M. A., Mills, D. C., Klassen, J. S. & Feldman, M. F. (2007). Functional Characterization of Bacterial Oligosaccharyltransferases Involved in O-Linked Protein Glycosylation. *Journal of Bacteriology* **189**, 8088-8098.

79. Foster, S. L., Richardson, S. H. & Failla, M. L. (2001). Elevated Iron Status Increases Bacterial Invasion and Survival and Alters Cytokine/Chemokine mRNA Expression in Caco-2 Human Intestinal Cells. *The Journal of Nutrition* **131**, 1452-1458.

80. Friebel, A., Ilchmann, H., Aepfelbacher, M., Ehrbar, K., Machleidt, W. & Hardt, W.-D. (2001). SopE and SopE2 from *Salmonella* typhimurium Activate Different Sets of RhoGTPases of the Host Cell. *Journal of Biological Chemistry* **276**, 34035-34040.

81. Fu, Y. & Galan, J. E. (1999). A *Salmonella* protein antagonizes Rac-1 and Cdc42 to mediate host-cell recovery after bacterial invasion. *Nature* **401**, 293-297.

82. Fujino, T., Okuno, Y., Nakada, D., Aoyama, A., Fukai, K., Mukai, T. & Ueho, T. (1953). On the bacteriological examination of shirasu food poisoning. *Med. J. Osaka Univ* **4**, 299-304.

83. Fukui, S., Feizi, T., Galustian, C., Lawson, A. M. & Chai, W. (2002). Oligosaccharide microarrays for high-throughput detection and specificity assignments of carbohydrate-protein interactions. *Nat Biotech* **20**, 1011-1017.

84. Fürste, J. P., Pansegrau, W., Frank, R., Blöcker, H., Scholz, P., Bagdasarian, M. & Lanka, E. (1986). Molecular cloning of the plasmid RP4 primase region in a multi-host-range *tac*P expression vector. *Gene* **48**, 119-131.

85. Gaillard, J. L., Berche, P., Mounier, J., Richard, S. & Sansonetti, P. (1987). *In vitro* model of penetration and intracellular growth of *Listeria monocytogenes* in the human enterocyte-like cell line Caco-2. *Infection and Immunity* **55**, 2822-2829.

86. Gay, P., Le Coq, D., Steinmetz, M., Ferrari, E. & Hoch, J. A. (1983). Cloning structural gene sacB, which codes for exoenzyme levansucrase of *Bacillus subtilis*: expression of the gene in *Escherichia coli*. *Journal of Bacteriology* **153**, 1424-1431.

87. Gebhart, C., Ielmini, M. V., Reiz, B., Price, N. L., Aas, F. E., Koomey, M. & Feldman, M. F. (2012). Characterization of exogenous bacterial oligosaccharyltransferases in *Escherichia coli* reveals the potential for O-linked

protein glycosylation in *Vibrio cholerae* and *Burkholderia thailandensis*. *Glycobiology* **22**, 962-974.

88. Gedde, M. M., Higgins, D. E., Tilney, L. G. & Portnoy, D. A. (2000). Role of Listeriolysin O in Cell-to-Cell Spread of *Listeria monocytogenes*. *Infection and Immunity* **68**, 999-1003.
89. Giannasca, P. J., Giannasca, K. T., Leichtner, A. M. & Neutra, M. R. (1999). Human Intestinal M Cells Display the Sialyl Lewis A Antigen. *Infection and Immunity* **67**, 946-953.
90. Gil, A. I., Miranda, H., Lanata, C. F., Prada, A., Hall, E. R., Barreno, C. M., Nusrin, S., Bhuiyan, N. A., Sack, D. A. & Nair, G. B. (2007). O3:K6 Serotype of *Vibrio parahaemolyticus* identical to the global pandemic clone associated with diarrhea in Peru. *International Journal of Infectious Diseases* **11**, 324-328.
91. Gill, R. T., Valdes, J. J. & Bentley, W. E. (2000). A Comparative Study of Global Stress Gene Regulation in Response to Overexpression of Recombinant Proteins in *Escherichia coli*. *Metabolic Engineering* **2**, 178-189.
92. Girón, J. A., Torres, A. G., Freer, E. & Kaper, J. B. (2002). The flagella of enteropathogenic *Escherichia coli* mediate adherence to epithelial cells. *Molecular Microbiology* **44**, 361-379.
93. Gloux, K., Leclerc, M., Iliozer, H., L'Haridon, R., Manichanh, C., Corthier, G., Nalin, R., Blottière, H. M. & Doré, J. (2007). Development of High-Throughput Phenotyping of Metagenomic Clones from the Human Gut Microbiome for Modulation of Eukaryotic Cell Growth. *Applied and Environmental Microbiology* **73**, 3734-3737.
94. Gophna, U., Ron, E. Z. & Graur, D. (2003). Bacterial type III secretion systems are ancient and evolved by multiple horizontal-transfer events. *Gene* **312**, 151-163.
95. Gotoh, K., Kodama, T., Hiyoshi, H., Izutsu, K., Park, K. S., Dryselius, R., Akeda, Y., Honda, T. & Iida, T. (2010). Bile acid-induced virulence gene expression of *Vibrio parahaemolyticus* reveals a novel therapeutic potential for bile acid sequestrants. *PLoS ONE* **5**, e13365.
96. Goujon, M., McWilliam, H., Li, W., Valentin, F., Squizzato, S., Paern, J. & Lopez, R. (2010). A new bioinformatics analysis tools framework at EMBL–EBI. *Nucleic Acids Research* **38**, W695-W699.
97. Guglielmetti, S., Tamagnini, I., Mora, D., Minuzzo, M., Scarafoni, A., Arioli, S., Hellman, J., Karp, M. & Parini, C. (2008). Implication of an Outer Surface

Lipoprotein in Adhesion of Bifidobacterium bifidum to Caco-2 Cells. *Applied and Environmental Microbiology* **74**, 4695-4702.

98. Gustafsson, C., Govindarajan, S. & Minshull, J. (2004). Codon bias and heterologous protein expression. *Trends in Biotechnology* **22**, 346-353.

99. Hackney, C. R., Kleeman, E. G., Ray, B. & Speck, M. L. (1980). Adherence as a method of differentiating virulent and avirulent strains of *Vibrio parahaemolyticus*. *Applied and Environmental Microbiology* **40**, 652-658.

100. Hahn, H. P. (1997). The type-4 pilus is the major virulence-associated adhesin of *Pseudomonas aeruginosa* – a review. *Gene* **192**, 99-108.

101. Hamada, D., Higurashi, T., Mayanagi, K., Miyata, T., Fukui, T., Iida, T., Honda, T. & Yanagihara, I. (2007). Tetrameric Structure of Thermostable Direct Hemolysin from *Vibrio parahaemolyticus* Revealed by Ultracentrifugation, Small-angle X-ray Scattering and Electron Microscopy. *Journal of Molecular Biology* **365**, 187-195.

102. Hardt, W.-D., Chen, L.-M., Schuebel, K. E., Bustelo, X. R. & Galán, J. E. (1998). *S.* typhimurium Encodes an Activator of Rho GTPases that Induces Membrane Ruffling and Nuclear Responses in Host Cells. *Cell* **93**, 815-826.

103. Hartman, P. S. (1991). Transillumination can profoundly reduce transformation frequencies. *Biotechniques* **11**, 747-8.

104. Häse, C., Bauer, M. & Finkelstein, R. (1994). Genetic characterization of mannose-sensitive hemagglutinin (MSHA)-negative mutants of *Vibrio cholerae* derived by Tn5 mutagenesis. *Gene* **150**, 17.

105. Hegge, F. T., Hitchen, P. G., Aas, F. E., Kristiansen, H., Løvold, C., Egge-Jacobsen, W., Panico, M., Leong, W. Y., Bull, V., Virji, M., Morris, H. R., Dell, A. & Koomey, M. (2004). Unique modifications with phosphocholine and phosphoethanolamine define alternate antigenic forms of *Neisseria gonorrhoeae* type IV pili. *Proceedings of the National Academy of Sciences of the United States of America* **101**, 10798-10803.

106. Heidelberg, J. F., Eisen, J. A., Nelson, W. C., Clayton, R. A., Gwinn, M. L., Dodson, R. J., Haft, D. H., Hickey, E. K., Peterson, J. D., Umayam, L., Gill, S. R., Nelson, K. E., Read, T. D., Tettelin, H., Richardson, D., Ermolaeva, M. D., Vamathevan, J., Bass, S., Qin, H., Dragoi, I., Sellers, P., McDonald, L., Utterback, T., Fleishmann, R. D., Nierman, W. C., White, O., Salzberg, S. L., Smith, H. O., Colwell, R. R., Mekalanos, J. J., Venter, J. C. & Fraser, C. M. (2000). DNA sequence of both chromosomes of the cholera pathogen *Vibrio cholerae*. *Nature* **406**, 477-483.

107. Hélaine, S., Carbonnelle, E., Prouvensier, L., Beretti, J.-L., Nassif, X. & Pelicic, V. (2005). PilX, a pilus-associated protein essential for bacterial aggregation, is a key to pilus-facilitated attachment of *Neisseria meningitidis* to human cells. *Molecular Microbiology* **55**, 65-77.

108. Helaine, S., Dyer, D. H., Nassif, X., Pelicic, V. & Forest, K. T. (2007). 3D structure/function analysis of PilX reveals how minor pilins can modulate the virulence properties of type IV pili. *Proceedings of the National Academy of Sciences* **104**, 15888-15893.

109. Henry, S., Oriol, R. & Samuelsson, B. (1995). Lewis Histo-Blood Group System and Associated Secretory Phenotypes. *Vox Sanguinis* **69**, 166-182.

110. Hickey, T. E., Baqar, S., Bourgeois, A. L., Ewing, C. P. & Guerry, P. (1999). *Campylobacter jejuni*-Stimulated Secretion of Interleukin-8 by INT407 Cells. *Infection and Immunity* **67**, 88-93.

111. High, N., Mounier, J., Prevost, M. C. & Sansonetti, P. J. (1992). IpaB of *Shigella flexneri* causes entry into epithelial cells and escape from the phagocytic vacuole. *The EMBO journal* **11**, 1991.

112. Hirono, Yamashita & Aoki. (1998). Note: Molecular cloning of chitinase genes from *Vibrio anguillarum* and *V. parahaemolyticus*. *Journal of Applied Microbiology* **84**, 1175-1178.

113. Hiyoshi, H., Kodama, T., Iida, T. & Honda, T. (2010). Contribution of *Vibrio parahaemolyticus* Virulence Factors to Cytotoxicity, Enterotoxicity, and Lethality in Mice. *Infection and Immunity* **78**, 1772-1780.

114. Hiyoshi, H., Kodama, T., Saito, K., Gotoh, K., Matsuda, S., Akeda, Y., Honda, T. & Iida, T. (2011). VopV, an F-Actin-Binding Type III Secretion Effector, Is Required for *Vibrio parahaemolyticus*-Induced Enterotoxicity. *Cell Host & Microbe* **10**, 401-409.

115. Hoffmann, F. & Rinas, U. (2004). Stress induced by recombinant protein production in *Escherichia coli*. *Physiological Stress Responses in Bioprocesses*, 73-92.

116. Honda, T., Goshima, K., Takeda, Y., Sugino, Y. & Miwatani, T. (1976). Demonstration of the cardiotoxicity of the thermostable direct hemolysin (lethal toxin) produced by *Vibrio parahaemolyticus*. *Infection and Immunity* **13**, 163-171.

117. Honda, T., Iida, T., Akeda, Y. & Kodama, T. (2008). Sixty years of *Vibrio parahaemolyticus* research. *Microbe* **3**, 462-466.

118. Hulton, C. S. J., Seirafi, A., Hinton, J. C. D., Sidebotham, J. M., Waddell, L., Pavitt, G. D., Owen-Hughes, T., Spassky, A., Buc, H. & Higgins, C. F. (1990). Histone-like protein H1 (H-NS), DNA supercoiling, and gene expression in bacteria. *Cell* **63**, 631-642.

119. Iijima, Y., Yamada, H. & Shinoda, S. (1981). Adherence of *Vibrio parahaemolyticus* and its relation to pathogenicity. *Canadian Journal of Microbiology* **27**, 1252-1259.

120. Ilver, D., Arnqvist, A., Ögren, J., Frick, I.-M., Kersulyte, D., Incecik, E. T., Berg, D. E., Covacci, A., Engstrand, L. & Borén, T. (1998). *Helicobacter pylori* Adhesin Binding Fucosylated Histo-Blood Group Antigens Revealed by Retagging. *Science* **279**, 373-377.

121. Ireton, K., Payrastre, B. & Cossart, P. (1999). The *Listeria monocytogenes* Protein InlB Is an Agonist of Mammalian Phosphoinositide 3-Kinase. *Journal of Biological Chemistry* **274**, 17025-17032.

122. Isberg, R. R. & Barnes, P. (2001). Subversion of integrins by enteropathogenic *Yersinia*. *Journal of Cell Science* **114**, 21-28.

123. Ishijima, N., Suzuki, M., Ashida, H., Ichikawa, Y., Kanegae, Y., Saito, I., Borén, T., Haas, R., Sasakawa, C. & Mimuro, H. (2011). BabA-mediated Adherence Is a Potentiator of the *Helicobacter pylori* Type IV Secretion System Activity. *Journal of Biological Chemistry* **286**, 25256-25264.

124. Jahn, K. A., Biazik, J. M. & Braet, F. (2011). GM1 expression in caco-2 cells: Characterisation of a fundamental passage-dependent transformation of a cell line. *Journal of Pharmaceutical Sciences* **100**, 3751-3762.

125. Janion, C. (2008). Inducible SOS response system of DNA repair and mutagenesis in *Escherichia coli*. *International journal of biological sciences* **4**, 338.

126. Jennings, M. P., Jen, F. E. C., Roddam, L. F., Apicella, M. A. & Edwards, J. L. (2011). *Neisseria gonorrhoeae* pilin glycan contributes to CR3 activation during challenge of primary cervical epithelial cells. *Cellular Microbiology* **13**, 885-896.

127. Johnson, M., Zaretskaya, I., Raytselis, Y., Merezhuk, Y., McGinnis, S. & Madden, T. L. (2008). NCBI BLAST: a better web interface. *Nucleic Acids Research* **36**, W5-W9.

128. Jones, C. H., Pinkner, J. S., Roth, R., Heuser, J., Nicholes, A. V., Abraham, S. N. & Hultgren, S. J. (1995). FimH adhesin of type 1 pili is assembled into a fibrillar tip structure in the *Enterobacteriaceae*. *Proceedings of the National Academy of Sciences* **92**, 2081-2085.

129. Jostock, T. & Dubel, S. (2005). Screening of Molecular Repertoires by Microbial Surface Display. *Combinatorial Chemistry & High Throughput Screening* **8**, 127-133.

130. Justice, S. S., Hunstad, D. A., Seed, P. C. & Hultgren, S. J. (2006). Filamentation by *Escherichia coli* subverts innate defenses during urinary tract infection. *Proceedings of the National Academy of Sciences* **103**, 19884-19889.

131. Kachlany, S. C., Planet, P. J., DeSalle, R., Fine, D. H., Figurski, D. H. & Kaplan, J. B. (2001). flp-1, the first representative of a new pilin gene subfamily, is required for non-specific adherence of *Actinobacillus actinomycetemcomitans*. *Molecular Microbiology* **40**, 542-554.

132. Källström, H., Blackmer Gill, D., Albiger, B., Liszewski, M. K., Atkinson, J. P. & Jonsson, A.-B. (2001). Attachment of *Neisseria gonorrhoeae* to the cellular pilus receptor CD46: identification of domains important for bacterial adherence. *Cellular Microbiology* **3**, 133-143.

133. Källström, H., Liszewski, M. K., Atkinson, J. P. & Jonsson, A.-B. (1997). Membrane cofactor protein (MCP or CD46) is a cellular pilus receptor for pathogenic *Neisseria*. *Molecular Microbiology* **25**, 639-647.

134. Katoh, H. (1965). Studies on the growth rate of various food bacteria. *Japanese journal of bacteriology* **20**, 94.

135. Kenny, B., DeVinney, R., Stein, M., Reinscheid, D. J., Frey, E. A. & Finlay, B. B. (1997). Enteropathogenic *E. coli* (EPEC) Transfers Its Receptor for Intimate Adherence into Mammalian Cells. *Cell* **91**, 511-520.

136. Kerr, M. C. & Teasdale, R. D. (2009). Defining macropinocytosis. *Traffic* **10**, 364-371.

137. Kilcoyne, M., Gerlach, J. Q., Kane, M. & Joshi, L. (2012). Surface chemistry and linker effects on lectin-carbohydrate recognition for glycan microarrays. *Analytical Methods* **4**, 2721-2728.

138. Kirn, T. J., Lafferty, M. J., Sandoe, C. M. P. & Taylor, R. K. (2002). Delineation of pilin domains required for bacterial association into microcolonies and intestinal colonization by *Vibrio cholerae*. *Molecular Microbiology* **35**, 896-910.

139. Kita-Tsukamoto, K., Oyaizu, H., Nanba, K. & Simidu, U. (1993). Phylogenetic Relationships of Marine Bacteria, Mainly Members of the Family *Vibrionaceae*, Determined on the Basis of 16S rRNA Sequences. *International Journal of Systematic Bacteriology* **43**, 8-19.

140. Kline, K. A., Fälker, S., Dahlberg, S., Normark, S. & Henriques-Normark, B. (2009). Bacterial Adhesins in Host-Microbe Interactions. *Cell Host & Microbe* **5**, 580-592.

141. Klose, K. E. & Mekalanos, J. J. (2002). Distinct roles of an alternative sigma factor during both free-swimming and colonizing phases of the *Vibrio cholerae* pathogenic cycle. *Molecular Microbiology* **28**, 501-520.

142. Knight, R., Freeland, S. & Landweber, L. (2001). A simple model based on mutation and selection explains trends in codon and amino-acid usage and GC composition within and across genomes. *Genome Biology* **2**, research0010.1 - research0010.13.

143. Kodama, T., Gotoh, K., Hiyoshi, H., Morita, M., Izutsu, K., Akeda, Y., Park, K. S., Cantarelli, V. V., Dryselius, R. & Iida, T. (2010b). Two regulators of *Vibrio parahaemolyticus* play important roles in enterotoxicity by controlling the expression of genes in the Vp-PAI region. *PLoS ONE* **5**, e8678.

144. Kodama, T., Rokuda, M., Park, K.-S., Cantarelli, V. V., Matsuda, S., Iida, T. & Honda, T. (2007). Identification and characterization of VopT, a novel ADP-ribosyltransferase effector protein secreted via the *Vibrio parahaemolyticus* type III secretion system 2. *Cellular Microbiology* **9**, 2598-2609.

145. Kodama, T., Yamazaki, C., Park, K.-S., Akeda, Y., Iida, T. & Honda, T. (2010). Transcription of *Vibrio parahaemolyticus* T3SS1 genes is regulated by a dual regulation system consisting of the ExsACDE regulatory cascade and H-NS. *FEMS Microbiology Letters* **311**, 10-17.

146. Kolappan, S., Roos, J., Yuen, A. S. W., Pierce, O. M. & Craig, L. (2012). Structural Characterization of CFA/III and Longus Type IVb Pili from Enterotoxigenic *Escherichia coli*. *Journal of Bacteriology* **194**, 2725-2735.

147. Kovach, M. E., Shaffer, M. D. & Peterson, K. M. (1996). A putative integrase gene defines the distal end of a large cluster of ToxR-regulated colonization genes in *Vibrio cholerae*. *Microbiology* **142**, 2165-2174.

148. Krachler, A. M., Ham, H. & Orth, K. (2011). Outer membrane adhesion factor multivalent adhesion molecule 7 initiates host cell binding during infection by Gram-negative pathogens. *Proceedings of the National Academy of Sciences* **108**, 11614-11619.

149. Krivan, H. C., Ginsburg, V. & Roberts, D. D. (1988). *Pseudomonas aeruginosa* and *Pseudomonas cepacia* isolated from cystic fibrosis patients bind specifically to

gangliotetraosylceramide (asialo GM1) and gangliotriaosylceramide (asialo GM2). *Archives of Biochemistry and Biophysics* **260**, 493-496.

150. Krogfelt, K. A., Bergmans, H. & Klemm, P. (1990). Direct evidence that the FimH protein is the mannose-specific adhesin of *Escherichia coli* type 1 fimbriae. *Infection and Immunity* **58**, 1995-1998.

151. Kubori, T. & Galán, J. E. (2003). Temporal Regulation of *Salmonella* Virulence Effector Function by Proteasome-Dependent Protein Degradation. *Cell* **115**, 333-342.

152. Kubori, T., Sukhan, A., Aizawa, S.-I. & Galán, J. E. (2000). Molecular characterization and assembly of the needle complex of the *Salmonella typhimurium* type III protein secretion system. *Proceedings of the National Academy of Sciences* **97**, 10225-10230.

153. Kumar, S., Nei, M., Dudley, J. & Tamura, K. (2008). MEGA: A biologist-centric software for evolutionary analysis of DNA and protein sequences. *Briefings in Bioinformatics* **9**, 299-306.

154. Lecuit, M., Hurme, R., Pizarro-Cerdá, J., Ohayon, H., Geiger, B. & Cossart, P. (2000). A role for α- and β-catenins in bacterial uptake. *Proceedings of the National Academy of Sciences* **97**, 10008-10013.

155. Lecuit, M., Ohayon, H., Braun, L., Mengaud, J. & Cossart, P. (1997). Internalin of *Listeria monocytogenes* with an intact leucine-rich repeat region is sufficient to promote internalization. *Infection and Immunity* **65**, 5309-19.

156. Lee, J. S. (1972). Inactivation of *Vibrio parahaemolyticus* in Distilled Water. *Applied Microbiology* **23**, 166-167.

157. Lee, W. C., Lee, M. J., Kim, J. S. & Park, S. Y. (2001). Foodborne illness outbreaks in Korea and Japan studied retrospectively. *Journal of Food Protection*® **64**, 899-902.

158. Leo, J. C., Elovaara, H., Brodsky, B., Skurnik, M. & Goldman, A. (2008). The *Yersinia* adhesin YadA binds to a collagenous triple-helical conformation but without sequence specificity. *Protein Engineering Design and Selection* **21**, 475-484.

159. Linkous, D. A. & Oliver, J. D. (1999). Pathogenesis of *Vibrio vulnificus*. *FEMS Microbiology Letters* **174**, 207-214.

160. Liverman, A. D. B., Cheng, H.-C., Trosky, J. E., Leung, D. W., Yarbrough, M. L., Burdette, D. L., Rosen, M. K. & Orth, K. (2007). Arp2/3-independent assembly of actin by *Vibrio* type III effector VopL. *Proceedings of the National Academy of Sciences* **104**, 17117-17122.

161. Lynch, T., Livingstone, S., Buenaventura, E., Lutter, E., Fedwick, J., Buret, A. G., Graham, D. & DeVinney, R. (2005). *Vibrio parahaemolyticus* Disruption of Epithelial Cell Tight Junctions Occurs Independently of Toxin Production. *Infection and Immunity* **73**, 1275-1283.

162. Magnusson, K. E., Davies, J., Grundström, T., Kihlström, E. & Normark, S. (1980). Surface charge and hydrophobicity of *Salmonella*, *E. coli*, Gonococci in relation to their tendency to associate with animal cells. *Scandinavian journal of infectious diseases. Supplementum* **Suppl 24**, 135-140.

163. Mahdavi, J., Sondén, B., Hurtig, M., Olfat, F. O., Forsberg, L., Roche, N., Ångström, J., Larsson, T., Teneberg, S., Karlsson, K.-A., Altraja, S., Wadström, T., Kersulyte, D., Berg, D. E., Dubois, A., Petersson, C., Magnusson, K.-E., Norberg, T., Lindh, F., Lundskog, B. B., Arnqvist, A., Hammarström, L. & Borén, T. (2002). *Helicobacter pylori* SabA Adhesin in Persistent Infection and Chronic Inflammation. *Science* **297**, 573-578.

164. Makino, K., Oshima, K., Kurokawa, K., Yokoyama, K., Uda, T., Tagomori, K., Iijima, Y., Najima, M., Nakano, M., Yamashita, A., Kubota, Y., Kimura, S., Yasunaga, T., Honda, T., Shinagawa, H., Hattori, M. & Iida, T. (2003). Genome sequence of *Vibrio parahaemolyticus*: a pathogenic mechanism distinct from that of *V cholerae*. *The Lancet* **361**, 743-749.

165. Mantile, G., Miele, L., Cordella-Miele, E., Singh, G., Katyal, S. & Mukherjee, A. (1993). Human Clara cell 10-kDa protein is the counterpart of rabbit uteroglobin. *Journal of Biological Chemistry* **268**, 20343-20351.

166. Marceau, M., Forest, K., Béretti, J.-L., Tainer, J. & Nassif, X. (1998). Consequences of the loss of O-linked glycosylation of meningococcal type IV pilin on piliation and pilus-mediated adhesion. *Molecular Microbiology* **27**, 705-715.

167. Marceau, M. & Nassif, X. (1999). Role of Glycosylation at Ser63 in Production of Soluble Pilin in Pathogenic *Neisseria*. *Journal of Bacteriology* **181**, 656-661.

168. Marionneau, S., Cailleau-Thomas, A., Rocher, J., Le Moullac-Vaidye, B., Ruvoën, N., Clément, M. & Le Pendu, J. (2001). ABH and Lewis histo-blood group antigens, a model for the meaning of oligosaccharide diversity in the face of a changing world. *Biochimie* **83**, 565-573.

169. Marsh, J. W. & Taylor, R. K. (1999). Genetic and Transcriptional Analyses of the *Vibrio cholerae* Mannose-Sensitive Hemagglutinin Type 4 Pilus Gene Locus. *Journal of Bacteriology* **181**, 1110-1117.

170. Martinez-Urtaza, J., Simental, L., Velasco, D., DePaola, A., Ishibashi, M., Nakaguchi, Y., Nishibuchi, M., Carrera-Flores, D., Rey-Alvarez, C. & Pousa, A. (2005). Pandemic *Vibrio parahaemolyticus* O3:K6, Europe. *Emerging infectious diseases* **11**, 1319-1320.

171. Matlawska-Wasowska, K., Finn, R., Mustel, A., O'Byrne, C., Baird, A., Coffey, E. & Boyd, A. (2010). The *Vibrio parahaemolyticus* Type III Secretion Systems manipulate host cell MAPK for critical steps in pathogenesis. *BMC Microbiology* **10**, 329.

172. Mattick, J. S. (2002). Type IV pili and twitching motility. *Annual Reviews in Microbiology* **56**, 289-314.

173. McBroom, C. R., Samanen, C. H. & Goldstein, I. (1972). [16] Carbohydrate antigens: Coupling of carbohydrates to proteins by diazonium and phenylisothiocyanate reactions. *Methods in enzymology* **28**, 212-219.

174. McCaw, M. L., Lykken, G. L., Singh, P. K. & Yahr, T. L. (2002). ExsD is a negative regulator of the *Pseudomonas aeruginosa* type III secretion regulon. *Molecular Microbiology* **46**, 1123-1133.

175. McLaughlin, J. B., DePaola, A., Bopp, C. A., Martinek, K. A., Napolilli, N. P., Allison, C. G., Murray, S. L., Thompson, E. C., Bird, M. M. & Middaugh, J. P. (2005). Outbreak of *Vibrio parahaemolyticus* gastroenteritis associated with Alaskan oysters. *New England Journal of Medicine* **353**, 1463-1470.

176. Meibom, K. L., Li, X. B., Nielsen, A. T., Wu, C.-Y., Roseman, S. & Schoolnik, G. K. (2004). The *Vibrio cholerae* chitin utilization program. *Proceedings of the National Academy of Sciences of the United States of America* **101**, 2524-2529.

177. Mengaud, J., Ohayon, H., Gounon, P., Mège, R. M. & Cossart, P. (1996). E-cadherin is the receptor for internalin, a surface protein required for entry of *L. monocytogenes* into epithelial cells. *Cell* **84**, 923-932.

178. Méresse, S., Steele-Mortimer, O., Finlay, B. B. & Gorvel, J. P. (1999). The rab7 GTPase controls the maturation of *Salmonella* typhimurium-containing vacuoles in HeLa cells. *The EMBO journal* **18**, 4394-4403.

179. Merritt, E. A., Sarfaty, S., Akker, F. V. D., L'Hoir, C., Martial, J. A. & Hol, W. G. J. (1994). Crystal structure of cholera toxin B-pentamer bound to receptor GM1 pentasaccharide. *Protein Science* **3**, 166-175.

180. Miyamoto, Y., Kato, T., Obara, Y., Akiyama, S., Takizawa, K. & Yamai, S. (1969). *In vitro* hemolytic characteristic of *Vibrio parahaemolyticus*: its close correlation with human pathogenicity. *Journal of Bacteriology* **100**, 1147.

181. Miyamoto, Y., Obara, Y., Nikkawa, T., Yamai, S., Kato, T., Yamada, Y. & Ohashi, M. (1980). Simplified Purification and Biophysicochemical Characteristics of Kanagawa Phenomenon-Associated Hemolysin of *Vibrio parahaemolyticus*. *Infection and Immunity* **28**, 567-576.

182. Mollicone, R., Bara, J., Le Pendu, J. & Oriol, R. (1985). Immunohistologic pattern of type 1 (Lea, Leb) and type 2 (X, Y, H) blood group-related antigens in the human pyloric and duodenal mucosae. *Laboratory investigation; a journal of technical methods and pathology* **53**, 219-227.

183. Monack, D. M., Raupach, B., Hromockyj, A. E. & Falkow, S. (1996). *Salmonella* typhimurium invasion induces apoptosis in infected macrophages. *Proceedings of the National Academy of Sciences* **93**, 9833-9838.

184. Moran, A. P., Gupta, A. & Joshi, L. (2011). Sweet-talk: role of host glycosylation in bacterial pathogenesis of the gastrointestinal tract. *Gut* **60**, 1412-1425.

185. Morita, Y., Kodama, K., Shiota, S., Mine, T., Kataoka, A., Mizushima, T. & Tsuchiya, T. (1998). NorM, a Putative Multidrug Efflux Protein, of *Vibrio parahaemolyticus* and Its Homolog in *Escherichia coli*. *Antimicrobial Agents and Chemotherapy* **42**, 1778-1782.

186. Morona, R., Klose, M. & Henning, U. (1984). *Escherichia coli* K-12 outer membrane protein (OmpA) as a bacteriophage receptor: analysis of mutant genes expressing altered proteins. *Journal of Bacteriology* **159**, 570-578.

187. Morrow, A. L., Ruiz-Palacios, G. M., Jiang, X. & Newburg, D. S. (2005). Human-Milk Glycans That Inhibit Pathogen Binding Protect Breast-feeding Infants against Infectious Diarrhea. *The Journal of Nutrition* **135**, 1304-1307.

188. Mota, L. J. & Cornelis, G. R. (2005). The bacterial injection kit: type III secretion systems. *Annals of medicine* **37**, 234-249.

189. Mukai, T., Asasaka, T., Sato, E., Mori, K., Matsumoto, M. & Ohori, H. (2002). Inhibition of binding of *Helicobacter pylori* to the glycolipid receptors by probiotic *Lactobacillus reuteri*. *FEMS Immunology & Medical Microbiology* **32**, 105-110.

190. Nachlas, M. M., Margulies, S. I., Goldberg, J. D. & Seligman, A. M. (1960). The determination of lactic dehydrogenase with a tetrazolium salt. *Analytical biochemistry* **1**, 317-326.

191. Nagayama, K., Oguchi, T., Arita, M. & Honda, T. (1994). Correlation between cell-associated mannose-sensitive hemagglutination by *Vibrio parahaemolyticus* and adherence to a human colonic cell line Caco-2. *FEMS Microbiology Letters* **120**, 207-210.

192. Nagayama, K., Oguchi, T., Arita, M. & Honda, T. (1995). Purification and characterization of a cell-associated hemagglutinin of *Vibrio parahaemolyticus*. *Infection and Immunity* **63**, 1987-1992.

193. Nagy, B., Moon, H. W., Isaacson, R. E., To, C. C. & Brinton, C. C. (1978). Immunization of suckling pigs against enteric enterotoxigenic *Escherichia coli* infection by vaccinating dams with purified pili. *Infection and Immunity* **21**, 269-274.

194. Nair, G. B., Ramamurthy, T., Bhattacharya, S. K., Dutta, B., Takeda, Y. & Sack, D. A. (2007). Global Dissemination of *Vibrio parahaemolyticus* Serotype O3:K6 and Its Serovariants. *Clinical Microbiology Reviews* **20**, 39-48.

195. Nakasone, N., Insisengmay, S. & Iwanaga, M. (2000). Characterization of the pili isolated from *Vibrio parahaemolyticus* O3: K6. *The Southeast Asian Journal of Tropical Medicine and Public Health* **31**, 360-365.

196. Nakasone, N. & Iwanaga, M. (1990). Pili of a *Vibrio parahaemolyticus* strain as a possible colonization factor. *Infection and Immunity* **58**, 61-69.

197. Nakasone, N. & Iwanaga, M. (1991). Purification and characterization of pili isolated from *Vibrio parahaemolyticus* Na2. *Infection and Immunity* **59**, 726-728.

198. Newton, A., Kendall, M., Vugia, D. J., Henao, O. L. & Mahon, B. E. (2012). Increasing Rates of Vibriosis in the United States, 1996–2010: Review of Surveillance Data From 2 Systems. *Clinical Infectious Diseases* **54**, S391-S395.

199. Nicholls, L., Grant, T. H. & Robins-Browne, R. M. (2002). Identification of a novel genetic locus that is required for *in vitro* adhesion of a clinical isolate of enterohaemorrhagic *Escherichia coli* to epithelial cells. *Molecular Microbiology* **35**, 275-288.

200. Nishibuchi, M., Fasano, A., Russell, R. G. & Kaper, J. B. (1992). Enterotoxigenicity of *Vibrio parahaemolyticus* with and without genes encoding thermostable direct hemolysin. *Infection and Immunity* **60**, 3539-3545.

201. Nishibuchi, M. & Kaper, J. B. (1990). Duplication and variation of the thermostable direct haemolysin (tdh) gene in *Vibrio parahaemolyticus*. *Molecular Microbiology* **4**, 87-99.

202. Nye, M. B., Pfau, J. D., Skorupski, K. & Taylor, R. K. (2000). *Vibrio cholerae* H-NS Silences Virulence Gene Expression at Multiple Steps in the ToxR Regulatory Cascade. *Journal of Bacteriology* **182**, 4295-4303.

203. Oelschlaeger, T. A. (2001). Adhesins as invasins. *International Journal of Medical Microbiology* **291**, 7-14.

204. Ogawa, M., Handa, Y., Ashida, H., Suzuki, M. & Sasakawa, C. (2008). The versatility of *Shigella* effectors. *Nat Rev Micro* **6**, 11-16.

205. Ogawa, M. & Sasakawa, C. (2006). Intracellular survival of *Shigella*. *Cellular Microbiology* **8**, 177-184.

206. Okada, K., Iida, T., Kita-Tsukamoto, K. & Honda, T. (2005). Vibrios Commonly Possess Two Chromosomes. *Journal of Bacteriology* **187**, 752-757.

207. Okuda, J., Ishibashi, M., Hayakawa, E., Nishino, T., Takeda, Y., Mukhopadhyay, A. K., Garg, S., Bhattacharya, S. K., Nair, G. B. & Nishibuchi, M. (1997). Emergence of a unique O3:K6 clone of *Vibrio parahaemolyticus* in Calcutta, India, and isolation of strains from the same clonal group from Southeast Asian travelers arriving in Japan. *Journal of Clinical Microbiology* **35**, 3150-5.

208. Ono, T., Park, K.-S., Ueta, M., Iida, T. & Honda, T. (2006). Identification of Proteins Secreted via *Vibrio parahaemolyticus* Type III Secretion System 1. *Infection and Immunity* **74**, 1032-1042.

209. Opitz, B., Püschel, A., Beermann, W., Hocke, A. C., Förster, S., Schmeck, B., van Laak, V., Chakraborty, T., Suttorp, N. & Hippenstiel, S. (2006). *Listeria monocytogenes* Activated p38 MAPK and Induced IL-8 Secretion in a Nucleotide-Binding Oligomerization Domain 1-Dependent Manner in Endothelial Cells. *The Journal of Immunology* **176**, 484-490.

210. Orth, K., Palmer, L. E., Bao, Z. Q., Stewart, S., Rudolph, A. E., Bliska, J. B. & Dixon, J. E. (1999). Inhibition of the Mitogen-Activated Protein Kinase Kinase Superfamily by a *Yersinia* Effector. *Science* **285**, 1920-1923.

211. Pallesen, L., Poulsen, L. K., Christiansen, G. & Klemm, P. (1995). Chimeric FimH adhesin of type 1 fimbriae: a bacterial surface display system for heterologous sequences. *Microbiology* **141**, 2839-2848.

212. Panina, E. M., Mattoo, S., Griffith, N., Kozak, N. A., Yuk, M. H. & Miller, J. F. (2005). A genome-wide screen identifies a *Bordetella* type III secretion effector and candidate effectors in other species. *Molecular Microbiology* **58**, 267-279.

213. Parge, H. E., Forest, K. T., Hickey, M. J., Christensen, D. A., Getzoff, E. D. & Tainer, J. A. (1995). Structure of the fibre-forming protein pilin at 2.6 A resolution. *Nature* **378**, 32-38.

214. Park, K.-S., Ono, T., Rokuda, M., Jang, M.-H., Okada, K., Iida, T. & Honda, T. (2004). Functional Characterization of Two Type III Secretion Systems of *Vibrio parahaemolyticus*. *Infection and Immunity* **72**, 6659-6665.

215. Patel, J. C. & Galán, J. E. (2006). Differential activation and function of Rho GTPases during *Salmonella*–host cell interactions. *The Journal of cell biology* **175**, 453-463.

216. Pautsch, A. & Schulz, G. E. (2000). High-resolution structure of the OmpA membrane domain. *Journal of Molecular Biology* **298**, 273-282.

217. Pelicic, V. (2008). Type IV pili: *e pluribus unum*? *Molecular Microbiology* **68**, 827-837.

218. Peterson, K. M. & Mekalanos, J. J. (1988). Characterization of the *Vibrio cholerae* ToxR regulon: identification of novel genes involved in intestinal colonization. *Infection and Immunity* **56**, 2822-2829.

219. Philippe, N., Alcaraz, J.-P., Coursange, E., Geiselmann, J. & Schneider, D. (2004). Improvement of pCVD442, a suicide plasmid for gene allele exchange in bacteria. *Plasmid* **51**, 246-255.

220. Piddock, L. J. V. (2006). Multidrug-resistance efflux pumps? not just for resistance. *Nat Rev Micro* **4**, 629-636.

221. Poirel, L., Liard, A., Rodriguez-Martinez, J. M. & Nordmann, P. (2005). *Vibrionaceae* as a possible source of Qnr-like quinolone resistance determinants. *Journal of Antimicrobial Chemotherapy* **56**, 1118-1121.

222. Power, P. M., Roddam, L. F., Dieckelmann, M., Srikhanta, Y. N., Cheng Tan, Y., Berrington, A. W. & Jennings, M. P. (2000). Genetic characterization of pilin glycosylation in *Neisseria meningitidis*. *Microbiology* **146**, 967-979.

223. Power, P. M., Roddam, L. F., Rutter, K., Fitzpatrick, S. Z., Srikhanta, Y. N. & Jennings, M. P. (2003). Genetic characterization of pilin glycosylation and phase variation in *Neisseria meningitidis*. *Molecular Microbiology* **49**, 833-847.

224. Power, P. M., Seib, K. L. & Jennings, M. P. (2006). Pilin glycosylation in *Neisseria meningitidis* occurs by a similar pathway to wzy-dependent O-antigen biosynthesis in *Escherichia coli*. *Biochemical and Biophysical Research Communications* **347**, 904-908.

225. Prasadarao, N. V., Blom, A. M., Villoutreix, B. O. & Linsangan, L. C. (2002). A Novel Interaction of Outer Membrane Protein A with C4b Binding Protein Mediates Serum Resistance of *Escherichia coli* K1. *The Journal of Immunology* **169**, 6352-6360.

226. Prasadarao, N. V., Wass, C. A. & Kim, K. S. (1996). Endothelial cell GlcNAc beta 1-4GlcNAc epitopes for outer membrane protein A enhance traversal of *Escherichia coli* across the blood-brain barrier. *Infection and Immunity* **64**, 154-60.

227. Prinz, C., Schöniger, M., Rad, R., Becker, I., Keiditsch, E., Wagenpfeil, S., Classen, M., Rösch, T., Schepp, W. & Gerhard, M. (2001). Key Importance of the *Helicobacter pylori* Adherence Factor Blood Group Antigen Binding Adhesin during Chronic Gastric Inflammation. *Cancer Research* **61**, 1903-1909.

228. Pujol, C., Eugène, E., Marceau, M. & Nassif, X. (1999). The meningococcal PilT protein is required for induction of intimate attachment to epithelial cells following pilus-mediated adhesion. *Proceedings of the National Academy of Sciences* **96**, 4017-4022.

229. Punta, M., Coggill, P. C., Eberhardt, R. Y., Mistry, J., Tate, J., Boursnell, C., Pang, N., Forslund, K., Ceric, G., Clements, J., Heger, A., Holm, L., Sonnhammer, E. L. L., Eddy, S. R., Bateman, A. & Finn, R. D. (2012). The Pfam protein families database. *Nucleic Acids Research* **40**, D290-D301.

230. Qadri, F., Shamsul Alam, M., Nishibuchi, M., Rahman, T., Alam, N. H., Chisti, J., Kondo, S., Sugiyama, J., Bhuiyan, N. A., Mathan, M. M., Sack, D. A. & Nair, G. B. (2003). Adaptive and Inflammatory Immune Responses in Patients Infected with Strains of *Vibrio parahaemolyticus*. *Journal of Infectious Diseases* **187**, 1085-1096.

231. Quinlan, M. E., Heuser, J. E., Kerkhoff, E. & Dyche Mullins, R. (2005). *Drosophila* Spire is an actin nucleation factor. *Nature* **433**, 382-388.

232. Quinlan, M. E. & Kerkhoff, E. (2008). Actin nucleation: bacteria get in-Spired. *Nat Cell Biol* **10**, 13-15.

233. Ralph, A. & Currie, B. J. (2007). *Vibrio vulnificus* and *V. parahaemolyticus* necrotising fasciitis in fishermen visiting an estuarine tropical northern Australian location. *Journal of Infection* **54**, e111-e114.

234. Reyrat, J.-M., Pelicic, V., Gicquel, B. & Rappuoli, R. (1998). Counterselectable Markers: Untapped Tools for Bacterial Genetics and Pathogenesis. *Infection and Immunity* **66**, 4011-4017.

235. Rich, K. A., Burkett, C. & Webster, P. (2003). Cytoplasmic bacteria can be targets for autophagy. *Cellular Microbiology* **5**, 455-468.

236. Ridley, A. J. (2006). Rho GTPases and actin dynamics in membrane protrusions and vesicle trafficking. *Trends in Cell Biology* **16**, 522-529.

237. Rillahan, C. D. & Paulson, J. C. (2011). Glycan microarrays for decoding the glycome. *Annual review of biochemistry* **80**, 797-823.

238. Ritchie, J. M., Rui, H., Zhou, X., Iida, T., Kodoma, T., Ito, S., Davis, B. M., Bronson, R. T. & Waldor, M. K. (2012). Inflammation and disintegration of intestinal villi in an experimental model for *Vibrio parahaemolyticus*-induced diarrhea. *PLoS pathogens* **8**, e1002593.

239. Rosqvist, R., Forsberg, Å., Rimpiläinen, M., Bergman, T. & Wolf-Watz, H. (1990). The cytotoxic protein YopE of *Yersinia* obstructs the primary host defence. *Molecular Microbiology* **4**, 657-667.

240. Saadi, A. T., Weir, D. M., Poxton, I. R., Stewart, J., Essery, S. D., Caroline Blackwell, C., Raza, M. W. & Busuttil, A. (1994). Isolation of an adhesin from *Staphylococcus aureus* that binds Lewis blood group antigen and its relevance to sudden infant death syndrome. *FEMS Immunology and Medical Microbiology* **8**, 315-320.

241. Sääf, A. M., Halbleib, J. M., Chen, X., Yuen, S. T., Leung, S. Y., Nelson, W. J. & Brown, P. O. (2007). Parallels between global transcriptional programs of polarizing Caco-2 intestinal epithelial cells *in vitro* and gene expression programs in normal colon and colon cancer. *Molecular biology of the cell* **18**, 4245-4260.

242. Saga, T., Kaku, M., Onodera, Y., Yamachika, S., Sato, K. & Takase, H. (2005). *Vibrio parahaemolyticus* Chromosomal *qnr* Homologue *VPA0095*: Demonstration by Transformation with a Mutated Gene of Its Potential To Reduce Quinolone Susceptibility in *Escherichia coli*. *Antimicrobial Agents and Chemotherapy* **49**, 2144-2145.

243. Sai Sudha, P., Devaraj, H. & Devaraj, N. (2001). Adherence of *Shigella dysenteriae* 1 to human colonic mucin. *Current Microbiology* **42**, 381-387.

244. Saitoh, T., Natomi, H., Zhao, W., Okuzumi, K., Sugano, K., Iwamori, M. & Nagai, Y. (1991). Identification of glycolipid receptors for *Helicobacter pylori* by TLC-immunostaining. *FEBS Letters* **282**, 385-387.

245. Sakamoto, J., Furukawa, K., Cordon-Cardo, C., Yin, B. W. T., Rettig, W. J., Oettgen, H. F., Old, L. J. & Lloyd, K. O. (1986). Expression of Lewisa, Lewisb, X, and Y

Blood Group Antigens in Human Colonic Tumors and Normal Tissue and in Human Tumor-derived Cell Lines. *Cancer Research* **46**, 1553-1561.

246. Sakazaki, R., Iwanami, S. & Fukumi, H. (1963). Studies on the enteropathogenic, facultatively halophilic bacteria, *Vibrio parahaemolyticus*. Cultural and biochemical properties and its taxonomic position. *Japanese journal of medical science & biology* **16**, 161.

247. Sarkar, M. & Chaudhuri, K. (2004). Association of adherence and motility in interleukin 8 induction in human intestinal epithelial cells by *Vibrio cholerae*. *Microbes and Infection* **6**, 676-685.

248. Schütz, M., Weiss, E.-M., Schindler, M., Hallström, T., Zipfel, P. F., Linke, D. & Autenrieth, I. B. (2010). Trimer Stability of YadA Is Critical for Virulence of *Yersinia enterocolitica*. *Infection and Immunity* **78**, 2677-2690.

249. Schweizer, M. & Henning, U. (1977). Action of a major outer cell envelope membrane protein in conjugation of *Escherichia coli* K-12. *Journal of Bacteriology* **129**, 1651-1652.

250. Seveau, S., Tham, T. N., Payrastre, B., Hoppe, A. D., Swanson, J. A. & Cossart, P. (2007). A FRET analysis to unravel the role of cholesterol in Rac1 and PI 3-kinase activation in the InlB/Met signalling pathway. *Cellular Microbiology* **9**, 790-803.

251. Shashikant, C. S., L. Carr, J., Bhargava, J., Bentley, K. L. & Ruddle, F. H. (1998). Recombinogenic targeting: a new approach to genomic analysis - a review. *Gene* **223**, 9-20.

252. Shen, Y., Naujokas, M., Park, M. & Ireton, K. (2000). InlB-Dependent Internalization of *Listeria* Is Mediated by the Met Receptor Tyrosine Kinase. *Cell* **103**, 501-510.

253. Sheth, H. B., Lee, K. K., Wong, W. Y., Srivastava, G., Hindsgaul, O., Hodges, R. S., Paranchych, W. & Irvin, R. T. (1994). The pili of *Pseudomonas aeruginosa* strains PAK and PAO bind specifically to the carbohydrate sequence βGalNAc(1–4)βGal found in glycosphingolipids asialo-GM1 and asialo-GM2. *Molecular Microbiology* **11**, 715-723.

254. Shime-Hattori, A., Iida, T., Arita, M., Park, K.-S., Kodama, T. & Honda, T. (2006). Two type IV pili of *Vibrio parahaemolyticus* play different roles in biofilm formation. *FEMS Microbiology Letters* **264**, 89-97.

255. Shimohata, T., Nakano, M., Lian, X., Shigeyama, T., Iba, H., Hamamoto, A., Yoshida, M., Harada, N., Yamamoto, H., Yamato, M., Mawatari, K., Tamaki, T., Nakaya, Y. & Takahashi, A. (2011). *Vibrio parahaemolyticus* Infection Induces

Modulation of IL-8 Secretion Through Dual Pathway via VP1680 in Caco-2 Cells. *Journal of Infectious Diseases* **203**, 537-544.

256. Simidu, U., Kaneko, E. & Taga, N. (1977). Microbiological studies of Tokyo Bay. *Microbial Ecology* **3**, 173-191.

257. Smedley, J. G., Jewell, E., Roguskie, J., Horzempa, J., Syboldt, A., Stolz, D. B. & Castric, P. (2005). Influence of Pilin Glycosylation on *Pseudomonas aeruginosa* 1244 Pilus Function. *Infection and Immunity* **73**, 7922-7931.

258. Smith, S. G. J., Mahon, V., Lambert, M. A. & Fagan, R. P. (2007). A molecular Swiss army knife: OmpA structure, function and expression. *FEMS Microbiology Letters* **273**, 1-11.

259. Sory, M.-P. & Cornelis, G. R. (1994). Translocation of a hybrid YopE-adenylate cyclase from *Yersinia enterocolitica* into HeLa cells. *Molecular Microbiology* **14**, 583-594.

260. Soto, G. E. & Hultgren, S. J. (1999). Bacterial Adhesins: Common Themes and Variations in Architecture and Assembly. *Journal of Bacteriology* **181**, 1059-1071.

261. Sousa, S., Cabanes, D., Bougnères, L., Lecuit, M., Sansonetti, P., Tran-Van-Nhieu, G. & Cossart, P. (2007). Src, cortactin and Arp2/3 complex are required for E-cadherin-mediated internalization of *Listeria* into cells. *Cellular Microbiology* **9**, 2629-2643.

262. Speert, D. P., Loh, B. A., Cabral, D. A. & Salit, I. E. (1986). Nonopsonic phagocytosis of nonmucoid *Pseudomonas aeruginosa* by human neutrophils and monocyte-derived macrophages is correlated with bacterial piliation and hydrophobicity. *Infection and Immunity* **53**, 207-212.

263. Stabb, E. V. & Ruby, E. G. (2002). RP4-based plasmids for conjugation between *Escherichia coli* and members of the *vibrionaceae*. In *Methods in Enzymology* (Virginia L. Clark, P. M. B., ed.), Vol. Volume 358, pp. 413-426. Academic Press.

264. Stahlhut, S. G., Schroll, C., Harmsen, M., Struve, C. & Krogfelt, K. A. (2010). Screening for genes involved in *Klebsiella pneumoniae* biofilm formation using a fosmid library. *FEMS Immunology & Medical Microbiology* **59**, 521-524.

265. Steele-Mortimer, O. (2008). The *Salmonella*-containing vacuole—Moving with the times. *Current Opinion in Microbiology* **11**, 38-45.

266. Stenström, T. A. & Kjelleberg, S. (1985). Fimbriae mediated nonspecific adhesion of *Salmonella* typhimurium to mineral particles. *Archives of Microbiology* **143**, 6-10.

267. Stimson, E., Virji, M., Makepeace, K., Dell, A., Morris, H. R., Payne, G., Saunders, J. R., Jennings, M. P., Barker, S., Panico, M., Blench, I. & Moxon, E. R. (1995).

Meningococcal pilin: a glycoprotein substituted with digalactosyl 2,4-diacetamido-2,4,6-trideoxyhexose. *Molecular Microbiology* **17**, 1201-1214.

268. Sukumaran, S. K., Shimada, H. & Prasadarao, N. V. (2003). Entry and Intracellular Replication of *Escherichia coli* K1 in Macrophages Require Expression of Outer Membrane Protein A. *Infection and Immunity* **71**, 5951-5961.

269. Sun, D., Mekalanos, J. J. & Taylor, R. K. (1990). Antibodies Directed against the Toxin-Coregulated Pilus Isolated from *Vibrio cholerae* Provide Protection in the Infant Mouse Experimental Cholera Model. *Journal of Infectious Diseases* **161**, 1231-1236.

270. Suwanto, A. & Kaplan, S. (1989). Physical and genetic mapping of the *Rhodobacter sphaeroides* 2.4.1 genome: presence of two unique circular chromosomes. *Journal of Bacteriology* **171**, 5850-5859.

271. Tacket, C. O., Taylor, R. K., Losonsky, G., Lim, Y., Nataro, J. P., Kaper, J. B. & Levine, M. M. (1998). Investigation of the Roles of Toxin-Coregulated Pili and Mannose-Sensitive Hemagglutinin Pili in the Pathogenesis of *Vibrio cholerae* O139 Infection. *Infection and Immunity* **66**, 692-695.

272. Takikawa, I. (1958). Studies on pathogenic halophilic bacteria. *Yokohama medical bulletin* **9**, 313.

273. Tam, V. C., Serruto, D., Dziejman, M., Brieher, W. & Mekalanos, J. J. (2007). A Type III Secretion System in *Vibrio cholerae* Translocates a Formin/Spire Hybrid-like Actin Nucleator to Promote Intestinal Colonization. *Cell Host & Microbe* **1**, 95-107.

274. Tamano, K., Aizawa, S.-I., Katayama, E., Nonaka, T., Imajoh-Ohmi, S., Kuwae, A., Nagai, S. & Sasakawa, C. (2000). Supramolecular structure of the *Shigella* type III secretion machinery: the needle part is changeable in length and essential for delivery of effectors. *EMBO J* **19**, 3876-3887.

275. Terpe, K. (2006). Overview of bacterial expression systems for heterologous protein production: from molecular and biochemical fundamentals to commercial systems. *Applied Microbiology and Biotechnology* **72**, 211-222.

276. Tertti, R., Skurnik, M., Vartio, T. & Kuusela, P. (1992). Adhesion protein YadA of *Yersinia* species mediates binding of bacteria to fibronectin. *Infection and Immunity* **60**, 3021-3024.

277. Thelin, K. H. & Taylor, R. K. (1996). Toxin-coregulated pilus, but not mannose-sensitive hemagglutinin, is required for colonization by *Vibrio cholerae* O1 El Tor biotype and O139 strains. *Infection and Immunity* **64**, 2853-6.

278. Thompson, F. L., Austin, B. & Swings, J. (2006). *The biology of vibrios*, ASM Press.

279. Thompson, F. L., Iida, T. & Swings, J. (2004). Biodiversity of Vibrios. *Microbiology and Molecular Biology Reviews* **68**, 403-431.

280. Toranzo, A. E., Magariños, B. & Romalde, J. L. (2005). A review of the main bacterial fish diseases in mariculture systems. *Aquaculture* **246**, 37-61.

281. Tramont, E. C. (1989). Gonococcal vaccines. *Clinical Microbiology Reviews* **2**, S74-S77.

282. Tran, J. H., Jacoby, G. A. & Hooper, D. C. (2005). Interaction of the Plasmid-Encoded Quinolone Resistance Protein Qnr with *Escherichia coli* DNA Gyrase. *Antimicrobial Agents and Chemotherapy* **49**, 118-125.

283. Tran Van Nhieu, G., Caron, E., Hall, A. & Sansonetti, P. J. (1999). IpaC induces actin polymerization and filopodia formation during *Shigella* entry into epithelial cells. *EMBO J* **18**, 3249-3262.

284. Troisfontaines, P. & Cornelis, G. R. (2005). Type III Secretion: More Systems Than You Think. *Physiology* **20**, 326-339.

285. Trosky, J. E., Li, Y., Mukherjee, S., Keitany, G., Ball, H. & Orth, K. (2007). VopA Inhibits ATP Binding by Acetylating the Catalytic Loop of MAPK Kinases. *Journal of Biological Chemistry* **282**, 34299-34305.

286. Trosky, J. E., Mukherjee, S., Burdette, D. L., Roberts, M., McCarter, L., Siegel, R. M. & Orth, K. (2004). Inhibition of MAPK Signaling Pathways by VopA from *Vibrio parahaemolyticus*. *Journal of Biological Chemistry* **279**, 51953-51957.

287. Tweedy, J. M., Park, R. W. A. & Hodgkiss, W. (1968). Evidence for the Presence of Fimbriae (Pili) on *Vibrio* Species. *Journal of General Microbiology* **51**, 235-244.

288. Vandy, S., Leakhann, S., Phalmony, H., Denny, J. & Roces, M. C. (2012). *Vibrio parahaemolyticus* enteritis outbreak following a wedding banquet in a rural village–Kampong Speu, Cambodia, April 2012. *Western Pacific Surveillance and Response Journal* **3**, 1-4.

289. Virji, M., Kayhty, H., Ferguson, D., Alexandrescu, C., Heckels, J. & Moxon, E. (2006). The role of pili in the interactions of pathogenic *Neisseria* with cultured human endothelial cells. *Molecular Microbiology* **5**, 1831-1841.

290. Vongxay, K., Wang, S., Zhang, X., Wu, B., Hu, H., Pan, Z., Chen, S. & Fang, W. (2008). Pathogenetic characterization of *Vibrio parahaemolyticus* isolates from clinical and seafood sources. *International journal of food microbiology* **126**, 71-75.

291. Walker, G. C. (1985). Inducible DNA repair systems. *Annual review of biochemistry* **54**, 425-457.

292. Wang, X. H. & Leung, K. Y. (2000). Biochemical characterization of different types of adherence of *Vibrio* species to fish epithelial cells. *Microbiology* **146**, 989-998.

293. Waterfield, N. R., Sanchez-Contreras, M., Eleftherianos, I., Dowling, A., Yang, G., Wilkinson, P., Parkhill, J., Thomson, N., Reynolds, S. E., Bode, H. B., Dorus, S. & ffrench-Constant, R. H. (2008). Rapid Virulence Annotation (RVA): Identification of virulence factors using a bacterial genome library and multiple invertebrate hosts. *Proceedings of the National Academy of Sciences* **105**, 15967-15972.

294. Watnick, P. I., Fullner, K. J. & Kolter, R. (1999). A Role for the Mannose-Sensitive Hemagglutinin in Biofilm Formation by *Vibrio cholerae* El Tor. *Journal of Bacteriology* **181**, 3606-3609.

295. Welch, M. D., Rosenblatt, J., Skoble, J., Portnoy, D. A. & Mitchison, T. J. (1998). Interaction of human Arp2/3 complex and the *Listeria monocytogenes* ActA protein in actin filament nucleation. *Science* **281**, 105-108.

296. Wells, C. L., Van De Westerlo, E. M. A., Jechorek, R. P. & Erlandsen, S. L. (1996). Intracellular survival of enteric bacteria in cultured human enterocytes. *Shock* **6**, 27-34.

297. Whitchurch, C. B., Hobbs, M., Livingston, S. P., Krishnapillai, V. & Mattick, J. S. (1991). Characterisation of a *Pseudomonas aeruginosa* twitching motility gene and evidence for a specialised protein export system widespread in eubacteria. *Gene* **101**, 33-44.

298. Wiedemann, A., Linder, S., Grassl, G., Albert, M., Autenrieth, I. & Aepfelbacher, M. (2001). *Yersinia enterocolitica* invasin triggers phagocytosis via β1 integrins, CDC42Hs and WASp in macrophages. *Cellular Microbiology* **3**, 693-702.

299. Wieland, T., Faulstich, H. & Fiume, L. (1978). Amatoxins, Phallotoxins, Phallolysin, and Antamanide: The Biologically Active Components of Poisonous *Amanita* Mushroom. *Critical Reviews in Biochemistry and Molecular Biology* **5**, 185-260.

300. Wood, M. W., Rosqvist, R., Mullan, P. B., Edwards, M. H. & Galyov, E. E. (1996). SopE, a secreted protein of *Salmonella* dublin, is translocated into the target

eukaryotic cell via a sip-dependent mechanism and promotes bacterial entry. *Molecular Microbiology* **22**, 327-338.

301. Wulf, E., Deboben, A., Bautz, F. A., Faulstich, H. & Wieland, T. (1979). Fluorescent phallotoxin, a tool for the visualization of cellular actin. *Proceedings of the National Academy of Sciences* **76**, 4498-4502.

302. Xiao, Y. & Hutcheson, S. W. (1994). A single promoter sequence recognized by a newly identified alternate sigma factor directs expression of pathogenicity and host range determinants in *Pseudomonas syringae*. *Journal of Bacteriology* **176**, 3089-3091.

303. Xicohtencatl-Cortes, J., Monteiro-Neto, V., Ledesma, M. A., Jordan, D. M., Francetic, O., Kaper, J. B., Puente, J. L. & Girón, J. A. (2007). Intestinal adherence associated with type IV pili of enterohemorrhagic *Escherichia coli* O157:H7. *The Journal of Clinical Investigation* **117**, 3519-3529.

304. Yabuuchi, E., Miwatani, T., Takeda, Y. & Arita, M. (1974). Flagellar morphology of *Vibrio parahaemolyticus*. *Japanese journal of microbiology* **18**, 295.

305. Yahr, T. L. & Frank, D. W. (1994). Transcriptional organization of the trans-regulatory locus which controls exoenzyme S synthesis in *Pseudomonas aeruginosa*. *Journal of Bacteriology* **176**, 3832-3838.

306. Yamamoto, T. & Yokota, T. (1989). Adherence targets of *Vibrio parahaemolyticus* in human small intestines. *Infection and Immunity* **57**, 2410-2419.

307. Yanagihara, I., Nakahira, K., Yamane, T., Kaieda, S., Mayanagi, K., Hamada, D., Fukui, T., Ohnishi, K., Kajiyama, S. i., Shimizu, T., Sato, M., Ikegami, T., Ikeguchi, M., Honda, T. & Hashimoto, H. (2010). Structure and Functional Characterization of *Vibrio parahaemolyticus* Thermostable Direct Hemolysin. *Journal of Biological Chemistry* **285**, 16267-16274.

308. Yarbrough, M. L., Li, Y., Kinch, L. N., Grishin, N. V., Ball, H. L. & Orth, K. (2009). AMPylation of Rho GTPases by Vibrio VopS Disrupts Effector Binding and Downstream Signaling. *Science* **323**, 269-272.

309. Yoshida, S., Katayama, E., Kuwae, A., Mimuro, H., Suzuki, T. & Sasakawa, C. (2002). *Shigella* deliver an effector protein to trigger host microtubule destabilization, which promotes Rac1 activity and efficient bacterial internalization. *EMBO J* **21**, 2923-2935.

310. Yu, N. Y., Wagner, J. R., Laird, M. R., Melli, G., Rey, S., Lo, R., Dao, P., Sahinalp, S. C., Ester, M., Foster, L. J. & Brinkman, F. S. L. (2010). PSORTb 3.0: improved

protein subcellular localization prediction with refined localization subcategories and predictive capabilities for all prokaryotes. *Bioinformatics* **26**, 1608-1615.

311. Yu, Y., Yang, H., Li, J., Zhang, P., Wu, B., Zhu, B., Zhang, Y. & Fang, W. (2012). Putative type VI secretion systems of *Vibrio parahaemolyticus* contribute to adhesion to cultured cell monolayers. *Archives of Microbiology*, 1-9.
312. Zanetti, S., Deriu, A., Volterra, L., Falchi, M. P., Molicotti, P., Fadda, G. & Sechi, L. (2000). Virulence factors in *Vibrio alginolyticus* strains isolated from aquatic environments. *Annali di igiene : medicina preventiva e di comunita* **12**, 487-491.
313. Zhang, L., Krachler, Anne M., Broberg, Christopher A., Li, Y., Mirzaei, H., Gilpin, Christopher J. & Orth, K. (2012). Type III Effector VopC Mediates Invasion for *Vibrio* Species. *Cell Reports* **1**, 453-460.
314. Zhou, D., Mooseker, M. S. & Galán, J. E. (1999). Role of the *S.* typhimurium Actin-Binding Protein SipA in Bacterial Internalization. *Science* **283**, 2092-2095.
315. Zhou, G., Mo, W.-J., Sebbel, P., Min, G., Neubert, T. A., Glockshuber, R., Wu, X.-R., Sun, T.-T. & Kong, X.-P. (2001). Uroplakin Ia is the urothelial receptor for uropathogenic *Escherichia coli*: evidence from *in vitro* FimH binding. *Journal of Cell Science* **114**, 4095-4103.
316. Zhou, X., Shah, D. H., Konkel, M. E. & Call, D. R. (2008). Type III secretion system 1 genes in *Vibrio parahaemolyticus* are positively regulated by ExsA and negatively regulated by ExsD. *Molecular Microbiology* **69**, 747-764.